uOttawa

L'Université canadienne
Canada's university

FACULTÉ DES ÉTUDES SUPÉRIEURES ET POSTDOCTORALES

uOttawa

L'Université canadienne
Canada's university

FACULTY OF GRADUATE AND POSTDOCTORAL STUDIES

Thanh Huyen Dang
AUTEUR DE LA THÈSE / AUTHOR OF THESIS

Ph.D. (Environmental Engineering)
GRADE / DEGREE

School of Information Technology and Engineering
FACULTÉ, ÉCOLE, DÉPARTEMENT / FACULTY, SCHOOL, DEPARTMENT

Surface Modifying Macromolecules (SMM) – Incorporated Ultrafiltration Membranes for Natural Organic Matter (NOM) Removal: Characterization and Cleaning

TITRE DE LA THÈSE / TITLE OF THESIS

R. Narbaitz
DIRECTEUR (DIRECTRICE) DE LA THÈSE / THESIS SUPERVISOR

CO-DIRECTEUR (CO-DIRECTRICE) DE LA THÈSE / THESIS CO-SUPERVISOR

EXAMINATEURS (EXAMINATRICES) DE LA THÈSE / THESIS EXAMINERS

O. Basu

K. Kennedy

J. Kilduff

A. Tremblay

Gary W. Slater
Le Doyen de la Faculté des études supérieures et postdoctorales / Dean of the Faculty of Graduate and Postdoctoral Studies

SURFACE MODIFYING MACROMOLECULES (SMM) - INCORPORATED ULTRAFILTRATION MEMBRANES FOR NATURAL ORGANIC MATTER (NOM) REMOVAL: CHARACTERIZATION AND CLEANING

by

THANH HUYEN DANG

Ph.D. Thesis

Submitted to the School of Graduate Studies and Research

Under the supervision of Dr. Roberto M. Narbaitz

In partial fulfillment of the requirements for the degree of Ph.D. in Environmental Engineering

Ottawa-Carleton Joint Institute of Environmental Engineering
Department of Civil Engineering
University of Ottawa
Ottawa, Ontario
Canada, K1N 6N5

Your file Votre référence
ISBN: 978-0-494-61366-5
Our file Notre référence
ISBN: 978-0-494-61366-5

ABSTRACT

Membrane technology is an indispensable treatment alternative for utilities with complex water and wastewater management needs. There are a variety of state-of-art membrane solutions for potable water treatment including removing disinfection by-product (DBP) precursors, softening, acting as a physical barrier for virus, pathogens and bacteria removal, and even converting brackish groundwater and other marginal sources into safe drinking water.

One of the shortcomings of membrane technology is the propensity of the membranes to become fouled. In other words, the permeate flux decreases with time and membrane surface is covered by foulants such as natural organic matter (NOM) present in water sources. Although there are different techniques used in fouling reduction, this thesis focuses only on two approaches to solve this problem; they are membrane modification and membrane cleaning. For the first approach, two types of surface modifying macromolecules (i.e., hydrophobic nSMM and hydrophilic LSMM) were employed. The key objective is to change the membrane surface characteristics to better retain the foulant and enhance water permeation. A new casting technique (called as double-pass casting method) was also developed to hopefully produce better defect-free membranes. The second approach aimed at exploring the cleaning of fouled membranes in terms of cleaning apparatus, chemicals, protocols, frequencies and the effects of membrane hydrophilicity (via additive incorporation). The membranes developed in this study were evaluated and fouled by filtering raw Ottawa River water, so the principal foulant was NOM.

Blending of nSMM made the polyethersulfone (PES) membranes more hydrophobic, gave them a narrow pore size, and at the same time it hindered the penetration of water to the permeate side. Among the five modification factors studied such as polymer concentration, additive concentration, casting speed, thickness and post-treatment, only the additive concentration impacted the membrane performance (i.e., DOC removal and flux reduction) to a statistically significant level. The double-pass casting approach had a statistically significant effect on membrane morphology (smoothness of the surfaces and

cross-sectional structure), and also helped increase the permeate flux and the water production but DOC rejection was lowered. It can be concluded that addition of nSMM in membrane modification is not a good choice for the purpose of treating drink water. The incorporation of LSMM showed a more promising result. The PES-LSMM membranes had the highest flux resistance and highest TOC rejection (approximately 80%) in comparison with similar commercial ultrafiltration (UF) membranes. Besides PES base polymer, the LSMM can be miscible with a lot of other base polymers such as CA, PEI, PS, PVDF. Nevertheless, only PVDF membranes apparently had benefits from this hydrophilic additive with high flux changes or water production.

Four types of UF cells have been evaluated in the cleaning stage including a stirred UF cell, a SEPA cell, a single CF cell and a six-CF cell- in parallel system. The performance of the first three single cells in terms of flux was similar for the first testing cycle and then deviated in subsequent cycles due to different degree of NOM deposition and the ease of cleaning corresponding with different cell geometries. The six-cell-in-parallel system behaved quite differently from the single cell CF system. Cleaning efficiency at bench-scale had no significant difference regardless of cell type as long as a short cleaning frequency (i.e., 30 min) was employed. However, the SEPA cell is recommended for long-term cleaning test (several hours) since its design simulates better a real spiral wound membrane module with feed spacers and permeate carriers on the feed and permeate side of the membrane sheets, respectfully. The combination of backwashing and chemical cleaning protocol gave the highest cleaning efficiency since both reversible fouling and most of irreversible fouling was removed. When only chemicals alone were used, the sodium tripolyphosphate seemed to be the most effective reagent for both membranes with and without the LSMM additive. Overall, the incorporation of the LSMM additive did not statistically enhance cleaning efficiency.

RÉSUMÉ

La technologie de membrane est une alternative de traitement indispensable pour les utilités avec les eaux complexes et les besoins d'administration d'eaux usées. Il y a une variété de solutions en ce qui concerne l'utilisation de membrane d'état-d'art pour le traitement d'eau potable incluant l'enlèvement des produits dérivé par le désinfection (DDP), l'adoucissement d'eau, la création d'une barrière physique pour l'enlèvement de virus, de pathogènes et de bactéries et même la conversion de l'eau salé de la nappe phréatique et d'autres sources marginales en eau potable.

Un des désavantages de technologie membraneuse est la prédisposition des membranes de devenir pollué. Autrement dit, le flux de perméat diminu avec le temps et la surface membraneuse deviennent couvertes par des particules en suspension comme la matière organique naturelle (NOM) présent dans les sources d'eau. Bien qu'il y ait de différentes techniques utilisées dans la réduction de foulants, cette thèse est concentrée seulement sur deux approches pour résoudre ces problèmes, ils sont la modification de membrane et le nettoyage membraneux. Pour la première approche, deux types de surface qui modifies les macromolécules (c'est-à-dire, nSMM hydrophobe et hydrophilic LSMM) ont été employés. L'objectif principale est de changer les caractéristiques de la surface de la membrane pour empêcher l'encrassement et améliorer la perméabilité d'eau. Une nouvelle technique de casting (appelé la méthode double passe) a été aussi développée qui pourrait avec optimisme produire des meilleurs membranes sans défaut. La deuxième approche visait à explorer le nettoyage de membranes polluées du point de vue de l'appareil de nettoyage, des produits chimiques, des protocoles, des fréquences et des effets de membrane hydrophilic (via l'incorporation d'additive). Les membranes développées dans cette étude ont été évaluées et polluées en filtrant de l'eau brute de la Rivière d'Ottawa, donc le principal foulant était NOM.

Le mélange d'additive nSMM a tranformé les membranes polyethersulfone (PES) plus hydrophobe, a réduit la grandeur des pores, en même temps affectant la pénétration d'eau sur le côté des perméats. Parmi les cinq facteurs de modification étudiés comme la

concentration de polymère, la concentration d'additive, la vitesse de moulage, l'épaisseur et le post-traitement, seulement la concentration d'additive a eu un impact sur la performance de la membrane (c'est-à-dire, l'enlèvement de DOC et la réduction de flux) à un niveau statistiquement significatif. La méthode double passe avait un effet statistiquement significatif sur la morphologie membraneuse (l'aspect lisse des surfaces et de la structure trans-à éléments) et a aussi aidé à augmenter le flux pénètre et la production d'eau mais le refus de DOC a été baissé. Il peut être conclu que l'addition de nSMM pour la modification de membrane n'est pas un bon choix pour le but de traiter de l'eau potable. L'incorporation de LSMM a démontré un résultat plus prometteur. Les membranes PES-LSMM avaient la plus haute résistance de flux et le plus haut refus de TOC (environ 80%) en comparaison avec d'autre membranes d'ultrafiltration (UF) commerciale semblable. En plus du polymère de base de PES, le LSMM peut être mêlable avec beaucoup d'autres polymères de base comme le CA, PEI, PS, PVDF. Quand même, seulement les membranes de PVDF avaient apparemment des avantages de cet additif hydrophilic accompagnie par de hauts changements de flux ou de production d'eau.

Quatre types de cellules UF ont été évalués dans l'étape du nettoyage de membrane en incluant une cellule UF remuée, une cellule SEPA, un cellule CF et un système "six cellules en parallèle". La performance des trois premières cellules en terme de flux était semblable pour le premier cycle d'essai et a ensuite dévié dans les cycles ultérieurs en raison du différent degré de déposition de NOM et à l'aisance de nettoyer en comparaison avec les différentes géométries de cellule. Le système "six cellules en parallèle" s'est comporté tout à fait différemment du système avec le simple cellule CF. L'efficacité du nettoyage à l'échelle de banc n'avait aucune différence significative sans tenir compte du type de cellule aussi longtemps qu'une fréquence de nettoyage courte (c'est-à-dire, 30 minute) est employée. Pourtant, la cellule SEPA est recommandée pour le test de nettoyage à long terme (plusieurs heures) puisque sa conception simule mieux un vrai module en spirale enroulé, car la cellule SEPA contient des matériaux qui crées des espaces entre le membrane et la cellule pour mieux tranférer le perméat. La combinaison de backwashing et le protocole de nettoyage chimique a donné la plus haute efficacité de

nettoyage puisque tout l'encrassement réversible et la plupart d'encrassement irréversible a été enlevé. Quand seulement les produits chimiques ont été utilisés, le sodium tripolyphosphate a semblé être l'agent le plus efficace pour les deux membranes avec et sans additif LSMM. En tout, l'incorporation de l'additif LSSM n'a pas amélioré à un niveau statiquement significatif l'éfficacité du nettoyage.

Xin dành tặng cuốn Luận văn này đến những người tôi yêu quý nhất...

Đến người chồng yêu quý của tôi: Hoàng Anh Tuấn. Không có anh, em sẽ không bao giờ có được như ngày hôm nay. Tình yêu, tấm lòng, sự hy sinh và sự chia sẻ của anh khiến em luôn là người hạnh phúc nhất trên đời này.

Đến bố mẹ tôi: Đặng Bá Giai, Bùi Thị Sính và bố mẹ chồng tôi: Hoàng Phú, Ngô Thị Thoa, những người luôn ở bên tôi, động viên và ủng hộ tôi hết lòng.

Đến các anh chị của tôi: Đặng Việt Yên, Đặng Thuý Bình, Hoàng Việt Dũng, đã luôn gắn bó, giúp đỡ tôi về vật chất và tinh thần, giúp tôi quên đi nỗi khắc khoải khi xa quê hương.

Đến bà tôi, người đã không còn sống để chứng kiến những thành công tôi có được hôm nay. Tôi đã phải lên đường đi du học mà không kịp nhìn thấy bà khi bà mất. Quyển luận văn này như ngàn lời tạ lỗi của tôi với bà.

ACKNOWLEDGMENTS

I would like to express all my great gratitude to Dr. Roberto M. Narbaitz, for giving me the opportunity to work in this project, for believing in me, for his continued encouragement, for his support and guidance. I am very grateful to Dr. Takeshi Matsuura, for his invaluable guidance, comments and suggestions throughout this research.

My special thanks to Anh Nguyen, who encouraged and helped me in the early days when I started this program, a person who suggested ideas to the success I have achieved today.

My sincere recognition to Dr. Dipak Rana for helping me with all SMMs systhesis and for his cooperation in the project.

I am indebted to my professors at Civil Engineering Department, Dr. L. Fernandes, Dr. K. Kennedy, Dr. R. Droste, Dr. Skaff as well as professors in Chemical and Biological Department, Dr. Tremblay, Dr. Dubé, Dr. Tezel and Dr. Kruczek.

My sincere thanks to Francisco Aposaga (Frank) at the Civil Engineering Department, for all his help and patience in the laboratory. To the technicians at the Chemical Engineering Department, Gérard Nina, Franco Ziroldo and especially my dear "problem-solver" Louis Tremblay. To Yolande Hogan and Manon Racine for their administrative help.

A very special thanks to my best friends Adel Medlej and Omar Al-Attas, to my earnest friends Ha Nguyen, Adrian Filip, Ivory and Gordie Tremaine for the time that we shared, for always being there when I needed you.

I am very grateful to my fellow graduate students and friends Amy Westgate, Anne-Marie Garand-Sheridan, Megan Storrar, Muna Albanna, Juan Marin-Hernandez, Kate Zheng, Cigdem Eskicioglu, Jill Hass, Nuno Miguel, Samer Jabbour, Mansour Navidpour, Rafael Flores Vera for the lovely time we shared together at University of Ottawa.

Thanks to all students, classmates and staff at the Civil and Chemical-Biological Engineering Departments, University of Ottawa; to all Vietnamese fellows in Ottawa for countless times we gathered and shared with great fun and excitement.

I would like to acknowledge Dr. K. C. Khulbe (Department of Chemical Engineering), for the AFM analysis; to Mr. Andy Campbell (Britannia Water Treatment Plant), for his help in the collection of the Ottawa River water.

This project was possible thanks to Vietnam Government (Vietnamese Overseas Scholarship Programs -VOSP), Materials and Manufacturing Ontario (MMO), Natural Sciences and Engineering Research Council of Canada (NSERC) and University of Ottawa for their financial support.

TABLE OF CONTENTS

LIST OF TABLES

LIST OF FIGURES

Nomenclature

A	Surface area of membranes (cm^2)
C_b	Bulk concentration (mg/l)
d_p	Pore diameter (nm)
d_s	Solute diameter (nm)
f_i	Fraction of pores with diameter d_i (dimensionless)
J	Total flux (m^3/m^2-s)
J_i	Solvent flux for pores with diameter d_i (m^3/m^2-s)
$J_{pure\ water}$	flux of pure water ($L/m^2/h$)
$J_{fouled\ water}$	flux of fouled water ($L/m^2/h$)
M_n	number average molecular weight (dalton)
M_w	weight average molecular weight (dalton)
N	Number of pores per unit area
N_i	Density of pores with diameter d_i (dimensionless)
ΔP	Pressure (Pa)
R_a	Roughness of membrane surface (nm)
R_c	resistance of cake (m^{-1})
R_m	resistance of membrane (m^{-1})
T_g	glass transition temperature (^oC)
ε_s	Surface porosity (%)
η	Solvent viscosity ($N.s/m^2$)
μ	fluid viscosity ($N.s/m^2$)
μ_p	Geometric mean of the pore diameter (dimensionless)
σ_p	Geometric standard deviation (dimensionless)
α	Specific pore blockage efficiency (%)
σ_{inter}	Blocked area per unit filtrate volume (m^2/m^3)
δ_m	Cake thickness (mm)
χ	Mean pore sizes (nm)
γ_s	Surface tension (mJ/m^2)

Abbreviations

AFM	Atomic Force Microscopy
ANOVA	Analysis of variance
ATR	Attenuated total reflection
BSA	Bovine serum albumin
Cl_2	Chlorine
CF	Crossflow
D/DBPs	Disinfectant/Disinfectant-by-products
DBPs	Disinfection by-products
DEG	Diethylene glycol
DIA	Dialysis
DMAc	N,N-dimethyl acetamide
DOC	Dissolved Organic Carbon
DSC	Differential scanning calorimeter
ED	Electrodialysis
EDTA	Ethylenediamine Tetraacetic Acid
FTIR	Fourier transform infrared
GD	Gas diffusion
GP	Gas permeation
GPC	Gel permeation chromatography
HAA	Haloacetic acids
HEMA	Hydroxy-ethyl-methacrylate
HF	Hollow fiber
ICP-AES	Inductively coupled plasma - atomic emission spectrometry
LSMMs	Hydrophilic Surface Modifying Macromolecules
MDI	Diphenylmethane diisocyanate
MF	Microfiltration
MQ	Milli-Q (ultrapure) water
MPC	Methacryloyloxyethylphosphorylcholine
MW	Molecular weight
MWCO	Molecular Weight Cut-off

NF	Nanofiltration
NMP	N-methyl pyrrolidone
NMR	Nuclear magnetic resonance
NOM	Natural organic matter
nSMM	Hydrophobic Surface Modifying Macromolecules
OFA	Oligomeric fluoro-alcohol
ORW	Ottawa River Water
PA	Polyamide
PAI	Poly(amide imide)
PAN	Polyacrylonitrile
PC	Polycarbonate
PDMS	α,ω-aminopropyl poly(dimethyl siloxane)
PE	Polyesters
PEG	Polyethylene glycol
PEI	Polyetherimide
PEO	Polyethylene oxide
PES	Polyethersulfone
PP	Polypropylene
PPG	Polypropylene glycol
PPO	Polypropylene diol
PS	Polysulfone
PTFE	Polytetrafluoroethylene
PV	Pervaporation
PVC	Polyvivylchloride
PVDF	Poly(vinylidene-fluoroethylene)
PVP	Polyvinylpyrrolidone
PWP	Pure Water Permeation
RO	Reverse osmosis
SEC	Size exclusion chromatography
SEM	Scanning Electron Microscopy
SMMs	Surface Modifying Macromolecules

TDS	Total dissolved solids
THMs	Trihalomethanes
THF	Tetrahydrofuran
TOC	Total organic carbon
UF	Ultrafiltration
VOCs	Volatile organic compounds
XPS	X-ray photoelectron spectroscopy

CHAPTER 1

INTRODUCTION

1.1 Background

Membrane technologies are presently playing an important role in water treatment in many countries. Under certain circumstances, a membrane unit can replace an entire conventional water treatment chain (Fig 1.1). The potential advantages of membrane technologies include more reliable virus and protozoa removal, limited use of chemicals, disinfection without forming disinfection by-products (DBPs), more compact systems and potential for fully automated operation.

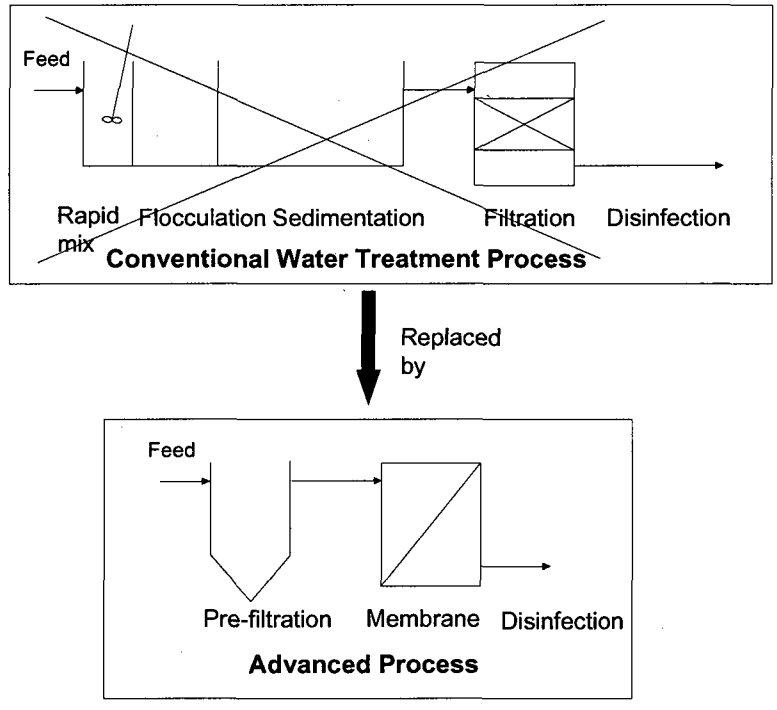

Figure 1.1. Comparison of conventional water treatment process and membrane process

There has been an exponential increase in microfiltration and ultrafiltration systems in the expansion of old water treatment plants and newly designed plants, which is significant proof of its merits (Amy et al., 2007). The primary reasons for this growth have been more reliable *Giardia* and *Cryptosporidium* control at competitive cost. Ultrafiltration particularly has been the focus of much interest since (i) It deals with the separation of

fairly large molecules like proteins, starches and gums, and some natural organic matter (NOM); (ii) It requires fairly low operating pressures (10-100 psig), which will lower equipment and pumping cost; (iii) No complicated heat transfer, heat-generating equipment or condensers are needed and (iv) It can operate at ambient temperature (Cheryan, 1986). Despite their many advantages, membrane processes still have to face with one significant constraint: FOULING, the flux reduction with time. Fouling affects the membrane's effectiveness and lifespan. A number of strategies have been applied to reduce the impact of fouling such as pretreatment, system operation optimization, optimization of membrane module configurations, chemical or hydraulic washing and membrane modification (Anselme and Jacobs, 1996).

The approach chosen for this study is to investigate improved resistance to fouling and cleaning through *membrane modification* i.e., development of new membranes via the addition of various tailor-made polymeric additives. The two main groups of additives are (hydrophobic) surface modifying macromolecules (SMMs) and hydrophilic surface modifying macromolecules (LSMMs). The modification method using SMMs has actually been developed since the early 1990s by Matsuura, Santerre, Narbaitz and coworkers (Pham, 1995; Tang et al., 1996; Hamza et al., 1997; Ho et al., 2000; Mosqueda-Jimenez, 2003; Rana et al., 2005; Nguyen, 2005; Kasemura et al., 1993). Much of this work has focused on ultrafiltration membranes for the production of drinking water from river water. Many SMMs/LSMMs have been synthesized to make the membrane surfaces more hydrophobic or more hydrophilic. These additives were incorporated to be compatible with polyethersulfone (PES) as a base polymer. However, this is not a trivial matter as some casting solutions prepared with certain proportions of PES and the surface modifying additives do not mix well and produce defective membranes. In addition the compatibility of SMM/LSMM has not been evaluated in conjunction with other base polymers. Moreover, no research on the efficiency of cleaning of these surface modified membranes has been conducted so far. The casting technique (single pass) used for making membranes has caused troubles sometimes with colony of pinholes or defect membranes.

1.2 Hypothesis

This thesis focuses on exploring the capabilities of surface modified ultrafiltration membranes and improving them. Based on the proposed work, the following *hypotheses* are proposed:

- The double-pass method, which is a modification from traditional casting technique, will produce more defect-free PES membranes since the second pass would cover defects such as any pinholes present.
- The more hydrophilic LSMM-PES membranes will be easier to clean than the hydrophobic SMM-PES membranes because of their smooth and water-liking surfaces.
- LSMM is a membrane additive that can also be used to improve membranes cast using different base polymer such as PVDF, PS, PEI and CA.

1.3 Scope of the research

The study is divided into three stages in order to address these hypotheses:

- ***Stage 1***: Develop the best hydrophilic/hydrophobic PES-based membranes by changing the LSMM/SMM percent and casting method, and then compare them with the commercial UF membranes. The hydrophobic SMM-PES membranes were developed to contrast with the hydrophilic LSMM-PES membranes and determine the impact of hydrophilicity/hydrophobicity on cleaning efficiency (during stage 2).
- ***Stage 2***: Assess the regeneration of modified membranes upon cleaning, in which the best cleaning procedures, best apparatus and best cleaning chemicals would be evaluated and disclosed.
- ***Stage 3***: Evaluate the performance of LSMM-blended UF membranes with different base polymers in terms of membrane hydrophilicity and fluxes.

To achieve the above objectives, the following tasks need to be undertaken: membrane preparation, membrane and water source characterization, and membrane testing. The testing will concentrate on the evaluation of the change of membrane properties

(porosity, MWCO, hydrophobicity, charge, surface morphology) and membrane performance (fluxes, NOM removal and water production).

1.4 Thesis organization

This thesis is organized as a paper-format thesis. The main results presented in Chapter 4 to Chapter 8, were prepared in a journal manuscript format.

Chapter 4 and 5 present the results of the first stage of the study, and also answer the first two hypotheses. The purpose of this stage is to develop the best modified PES membranes by incorporating LSMM/SMM additives into the casting solutions. Evaluation of manufacturing conditions on the development of these membranes is greatly concerned, for instance, concentration of additives, membrane thickness, casting technique, casting speed, etc. Data on other effects of manufacturing conditions for manufacturing hydrophobic nSMM membranes are presented in Chapter 4. The manuscript shown as chapter 4 was submitted to *Journal of Applied Polymer Science.* Chapter 5 proposes a new casting technique that would be able to overcome the hard-to-cast solutions during the membrane manufacture. The manuscript shown as chapter 5 was published by *Journal of Membrane Science, Volume 323, Issue 1, 2008, 45-52.*

In Chapter 6, the best experimental PES-LSMM membranes are compared with commercially available UF membranes to explore how good our experimental membranes are. Our modified membranes are evaluated in terms of characteristics and performance with nine commercial membranes from Osmonics and Amicon. Part of this chapter was presented in 2007 ACE Annual Conference and Exhibition held by American Water Works Association in Toronto, Ontario, Canada, June 24-28, 2007. The manuscript shown as chapter 6 was published by *Water Quality Research Journal of Canada, Volume 41, Issue 1, 2006, 84–93.*

Chapter 7 describes the results of Stage 2 which investigated the impact of membrane modification on membrane cleaning. In this chapter, the assessment not only focused on the impact of membrane modification but also the selection of bench-scale membrane

cleaning apparatus and cleaning frequency. This paper was submitted to the *Journal of Environmental Engineering (ASCE)* for publication.

Finally, the results of the third stage are reported in Chapter 8 and also give a complete answer for the third hypothesis. This chapter studies the impact of LSMM blending with different base polymers to modify their hydrophilicity. The modified membranes were compared in terms of flux and changes in hydrophilicity. This manuscript shown as Chapter 8 was accepted for publication in *Journal of Applied Polymer Science.*

In addition, a summary of the whole research is conducted including the introduction of the main additive (LSMM) that was used throughout the study; its synthesis procedure; manufacture of LSMM-blended PES membranes; blending of LSMM with other base polymers and cleaning. This is shown as Appendix S, Summary of the Project, and was printed in the *proceeding, 2008 IWA North American Membrane Research Conference* in Amherst, Massachusetts, USA, August 10-13, 2008. The presentation earned a $1000 award during the Student Competition.

As the results chapters are journal manuscripts, that have content limits, not all the research results from the five years of doctoral research could be presented within the results chapters, so 19 appendices were included. It should be noted that even though some chapters have been published, their contents have modified slightly to meet the requirement of thesis defense's committee.

CHAPTER 2

LITERATURE REVIEW

The following literature review will discuss membrane processes and some related matters, primarily fouling and cleaning.

2.1 Membrane processes

2.1.1 General

Compared with conventional separation processes, membrane separation processes are often more capital and energy efficient (Ho and Sirkar, 1992). A membrane process allows selective and controlled transfer of one species from one bulk phase to another bulk phase separated by the membrane. According to Aptel and Buckley (1996), a general classification of membrane processes can be obtained by considering the driving forces (i.e., pressure, activity and electrical potential).

Among the pressure-driven operations across the membranes, there are four types of processes namely reverse osmosis (RO), nanofiltration (NF), ultrafiltration (UF) and microfiltration (MF) (Figure 2.1). In RO, the solvent of feed solution is transferred through a dense membrane to retain salts and low molecular-weight (MW) solutes. To produce "pure" water from a saline solution, the osmotic pressure of the solution must be exceeded in the brine, for instance, the high pressure of 5-8 MPa is required for the process to work. NF, also called low-pressure RO or membrane softening, lies between RO and UF in terms of pressure requirement and selectivity. Its pressure requirement is typically from 0.5 to 1.5 MPa and it is often employed for softening, color removal and organics control. In water treatment, UF can be defined as a clarification and disinfection membrane process in drinking water treatment. UF membranes are porous and remove all types of microorganisms, including protozoa, bacteria and some viruses, and all types of particles. However, the small solutes (<10 nm diameter) are not retained by UF. The driving pressure of UF system is low (50-500kPa). Pressure in MF system is a bit less than UF, however, they are more distinguished through pore sizes. Those of MF are

greater than 0.1μm while UF pore sizes are generally from 0.01-0.1 μm. The similarity in pressure requirements arises from the fact that many commercial UF membranes purposely have pores of almost same size as MF membranes so that they have high fluxes in order to be cost competitive. This arises because current drinking water standards do not include standards for viruses or other contaminants which could be removed by UF membranes, not by MF membranes. However, for some industrial application, such as whey processing and milk treatment, there is a clear need for UF membranes.

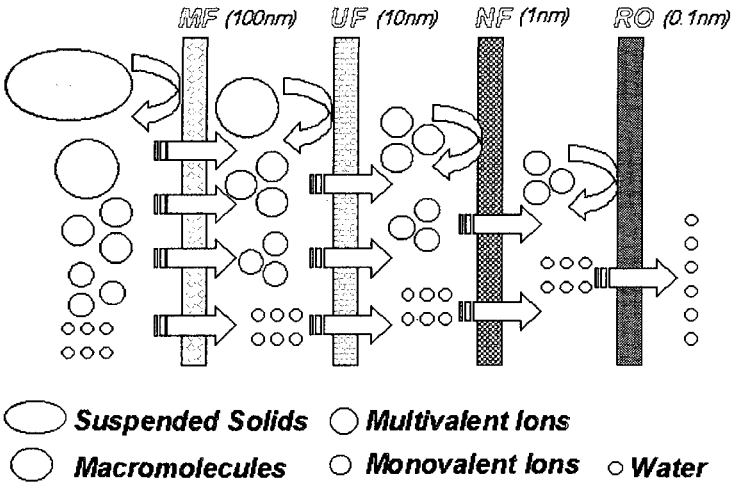

Figure 2.1. Ranges of separation (Kim and Elimelech, 2001)

There are three other types of membrane processes used particularly for gas separation: gas permeation (GP), gas diffusion (GD) and pervaporation (PV). In these processes, the driving force is activity difference across the membranes. On the other hand, dialysis (DIA) and electrodialysis (ED) are used to purify liquids based on concentration or electrical potential differences as the driving forces instead of transmembrane pressure differences.

Membranes can be also classified according to different criteria such as mechanism of separation (i.e., difference in sizes, solubility and diffusivity or charges), morphology (symmetric and anisotropic) - see Figure 2.2, geometry (flat and cylinder) and chemical nature (organic or inorganic materials).

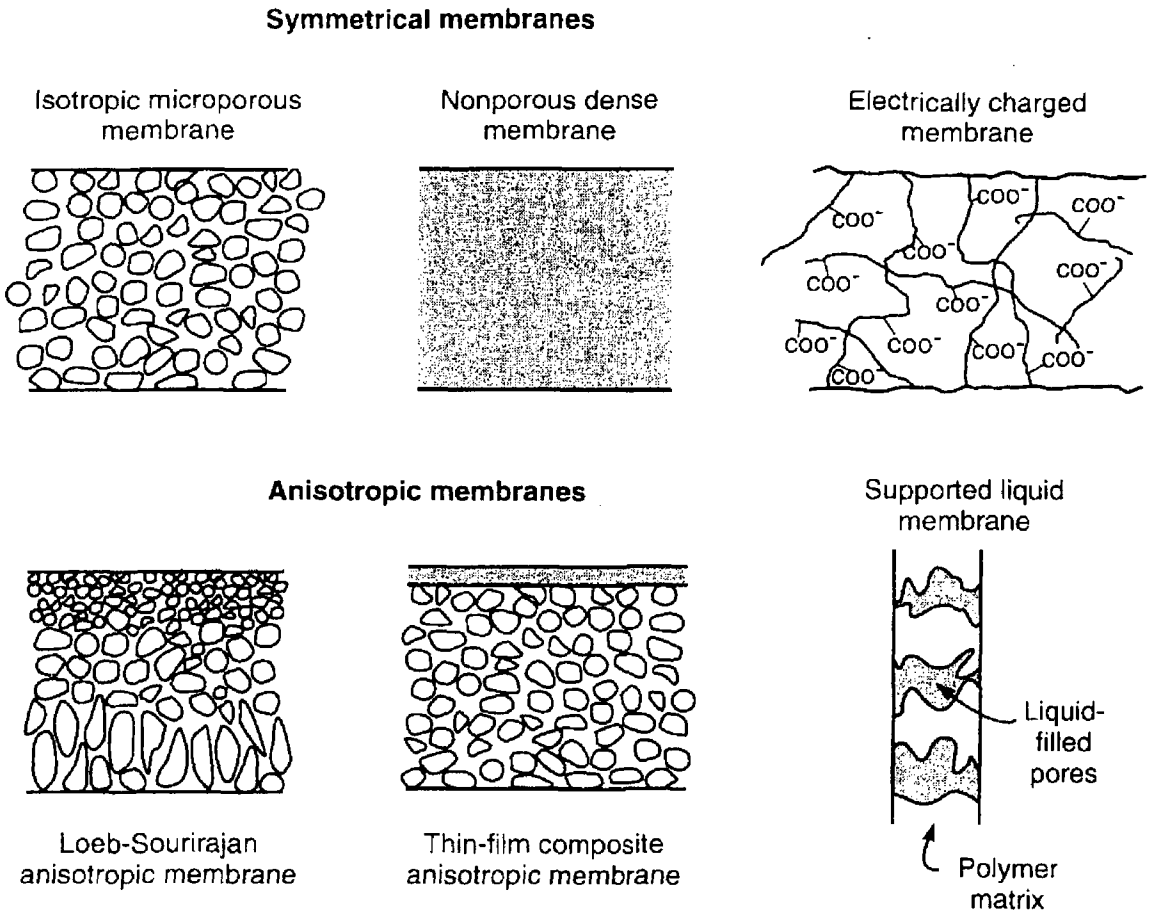

Figure 2.2. Schematic diagrams of the principal types of membranes (Baker, 2004)

This study will focus mainly on ultrafiltration for water treatment because of its increasing applications, and it is the current focus of our research group.

2.1.2 Preparation and materials

There are a number of techniques can be applied for preparation of membranes: sintering, solution casting, melt extruded film, stretching, track etching and template leaching for isotropic membranes; coating, interfacial polymerization and phase inversion for anisotropic membranes (Aptel and Buckley, 1996). Currently the most common type of RO and NF membranes are thin film composite membranes, however they can also be prepared with other techniques such as the phase inversion technique. MF and UF membranes are single layer membranes as opposed to composites. The preparation of composite membranes requires the preparation of the support layer and the creation of an upper separation layer by coating and or interfacial polymerization. Sintering, stretching

and track etching are only used in the preparation of MF membranes Phase inversion is a more common technique to make UF membranes. As stated above, UF membranes are our focus of this research, accordingly the following solely discusses the phase inversion technique and materials for UF membrane fabrication.

There are two basic types of the phase inversion technique: the wet process (developed by Loeb and Sourirajan, 1962) and the dry process (developed by Kesting, 1985). The difference is that in the wet process, the casting solution is fairly concentrated and the solvent is allowed to evaporate only partially, while in the dry process the casting solution is diluted and the solvent can evaporate completely. Baker (2004) summarized the simplest and most commonly used technique (i.e. the phase inversion in wet process) as follows: A polymer is dissolved in a two-component solvent mixture consisting of a volatile solvent, in which the polymer is readily soluble, and a less volatile non-solvent. The polymer solution is cast onto a glass plate. The film is left to stand for 10-100s to allow the volatile solvent evaporate, after which the film is immersed in a water bath to precipitate and form the membrane. This is also called polymer precipitation by water. The membrane can be possibly post-treated by annealing in a bath of hot water. In the case of polymer precipitation by solvent evaporation, the time required is longer since the casting film is not immersed in the water right after casting but the precipitation of the film continues until the membrane structure is completely formed. As the result, membranes formed by solvent evaporation are only modestly anisotropic and have larger pores (Baker, 2004).

One of the main problems of membrane making is membrane imperfection. Membranes could have holes and/or colonies of pinholes. These defects affect significantly the performance (e.g., solute rejection or fluxes) and also the membranes deteriorate faster. Several methods have been introduced in the literature to modify the traditional phase inversion technique. For instance, Pereira et al., (2001) investigated the simultaneous casting of two different polymer solutions to form the top and support layers of the membrane, respectively. Polyetherimide and polyethersulfone were used as base polymers. A polymer solution composed of Lewis acid and polyvinylpyrrolidone (PVP) to form the support layer. In order to form the top layer, different polymer solutions

composed of a volatile component tetrahydrofuran (THF) were used. They concluded that it was possible to promote adhesion of layers formed by different polymers resulting in a stable membrane film. Willem (2006) cast two or more polymer solutions (one after another, no waiting time) to produce membranes of multilayered structure. They claimed that the multilayer microporous membrane was free of a dense interfacial layer between layers. In addition, adjacent layers were inseparable and integral with one another, and were free of macrovoids. Preparing these membranes on non-woven fiber support allowed the formation of better controlled, higher integrity, multilayer microporous membranes with improved fluxes. Certainly, there are more ways to improve membrane performance and the selection of membrane preparation techniques depends on types of membranes and casting solutions.

The choice of materials required for porous membranes (e.g., UF membranes) are not only determined by the flux, rejection, reproducibility and recovery (after fouling) but also by their chemical and thermal properties (Mulder, 1996). Two main groups often mentioned in the literature are inorganic (metal, ceramics, glasses, etc.) and organic (polymeric). Inorganic membranes generally have superior mechanical, chemical and thermal stability relative to organic membranes; however, they are brittle, more expensive and not as compact. Thus, organic membranes are far more commonly used than inorganic membranes.

The selection of a base polymer for the organic membranes is not arbitrary, but rather based on very specific properties, originating from structural factors (Mulder, 1996). According to Zeman and Zydney (1996), to be successful in membrane manufacturing, the polymer must: (i) have suitable properties for the target application; (ii) be compatible with the selected membrane formation technology; (iii) be available and affordable and (iv) be a good membrane former. UF membranes are generally prepared from amorphous polymer which can generate, regulate and control the small pore sizes with relative ease (Anselme and Jacobs, 1996). In contrast, MF membranes are often made of crystalline polymers, which show high chemical resistance, thermal stability and compact less due to the hindrance of free rotation of polymer segments. Mulder (1996) discussed several classes of polymers that could be employed for the manufacture of MF and UF

membranes including: polycarbonates (PC), polyethylene derivatives, cellulose and its derivatives, polyamides (PA), and polysulfones (PS)/polyethersulfones (PES). Manufacturing techniques will be dictated by the types of membranes, e.g., UF membranes are generally prepared by the phase inversion technique as opposed to sintering or track-etching used for MF membranes.

Polycarbonates have excellent thermal and mechanical properties, thus, they are suitable for a track-etching technique. As a result, they are more appropriate for MF membranes (Mulder, 1996).

Polyethylene derivatives such as poly(vinylidene-fluoroethylene) (PVDF), polytetrafluoroethylene (PTFE), polypropylene (PP) are all hydrophobic and highly crystalline polymers. They exhibit good to excellent chemical and thermal stability. PVDF is resistant to most inorganic and organic acids and can be used in a wide pH range. It is resistant to oxidizing environments including ozone, which is used in water disinfection. Although PVDF is not as good as PTFE in term of these properties; it is preferable in use because of its high solubility in such solvents as dimethylformamide (DMF) and dimethylacetamide (DAMc) (Mulder, 1996).

Cellulose and its derivatives, e.g., cellulose acetate (CA) and cellulose nitrate (CN), on the other hand, are very hydrophilic and have a large degree of crystalinity. They are more attractive as membrane materials due to their low adsorption tendencies; hence, they are easier to clean after being fouled. Countering their outstanding membrane properties is that cellulose derivatives are very sensitive to thermal, chemical and biological degradation.

Polyamides also show good chemical, thermal and hydrolytic stabilities. While aromatic polyamides are mostly used in reverse osmosis, the aliphatic polyamides are commonly used in MF/UF. However, they have low compatibility with other polymers and solvents.

Polyetherimide (PEI) is an amorphous thermoplastic characterized by high heat resistance, high strength and excellent electrical properties that remain stable over a wide range of temperatures , It also has excellent processability. Moreover, PEI is a high

performance engineering thermoplastic. It has high strength and rigidity at elevated temperatures, long term heat resistance, dimensional stability and good electrical properties. Like other amorphous, high temperature resins, PEI has outstanding dimensional stability and is inherently flame retardant. PEI resists chemicals, such as hydrocarbons, alcohols and halogenated solvents (Nunes and Peinemann, 2001).

Polysulfones and polyethersulfones are very important polymers, which are not only used as basic materials for UF membranes but also as support materials for composite membranes (i.e., NF and RO). These polymers possess very good chemical stability and high glass transition temperature. PS polymers are more hydrophobic and more suitable when mechanical strength and thermal stability are prime requirements. The main limitation of PS, as well as PES, is the apparent low-pressure limit. As the result, PS and PES are strongly compacted at high pressures, resulting in flux decrease even with non-fouling solutions. PES is slightly more hydrophilic than PS and shows high compatibility with other polymers (Zeman and Zedney, 1996). Since the main chain of PES is relatively simple, it has a high capacity for modification. PES, therefore, is often selected as the host polymer in modified membranes. PES can withstand chlorine contact to 200 mg/l for short periods of time for cleaning or solutions with pH values between 1 to 13 and temperatures up to 75°C. In addition, PES is commercially available and relatively inexpensive. It is the most widely used polymers for manufacturing UF membranes (Hamza et al., 1997). However, one known disadvantage of PES is its high fouling potential due to the relatively hydrophobic characteristics.

2.2 Membrane characterization

Membrane characteristics are certainly very important factors in membrane process performance. Exploration of solute-membrane interactions to have a better perception of fouling phenomenon at membrane surfaces or improvements in surface modification techniques can not be made without an in-depth knowledge of the chemical and physical properties of membranes. Several techniques, such as contact angle measurement, electrokinetic measurement, solute transport test, bubble point test, atomic force

microscopy (AFM) and scanning electron microscopy (SEM), can be employed to determine surface membrane properties, as discussed next.

2.2.1 Hydrophilicity

Contact angle measurement is considered to be the simplest surface analysis technique. It is still the most convenient index of membrane hydrophilicity if measuring methods and times are kept consistent (Amy et al., 2001), the surface of solid is smooth, chemically homogenous and rigid (Chan, 1994) and water is used as a testing liquid. The lower the values of contact angles, the more hydrophilic membranes are. Advancing contact angles have been used commonly to assess the hydrophilicity since they reflect directly the degree of affinity to water of membrane surfaces. It characterizes the ability of a given liquid to spread on a surface caused by the active force exerted by the solid on the liquid. PES membranes have been proved rather hydrophobic with advancing contact angles of approximately 70 (Pham, 1995; Mosqueda-Jimenez, 2003; Nguyen, 2005). Adding hydrophobic surface molecules increased the contact angles remarkably e.g., more than 110 degrees (Pham, 1995; Ho et al., 2000). In contrast, incorporation of hydrophilic additives into PES membranes made them more hydrophilic with contact angles of about 50 degrees (Dang et al., 2006). Hydrophilic membranes, e.g. cellulose acetate membranes, have been proved to achieve more water production, less adsorption and easier cleaning (Zeman and Zydney, 1996). It appears hydrophilicity may have positive impacts on membrane fouling mitigation. The fouling mechanism may be revealed by checking contact angle before and after the membranes are fouled and cleaned. Nabe et al. (1997) found that the contact angles increased after being fouled with Bovine serum albumin (BSA) suggesting protein adsorption to the membrane surfaces. However, it was found that cleaning of various types of membranes fouled with river water either increased or decreased the contact angles and the contact angles of all membranes after cleaning became more uniform. This suggested the occurrence of NOM adsorption in which some foulants penetrated into and stayed in the membrane pores without being removed by NaOH cleaning (Dang et al., 2006).

2.2.2 Charge

One of the main causes of fouling is particle-particle and particle-membrane interactions. It has been shown that if membrane has the same type of charge as the particles/molecules in the solution, it is less apt to be fouled (Brink and Romijn, 1990; Gekas and Hallstrom, 1990; Meireles et al., 1991; Golander and Kiss, 1988). Charge of membranes can be measured in terms of Zeta potential, the electrical potential at the actual shear plane between the charged surface and the bulk solution. Measurement of membrane surface charge can be based on four phenomena (4 electrokinetic methods): (i) Electrophoresis, (ii) Electroosmosis, (iii) Sedimentation potential (Dorn effect) and (iv) Streaming potential (Letterman et al., 1999). Electrophoresis is effective for the study of powder dispersions so it only can be used after grinding the membrane, but the newly formed surface will likely differ considerably from the original surface. Electroosmosis is the transport of water through a capillary under the influence of a potential gradient. In this method, the charge is determined based on the slope of the flow rate versus applied current graph. Sedimentation potential is the potential difference caused by the sedimentation of particles in the field of gravity or in a centrifuge, between two identical electrodes at different levels. This method is not suitable for application in membrane technology. Streaming potential is found by applying a pressure (ΔP) across a porous medium and by measuring the resulting electrical potential (ΔE) with electrodes in the bulk electrolyte solutions on either side of the porous medium. Electroosmosis and streaming potential have been shown to be more relevant for membrane analysis (Fievet et al., 2000). Even so, electroosmosis yielded greater zeta potential values then those determined by streaming potential measurement for identical pH and ionic strength. This suggested the location of the shearing plane depends on the electrokinetic methods used (Fievet et al., 2000; Szymczyk et al., 1998). In addition, several other methods have been tried to characterize membrane-solution interface, i.e., membrane potential E_m (Fievet et al., 2000; Sbai et al., 2003); electrolyte conductivity measurement λ_{pore} (Szymczyk et al., 1999; Fievet et al., 2000; Sbai et al., 2003); electroviscous effect (Huisman et al., 1998; Fievet et al., 2003; Sbai et al., 2003) and by measurement of salt retention (Huisman et al., 2000; Martinez et al., 2002).

For UF membranes, the streaming potential reflects more the potentials of membrane pores than of the membrane surface (Childress and Elimelech, 1996). The charges to be considered in transfer analysis are those along the pore walls. Classical measurement methods have to be adapted to the specificity of porous membranes and particularly to ultrafiltration membranes as their average pore sizes (~10 nm) and their average fluxes are low. Pore streaming potential is induced when the electrolyte solution flows through the membrane whereas surface streaming potential (for RO and NF) is the induced potential when the electrolyte solution flows tangential to the membrane (Childress and Elimelech, 1996). Membranes can have positive or negative charges while NOM' charges are mostly negative. Thus, quantification of the charge of membranes helps decide if NOM-membrane electrostatic interactions are favorable (in the case of a positively charged membrane) or opposed/unfavorable (in the case of a negatively charged membrane). Shim et al. (2002) concluded the fouled membrane that had adsorbed with negative charge NOM exhibited a greater negative surface charge. After cleaning, the positive charges increased since some NOM was removed. The charges of PES membranes with hydrophilic and hydrophobic additives have not been explored yet and still a question.

2.2.3 Molecular weight cutoff

MWCO of the membrane (defined as the molecular weight that yields 90% solute separation) is generally determined by the solute transport method. This method measures the separation of several non-adsorbing solutes (polyethylene glycols, PEG, or dextran) of known molecular sizes to ascertain the sizes of membrane pores. The solute separation, f, in percent is computed based on the solute concentrations in the permeate and in the bulk of feed solutions assuming the effect of concentration polarization on separation is negligible (Singh et al., 1998). The plot of solute separation versus solute diameter (straight line on log-normal probability paper) gives the values of mean solute size and solute geometric standard deviation or mean pore size, geometric standard deviation and MWCO of the membranes. This approach ignores the dependence of solute separation on steric and hydrodynamic interactions between solute and pores (Singh et al., 1998). The MWCOs determined from the above method (i.e., based on actual

rejection-values using PEG or dextran) however were often lower than the data provided by the manufacturers (Kim et al., 1994; Cho et al., 2000) and different from the effective MWCOs (actual rejection size). One of the reasons is due to restricted diffusion of molecules with different sizes through membranes. Thus, it was expectedly that although 95% of NOM in Ottawa River water had molecular weights less than 30 kDa, only 70% of NOM rejection was achieved with the membranes whose MWCOs were about 50 kDal (Nguyen, 2005). The effects of electrostatic repulsion, hydrodynamic operating conditions and type (structure) of probe molecules might also contribute for this result (Cho et al., 2000). MWCO therefore is not truly a precise indicator for membrane evaluation of solute rejection. It, however, can relatively indicate the range of membrane pores and the solutes it will separate. For that reason, this characteristic is still used to determine the approximate pore sizes within newly-developed membranes.

2.2.4 Pore size, porosity, pore size distribution

Values of the average pore size, porosity and pore size distribution can be obtained by several techniques including solute transport, atomic force microscopy (AFM) and the bubble point method. The solute transport was described in detail in the section 2.2.3. The bubble point is a widely-recommended method for measuring pore sizes and testing the integrity of the membranes (Cheryan, 1986). This method, nevertheless, had a limited use since its key assumption of a zero contact angle is not achieved. The air usually passed through the largest pore on membrane surface first, thus this technique was really a measure of the largest pore size (Cheryan, 1986). The pore sizes also can be measured via AFM. They, however, were about 2-4 times higher than those by solute transport method (Khayet et al., 2002; Singh et al., 1998). The difference was explained by the characteristics of the two methods. The pore sizes obtained from a solute separation corresponded to a minimal size of the pore constriction experienced by the solute as passing through the pores, while pore sizes measured by AFM corresponded to the pore entrances which were of funnel shape and had maximum open at the entrance (Bessieres et al., 1996). Of the three methods, the solute transport seems to be the most reliable technique and followed by AFM.

Efficient membranes should have pores smaller than target solute molecules and high pore density (Alsari et al., 2001) so that they can remove more contaminants such as humic substances from water, and yet achieve high permeation fluxes.

2.2.5 Image of membranes- roughness

The study of the skin layer morphology of synthetic polymeric membranes can help to elucidate the separation mechanism, since the pore structure and especially surface images determine the intrinsic permeation properties. Scanning Electron Microscopy (SEM) is known to be a powerful tool for interpreting the relationship between membrane surface morphology and fouling phenomena. The principles of this method are detailed by Chan (1994). A key limit of SEM is that high-resolution SEM, which requires high-energy electrons, can cause structural and chemical changes at polymer surfaces. To minimize beam damages, membrane samples must be coated with a heavy metal, such as gold, platinum or palladium. Even so, the coating process itself may be destructive and obscure finer details. Consequently, the structure of an ultrafiltration or microfiltration membrane, as revealed by scanning electron microscopy, may not be identical to that which existed prior to its conversion into a specimen suitable for SEM examination. Despite this limit, SEM has still been used in a number of studies in membrane fields because of its simple and clear three-dimensional images of surfaces (Ulbricht and Belfort, 1996; Tang et al., 1996). In contrast to SEM, AFM can be performed on wet ultrafiltration membranes (Fritzsche et al., 1992) so it gives better and more reliable results. Upon using AFM, membrane roughness can be quantified through the measurement of the mean roughness, R_a, which represents the value of surface relative to the center plane for which the columns enclosed by the images above and below this plane are equal.

Surface roughness is usually related to many other parameters. Singh et al. (1998) found that roughness became higher when MWCO increased since high MWCO membranes had less tightly packed nodules/aggregates in the skin layer. The same trend was observed by many other researchers (Fritzsche et al., 1992; Bessieres et al., 1996). Hirose et al. (1996) found that an increase in surface roughness resulted in a higher water permeation flux and a decreased the tendency to foul since a rougher surface might create

more turbulent flow conditions adjacent to the membrane surface. However, it was not always the case. Several researchers concluded that the smooth membranes gave the higher initial and final fluxes (Nabe et al., 1997; Dang et al., 2006). Assuming no other factors are at play, membranes that have higher roughness should retain more foulants since it is easier for them to accumulate in the valleys within the rough membrane surfaces. It was shown by Nabe et al. (1997) that the average roughness of membranes reduced after adsorbing protein. They also observed that the cleaning index, used as a measure of performance, was worse for smooth membranes than that for much rougher ones.

2.3 Membrane fouling

Today's membranes have five to ten times the flux and better selectivity than membranes available 30 years ago (Baker, 2004). As the result of these improvements, the main factor determining system performance is membrane fouling.

2.3.1 Fouling mechanisms

As to reduce fouling phenomenon as well as decrease the cost for recovery of membrane performance, an understanding of fouling mechanisms is important. Mechanisms leading to membrane fouling were described in detail by many researchers (Hermia, 1982; Bowen et al., 1995; Anselme and Jacob, 1996). Basically, there are four different physical-based types of fouling: complete blocking of the pores (pore plugging), intermediate blocking (long term adsorption), cake filtration or boundary layer resistance and standard blocking or pore constriction (direct adsorption) (Figure 2.3). Complete blocking occurs when each particle arriving to the membrane blocks entirely one or more pores with no superposition of particles. Intermediate blocking takes place as each particle settles on other previously-arrived particles already blocking some pores or directly blocking some membrane areas. During cake filtration, each new foulant particle adheres to (or rests on) one or more previously arrived foulant particles that are already blocking some pores. However, in cake filtration there is no direct contact between the newly arrived foulant particles and the membrane surface. When each particle arriving to the membrane is deposited into the internal pore walls, leading to a decrease in the pore

volume, it is called standard blocking. Given these descriptions and that there will be an uneven distribution of different membrane pore sizes as well as solute molecular sizes, it is clear that all the above mechanisms may predominate at various times for a filtration cycle. For the first three mechanisms, the solute molecules are bigger than membrane pore sizes, thus fouling occurs outside of pore walls. For the standard blocking, however, the particles (solute molecules) deposit along the pore walls since they are smaller than membrane pores.

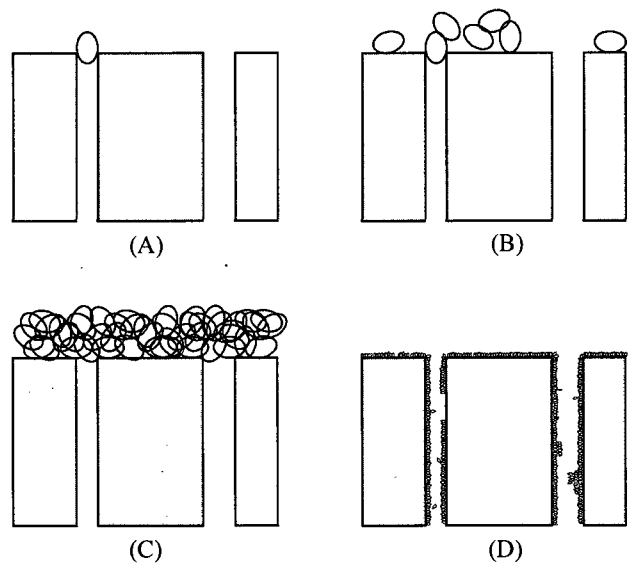

Figure 2.3. Four types of fouling mechanisms (A) complete blocking, (B) intermediate blocking, (C) cake filtration, (D) standard blocking. (Bowen et al., 1995)

Identification of the controlling fouling mechanism is often conducted via modelling the flux reduction using mathematical methods. Several models have been developed based on these four basic fouling mechanisms to calculate the flux reduction of each in terms of J_v/J_o, where J_o, J_v are the initial and final filtrate fluxes, respectively. Hermia (1982) reviewed and compared these different models for dead-end filtration as in Table 2.1.
These models assume that a single type of fouling controls the filtration behaviour. In reality, fouling on membranes is sometimes more complicated and can be caused by a combination of these mechanisms.

Table 2.1 Four different fouling-estimated models

Model	Constant	Equation
Complete blocking	$K_{block} = \frac{\alpha_{block} A J_o C_b}{N_o}$	$\frac{J_v}{J_o} = \exp(-K_{block} t)$
Intermediate blocking	$K_{inter} = \frac{\sigma_{inter} \Delta P}{\mu R_{inter} J_o}$	$\frac{J_v}{J_o} = (1 + K_{inter} t)^{-1}$
Cake filtration	$K_{cake} = \frac{2\alpha_{cake} J_o C_b}{R_m}$	$\frac{J_v}{J_o} = (1 + K_{cake} t)^{-1/2}$
Standard blocking (or pore constriction)	$K_{std} = \frac{\alpha_{pore} A J_o C_b}{\pi r_p^2 \delta_m}$	$\frac{J_v}{J_o} = (1 + K_{std} t)^{-2}$

J_V is filtrate flux, J_0 is initial filtrate flux through the clean membrane; K_{block} is constant in complete blocking model, α_{block} provides a measure of the pore blockage efficiency; K_{inter} is constant in intermediate blocking model, α_{inter} is blocked area per unit filtrate volume; K_{std} is constant in pore constriction model, α_{pore} is pore constriction efficiency; K_{cake} is constant in cake filtration model, α_{cake} is specific cake resistance;

Accordingly a number of dual mechanism models have been developed (Kilduff et al., 2002; Mosqueda-Jimenez et al., 2006). It may be composed of surface fouling and internal fouling (Figure 2.4).

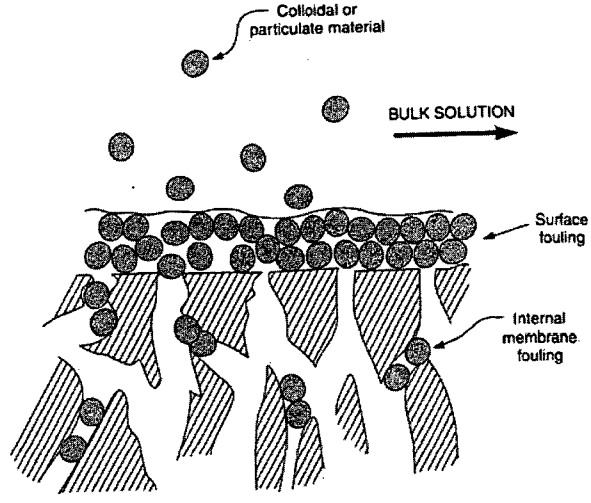

Figure 2.4. Schematic representation of fouling on membranes (Baker, 2004)

Surface fouling is the deposition of solid material on the membrane that consolidates over time. This fouling layer can be controlled by high turbulence, regular cleaning and using hydrophilic or charged membranes to minimize adhesion to the membrane surface. This is generally reversible. Internal fouling is caused by penetration of solid material into the membrane, which results in plugging of the pores. Internal fouling is generally irreversible (Baker, 2004).

2.3.2 Types of foulants

Almost every component in the feed stream can foul a membrane to some extent (Cheryan, 1986). They are so called foulants. Basically, there are two main types: inorganic foulants and organic foulants.

2.3.2.1 Inorganic foulants

A wide range of inorganic species can cause fouling including calcium sulphate, calcium carbonate, calcium phosphate, silica, metal oxides and hydroxides (particularly of iron and aluminum), colloidal sulphur, and other inorganic particulates (Zeman and Zedney, 1996). On one hand, they interact with the membrane directly and precipitate on/within the porous structure of the membrane. Dissolved metal precipitation, which leads to the formation of an iron oxide and manganese cake on the membrane, is the phenomenon that has been identified most frequently in operating treatment plants (Anselme and Jacobs, 1996). On the other hand, they contribute to the ionic strength of the solution, which in turns affects the conformation and dispersion of other organic foulants and leads to faster organic fouling (Cheryan, 1986). For instance, calcium salts can bind to negatively charged groups on the membrane by electrostatic effects, resulting in a "salt bridge" between the membranes and proteins, which will lead to faster flux reduction.

To control precipitation or flocculation, adjustment of the physical parameters, such as pH and temperature, is the best strategy since they relate to the salt solubility. As the temperature increases, the solubility of mineral salts often decreases, so it increases the chance of deposition. More favourable permeation rates can be achieved at high temperature with decreasing feed viscosity (Wiesner and Aptel, 1996). Nonetheless, the

only way to overcome the conformation and dispersion of other organic foulants is to add chemicals. Aluminium and iron coagulants are often added to surface water prior to hollow fibre MF or UF treatment to improve particle and organic rejection. Calcium-sequestering reagents, such as EDTA or citrates, were also added to the feed water prior to UF for the removal of whey proteins (Cheryan, 1986). Increase in pH in this case could result in greater fouling because the salts are more stable.

2.3.2.2 Organic foulants

NOM and proteins are the two types of organic foulants most cited recently in the literature. Protein is found to be a major foulant in ultrafiltration of food and biological systems (Cheryan, 1986). They tend to have high concentrations at the membrane surface as being rejected by the membrane and easily form a "gel" to hinder the permeating through the membrane. In protein fouling, it is very important to consider simultaneously the effects of pH, ionic strength and nature of salts because pH and ionic strength relate to changes in the protein packing density associated with electrostatic repulsive forces between charged proteins within the deposit (Zeman and Zedney, 1996).

In drinking water treatment, NOM however has been implicated as a mayor foulant (Hong and Elimelech, 1997). The presence of NOM in the water appears to reduce the sensitivity of permeate flux to pH while also reducing the permeate flux at all values of pH due to adsorptive fouling (Wiesner and Aptel, 1996). NOM is composed of both humic and non-humic substances corresponding to the hydrophobic and hydrophilic components. Humic substance accounts for a large part of the organic matter in water. They are amorphous, brown or black, hydrophilic, acidic, polydisperse substances of molecular weights ranging from hundreds to tens of thousands (Schnitzer and Khan, 1972). Based on their solubility in alkali and acid, the humic substance can be divided into three main fractions: (i) humic acids, which are soluble in pH>2; (ii) fulvic acids, which are soluble in all pH; and (iii) the humin fraction which is not soluble at all. It has been suggested that the three humic fractions are similar to each other in structure but they differ in molecular weight, ultimate analysis and functional group content. The non humic substances contain such fractions as hydrophilic acids, proteins, amino acids,

polysaccharide and carbohydrates. The polysaccharide fraction of NOM determined by pyrolysis-GC/MS or LC-OCD was proved by many researchers one of the principal foulants of UF membranes (Mallevialle et al., 1989; Kimura et al., 2004 and Kennedy et al., 2005a). In addition to their effect on membrane fouling, the NOM has been shown to play a key role in the cohesion of colloids deposited on membranes. Analysis of the organic foulants in natural waters and their relative concentration in the cake formation suggest that polyphenolic compounds, proteins and polysaccharides bind together colloids and may cement the cake to the membrane surface (Wiesner and Aptel, 1996).

The degree of NOM-membrane interactions can be affected by NOM properties (NOM concentration, humic/non-humic fraction, molecular weight distribution, charge), membrane properties (physical structure, surface/pore charge, hydrophobicity), ion competitions and operating conditions (Cho et al., 1999). Scientific research incorporates a number of chemical and physical methods for the characterization of NOM. Analyses of humic substances by chemical methods include ultimate analysis and functional groups (determining carboxyl groups, total hydroxyls, phenolic hydroxyls, alcoholic hydroxyls, carbonyls, methoxyls, etc. in humic substances). Physical characterization methods are less complex and consist of spectroscopic analysis, electrometric titrations, molecular weight measurements, viscosity, electron microscopic examination and thermal analysis.

2.3.3 Fouling control

As fouling significantly affects membrane performance and the cost of water treatment, fouling control has received a great deal of attentions in the past several decades. Some of the major fouling minimization tactics are pretreatment, operation conditions adjustment, cleaning and materials modification. Within the scope of this study and as a key point of this thesis, only the last two techniques will be discussed in details as separate sections.

2.4 Membrane cleaning

Regular cleaning is very much a part of the operation of a membrane plant. However, the kind of cleaning methods used, how frequently they are required and how they are related

to operating parameters should be assessed on a case-by case basis to ensure maximum recovery of membrane performance.

2.4.1. Apparatus for cleaning

There are possibly two main modes of operation used in cleaning experiments: cross-flow and dead end as the ones used in permeation tests. In the cross-flow geometry the feed flow is parallel to the membrane and perpendicular to the filtrate flow, resulting in three different streams: feed, permeate and retentate. Whereas dead-end devices only have a feed and permeate stream and the main flow direction is perpendicular to the membrane surface (Pellegrino, 2000).

By far, the most widely used lab apparatus to assess the cleaning of flat sheet membranes has been the dead-end cells, i.e., stirred batch UF cells from Amicon (Muñoz-Aguado et al., 1996; Tran-Ha et al., 1998; Kuzmenko et al., 2005). Crossflow cells have also been utilized in fouling and cleaning evaluations, especially the ones from Nitto Denko Corporation (Kimura et al., 2004; Shon et al., 2007) and the SEPA CF cell from GE Osmonics (Bodzek and Konieczny, 1998). The SEPA cell has been designated by the USEPA as the standard cell for evaluating the potential of membrane processes as part of the Information Collection Rule (ICR) (Mosqueda-Jimenez et al., 2003). Cleaning has also been performed by just soaking for a day the membrane coupons in glass vessels filled with chemical solutions (Arnal et al., 2008). Except for the last method, flat sheet membrane cleaning evaluations have been conducted using standard membrane filtration apparatus. Another cross-flow (CF) cell designed by Sourirajan and Matsuura (1985) has yet been tried for cleaning studies. This type of CF cell has been used extensively in our lab for permeation tests (Mosqueda-Jimenez et al., 2004cd; Rana et al., 2005; Dang et al., 2008). The cleaning performance would alter to some extent when different cells are utilized according to their different designs. So far there has been no direct comparison of the impact of the test cell type on the effectiveness of a given cleaning strategy. Accordingly there is not a bench-scale membrane system that is considered standard for membrane cleaning studies.

2.4.2. Cleaning protocols and chemicals

Cleaning or regeneration of membranes can be achieved by using physical, chemical, electrokinetic and ultrasonic methods. Physical methods include foam-ball swabbing of tubular membranes, hydrodynamic, backwashing, pure water flushing, air flushing, gas-liquid flushing, reverse flow, hot water treatment or a combination of these methods. Whereas, chemical methods mainly use various alkalis (sodium hydroxide, sodium hydrochlorite, sodium sulphite, aldehyde solution), acids (oxalic acid, citric acid, hydrochloric acid-citric acid-ammonium fluoride), surface-active agents (sodium percarbonate and potassium percarbonate), enzymes, detergents (perborate, complexing agents EDTA), disinfectants, etc. (Deqian, 1987). Electrokinetic methods are applied in some cases (wastewater treatment) in which high voltage (>100V) is pulsed in short interval or long duration. Combined physical and chemical methods have received more attention recently since they perform high quality cleanings. Anselme and Jacobs (1996) proposed potential cleaning methods for the following specific fouling mechanisms:

- For cake formation: hydraulic techniques such as flushing, backwashing
- For NOM adsorption: Chemical cleaning techniques are sometimes found difficult to break down completely the foulants. This type of fouling is slowly reversible because it requires desorption of the organic molecules.
- For materials precipitation: chemical cleaning and backwashing

Backwash has been found to be one of the most effective methods for controlling fouling in particular for hollow fiber (HF) membranes, while it has limited uses in only a few spiral wound membranes (i.e., membranes from TriSep Corporation). In general, a backwash pump is employed to reverse the permeate flow from the permeate side at an effective backwash pressure. Water pulsing or flushing on the other hand can be conducted from both sides. Depending on membrane types, module designs and other processing conditions, the flow direction will be selected. As a simple and non-corrosive method, backwashing or backflushing has been tried with many types of membranes and with various types of foulants. When using commercial membranes (KOCH Carbo-cor and ceramic membranes) for the treatment of wastewater composed of fresh water and seawater, Peng (2002) found that backflushing was more effective with Carbo-cor

membranes than for ceramic ones. With Carbo-cor membranes, cleaning with 1% NaOH together with air backflushing gave the highest flux recovery. Non-chemical cleaning methods, such as hot water flushing, air backflushing and pressured steam, were found effective in regenerating membrane flux for large pore Carbo-cor membranes. The duration of physical cleaning in HF is often from few seconds to 2 minutes after a filtration cycle of 30 min to 1 hour. The specific durations depend on types of feed water and the membrane modules.

In chemical cleaning, the choice of cleaning agents and cleaning conditions (pH, temperature and contact time) depended not only on the type of components deposited, but also on the chemical and thermal resistance of the membrane, the module and the rest of the equipment (Tragardh, 1989). Sometimes materials other than the membrane itself are the limiting factors. Cleaning agents are often circulated without pressure to prevent deeper penetration of the foulants into the membranes. Chemicals are often selected depending on specific foulants. Tragardh, (1989) concluded that if the problem was bacteria contamination, sodium hypochlorite (at maximum concentration of 200 ppm chlorine at normal temperature) or 5% hydrogen peroxide were recommended. Whereas if the problem was fouling layers of fat, oil or grease, non-ionic surfactants with anti-foaming properties (max. 1% water solution) were effective. Two percent (2%) solution of citric acid or a commercial cleaning solution of NOXOL 500 should be used for cleaning membranes fouled by divalent ions in waste feed or hard water. Other commercial cleaning agents such as NOXOL 735 or 771, on the other hand, worked well cleaning the precipitates of oxides, carbonates, phosphates or sulphates. The chemical and thermal resistance of membranes vary greatly depending on the primary polymer within the membrane. Polysulfone membranes are resistant to solutions with pH ranging from 1-13 and temperatures up to 80°C and quite resistant to oxidizing agents, such as hypochlorite. On the other hand, cellulose acetate membranes could be used only at temperatures up to 30-40°C and in the pH rang 3-8. Polyamides were strongly attacked by chlorine-containing cleaning agents. Generally, Tragardh (1989) recommended a cleaning cycle with following steps: (1) Product (foulants) removal from the system; (2) Rising with pure water; (3) Cleaning in one or more steps; (4) Rinsing with pure water; and (5) Disinfection.

Fouling by NOM adsorption is difficult to reverse or is slowly reversible because it requires desorption of the organic molecules. The use of oxidizing shocks (chlorine for instance) during membrane backwashing or chemical washing generally makes it possible to limit loss of membrane permeability. However, it has been shown that hydrophilic polymeric membranes are less sensitive to this type of cleaning than hydrophobic membranes since chemical bonds in the later are of higher energy and therefore are more difficult to break, even with chemical cleaning techniques (Mallevialle et al., 1989; Laine et al., 1989). Maartens et al. (1998) tried different cleaning methods with HF UF membranes in the removal of humics in natural brown water. The membranes were cleaned for different time intervals depending on the cleaning regime, at 100 kPa, 30°C. The alkaline cleaning solution combined with 0.1% Triton X100 (with NH_3) had a marked higher cleaning effect after the membrane was used for NOM removal (color rejection). The explanation for this was that the Triton X100 not only removed the foulants, but also adsorbed onto the membrane to cause a more open pores or create a more flexible membrane structure with a higher pure water permeation (PWP). Cleaning with strong chelating agents, such as EDTA, could most effectively remove the NOM fouling layer and restored permeate flux (Hong and Elimelech, 1997). This improvement was caused by disrupting the fouling layer structure through a ligand exchange reaction between EDTA and NOM-calcium complexes. Lee et al. (2001) reported that 0.1M NaCl solution was fairly effective in flux recovery in comparison to acid or alkaline reagent. However, Kimura et al. (2004) found that the foulants could not be desorbed significantly by NaCl solutions. They recognized that the oxidizing agent (NaClO) exhibited the best cleaning performance, then followed by NaOH and oxalic acid. The difference might be due to different sources of NOM and types of membranes. Table 2.2 summarizes several cleaning methods used in the literature for hollow fibre and flat sheet membranes.

Table 2.2 Cleaning methods used for UF hollow fibre and flat sheet membranes (cited from the literature)

Hollow fiber membranes

Membranes	Feed source	Cleaning method	Chemicals	Frequency/ Duration	Reference
Cellulose-accetate CA	Ibo River	BW+Chemicals	Sodium Hypochloride (3-5mg/l)	- BW : 20-70s/every 30 min	1, Labscale
Polysulfone PS	Cummberland River	BF + Chemicals	Acidic solution at 80oC	-Hourly BF -3 months/1 hour	2, Pilot-scale
PS	Wishkah River	Chemicals	Chlorine solution at 80oC	-No/1 hour	2, Pilot-scale
PS	Boise River	BF + Chemicals	Acidic+ chlorine solutions at 80oC	- Hourly BF - 01 month/1 hour	2, Pilot-scale
PS	Medina River	Chemicals	Acidic solution at 80oC	- twice per 1.5 month/1 hour	2, Pilot-scale
Polyethersulfone PES	Canal water	CP + BW		- CF: v=1.6m/s in 5s - BW: in 0.5 min	3, Lab-scale
PES	Canal water	PP + BW		-PP: 5 s/every 5min -BW: in 0.5 min	3, Lab-scale
Cellulose-triacetate CTA	Surface water	BW		- BW : every 45 min	4, Lab-scale
Polypropylene PP	Water from reservoir in Virginia	BW + chemicals	NaOH 1%	-BW: every 20 min - Chemical clean: every 300 hr	5, Lab-scale
CA	Water	Air sparging (air +BW)		Vair= 85ml/min	6, Lab-scale
Polypropylene	Hollywood reservoir	BW + air		-Compressed air @ 90psi -BW: 1-2.5min/every 30min	7, Pilot scale
Polyacrylo-nitrile PAN	Surface water	BW + chemicals			8, Pilot scale
	Drinking water	air-scrubbing		30 minutes	9, Pilot scale
PES/PVP	Delft canal	BW		30s after each filtration cycle of	10, Lab-

	water			30min	scale
PS	Reservoir	CF, BW, chemicals	(NaOH, NaOCl, citric acid)	Flush and BW: 10, 20, and 30 min; Chemical Soaking durations: 2, 4 and 6 h	11, Lab-scale

Flat sheet membranes

Polymers	**Source of water**	**Cleaning method**	**Chemical types**	**Duration**	**Reference**
PS	Chitose river	Sponge cleaning + chemicals	NaCl, HCl, EDTA, oxalic acid, NaOH, NaClO	Sponge cleaning for 60 min+chemical soaked for 24hr, room temp	12, Lab-scale
PS	Drinking water, fouled by whey protein solution	Flushing + chemicals	Cationic surfactant solution	Flushing (30min) + chemical clean (60min) 20°C	13, Lab-scale
PS	Irrigation pond.	Chemicals	NaHClO, NaOH, $CuSO_4$, citric acid, hydrogen peroxide	Soaked in chemicals for 12/24 hr at 25-40oC, concentration (0.5-10%)	14, Lab-scale
PES	Water fouled by BSA	Chemicals	HClO (hypochlorite)	Soaked in HClO	15, Lab-scale
Cellulose ether (CE-20) and PES-20	Water fouled by BSA	Chemicals	NaOCl, NaOH, H_2O_2, DI	Soaked in chemicals with different concentrations	16, Lab-scale
Sulfonated PS	Wastewater	Relaxation + Flushing		60 min filtration + 60' relaxation + 60' high v flushing	17, Lab-scale

References: [1](Nakatsuka et al., 1996); [2](Green and Tylla, 1998); [3](Kennedy et al., 1998); [4](Weber and Knauf, 1998); [5](Chellam et al., 1998); [6](Richter et al., 1999); [7](Karimi et al., 1999); [8](Takizawa et al., 2000); [9](Huang et al., 2000); [10](Kennedy et al., 2005b); [11](Liang et al, 2008); [12](Kimura et al., 2004, using Nitto Denko's CF cell); [13](Tran-Ha and Wiley, 1998, using stirred UF cell 100ml); [14](Arnal et al., 2008); [15](Arkhangelsky et al., 2007, using stirred UF cell 150ml); [16](Kuzmenko et al., 2005, using stirred UF cell 150ml); [17](Shon et al., 2005, using Nitto Denko's CF cell)

Abbreviations: BF: Backflushing; BW: Backwashing; CF: Crossflushing; PP: Pressure pulsing; Pb/Pf: backwashing pressure/filtration pressure

2.5 Membrane surface modification

2.5.1. General

Membrane modification is a fundamental approach since it centers on chemical development of a membrane materials so that membrane surfaces are less susceptible to fouling while the operational process is unchanged. Many surface modifying techniques have been researched including plasma surface modification technique (Ulbricht and Belfort, 1996), surface fluorination (Borisov et al., 1997), chemical coating (Dickson et al., 1998; Prakash et al., 2003; Chen and Tsai, 2004), chemical grafting (Wang et al., 2000; Zhao et al., 2005) or surface-active additives (Kasemura et al., 1993; Pham, 1995; Tang et al.,1996; Ho et al., 2000; Hamza et al., 1997; Mosqueda-Jimenez, 2003; Nguyen, 2005). Each method has its benefits and its disadvantages. The surface hydrophilicity of PS or PES membranes increased as treatment with water plasma and with He plasma, grafting with hydrophilic polymers such as 2 hydroxy-ethyl-methacrylate (HEMA) and acrylic or methacrylic acids or adding hydrophilic surface modifying macromolecules (LSMM 400, LSMM 600). These modifications in some cases enhanced permeability, decreased molecular-weigh cutoff of membranes and increased contaminant removal. Plasma and fluorination techniques, however, can not be easily controlled and may cause irreversible damage (Ulbricht and Belfort, 1996). Chemical coating and grafting require specific conditions which somewhat limit their use. Another disadvantage of many of these modification techniques is that they are complicated and require more than one step in the preparation process, usually making membranes then modifying their surface. Thus, an ideal technique should offer such characteristics as: (i) modification is limited to the surface without damaging it; b) the bulk properties of the polymer are kept relatively intact; c) only one step is required to obtain modified membranes. Blending the surface-active additive in the casting solution has presented almost all these characteristics and has been successfully used by Kasemura et al. (1993) as well as Matsuura, Santerre, Narbaitz and coworkers. Performance of surface-active additives and their impact on cleaning efficiency is the central focus of this thesis, thus they will be discussed more in detail in following section.

2.5.2. Surface Modifying Macromolecules (SMM and LSMM)

Surface modifying molecules (SMM), which are surface-active polymeric additives, have been manufactured and applied since the early 1990s (Kasemura et al., 1993; Hester and Mayes, 2002; Matsuura, Santerre, Narbaitz and coworkers). The characteristic of SMMs is that they are hydrophobic polymeric macromolecules and have a lower surface free energy than that of the base polymer; therefore, they have the ability to migrate preferentially toward a polymer-air interface (Fang, 1997).

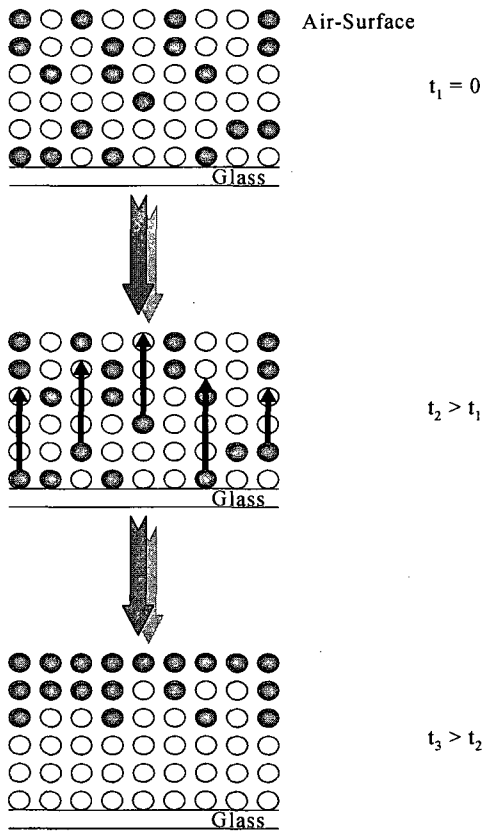

Figure 2.5. Migration of SMM to the membrane surface (Fang, 1997)

SMMs are blended with the casting solution containing the base polymer PES and a solvent (other additives may also be added); membrane is cast in air with the casting solution using wet or dry/wet phase inversion technique. During casting, SMMs preferably migrate to membrane surface and change the properties of membrane surfaces. Hence, a surface modified membrane is prepared using only a single casting step. The SMMs can be synthesized to be hydrophobic or hydrophilic polymeric additives. The

hydrophobicity of modified membranes depends on the SMM characteristics. Figure 2.5 illustrates the migration of the SMMs to the membrane surface with time. The dark circles represent SMM molecules while the open circles represent base polymer and solvent.

The SMMs were synthesized by a two-step solution polymerization method (Pham et al, 1999). The initial step involved the reaction of a diisocyanate with a polyol in a common solvent to form a urethane prepolymer solution. The reaction was then terminated by the addition of either hydrophobic or hydrophilic tails resulting in a polymer that would be precipitated. The precipitated polymer was then washed in 30 v/v % acetone-water mixture to leach out unreacted monomer before being dried in the oven at 50°C. Figure 2.6 presents a schematic of SMM synthesis and its hypothetical structure (Pham, 1995).

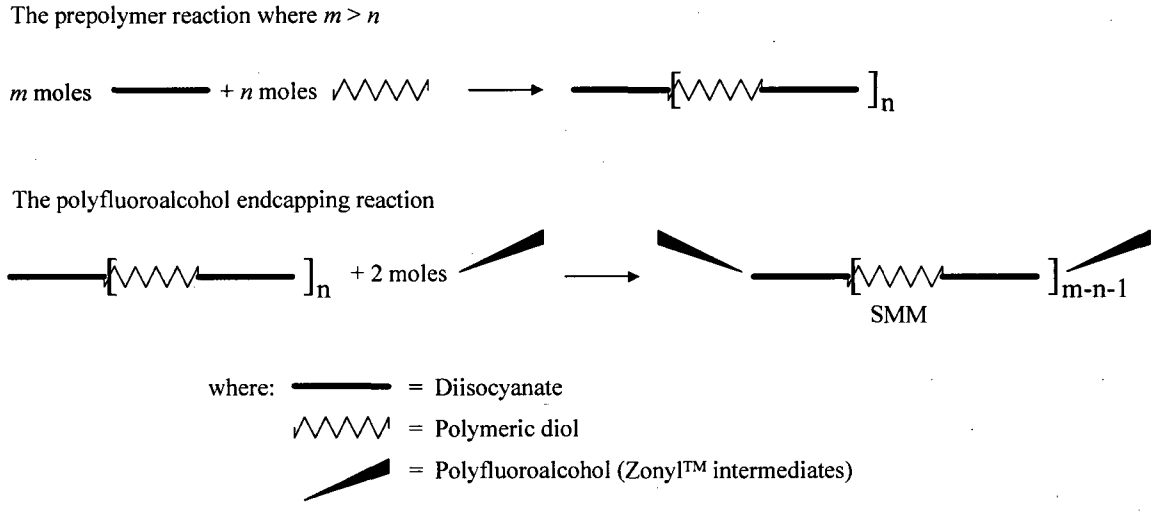

Figure 2.6. Scheme for SMM synthesis (Pham, 1995)

The main diisocynanates used for SMM preparation can be methylene bis-p- phenyl diisocyanate (MDI) (Pham ,1995; Ho et al. ,2000; Mandeep ,2001; Mosqueda-Jimenez, 2003) or hexamethylene diisocynate (HDI) (Tang et al., 1996). The polyols employed were polypropylene diol (PPO) (Pham, 1995; Ho et al., 2000; Mandeep, 2001; Mosqueda-Jimenez, 2003) or polytetramethylene oxide (PTMO) (Tang et al., 1996), polycaprolactone diol (PCL) (Ho et al., 2000), diethylene glycol (DEG) and hydroxyl diphenyl sulfone (DPS) (Mandeep, 2001; Mosqueda-Jimenez, 2003). The most commonly used solvent is N,N-dimethylacetamide (DMAC). Most of these main chains

were end-grouped with the low molecular weight fraction of an oligomeric fluoro-alcohol to create hydrophobic SMMs.

The SMM-PES membranes have been used in many fields including ultrafiltration, pervaporation and biomedical applications. The SMM additives did not enhance the fluxes or solute removal in ultrafiltration of surface water (Mosqueda-Jimenez, 2003) presumably because longer evaporation times were required for better membranes (i.e., greater SMM migration). The impact of SMMs to make a surface modified hydrophobic membrane was demonstrated by higher contact angles (Pham, 1995; Ho et al., 2000) and higher fluorine content (Tang et al., 1996; Pham et al., 1999), which indicated the migration of SMM to the membrane surface. The tensile strength and elongation tests showed that SMM modified membranes have stronger mechanical strength than unmodified membranes (Suk et al., 2002a). Recently Suk et al., (2006) synthesized a more hydrophobic SMM additive (referred to as nSMM) even under mild membrane preparation conditions (low evaporation temperature, 110°C and short evaporation time, 4 min) for membrane distillation. nSMM-blended membranes had the advancing contact angles up to 110°. It is of interest to assess if this new nSMM will help produce PES UF membranes that are suitable for NOM removal from surface water.

Hydrophilic membranes are generally considered to be less susceptible to fouling than hydrophobic membranes (Zeman and Zydney, 1996). Thus, effort on development of hydrophilic SMMs (referred to as LSMMs) has been started recently by Rana et al. (2005). The synthesis of LSMMs also followed the same two steps as that of SMMs. The difference was that in the second step, instead of using an oligomeric fluoro-alcohol, as in the previous hydrophobic SMM research, a hydrophilic oligomer, PEG, was used to end cap the main chain. The migration of hydrophobic SMM additives to the surface can be easily understood since the additive is more hydrophobic than the base polymer. In the case of hydrophilic SMMs, preferably migration to the surface can not be justified by the same approach because the additive is less hydrophobic than the base polymer. However, due to diffusion, acidic functional groups in PEG still have impact on membrane surfaces to a certain extent i.e., making the modified membranes more hydrophilic (Nguyen, 2005; Dang et al., 2006). Several different LSMMs were prepared using different molecular

weights of PEG. It should be noted that PEG with MW too high or too low made casting more difficult since the viscosity of casting solution were too high or too low, respectively. Of course, the performance of membranes depended also on other factors such as the percentage of base polymer, LSMM and solvent in the casting solution. The researchers therefore have tried to optimize the ratio so as to gain the best membrane performance. PVP addition as a pore forming additive was also evaluated (Nguyen, 2005; Nguyen et al., 2007). Summary of several LSMM membranes from the literature is cited in the Table 2.3.

Table 2.3 Summary of PES-LSMM membranes reported in the literature: casting compositions and effectiveness

Membrane code	Composition				Contact angles (°)	PWP ($l/m^2.h$)	TOC removal (%)
	PES (wt%)	LSMM (wt%)	NMP (wt%)	PVP (wt%)			
LSMM0 [1], 200	20	0	80	0	68.1±1.1	139±42.2	52
LSMM1.5 [1], 200	20	1.5	78.5	0	65.2±1.2	17±8.9	76
LSMM3 [1], 200	20	3	77	0	61.8±1.4	14±7.3	80
LSMM6 [1], 200	20	6	74	0	60.6±2.8	24.7±3.9	-
LSMM12 [1], 200	20	12	68	0	57.0±2.3	-	-
Control[2]	18	0	82	0	78.8± 2	143.8	73
LSMM4.5[2], 200	18	4.5	77.5	0	76.8±0.5	68.1	70.9
LSMM4.5P[2], 200	18	4.5	71.5	6	77.6±1	97.2	72.2
LSMM4.5[2], 400	18	4.5	77.5	0	72.5±1	135.7	66.9
LSMM4.5P[2], 400	18	4.5	71.5	6	73.0±1.3	145.0	66.3
LSMM4.5[2], 600	18	4.5	77.5	0	75.4±1	96.1	69.7
LSMM4.5P[2], 600	18	4.5	71.5	6	74.9±1	99.1	69.3
PES15-3[2], 200	15	3	82	0	77.5±1	-	-
PES18-3[2], 200	18	3	79	0	76.3±1	-	-
PES21-3[2], 200	21	3	76	0	76.0±1	-	-

Note: [1] Rana et al., 2005; [2] Nguyen, 2005
200, 400, 600 : MWs (Daltons) of PEG tail of the LSMM additive

Visual observations indicated that if the percent of LSMM in the solution was high (i.e. 6 or 12 wt%), the opacity of the casting solution increased (Rana et al., 2005) indicating

incomplete mixing of the base polymer, solvent and additive. In turn this increased the difficulty of casting the solution. However, within a range of LSMM concentrations LSMM yielded transparent casting solutions, and increasing the LSMM concentration slightly decreased the membrane average contact angles (or made membranes more hydrophilic). Considering that the contact angle of many of the PES-LSMM membranes in Table 2.3 have overlapping confidence intervals with those of the control membranes the name hydrophilic SMM or LSMM is not entirely appropriate. However, to maintain consistency with earlier papers involving this polymeric additive this dissertation used the same name for this additive. PES-LSMM membranes had higher flux, less flux reduction, less fouling and relatively high TOC removal (Rana et al., 2005; Nguyen et al., 2007).

Given some positive impacts of PES-LSMM membranes in ultrafiltration of surface water (our research focus) such as higher flux, less flux reduction, less fouling and relatively high TOC removal, it would be of interest to see if this type of experimental membrane can be competitive with the similar commercial UF membranes; or whether LSMM could improve the performance of LSMM membranes prepared with different base polymers other than PES. A study of SMM-blended PVDF membrane was tried by Khayet and Matsuura (2001) however it was for the separation of volatile organic compounds by pervaporation, not for the removal of NOM by UF membranes. Furthermore, as mentioned above, there has been a newly developed hydrophobic additive (called nSMM) that increased the contact angles tremendously even under mild casting condition. It is of interest to assess if this new nSMM will produce PES UF membranes that can be cleaned more effectively than PES-LSMM UF membranes after drinking water treatment applications. Likewise, a question about making defect-free membranes possible via modifying casting as discussed in section 2.1.2 is worth considering. Therefore, the following questions could be raised:

(1) Are these PES-LSMM membranes comparable with other commercial membranes?

(2) Are these LSMM additives compatible with other base polymers (e.g., PVDF, CA, PEI or PS) for ultrafiltration of surface water?

(3) Does the incorporation of nSMM produce good membranes for water treatment?

(4) Is there any way to fabricate defect-free membranes?

(5) Which additive, the nSMM or LSMM, is easier to clean? And to what extent does the performance of membranes enhance with the addition of modified additives upon cleaning?

(6) What kind of chemicals, cleaning protocols or cleaning apparatus is the best for cleaning these modified membranes?

(7) What bench-scale membrane filtration system is better for assessing the effectiveness of cleaning?

2.6 Hypothesis

These above concerns result in following **proposed hypothesis**:

- *The double-pass method, which is a modification from traditional casting technique, will produce more defect-free PES membranes since the second pass would cover defects such as any pinholes present.*
- *The more hydrophilic LSMM-PES membranes will be easier to clean than the hydrophobic SMM-PES membranes because of their smooth and water-liking surfaces.*
- *LSMM is a membrane additive that can also be used to improve membranes cast using different base polymer such as PVDF, PS, PEI and CA.*

Next chapter will describe in detail the materials and methods to resolve the above unknown issues.

CHAPTER 3

MATERIALS AND METHODS

This chapter describes the chemicals employed in this research and the techniques used in (a) feed water characterization; (b) membrane test protocol; (c) membrane modification and preparation; (d) membrane characterization and (e) membrane cleaning.

3.1 Methodology (Experimental Plan)

As stated in the Introduction chapter, the research was divided into three different stages. Figure 3.1 shows the flow diagram of the general methodology followed in this thesis.

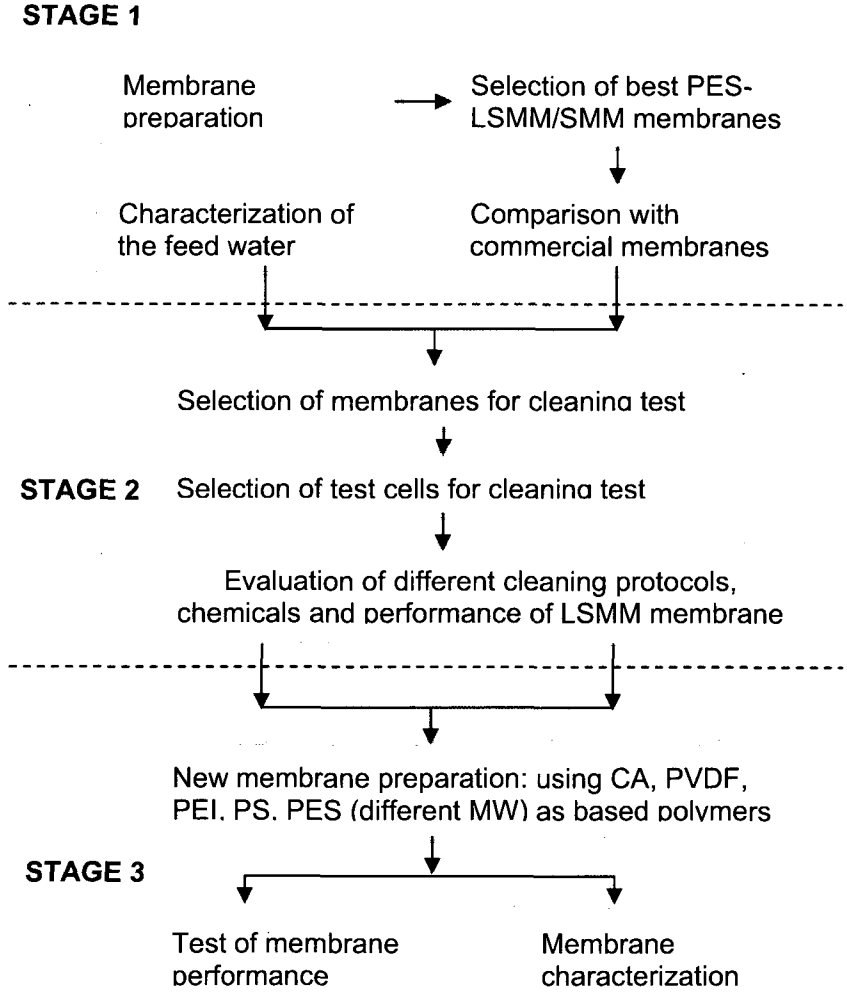

Figure 3.1. Methodology overview

Stage 1: Development of the best PES hydrophilic/hydrophobic membranes and comparison with similar commercial UF membranes

The goal of the first stage was to develop and optimize the manufacturing conditions to achieve the best hydrophobic and hydrophilic membranes possible by blending in tailor-made hydrophilic and hydrophobic additives. The variables were concentration of base polymer (PES), concentration of additives, thickness of membrane films, casting speed and casting technique. The best experimental membrane will be compared with the commercial UF membranes within the same range of molecular weight cut-off (MWCO). Parallel with the development of membranes, the feed water was also analyzed to assess the effect of water source (i.e., NOM) on fouling.

Stage 2: Regeneration of modified membranes upon cleaning

Improved amenability to cleaning is another potential benefit of surface modified membranes. In this stage, the assessment not only focused on the impact of membrane modification but also the selection of cleaning apparatus, cleaning chemicals and protocols. The most promising membranes from the first stage were used for cleaning test to assess the regeneration of modified membranes upon cleaning, in which the best cleaning procedures, best apparatus and best cleaning chemicals would be evaluated and disclosed. Results of this stage are presented in Chapter 7 and Appendix J.

Stage 3: Evaluation of the performance of LSMM-blended UF membranes with different base polymers

The hydrophilic LSMM has been proved to have positive impacts on the modification of PES based membranes and moreover it showed better impacts for surface water treatment than did hydrophobic SMM up to this point. Therefore, it is of interest to investigate the effect of LSMMs blending with various host polymers (other than PES) on the performance of UF membranes in the 3nd stage's test. Five polymers were selected as the base polymers to cover a wide range of hydrophilicity/phobicity spectrum: CA, PEI, PES, PS, and PVDF. The new PES polymer had MW of 18 kD, while the one in previous study had a MW of 31 kD.

In addition to the three stages of research, two other related concerns were investigated: (i) the effect of water source (i.e., NOM) storage on fouling and (ii) the study of membrane charge with and without the incorporation of surface additives LSMM.

3.2 Chemicals

The chemicals used for analysis in this project were of analytical grade while some of the chemicals for membrane preparation were of commercial grade unless stated otherwise. For membrane fabrication, base polymers, solvents and additives were the main three components. The base polymers (cellulose acetate, CA; polyetherimide, PEI; polyethersulfone, PES; polysulfone, PS; and polyvinylidene fluoride, PVDF) used in this research were cited in Table 3.1.

Table 3.1 Description of base polymers

Material descriptions	CAS number	Source
CA (Eastman 4650, Powder)	9004-35-7	Eastman Kodak Co., Rochester, NY
PEI (Ultem 1000, Natural Pellet)	61128-46-9	General Electric Co., Pittsfield, MA
PES (Victrex 4100P, Powder)	25667-42-9	ICI Advanced Materials, Billingham, Cleveland, England
PES (Ultrason E6020P, Porous Flake)	25608-63-3	BASF Aktiengesellschaft, Ludwigshafen, Germany
PS (Udel 3500, Pellet)	25135-51-7	Amoco Performance Products Inc., Atlanta, GA
PVDF (Kynar 740, Pellet)	24937-79-9	Elf Autochem Canada Inc., Oakville, ON, Canada

The 1-methyl-2-pyrrolidinone (NMP) (Sigma Aldrich, Milwaukee, WI) was used as a solvent. The hydrophilic additive, LSMM, was synthesized according to the method outlined by Rana et al. (2005). Details of LSMM synthesis are presented in Chapter 6. The hydrophobic additive, nSMM, was described in detail in Chapter 4 and it was synthesized following the procedure outlined by Suk et al., (2006).

Polyethylene glycol (PEG) and polyethylene oxide (PEO) (Aldrich Chemical, Milwaukee, WI) were used as probe solutes for the solute transport tests in MWCO determination. The molecular weight of the PEGs used were 1.5, 6, 10, 14, 20 and 35 kDal and for PEO the molecular weight was 100 kDal. Ethanol 99% (Fisher Scientific, Hampton, NH) was used to dry membranes.

The surface charges of membranes were calculated from the relationship of streaming potential at differential pressures. The background electrolyte for streaming potential determination was potassium chloride (KCl) (Sigma Aldrich, Milwaukee, WI). Potassium hydroxide (KOH) and hydrochloric acid (HCl) from Fisher Scientific, Hampton, NH were employed to adjust the pH.

For total organic carbon (TOC) analysis using an UV-persulfate based analzer, the following chemicals were used. The standards were prepared with potassium hydrogen phtalate (Fisher Chemicals, Fair Lawn, NJ). Sodium persulfate 95%, (VWR Canlab, Mississauga, ON) was used for organic carbon oxidation and phosphoric acid (Fisher Scientific, Hampton, NH) was used to acidify the samples, in order to convert carbonates to CO_2.

Supelite XAD8 (Supelco, Bellefonte, PA) and amberlite XAD4 (Sigma-Aldrich, Milwaukee, WI) were utilized as adsorption resins to isolate the hydrophobic, hydrophilic and transphilic fractions of NOM in the feed water i.e., Ottawa River water.

The following chemicals were used in the membrane cleaning tests: sodium hydroxide (NaOH) (EMD Chemicals Inc., Toronto, ON); citric acid (BDH Inc., Toronto, ON); sodium hypochlorite (NaOCl) and sodium tripolyphosphate ($Na_5P_3O_{10}$) (Fisher Scientific, Hampton, NH). These chemicals were recommended for cleaning by Hydranautics, a commercial manufacture and supplier of membranes.

Reagent-grade water was prepared with a Milli-Q Water System by Millipore (Bedford, MA) using mix bed ion exchange resins, synthetic activated carbon, organic scavengers and membranes. This ultrapure water is referred as MQ water. The supplier claims that the organic concentration of this water is less than 10 ppb.

3.3. Feed water characterization

NOM in Ottawa River Water (ORW) was characterized in detail to better understand the interactions between NOM and membranes. Beside some basic information such as total organic carbon (TOC), UV absorbance, hardness, color and molecular size fractionation, other variables including NOM fractions (hydrophobic acids, hydrophilic acids and transphilic acids) and size distribution were assessed in this study. Table 3.2 presents the detailed methods for each analysis. Details of these analytical methods are described in Appendix E.

Table 3.2 Method of analysis

Parameter	Method	Equipment
DOC	Standard method 5310C*	TOC analyzer
UV	Light absorbance at 254 nm	Beckman Spectrophotometer
pH	Standard method 4500-H^+ B*	Accumet pH memter 910
Conductivity	-	Oakton Conductivity Meter CON110
Color	Standard Method ASTM D1209*	Hach DR2800 Spectrophotometer
Turbidity	Standard method 2130B*	Hach 2100AN Turbidimeter
Alkalinity	Standard method 2320B*	Lab set-up
Total hardness	Standard method 2340C*	Lab set-up
Ca hardness	Standard method 2340B*	Lab set-up
MW distribution	Filtration of known-molecular-weight membranes	50-ml Amicon UF Stirred Cell
Isolation	Resin adsorption	XAD8/XAD4 columns
Size distribution	Static Light Scattering and Debye plot combination	Zetasizer Nano series

**Standard Methods, 1999*

The concentration of NOM was measured directly in terms of TOC using a UV-persulfate oxidation based TOC analyzer (Phoenix8000, Teledyne-Tekmar, Mason, OH). and UV absorbance at wave length of 254 ηm (UVA_{254}) was recorded by a spectrophotometer (DU-40, Beckman Coulter Inc., Fullerton, CA) using a 1-cm square

quartz cell. UV absorbance was used as TOC surrogate since they are linearly related. If TOC is an indicative of the mass material, UVA is an indicator of the NOM's aromatic characteristics. SUVA (l/mg.m) is also an indicator of the humic content (aromatic compound) of water and relates to UV absorption. It was calculated as the ratio of UVA_{254} and TOC. Waters with low SUVA values contain primarily non-humic organic matter. On the other hand, waters with high SUVA values (4-5 L/mg.m) generally are rich in humic substances (Mozia and Tomaszewska, 2004).

The apparent molecular weight distribution was determined by fractionation using ultrafiltration membranes and 50-ml Amicon UF Stirred Cell. In this method, the sample was sequentially filtered using UF membranes with decreasing MWCOs. The DOC concentration of a particular molecular weight fraction was calculated by subtracting the TOC concentration of the filtrate from one membrane from the TOC concentration of the filtrate from the membrane of the next larger nominal MWCO (Nilson and DiGiano, 1996). Regenerated cellulose membranes (Millipore, Bedford MA) with four different nominal molecular weight cut-offs: 5,000, 10,000, 30,000 and 300,000 daltons were employed. According to the manufacture, these membranes have a nonionic character, they are hydrophilic and exhibit a rejection efficiency of >98% for specific compounds above the nominal MWCO.

Organic fractions in the feed water (i.e., ORW) were isolated on the basic of hydrophobicity using nonionic macroporous sorbents (AmberliteXAD-8, AmberliteXAD-4, Sigma-Aldrich, Milwaukee, WI). The principle of this method is that as the water is passed through two columns containing AmberliteXAD-8 and AmberliteXAD-4 respectively, the hydrophobic fraction of NOM will be adsorbed by AmberliteXAD-8 and the transphilic fraction will be sorbed on AmberliteXAD-4. The hydrophilic fraction will be in the effluent. The hydrophobic fraction usually contains large MW NOM particles, the hydrophilic fraction-operationally defined as non-humic fraction composes of lower MW compounds (e.g., polysaccharides, amino acids, protein and etc.) and the transphilic fraction comprises particles with MW in between. The detailed procedure was described by Aiken et al. (1992) and Leenheer et al., (2000).

NOM particle size distribution was determined using Zetasizer Nano series equipment. This analysis employed the principle of Static Light Scattering (SLS) and Debye plot combination. SLS is a non-invasive technique used to characterize the molecules in solution. The particles in a sample is illuminated by a light source such as a laser, with the particles scattering the light in all directions, then the time-averaged intensity of scattered light is measured. Molecular weight of NOM is also able to assessed using this equipment. In order to analyze the molecular weight of particles in the solution, a calibration curve with Toluene solutions (different concentrations) should be set up. Since NOM is a very complex compound, the MW of NOM was not interested in this study but only size distribution of NOM. Refer to Appendix E for details of this analysis.

Given that the NOM water was often stored for a month or more for testing, a study of the effect of storage on NOM characteristics was conducted (Appendix A). The brief results were that upon storage, TOC, color and turbidity decreased; hydrophobic fraction (which composes of large MW particles) decreased while the fractions of hydrophilic with lower MW particles) and transphilic of NOM increased as a compensatory. It is likely due to either the settlement of particles under gravity or the break-down of NOM by some anaerobic bacteria. It would be recommended to keep water at 4°C with no acidification and mix the water before sampling to at least guarantee the TOC value of the water source. Ideally, mixing should be maintained continuously during the storage period.

3.4. Membrane preparation and characterization

3.4.1 Preparation of LSMM and nSMM additives

Basically, the synthesis of general surface additives involves in two steps: synthesizing a segmented block oligomeric prepolymer by reacting a diisocyanate with an oligomeric polyol, and then end-capping the prepolymer with a hydrophilic or hydrophobic oligomer to produce the hydrophilic or hydrophobic macromolecules. The specific diisocyanate and oligomeric polyol were chosen depending on the types of additives.

There were many types of LSMM which have been synthesized according to the method outlined by Rana et al. (2005). The chosen LSMM for this study (LSMM6) was

synthesized by end-capping the urethane prepolymer with PEG having average molecular weight of 600 Daltons. The urethane prepolymer was formed from the reaction of methylene bis-p-phenyl isocyanate (MDI) with poly(propylene glycol) (PPG) dissolved in N,N-dimethylacetamide (DMAc) solvent. Structures of nSMM and LSMM are shown in Figure 3.2. The values of the n and q were calculated from the average molecular weight of PPG and of PEG, which are 7.02 and 13.23, respectively. Based on the stoichiometry of the synthesis and the molecular weights, the repeat unit of m was calculated to be 30.57. Average molecular weights (weight average molecular weight, Mw, and number average molecular weight, Mn) and polydispersity index (PDI, Mw/Mn) were measured by gel permeation chromatography (GPC) (Waters Associates, Milford, MA). The polymer molecular weights were calculated using the universal calibration curve. The characteristics of the LSMM in this study was Mn = 1.28x104, Mw = 3.63 x104, PDI =2.83.

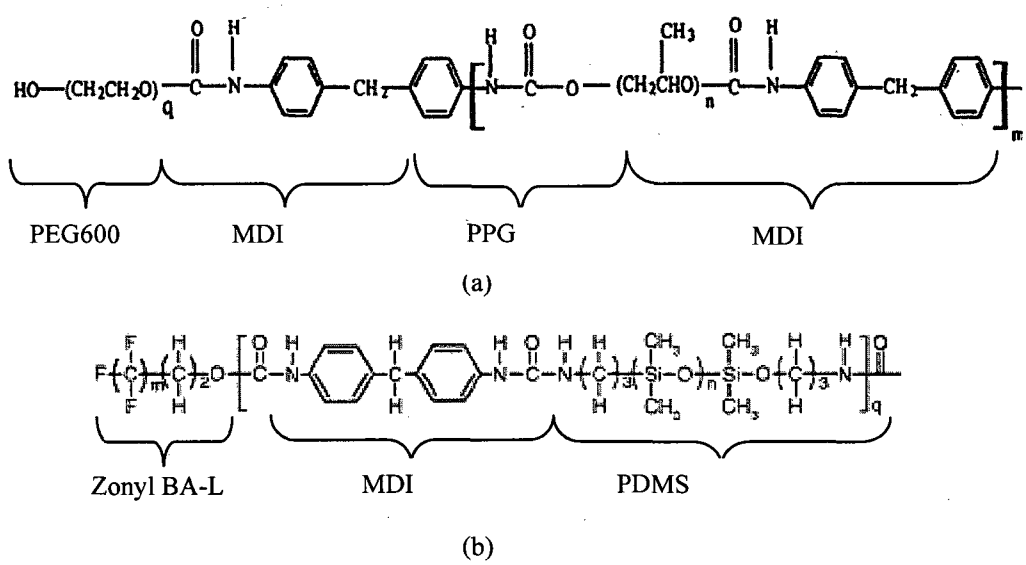

Figure 3.2. Chemical structures of (a) LSMM and (b) nSMM

For the preparation of nSMM, the MDI and polydimethylsiloxane (PDMS) were dissolved in tetrahydrofurane (THF) solvent to produce prepolymer, then end-capped with Zonyl BA-L. More information of nSMM can be referred to in Suk, et al (2006). This additive was claimed by the authors to enhance significantly PES membrane hydrophobicity. In the current study, the values of M_n and M_w of the nSMM were 12.8

and 27.1 kD, respectively. The glass transition temperature (T_g) of the nSMM was above 280 °C. The values of the n and m have been calculated as 9.81 and 22.58, respectively.

3.4.2 Membrane fabrication

All membranes were prepared using the phase inversion technique described by Matsuura (1994). This technique was particularly chosen because it can be used for a wide variety of polymers and it is simply effective. The membranes were modified by incorporating LSMM or nSMM into the casting solutions. Practically, the casting solution should contain: 0-6 wt% of additive; 10-25 wt% of the relatively hydrophobic base polymer like PES; 0-20 wt% of the hydrophilic pore forming polymer miscible with the base polymer (any one or a combination of PVP and PEG) and the rest was solvent (NMP) (Nguyen, 2005). In stage 1, the additive concentration chosen was 0.5, 1.5, 3.0 and 4.5 wt%; the base polymer PES was selected at 14, 16 and 18 wt%. No pore-forming polymer was used. The reason of not using higher percent of PES or not employing pore-forming polymers is explained in following section (section 3.4.3). NMP was used as opposed to DMAc because NMP is less toxic although DMAc is the most powerful solvent. The LSMM/nSMM additives and PES (MW of 31kD) powder were stored in a dessicator under vacuum. The bottle had a narrow mouth and a Teflon lined cap. The additive was first dissolved in a glass bottle of pre-determined NMP solvent by putting in an incubator orbital shaker (model G24, New Brunswick Scientific Co., Inc., Edison, NJ) for several hours. After the additive LSMM/nSMM was dissolved, PES was added and the bottle was capped and sealed with electric tape. The bottles were then spun again in the orbital shaker for several hours, usually overnight. It was crucial to dissolve the additives prior to PES since the additives could not be dissolved completely and quickly if added simultaneously with the PES. If the solution contained visible impurities probably originating from the additives or the polymer powder, it was filtered through 5.0 μm Teflon PTFE 47-mm disc (Cat # LSWP04700, Millipore, Bedford, MA) using a stainless steel pressure filter (XX4004700, Millipore, Bedford, MA) under nitrogen gas at 10 to 40 psig. After filtration, the solution was left in a desiccator to degas (remove air bubbles) until it was used. Each batch (bottle) of casting solution can make up to 10 sheets of membranes, each sheet is 11-cm wide by 15-cm long.

Samples of the casting solutions taken from the desiccator were characterized in terms of solution viscosity and surface tension. The solution viscosity was measured by rotational viscometer (LVT C2443, Brookfield Co., Middleboro, MA). The values were obtained by multiplying the dial reading number (corresponding to the torque required to rotate a spindle at a constant speed) by the spindle factor. Details of the calibration and measurement of solution viscosity are presented in Appendix P. The surface tensions of casting solutions were analyzed by using Pendant Drop software installed in VCA Optima goniometer (AST Products, Inc., Billerica, MA). This software employs pendant drop image analysis through video-image digitization and numerical curve-fitting using Laplace equation of capillarity. Surface tension data for some solutions is presented in Chapter 5.

Casting was conducted under the fume hood (8% humidity, 22±0.5 °C) to minimize the effect of humidity in membrane film nucleation. First, the polymeric solution was poured over a dust-free and smooth glass plate, and the membrane film was formed by dragging swiftly over the solution with a bronze casting bar. The gap between casting bar and glass plate was constant and corresponds to the nominal thickness of the membrane films. The gap varied from 200 μm to 280 μm. The wettability of glass plate was 66°. Second, the glass plate with the film was immersed into a 4°C coagulation bath (iced water). In this step, gelation, or the exchange of solvent (NMP) and nonsolvent (distilled water) occurred, resulting in the hardening of the membrane. The hardened membranes eventually peeled-off by themselves from the glass plate. They were stored in MQ water at 4°C until they were used. Between membrane castings, the glass plates were cleaned with a dilute solution of lab grade detergent (Contrex ©) and rinsed thoroughly with distilled water. It should be noted that the membranes, once became hardened, would be examined for defects (pinholes, wrinkles and impurities) by being placed on a light box. Membrane coupons were cut off from the membrane sheets in the areas free from defects. Even though extreme care was taken while making membranes, there was always a difference in performance among coupons cut off from different locations of the same sheet. The difference performance of those coupons is discussed in Appendix Q.

If the casting solution was well mixed, air free and dust free, the chances of having defects were small. However, if there were bubbles (air) in the solution, the defects

(pinholes) would be easily detected when a traditional casting method (using single spread) was employed. This thesis investigated a new casting technique that applied a double-pass casting to overcome these problems. Basically, the second casting motion (double pass) is hypothesized to cover the holes and/or valleys created during the nucleation of polymer-lean phase (de-mixing) after the first casting movement, resulting in smoother and hole-free membranes. Details of this new technique and its outcome are described in Chapter 5.

3.4.3 Selection of variable limits for membrane casting

As mentioned previously, the membrane casting variables studied were concentration of base polymer(s), concentration of additives, thickness of membrane films, casting speed, and casting technique. The selection of component concentration values was based on similar studies in the literature and followed the principle: 0-6 wt% of additive; 10-25 wt% of PES; 0-20 wt% of PVP or PEG and the rest of solvent (NMP).

According to the literature, in the range of 1.5 to 6 wt% of LSMM and constant 20 wt% of PES, contact angles became slightly decrease, had smaller mean pore sizes and higher solute (PEG) rejection (Rana et al., 2005). Nguyen (2005) found 18 wt% of PES, 4.5 wt% of LSMM and no PVP achieved the best flux and NOM removal. 18 wt% was also preferred mostly in recent researches especially with SMM-blended modification (Mosqueda-Jimenez et al., 2004cd, Zheng et al., 2006, Zhu et al., 2007). Basically the concentration should not be low to avoid making brittle membranes or high to produce very tight membranes. *Thus, in this research, 18 wt% of PES base polymer was chosen* since it was considered the "safe" number. The ratio PVP:PES of 1 to 3 was recommended in the membrane literature due to especially easy-to-cast factor (Mosqueda-Jimenez, 2003). They however disclosed that besides increasing the casting solution viscosity and facilitating membrane manufacturing, the addition of PVP did not have any favorable impacts to membrane characteristics and performance. Apparently a wider pore size distribution made them more susceptible to mechanical compaction. No improvement in fluxes and NOM removal. Fouling was severe for membranes with PVP (Nguyen et al., 2007). *Therefore, PVP was not added in the casting solution in this thesis.* The remaining variable in the casting solution was concentration of additives. The

detailed values for all variables to make both SMM and LSMM membranes are shown in Table 3.3.

Table 3.3 Variable setting

PES-nSMM membranes		**PES-LSMM membranes**	
Additive concentration	0.5; 1.5; 3.0; 4.5 (wt %)	*Additive concentration*	0.25; 0.5; 3.0; 4.5 (wt %)
Film thickness	200 versus 250 (μm)	*Film thickness*	200 versus 250 (μm)
Casting speed	5.5 cm/s (fast) versus 11 cm/s (slow)	*Casting speed*	1.5 cm/s (very fast)
Casting method	Double pass versus single pass	*Casting method*	Double pass versus single pass

Based on the discussion of the literature, the values of experimental variables (additive concentration, film thickness and casting method) are readily understood. The reason for the slower casting speed of PES-nSMM membranes is that their casting solutions were more viscous and harder to cast to obtain defect-free membranes. The casting speed values were chosen after several trials. It should be noted here that a slower casting speed often leads to tighter membranes, resulting in lower water permeation rates. For the PES-LSMM membranes, there were no quality problems with spreading the solutions at a fast speed, thus, only one casting speed was applied.

In conclusion, optimization of each component's contents requires dozens of membrane manufacturing and testing with replicates. Like while, this optimum ratio may work for a specific solute, not the others. The detailed results of membrane preparation and performance are presented in Chapter 4.

3.4.4 Membrane characterization

Representative membrane samples were characterized after they were dried. Three methods of drying membranes were tried in this study to compare the performance. The first method, called as chemical drying method or solvent exchange technique (Matsuura, 1994), used ethanol solution with different concentrations. The membranes were

sequentially submerged in four ethanol/water solutions (25, 50, 75 and 100% w/w ethanol) to remove the water from the membrane. The soaking in each of these solutions lasted at least 6 h. After the last immersion, each membrane sheet was placed between filter papers to dry at room temperature. The second method, called physical method, basically involved in drying membranes in an oven at 75°C for at least two days until the weight of dry membranes were unchanged. The third method, called natural drying method, was the simplest one in which the membranes were plainly placed between filter papers for 7 days. The results showed that there was no significantly difference among the three methods, thus the natural drying method was used prior to contact angle analysis. Details of the comparison are presented in Appendix I.

The membrane characteristics evaluated in this dissertation were contact angles, surface charge, water content, porosity, MWCO, roughness, surfaces and cross-sectional images.

Contact angles of the membranes were explored using a goniometer (VCA Optima Surface Analysis System, AST Products, Inc., Billerica, MA). The sessile drop method, which is based on the principle of the three-phase equilibrium that occurs at the solid/liquid/air interface, was used to determine the membrane surface contact angles. Dry membranes were cut into 5 x 25mm pieces and fixed onto 25 x 75 x 1mm superfrost micro slides (VWR, Mississauga, ON) using electrical tape. Advancing contact angles were determined as the critical angles at which the edge of contact between water drop and membrane expands. The water drop volume ranged from 2.5 to 3.0 μL. The reported contact angles are the average of ten measurements on three membrane samples. According to the manufacturer, the accuracy of this analyzer is ± 0.1 degrees. In addition to advancing contact angles, monitoring of contact angles with time also indicated the affinity to water of that membrane. These data were reported somewhere in Chapter 5 and in Appendix H. Monitoring the contact angles as a function of time has been used increasingly as a interchangeable with advancing (highest possible contact angles) or receding contact angles (lowest possible contact angles). Additionally, since there were two types of goniometers available in the lab, a diminutive study was done by an exchanged student from France (summer period) to compare the results obtained from the two equipments. The first goniometer (C860 701, Sherr Tumico, Germany) was an old style analyzer. The water drop images reflected on the round glass plate were observed

intuitively and contact angles were measured manually. The second one was VCA Optima goniometer (AST Products, Inc., Billerica, MA) which applies more recent technology. Water drop images were snapped by the inside digital camera and contact angles were automatically calculated by the Pendant drop software. The data obtained from the two goniometers were evaluated in detail in Appendix G. Except for the data in Chapter 6, all contact angle measurements reported in this thesis were generated by the more modern goniometer (i.e., VCA Optima).

The ***zeta potential*** of the membrane surface was determined using a modified version of the system described by Szymczyk et al. (1998). Zeta potentials were calculated from the streaming potential versus differential pressure graphs using the Helmholtz-Smoluchowski equation (Nystrom et al., 1994). Ag/AgCl electrodes were prepared with anodic deposition of chloride on silver from a 0.0001M HCl solution using a current density of about 0.2 mA/cm^2. The electrodes were stored in a 0.5M KCl solution overnight to prevent build-up of charge. All the streaming potential measurements were performed at room temperature (25±0.5°C), pH 7±0.1 and 0.001M KCl solution as the electrolyte. Details of this method and a manual for conducting these measurements can be referred to in Appendices E and F, respectively. Likewise, a preliminary study of membrane charges with and without additives was conducted to observe the effect of the charged SMM on membrane surface charges (See Appendix B). The study showed no significant change in membrane surface charge and there was considerable variability in the measurements, accordingly these results are presented as an appendix rather than within the body of the thesis.

Porosity, pore density and mean pore size were obtained through the solute transport method (Singh et al., 1998). It is essentially a continuation of the ultrafiltration test in which the feed is changed to solutions of different known molecular weight solutes for one-hour periods. The feed concentrations were 100 mg/L solutions of PEG with molecular weights of 1.5, 6, 10, 14, 20, 35 kDal and PEO with molecular weight of 100 kDal. The membrane system was flushed with ultra-pure water for one hour after each PEG/PEO solution circulation tests. At the end of the hour the PWP rate was re-measured to corroborate that the solute transport tests had not altered the flux (i.e., fouled the membrane). The feed and permeate samples were collected and analyzed for DOC

concentrations using a thermal oxidation-based DOC analyzer (Phoenix 9000, Teledyne-Tekmar, Mason, OH). The ***MWCO***, which is the molecular weight that would yield 90% solute separation, was determined based on the solute transport data. These data were assessed using log-normal probability function model to describe the membrane sieving curves and the Hagen-Poiseuille equation for surface porosity (Singh et al., 1998). All mathematical equations and sample determinations are presented in Appendix M.

The ***surface roughness*** was determined using a Nanoscope III atomic force microscope (AFM) equipped with a 1533D scanner (Digital Instruments, Gainesville, FL). Pieces of dried flat-sheet membranes were cut and fixed over magnetic disks with two-sided adhesive tape. The laser beam of the AFM was focused on a pre-selected spot of the surface prior to the engagement of the cantilever (Khayet et al., 2002). A tapping mode AFM in air was used to generate the AFM images. The roughness was obtained in terms of the root mean square of the average height of the membrane surface peaks. Results of AFM are shown in Appendix N.

A model JSM-6400 JEOL (Japan Electron Optics Limited, Japan) SEM was employed to capture the *images of cross-sectional area* of the dry membranes (see Appendix O for details). Prior to SEM observation, samples were submerged in liquid nitrogen, torn using tweezers and mounted in chair-shaped sample holders for the SEM with double-sided tape; then, they were coated under vacuum with a thin layer (60% gold and 40% palladium) in a Hummer VII sputting system (Anatech, Springfield, VA).

Water content defined by equation [1] was determined by gravimetric analysis.

$$W_{\%} = \frac{W_{wet} - W_{dry}}{W_{wet}} x100 \qquad [3.1]$$

Where, W_{wet} and W_{dry} are mass (g) of the wet and dry membranes, respectively. The wet membranes were cut into 5.5cm x 3.5cm pieces and placed into an aluminum tray. Usually three same-dimension pieces of a membrane were put on a tray. The wet membranes with trays were put into an oven (75°C) for two days (Sivakumar et al., 2006). The membrane samples were weighed before (W_{wet}) and after drying (W_{dry}) using

an analytical balance. Three measurements were conducted for each membrane type and the average values were reported.

3.5. Membrane testing

3.5.1 System set-up and testing protocol

The ultrafiltration flat sheet membranes were evaluated by a bench-scale set-up frequently used at our labs and other Canadian labs (Fig 3.3).

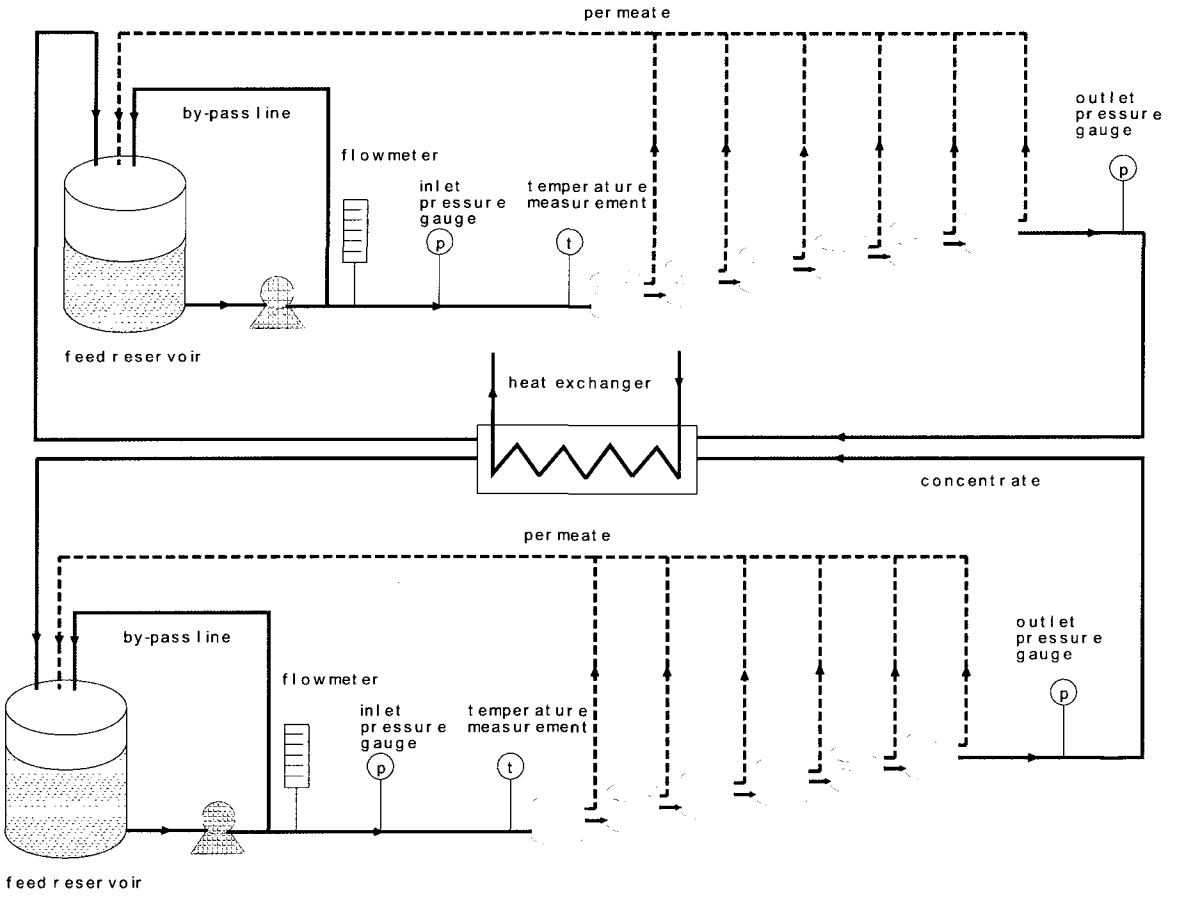

Figure 3.3. Experimental setup for Flat sheet membranes' test

The experimental set-up comprised two systems of six small cross-flow (CF) cells in series. Each cell was used to test one 52 mm diameter flat sheet membrane coupon. The CF cell (Figure 3.4) was made of 316 stainless steel and based on the design described by Sourirajan and Matsuura (1985). The cell had a relatively large cross-sectional area for fluid flow at the entrance and the exit, thus the pressure drop across the cell is less than 7

kPa gauge (1 psig) per cell. The cell also had a thinner channel flow design above the membrane surface, which allowed a relatively high fluid velocity parallel to the membrane surface. It should be noted when placing the membrane coupon on the cell, membrane surfaces (shiny and smooth face for LSMM membranes, rough face for SMM membranes and smooth face for commercial membranes) should face downward. Failure to do so leads to the NOM deposition on the wrong side (permeate side) which confused the data interpretation of membrane performance (i.e., NOM removal).

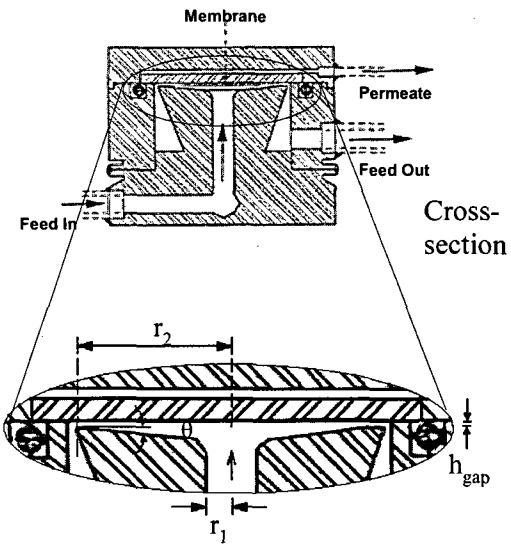

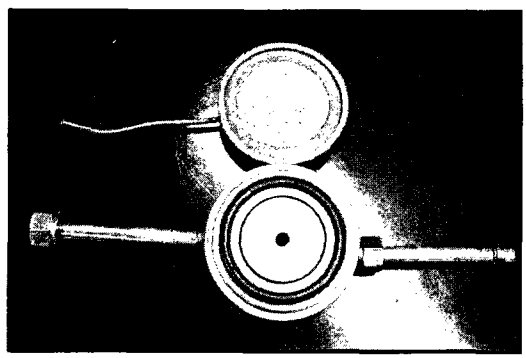

Upper and lower parts of CF cell

Figure 3.4. CF cell

During the filtration tests, feed water from 10-L low density polyethylene carboy (Nalgene, Rochester, NY) was pumped by a diaphragm Hydracell pump (Model M-03, Wanner Engineering Inc., Minneapolis, MN). A bypass line was installed to decrease the flow delivered to the cells. The flow of the feed stream was measured by a flowmeter (P-32025-20, Gilmont Instruments, Barrington, IL), and the inlet pressure was measured by a pressure gauge (MG-68027-06, Cole-Parmer, Vernon Hills, IL). The concentrate stream was passed through a concentric tube heat exchanger where a 13 L heated/refrigerated circulator unit (Model 1150A, VWR, West Chester, PA) maintained the concentrate at room temperature prior to recirculation to the feed reservoir. The permeate stream was also continuously recycled to the feed reservoir, except when samples were collected for TOC analysis. After the permeate flux was measured by weighing, it was returned to the feed tank At the beginning of the test permeate flux was measured every 10 or 15 minutes, then after 30 minutes, and as the time went on, the measurement were taken less

frequently. All tubing was clear PVC (Nalgene); valves, and flowmeter are made of 316 stainless steel.

The feed flowrate of 1.1 Lpm was selected to have a laminar flow inside the cells and it allowed the pressure drop within the system (six cells) of less than 14 kPa (2 psig) from the first to the last cell (Mosqueda-Jimenez et a., 2004a). The pressure used was recommended by the previous studies for its reasonable value within the UF operating range, not to high to reduce costs and no to low to insure the reasonable fluxes. The filtration test protocol was that described by Nguyen et al., (2007). Membranes were pre-compacted by filtering MQ water for one hour at 552 kPa (80 psig) and room temperature. The purpose of pre-compaction was to minimize flux reduction due to membrane compaction in subsequent tests while avoiding a significant impact on membranes pore structure. This was followed by 50 hours of pure water permeation (PWP) monitoring, i.e., MQ water filtration at 345 kPa (50 psig) and room temperature. A solute transport test was usually followed for pore characterization and then the test procedure was completed with a 144 hour long fouling test using Ottawa River water (same feed flow rate and pressure). The duration of the PWP run was chosen as 50 hours since it took that long to reach a steady state in terms of permeate flux. Additionally, a study of the impact of transmembrane pressures on the fluxes of experimental membranes was conducted in parallel (see Appendix D) to further understand this aspect. The flux and DOC removal were affected remarkably when different transmembrane pressures were tried. A study on post treatment (chemical treatment after membrane manufacture) was also done to improve the flux especially for hydrophobic membranes, whose fluxes were quite low during preliminary tests (Appendix C). It was found that the post-treatment had improved the flux to some extent.

Fluxes and DOC were monitored at defined intervals. The fluxes were recorded by checking the mass or volume of water collected over a given time. A comparison was made between measuring the mass versus volume collected and the methods were found interchangeable (Garand-Sheridan, 2008), however the mass based method was applied for membranes with low permeability where volumetric measurements were virtually impossible. At the end of each experiment, the actual permeation (fouled with brown NOM) area was checked, using a Manostat caliper by IQ Instruments (Switzerland). The

whole system was thoroughly cleaned by 1-hour flow-through with distilled water. To guarantee contaminant- free condition before the next test, cells were taken apart to clean one by one with soap and MQ water. Performance of membranes was determined with following indices.

3.5.2 Membrane performance parameters

Even though the most important performance parameters in membrane evaluation often are permeate flux and solute rejection, some of the following parameters were alternatively used to elucidate the membrane performance in this study.

(a) *Pure water permeation flux* (PWP – $L/m^2/h$): monitored the steady state pure water permeate flux through pristine membranes.

From the general equation of flux determination:

$$J = \frac{Q}{A} \qquad [3.2]$$

Where J: Measured flux ($L/m^2/h$)

Q: Water flowrate determined after 50 hours (L/h or mL/min)

A: Membrane area (m^2)

(b) *Specific flux*, $J_{sp,T}$ ($L/m^2/h$):

To account for temperature effect, the flux may be expressed as specific flux, J_{sp}, at a specific temperature, typically 20°C:

$$J_{sp,20^\circ C} = J_T \left(\frac{\mu_T}{\mu_{Sp,20^\circ C}} \right) \qquad [3.3]$$

Where $J_{sp,20^\circ C}$: Specific flux at 20°C ($L/m^2/h$)

J_T: Measured flux ($L/m^2/h$) at the operating temperature T (°C)

μ_T and $\mu_{sp,20^\circ C}$: Permeate viscosities at temperatures T and 20°C, respectively ($N.s/m^2$)

(c) *Normalized standard flux*, *NSF* ($L/m^2/h/bar$): This term accounts for the pressure effect.

$$NSF = \frac{J}{\Delta P} \quad [3.4]$$

Where NSF: Normalized standard flux ($L/m^2/h/bar$)

ΔP: Transmembrane pressure (N/m^2)

(d) *Long-term flux reduction* $(\%) = \frac{J_{wi} - J_{wf}}{J_{wi}} x100$ [3.5]

Where J_{wi}, J_{wf}: Initial flux and final flux of the fouling test period (with surface water as feed water) ($L/m^2/h$).

(e) *Normalized flux reduction* $= \frac{J_{wi} - J_{wf}}{J_{wi}.\Delta P} x100$, accounting for the pressure effect on the flux reduction. [3.6]

(f) *Membrane hydraulic resistance*, R_m.

This index refers to the resistance of membranes with pure water only.

$$R_m = \frac{\Delta P}{\mu . J_{wo}} \quad [3.7]$$

μ: Viscosity of water at temperature T ($N.s/m^2$)

J_{wo}: Initial flux with pure MQ water ($L/m^2/h$)

(g) *NOM removal* $= \frac{C_b - C_p}{C_b} x100\%$ [3.8]

presents the capacity of retaining solutes (NOM) of membranes.

Where C_b, C_p: Concentration of NOM in the feed and permeate at the end of the fouling test (mg/L)

(h) *NOM deposition* (on membrane surface) $(g/m^2) = \frac{W_{S+NOM} - W_{blank} - W_{beaker}}{A_m}$ [3.9]

$W_{(S+NOM)}$: Weight of the beaker containing 25ml solution (NaOH) and NOM after being dry in the oven at 105°C until the weight is consistent (g)

W_{blank}: Weight of the beaker containing 25ml solution (NaOH) only after being dry in the oven at 105°C until the weight is consistent (g)

W_{beaker}: Weight of clean beaker (g)

A_m (m^2): Fouled area of the membrane

This index is to quantify the NOM mass on membrane surface upon being fouled. The NOM-fouled membranes were immersed in 25 mL of 0.1 M NaOH within pre-weighed beakers. After the NOM was completely removed from the membrane coupons, all the coupons were removed from the beakers. The beakers were placed in an air-circulating oven at 105°C for 24 h to evaporate the water and then reweighed. The mass of NOM calculated by the difference between the dry weight of the beakers containers containing NOM and NaOH and that of the controls (containing just NaOH-W_{blank}) (Hong and Elimelech, 1997).

(i) *Flux changes due to surface modification* (%)= $\frac{J_{modified} - J_{control}}{J_{control}} x100$ [3.10]

This index refers to the flux improvement when the membranes are modified with additives.

$J_{modified}$: Flux of the membranes blended with LSMM/nSMM ($L/m^2/h$)

$J_{control}$: Flux of the control membranes (without LSMM/nSMM) ($L/m^2/h$)

(j) *Net Water production* = $P_{water} = \int_{t_0}^{t_f} J(t)dt$ [3.11]

Whereas P_{water}: Net water product (l/m^2)

J(t): flux as a function of time ($L/m^2/h$)

t_0: initial time of the fouling experiment (h)

t_f: time at the end of fouling test (h)

This indicates how much water this membrane can produce, one of evaluating indicators for membrane selection.

(k) *Degree of compaction* = regressed slope of water flux-time plot within the first 5 min of PWP test, after the precompaction period. This index quantifies the degree of compaction caused by the operating pressures. Discussion of this index was presented in Appendix R.

(l) *Flux recovery* FR: $FR = \frac{J_{wc}}{J_{wo}} x100\%$ [3.12]

Where J_{wc}: Pure water flux after cleaning test ($L/m^2/h$)

J_{wo}: Initial flux with pure MQ water ($L/m^2/h$)

This parameter is used importantly to assess the cleaning efficiency by comparing the pure water permeate flux before and after cleaning tests.

(m) *Solute resistance removal* $RR = \frac{R_{sw} - R_{sc}}{R_{sw}} x100\%$ [3.13]

Where $R_{sw} = \frac{\Delta P}{\mu . J_{wf}} - R_m$: Residual solute resistance of the fouled membranes [3.14]

$R_{sc} = \frac{\Delta P}{\mu . J_{wc}} - R_m$: Residual solute resistance of the cleaned membranes [3.15]

$R_m = \frac{\Delta P}{\mu . J_{wo}}$: Hydraulic membrane resistance

J_{wf}: flux at the end of fouling test period ($L/m^2/h$)

The last parameter specifies the capacity of removal of membrane resistance due to solute attachment on membrane surface.

The correlation between these above parameters in some cases helped provide an understanding of membrane performance as well.

3.6 Statistical analysis and modeling

3.6.1 Analysis of Variance (ANOVA) test

To test if the effect of the variables involved in the membrane casting (concentration of additive, thickness, SMM type, casting method, etc) was statistically significant, the ANOVA test was conducted using Minitab 15 statistical software (Minitab Inc. State College PA). The null hypothesis (H_0), in which the effect of any particular independent

variable on each of the response variables does not exist, was rejected if P-value ≤ 0.05 ($\alpha = 0.05$ or 5%). Therefore, for the P-values to be statistically significant they should be ≤ 0.05. Several types of ANOVA tests were used including one-way ANOVA, two-way ANOVA, General Linear Model and Balanced ANOVA-Mixed model. The chosen model was based on the complexity of the analyzed data set. The results of these statistical analyses are presented in Appendix L.

3.6.2. Modeling

In analysis, an empirical model of the system can often be built as a hypothesis of how the system could work or try to predict how an unforeseeable factor could affect the system. Two types of empirical modeling were used in this research to describe the fouling phenomenon occurring on membrane surface: Fouling Resistance Modeling and Fouling Mechanism Modeling.

According to the first modeling approach, fouling can be quantified by the resistance appearing due to formation of cake or gel layer on membrane surface during the filtration and the resistance removal can be determined via cleaning (Madaeni et al., 2001, Munoz-Aguado et al., 1996). The total resistance (m^{-1}) often includes the effects of membrane itself, solute adsorption, gel formation, cake formation, etc. The second modeling approach is to study the mechanisms leading to membrane fouling. The common practice consists of assuming that one of the four fouling mechanisms (e.g., cake formation, intermediate blocking, pore constriction (standard blocking) and complete blocking)) or combined mechanisms take place. The differential rate laws corresponding to all possible fouling mechanisms were proposed by Hermia (1982). Examples of the application of the two models are presented in Appendix K.

3.7 Comparison with commercial UF membranes

Previous studies pointed out fascinatingly that the newly modified PES-LSMM membranes was in the range of tight UF membranes with relatively smooth surface, small pore size and MWCO of approximately 60 kDal (Nguyen, 2005). However, there was not a direct comparison between these modified membranes and other UF membranes. A comparison study therefore was implemented to test and compare the performance of the LSMM membranes and nine commercial membranes with five (05) different types of

base polymers (polyethersulfone-PES, polysulfone-PS, cellulose acetate-CA, polyacrylonitrile-PAN and Cellulose-C) in the same range of molecular weight cutoff-MWCO (from 40 to 120 kDal). Table 3.4 presents basic information of these membranes.

Table 3.4 Description of commercial membranes

Type of Membrane	Manufacturer	Materials	Nominal MWCO (kDal)
XM50	Millipore	Regenerated Cellulose	50
Mil100	Millipore	PES	100
FO100	Millipore	Modified PS	100
FO50	Millipore	Modified PS	50
PAN100	GE Osmonics	PAN	100
PX150	GE Osmonics	PES	150
PU40	GE Osmonics	PES	40
EWH70	GE Osmonics	PS	70
CQ40	GE Osmonics	CA	40

All the membranes were coated with formaldehyde for preservation during storage and shipping. Hence, they were thoroughly rinsed with MQ water for several hours to clean this protection layer. These membranes were compared in terms of membrane characteristics (as in section 3.4.4) and in terms of membrane performance (as in section 3.4.6). The results from this study were presented in Chapter 6.

3.8. Membrane cleaning

3.8.1 Apparatus for membrane cleaning

As there is no bench-scale membrane filtration apparatus is considered as the standard for assessing membrane cleaning, four different types of apparatus were evaluated in this thesis. They included one dead-end and three cross-flow (CF) cells. The dead-end cell was a stirred UF cell (model 8400, Amicon®, Houston, TX), while the cross-flow cells were a SEPA cell (Osmonics®, Minnetonka, MN), a single CF cell and a six-CF cell-in-parallel system. The first two cells (stirred cell and SEPA cell) are standard and commercial units, whereas the last two systems were manufactured at the Department of

Civil Engineering's machine shop. In an attempt to minimize the variability due to membrane coupons while comparing the cleaning efficiency of the four cells, coupons of only one membrane type (commercial PES PU membranes provided by Osmonics) were chosen for this part of the study.

(a) Stirred UF cell (Amicon)

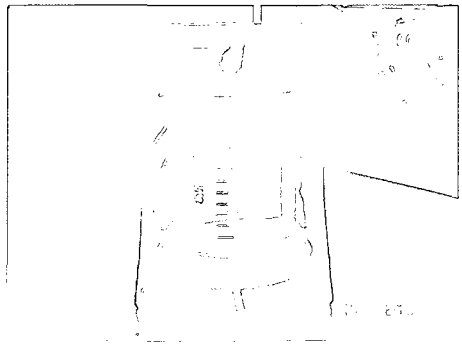

(b) SEPA cell (Osmonics)

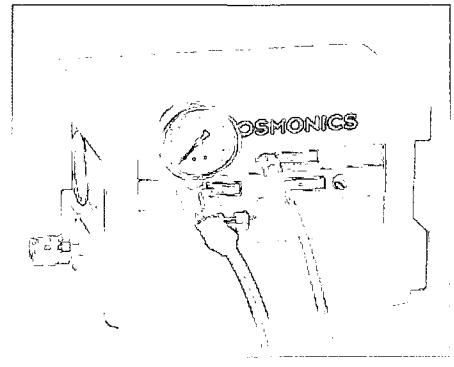

(c) Single CF cell (Non commercial one)

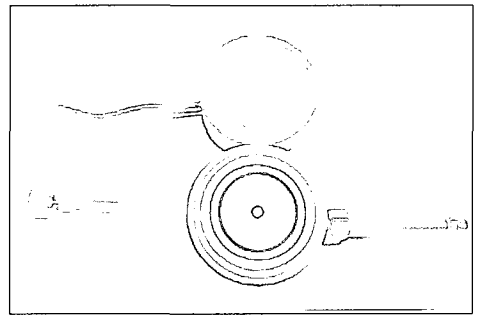

(d) Six-cell in parallel (Non commercial one)

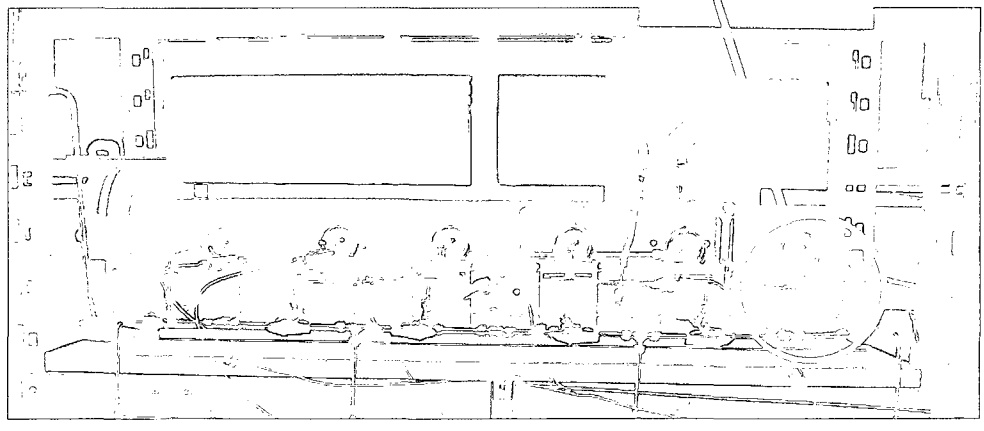

Figure 3.5. Cleaning systems

The stirred UF cell (Figure 3.5a) was chosen since it has been widely used for not only permeation tests but also cleaning studies. The cell is made of polysulfone and holds a volume capacity of 400ml. The minimum working volume is 10 ml. Effective area of membranes is 41.8 cm^2. The maximum operating pressure of this cell can be up to 517.5 kPa (75 psig) according to the manufacture.

The SEPA cell (Figure 3.5b) was selected because it has been recommended by Osmonics® to simulate the flow dynamics of larger commercially available membrane elements such as Osmonics® industrial separators (spiral-wound membrane elements) (Mosqueda-Jimenez et al., 2004a). Its body is made of 316 stainless steel. Effective membrane area is 155 cm^2 and its maximum operating pressure is up to 6900 kPa (1000 psig). A detailed description of these cells is presented in Chapter 7.

The single CF cell (Figure 3.5c) was made of 316 stainless steel and based on the design described by Sourirajan and Matsuura, 1985. Details of this cell have been described in section 3.5.1. The last system included six identical CF cells that had the same design as the single CF cell. The six-cell-in-parallel setup was constructed to be able to test six membrane coupons simultaneously and shorten the duration of the study. To maintain even flow rate and pressure distribution among the cells, pressure gauges and valves were installed for each cell (Figure 3.5d) and the flow-meters were installed before and after the cells to check the individual cell's flow-rate. The pressure and flow rate discrepancy among the cells was less than 6% and 5%, respectively. It is of interest to determine if the six-cell system produces similar cleaning efficiency to that of a single CF cell so that it could be reliably used for cleaning studies. It is worth noting that the membrane coupons were placed randomly on the cells and for the replicate tests, the placement of membrane coupons was again randomized.

3.8.2 Dead-end and cross-flow experimental set-up

Dead-end system

The stirred UF cell was set up in a batch dead-end filtration mode with a pressure of 345 kPa (50 psig) derived from a nitrogen cylinder (gas grade 4.8, BOC gas, Whitby, ON)

(Figure 3.6). The set-up was similar to the one for determination of MW distribution. The volume of the filtrate was continuously monitored using a balance and a stopwatch.

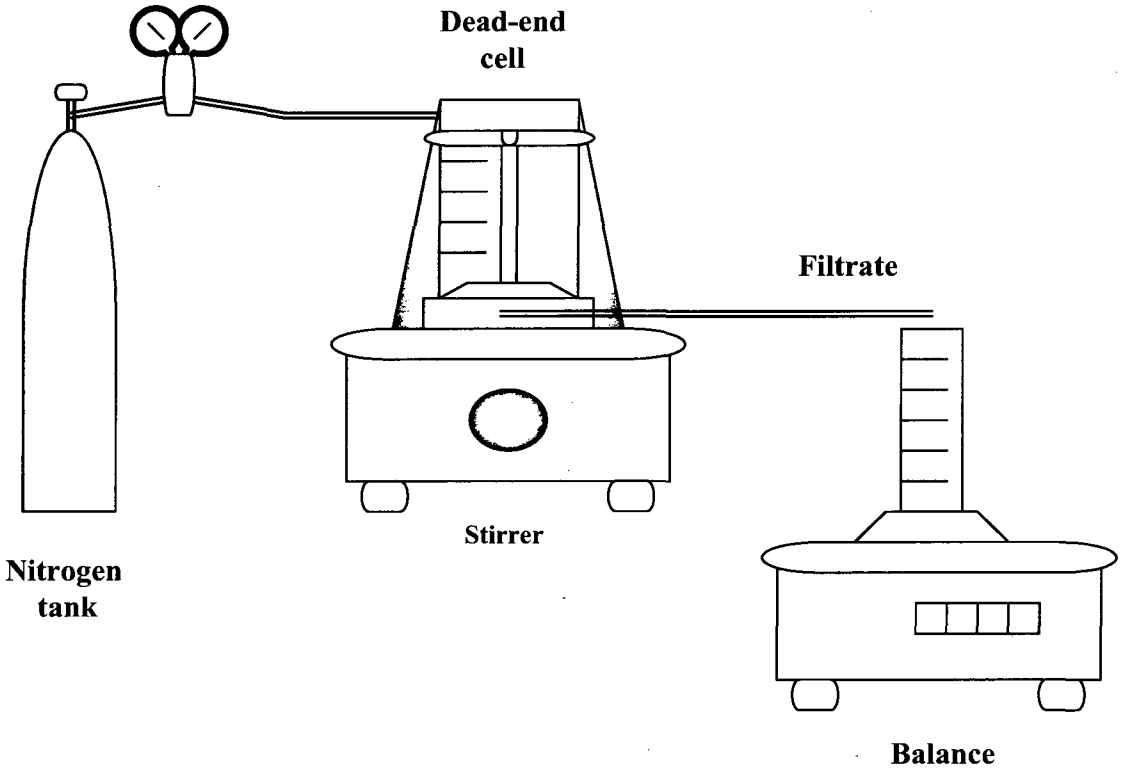

Figure 3.6. Dead-end system (After Mosqueda-Jimenez, 2003)

Due to the cell design, it was impossible to drive pressure from the permeate side (bottom end) of the membrane to the feed side to simulate backwashing, hence the membranes were flipped over and MQ water was pushed from the feed to the permeate side as in the normal filtration mode (50 psig pressure) to wash the membranes.

During the chemical cleaning, the chemical solutions were loaded in the feed chamber of the cell for a specific time with a stirrer on. Finally, the membranes were rinsed with MQ water prior to a new fouling-cleaning cycle.

Cross-flow systems

The experimental set-up for evaluating fouling, backwashing and chemical cleaning tests in cross-flow systems is presented in Figure 3.7. The membrane cell could be the SEPA cell, the single CF cell or the six CF cell-in-parallel system.

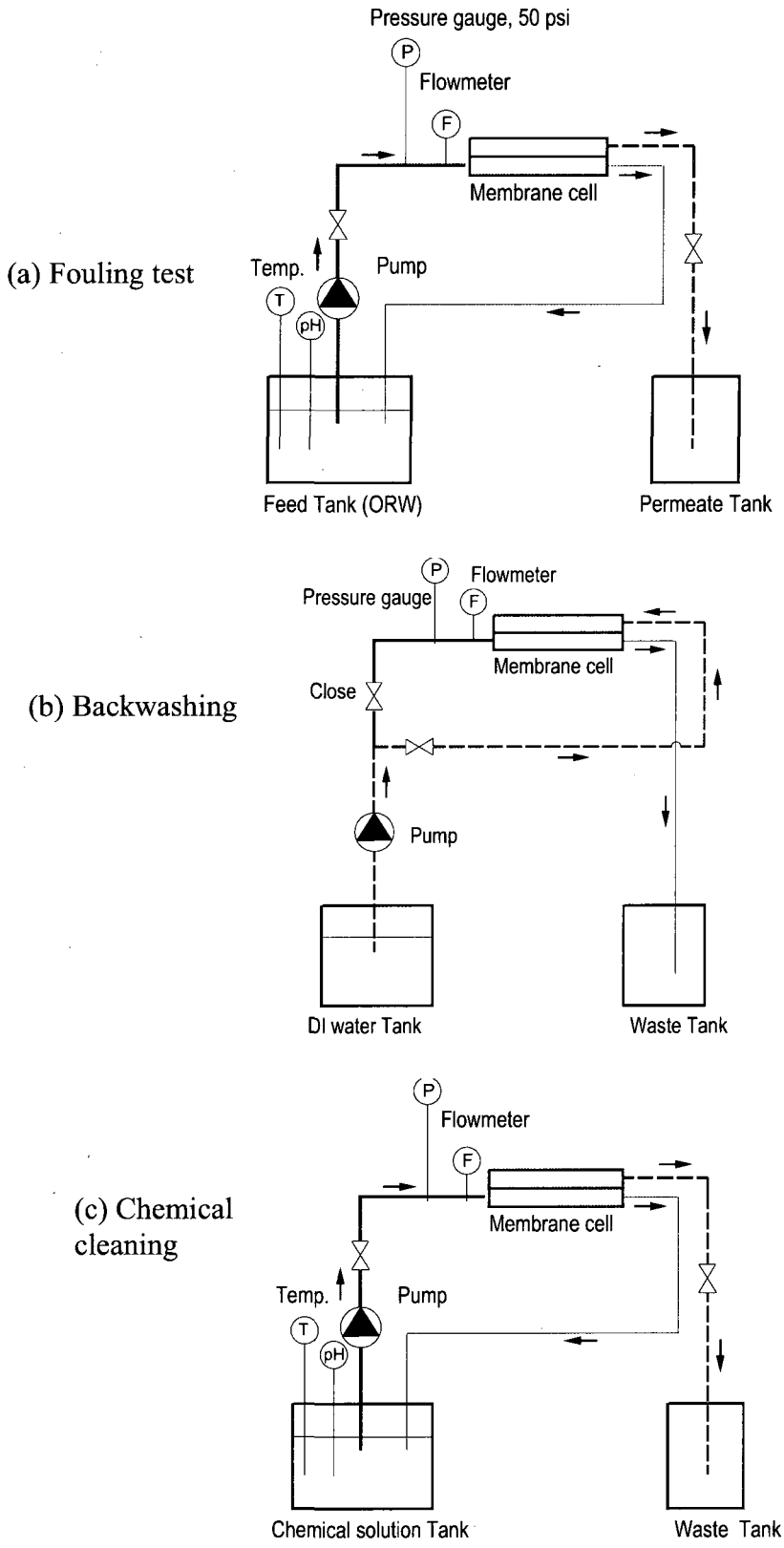

Figure 3.7. Schematic diagram of the apparatus for fouling and cleaning experiment

During the filtration (fouling) test, the river water was pumped from 10-L carboy reservoir by a diaphragm Hydracell pump. The flow of the feed stream was measured by a flowmeter (65MM, Gilmont Instruments, Barrington, IL), and the inlet pressure was measured by a pressure gauge (Cole-Parmer, Vernon Hills, IL). The flowrate was set at 0.4 Lpm and pressure of 50 psig for both fouling and BW tests. The lower flowrate was selected based on several cleaning studies in the literature (Bodzek and Konieczny, 1998; Cho et al., 2002). The permeate was collected in different tank while the retentate was recycled back to the feed tank. Permeate flux was measured at specified intervals.

For the 6-cell-in-parallel, the feed was split into two headers which each fed three identical CF cells. Two heads instead of one were implemented to ensure a more similar pressure and flow through each cell (i.e., shorter line to each cell). Metering valves (Swagelok: SS-6L and SS-4L, Ottawa Fluid System Technologies, Ottawa, ON) placed before and after each cell were used to control pressure, the pressure was monitored by pressure gauges (Swagelok: PGI-63C-PG300-LBG1, Ottawa Fluid System Technologies, Ottawa, ON) before each cell. Flowrate was monitored via one common rotameter (GF 8341-2516, Gilmont Instrument, Barnand Co., Barrington, IL). The retentate and permeate were all recycled back the feed tank. All the tubings were made of 316 stainless steel.

During the backwashing, MQ water was pumped in reverse direction for 10 min from the permeate side to detach the NOM on membrane surface. The valve to the inlet (feed side) of the cell was closed. In case of single CF cell and the 6-CF cell-in-parallel system, due to their cell design (i.e., very thin channel at the permeate side) it was required to disassemble the cell, flip over the membrane coupons and reassemble the cell in order to backwash them – same manner as with UF stirred cell. While flipping the membranes, care was taken at most to minimize the relocation of membranes. Prior to the chemical cleaning test or consequent fouling test with ORW, the membrane coupons had to be flipped over back as in normal filtration mode.

In the chemical cleaning step, the chemical solutions were circulated with no pressure for 15 min. After that the membranes were rinsed by circulating MQ within the system for 5 min. The pure water permeation rate was recorded again at 50 psig and 0.4 Lpm before

the new running cycle (fouling and cleaning) so as to be able to calculate the flux recovery (FR) by equation [3.12] and the solute resistance removal (RR) by equation [3.13].

In all cleaning tests, care was taken to ensure the system was under the same operating conditions (pH=7±0.5, room temperature) before each test. Fluxes and TOC analyses were conducted at a specified interval. The fouling and cleaning experiments were conducted in replicate at room temperature.

3.8.3 Cleaning chemicals

As described in section 3.1, there were several chemicals used for this cleaning stage such as NaOH, citric acid, NaOCl and $Na_5P_3O_{10}$ (sodium tripolyphosphate). The concentrations (Table 3.5) were chosen based on the recommendations of Hydranautics, a membrane company.

Table 3.5 Description of chemicals

Chemicals	Concentration	pH	Temperature (^{0}C)
NaOH	0.1M	12.5	23 ± 0.5
NaOH	0.1M	12.0	60 ± 0.5
Citric acid	0.1M	2	22 ± 0.5
NaOCl	0.01M	9.5	22 ± 0.5
$Na_5P_3O_{10}$	0.05M	11	22 ± 0.5

Note: Citric acid was not used alone but combined with NaOH solution. Basically, the citric acid was tried first for 7 min (a low pH cleaning is used first to remove foulants like mineral scale), then followed by 8 min of NaOH solution (a high pH cleaning is to remove organic materials). Total cleaning time is 15 min.

3.8.4 Cleaning protocols

Before describing the cleaning protocol, it is necessary to explain the associated fouling part of the protocol that was applied consistently because this period was one of the main parts in a fouling-cleaning cycle. The membranes were precompacted at 483 kPa (70 psig) for 30 min with MQ water to partly stabilize the membranes, then followed by the

fouling test with river water for a predefined period (every 30 min, 120 min or 240 min). A test on the impact of pre- compaction pressure was performed during this stage (See appendix S for details). Accordingly the pre-compaction was conducted at 483 kPa (70 psig) (instead of 552 kPa (80psig) pressure used in earlier stage) to minimize the change in membrane structure due to compaction associated with higher pressure. In addition, after 30 min pre-compaction, the pressure was released to 345 kPa (50 psig) and pure water permeate flux was recorded, called as J_{wo}. This parameter was used to compare with J_{wc}, the pure water flux of the membrane after being cleaned, to evaluate the flux recovery. In summary, one fouling-cleaning cycle always included 30 min precompaction + fouling test (30 min, 120 min or 240 min durations) + cleaning test (usually 10min BW and/or 15min chemical circulation + 5 min rinse with MQ water). It means that at the end of each fouling-cleaning cycle, the system was run with MQ water. The pressure at the end of rinsing period was raised (from the depressurized chemical cleaning cycle) to 345 kPa (50 psig) to measure the J_{wc} ($L/m^2/h$).

There were five protocols investigated for cleaning of NOM.

(1) Using chemical cleaning only (five chemicals in Table 3.5)

(2) Cross-flushing with MQ water

(3) Backwashing (BW) with MQ water

(4) Backwashing with hot MQ water (45°C is chosen since increasing temperature did not produce higher flux rate (Peng and Trembley, 2008)).

(5) Backwashing + Chemical (0.1M NaOH at 23°C, pH=12.5)

It should be noted that the objectives of stage 2 are to evaluate the impact of cleaning frequency (after every 30 min, 120 min or 240 min), cleaning chemicals (with different types of chemicals as listed above) and cleaning protocol besides the assessment of apparatus for cleaning (section 3.8.1).

To test the five different protocols, only the 120 min cleaning frequency was applied. It meant the membranes after being precompacted were filtered with river water for 120 min at 50 psig, followed by one of the five cleaning protocols, rinsed with MQ water, then repeated with another fouling-cleaning cycle. It was noted that membranes were

only precompacted once at the beginning. The backwashing duration was 10 min, the chemical circulation last 15 min and followed by a 5-min MQ water rinse. There were at least two fouling-cleaning cycles per test.

To test the impact of cleaning frequency, the BW + chemical combined protocol was chosen. The membranes were precompacted for 30 min, followed by a 30 min (or 120 min or 240 min) fouling test with river water, then cleaned by a BW + chemical combined procedure. After being rinsed for 5 min with MQ water, a new fouling-cleaning cycle started. The duration of BW and chemical circulation was 10 min and 15 min, respectively, except for the shortest 30 min frequency. For this short period, 5 min of BW and 10 min of chemical circulation were used.

To access the impact of different cleaning chemicals, the first protocol (using chemical only) was implemented with a cleaning frequency of 120 min. Each of the five types of chemicals or chemical combination was tested separately one at a time. During each cleaning test, the targeted chemical was circulated within the system for 15 min. At least two fouling-cleaning cycles were applied.

For most of the above tests, the six-cell-in-parallel system was utilized to shorten the experimental period. The experiments were conducted in duplicate.

3.8.5 Impact of membrane modification on surface cleaning

There were three different types of membranes used for this evaluation: two experimental membranes (control PES and PES-LSMM) and one commercial membrane. The PES-PU commercial membrane was chosen because it had the same base polymer (PES) as the experimental membranes and had quite similar characteristics (see Table 3.6). The first two were laboratory-made PES and PES-LSMM membranes. They are fabricated using PES base polymer with and without blending LSMM in NMP solvent as described in section 3.4.2. Details of LSMM can be found in section 3.4.1. For the PES-LSMM membranes, the additive LSMM was blended in the casting solution. The performance of membranes before and after cleaning was evaluated based on some parameters mentioned in section 3.4.6. The objective was to examine the cleaning performance of three PES membranes with different surface hydrophobicity.

Table 3.6 Characteristics of tested membranes

Membrane type	MWCO (kDal)	Mean pore size (nm)	Contact angle (^{0})	Surface charge (mV)	Roughness (nm)
PES	72	4.6	71.6	-6	1.27
PES-LSMM	70	4.35	70.1	-3	1.72
PES-PU	58	4.8	64.2	-3.3	0.67

Note that PES-nSMM membranes were not employed for the cleaning tests. The reason was that these hydrophobic membranes retained very little NOM on their surface, the membrane surfaces were quite clean. Certainly the NOM removal by these membranes was quite low compared with the commercial or the modified PES-LSMM membranes. Consequently, including PES-nSMM membranes, which have absolutely different performance, was not considered worthwhile for cleaning evaluation.

For the most critical part of this stage which was evaluation of modified membranes upon cleaning, all the tested membranes were compared using the BW + chemical cleaning method, and conducted on the six-cell-in-parallel system and Sepa cell. The results were reported in Chapter 7 and Appendix J. Fluxes and NOM rejection were monitored for assessment.

Table 3.7 Summarizes the variables and membranes used in this Cleaning section

Evaluation	Cell type	Cleaning protocol	Cleaning cycle	Cleaning frequency (fouling time)	Membrane types
Impact of Apparatus	- Sepa cell, - Stirred UF cell - Single CF cell - Six CF cell in parallel system	BW + Chemicals	10-15-5	4 hrs	PES PU
Impact of cleaning protocols	Six CF cell in parallel system	- Using chemicals only -Cross-flushing with MQ water - BW with MQ water (22°C) - BW with hot MQ water (45°C) - BW + Chemical (0.1M NaOH)	15-5 $t_{crossflush}$ =10 min t_{BW} =10 min t_{BW} =10 min 10-15-5	2 hrs	Control PES PES-LSMM PES PU
Impact of cleaning frequency	- Sepa cell, - Stirred UF cell - Six CF cell in parallel system	BW + Chemicals	10-15-5	0.5 hrs, 2 hrs, 4 hrs	Control PES PES-LSMM PES PU
Impact of chemicals	Six CF cell in parallel system	Using chemicals only	15-5	2 hrs	Control PES PES-LSMM PES PU
Impact of membrane types	- Sepa cell - Six CF cell in parallel system	- Using chemicals only - BW with MQ water (22°C) - BW + Chemicals	15-5 t_{BW} =10 min 10-15-5	2 hrs	Control PES PES-LSMM

Note: 15-5: $t_{chemicals} - t_{rinse}$ (min); 10-15-5: $t_{BW} - t_{chemicals} - t_{rinse}$ (min)
Except for 0.5 hrs frequency: t_{BW} = 5 min; $t_{chemicals}$ = 10 min and t_{rinse} = 5 min

3.9. Evaluation of the performance of LSMM-blended UF membranes with different base polymers

Five polymers were selected as the base polymers to cover a wide range of hydrophilicity/phobicity spectrum: CA, PEI, PES, PS, and PVDF. Note that a different MW of PES polymer was used (18 kD versus 31 kD).

It is recognized that the optimal base polymer/LSMM/solvent proportions are likely different for each base polymer. However, time constraints necessitated the selection of a single set of proportions. Based on the best results obtained with PES membranes, the percentage of LSMM additive was chosen limitedly as 0.5 wt% and 3.0 wt%. Higher additive percent did not guarantee a better performance. The concentration of all base polymers was kept constant of 18 wt%. The rest was NMP solvent. These proportions were applied for all base polymers to make it easier to compare.

The membrane fabrication followed the procedure described in section 3.4.2 in which the casting was conducted under the fume hood (8% humidity, 22±0.5 °C), the gap between the glass plate and casting bar was 200μm, and no migration time was incorporated prior to gelation in a 4°C coagulation bath.

First the casting solutions were visually checked for miscibility to see if LSMM was mixed well with those base polymers. The miscibility was further confirmed by analyzing the complete membranes using a Differential Scanning Calorimeter (DSC) equipped with a universal analysis 2000 program (DSC Q1000, TA Instruments, New Castle, DE). Second, the membrane properties and performance were evaluated in terms of the parameters discussed in section 3.4.4 and section 3.4.6. Detailed results of the stage 3 are shown in Chapter 8.

CHAPTER 4

KEY FACTORS EFFECTING THE MANUFACTURE OF HYDROPHOBIC UF MEMBRANES FOR SURFACE WATER TREATMENT

Huyen T. Dang[1], Dipak Rana[2], Roberto M. Narbaitz[1], Takeshi Matsuura[2]

[1]Dept. of Civil Engineering, and [2]Dept. of Chemical and Biological Engineering, University of Ottawa, 161 Louis Pasteur St., Ottawa, ON, K1N 6N5, Canada

4.1 Abstract

As part of the development of poly(ether sulfone) (PES) membranes whose surface is modified by the incorporation of a newly synthesized hydrophobic surface modifying macromolecule (nSMM) additive, this study investigates the impact of five key membrane preparation factors. They are concentration of PES, concentration of nSMM, casting thickness, casting speed and post-treatment conditions. The synthesis and characterizations of nSMM by nuclear magnetic resonance, gel permeation chromatography, differential scanning calorimeter, and elemental analysis have been presented. The changes in characteristics and performance of the membranes have been evaluated via Fourier transform infrared spectroscopy, contact angle analysis, scanning electron microscopy, and solute transport tests. The addition of 0.5 wt% of nSMM increased the contact angle of PES membranes by 20°, however higher nSMM concentrations did not increase the hydrophobicity any further. Only the additive concentration had a statistically significant impact on flux reduction and dissolved organic carbon (DOC) rejection. Even though other factors such as thickness may alter the pore characteristic, their effect on membrane performance was marginal.

Keywords: Polymeric membranes; hydrophobic additive; key effecting factors; solute rejection; mathematical model

4.2 Introduction

Porous integrally-asymmetric membranes are often made by the phase inversion method [1, 2]. This method is applied mainly in the preparation of membranes for dialysis, microfiltration (MF) and ultrafiltration (UF). Most commercial UF membranes are cast via this technique using a multi-component solution containing polymer(s), solvent(s) and non-solvent(s) or additive(s). In many cases, the pore characteristics (porosity, pore size) and skin layer morphology are modified by blending additives to the casting solution [3]. The additives can be inorganic salts (e.g., $LiNO_3$, LiCl, $ZnCl_2$, etc) or organic polymers (poly(vinyl pyrrolidone) (PVP), poly(ethylene glycol) (PEG), sulfonated poly(ether ether ketone), methacryloyloxyethylphosphorylcholine (MPC) copolymer, poly(amide imide) (PAI), etc) or nano-particles (TiO_2, Al_2O_3, etc) [4-12]. Although PVP or PEG acts as a surface modifying additive, their effects are temporary since they are water soluble and eventually leach out from the modified membrane. Since 1990s, our research group has been involved in the development of different types of hydrophobic surface modifying macromolecules (SMMs) to modify the membrane surface more permanently. Earlier studies with a hydrophobic SMM incorporation [13-15] did not result in a significant impact on membrane performance for drinking water treatment probably due to insufficiently migration of the particular SMM additive. A more rapidly migrating SMM has been developed (called as nSMM) for the preparation of pervaporation membranes [16]. The lead author's doctoral research plan included a comparison of the impact of hydrophobic/hydrophilic surface modification on the effectiveness of membrane cleaning. This manuscript however reports solely the preparation and performance of the more hydrophobic PES-nSMM membranes.

It is reported that the formation of membranes made by phase inversion technique depends on a number of material- and process-specific parameters including type and amount of base polymers, solvents, type and amount of additives, casting thickness, casting speed, post-treatment, conditions (temperature and composition) of coagulation bath and drying conditions [17]. This paper investigates the impact of five key preparation factors including concentration of PES, concentration of nSMM, casting thickness, casting speed and post-treatment conditions. Although the impacts would be

different with different types of additives, this research incorporates a broad comparison with other research dealing with membrane modification.

4.3 Experimental methods and analysis

4.3.1. Material

Poly(ether sulfone) (PES, Victrex 4100P, powder) was supplied by ICI Advanced Materials, Billingham, Cleveland, England, UK. 4,4-Methylene bis(phenyl isocyanate) (also known as diphenylmethane diisocyanate, MDI, 98%) was purchased from Sigma-Aldrich, Inc., St. Louis, MO, USA. Oligomeric fluoro-alcohol (OFA) (Zonyl fluorotelomer intermediate, 2-(perfluoroalkyl)ethanol, BA-L of average M_n 443 and 70 wt% fluorine was supplied by Aldrich Chemical Co., Milwaukee, WI, USA. The α,ω-aminopropyl poly(dimethyl siloxane) (PDMS) of average molecular weight 900 was purchased from Shin-Etsu Chemical Co. Ltd., Tokyo, Japan. Deuterated tetrahydrofuran (THF-d8, 99.5 at% D) was purchased from the CDN Isotopes, Point-Claire, PQ, Canada. Polyethylene glycol (PEG) and polyethylene oxide (PEO) (Aldrich Chemical Co., Milwaukee, WI) were used as probe solutes for the solute transport tests.

4.3.2. nSMM synthesis

The nSMM was synthesized using a two-step condensation polymerization method. MDI was distilled at 150°C under 0.5 torr. OFA and PDMS were degassed for 24 hrs under 0.5 mmHg. The first step was conducted in a common solvent (N,N-dimethyl acetamide, DMAc) to form polyurea prepolymer by the reaction of MDI with PDMS. Basically, 7.5 gm (0.03 mole) MDI dissolved in 50 ml DMAc was mixed with 18 gm (0.02 mole) PDMS in 100 ml DMAc. The prepolymer was then, in the second step, end-capped by the addition of OFA in the DMAc solvent resulting in formation of repeated polyurethane linkages. Here 8.86 gm (0.02 mole) OFA in 50 ml DMAc was used. The molar composition of nSMM is MDI: PDMS: OFA= 3:2:2. The polymer solution was precipitated in water and dried in an air circulation oven at 120 °C for 5 days. Figure 4.1 shows the steps involved in the nSMM synthesis. The chemical name of the nSMM is poly(urea-dimethylsiloxane-urethane) both ends capped by OFA. The polyurethane units

are expected to anchor the nSMM to the PES that makes up the bulk of the membrane, and thus minimize additive leaching.

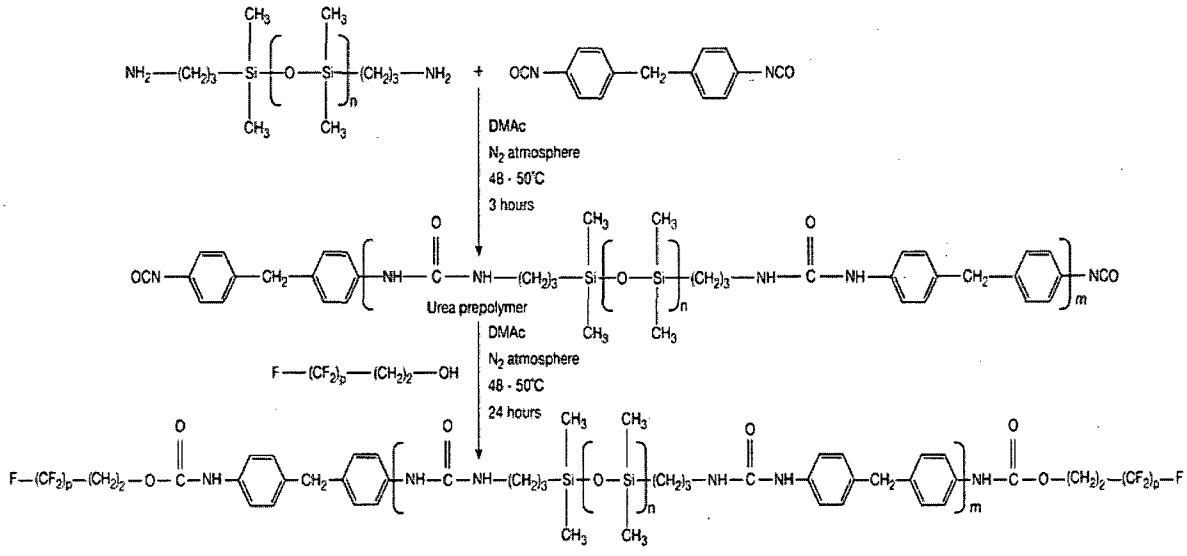

Figure 4.1. Schematics of nSMM synthesis

4.3.3. Polymeric additive's characterizations

Fluorine and silicone content in the nSMM were measured by using an oxygen flask bomb combustion technique (Oxygen Bomb Calorimeter, Gallenkamp & Co. Ltd., England). The elemental analysis of fluorine content in the nSMM was carried out using standard method in ASTM D3761. An accurate weight (10-50 mg) of nSMM was placed into oxygen flask bomb combustion. After pyro-hydrolysis, the fluorine (ion) was measured by an ion chromatography (Ion Chromatograph, Dionex DX1000, Sunnyvale, CA). The analysis of silicon content in the nSMM was performed by oxygen flask bomb combustion same way as fluorine analysis, followed by acid digestion and then analyzing for silicon by inductively coupled plasma - atomic emission spectrometry (ICP-AES, Varian Liberty 110, Varian Inc., Palo Alto, CA).

The glass transition temperature (Tg) was measured by a differential scanning calorimeter (DSC) equipped with a universal analysis 2000 program (DSC Q1000, TA Instruments, New Castle, DE). About 10 mg of polymer was put into an aluminum pan and crimped with another aluminum pan. The pans were then placed within the sample

chamber of the DSC. The polymer was annealed at about 280 °C for 10 min and then quenched to -50 °C, and scanned at a heating rate of 10 °C/min. The Tg value was recorded at the onset point of the corresponding heat capacity transition.

The number and weight average molecular weight of the synthesized nSMM were measured by gel permeation chromatography (GPC, model 410, Waters Associates, Milford, MA) equipped with a refractive index detector. Three UltraStyragel™ packed columns from Waters were placed in series. Tetrahydrofuran, THF, was used as the mobile phase at a flow rate of 0.3 mL/min at 40°C. The calibration of the GPC was performed using eight polystyrene (Shodex, Tokyo, Japan) standards with molecular weights between 1.3×10^3 and 3.15×10^6 g/mol. The standards and nSMM samples were prepared in THF (0.2 w/v% solutions) and Millenium 32 software (Waters) was used for the data acquisition.

A sample for nuclear magnetic resonance (NMR) analysis was prepared by dissolving as much polymer as possible in THF-d_8. The NMR data was collected on an AVANCE 300 NMR spectrometer (Bruker Corp., East Milton, ON). The ^{1}H NMR spectrum was acquired under quantitative conditions with 16 scans using a 30° pulse, and a 3.6 sec interpulse sequence.

4.3.4 Preparation of membranes

Casting solutions were prepared with different concentrations of PES base polymer (14, 16 and 18 wt%) and nSMM contents (0.5, 1.5, 3.0, and 4.5 wt%) dissolved in NMP solvent. These casting dopes were cast on a glass plate with a predetermined thickness (0.2 or 0.25 mm) at different casting speeds (1.5 cm/s – fast, and 0.25 cm/s- slow). The different film thicknesses were obtained by using casting bars with different gaps formed with the glass plate. The casting speed referred to the speed at which the casting bar was moved from one end of the glass plate to the other to create a roughly 165 cm^2 flat sheet film. The cast films were then immersed into the gelation media (water, 4°C) immediately until they hardened. The membrane preparation variables, whose impact was assessed, were PES concentration, nSMM concentration, thickness of the cast solution film and the casting speed. Table 4.1 shows the membrane code and the corresponding variables.

Table 4.1 Description of membranes

Membrane code	PES (wt%)	nSMM (wt%)	Thickness (mm)	Casting speed (cm/s)
M1	18	4.5	0.20	0.25
M2	18	4.5	0.20	1.5
M3	18	4.5	0.25	0.25
M4	18	4.5	0.25	1.50
M5	16	4.5	0.20	1.50
M6	14	4.5	0.20	1.50
M7	18	3.0	0.20	0.25
M8	18	3.0	0.20	1.50
M9	18	1.5	0.20	0.25
M10	18	1.5	0.20	1.50
M11	18	1.5	0.25	0.25
M12	18	1.5	0.25	1.50
M13	18	0.5	0.20	1.50
M14	18	0.5	0.25	1.50
M15	18	0.0	0.20	1.50

4.3.5. Membrane analysis and testing

The contact angle of membrane surfaces was measured using VCA Optima goniometer (AST Products, Inc., Billerica, MA). Water content was determined by gravimetric analysis [18]. Morphological examination of the top surface was made using scanning electron microscopy (SEM, model JSM-6400, Japan Electron Optics Limited, Japan). The pore size and the pore size distribution were determined by the solute transport method [19]. Fourier transform infrared (FTIR) spectroscopy was also used to observe the presence of functional groups in the membrane. The FTIR spectrometer (Varian 1000, Scimitar series, Varian Inc., Palo Alto, CA, USA) was equipped with diamond w/ZnSe lens single reflection attenuated total reflection (ATR) plate. An IR source at 45° incident angle was employed. Both top and bottom layers of the asymmetric membrane surface samples were mounted facing the crystal surface. The spectra were measured in the

transmittance mode over a wave number range of 4000 to 600 cm^{-1} at a resolution of 4 cm^{-1}.

All membrane tests followed the testing protocol described in detail by Dang et al., [19] and were using a six-crossflow cell-in-series system described by Mosqueda-Jimenez et al., [13]. Briefly, membranes were pre-compacted for one hour at 552 kPa (80 psig) and room temperature. This was followed by 50 hours of pure water permeation (PWP) monitoring (i.e. ultra-pure water filtration at 345 kPa (50 psig), at 1.1 Lpm flowrate and room temperature), then followed by the PEG/PEO solute transport quantification and completed by a 50-hour long filtration/fouling test using Ottawa River water (at the same feed flow rate and pressure). All filtration tests were conducted in duplicate.

4.4 Results and discussion

4.4.1 Polymer analysis

The fluorine and silicone content in the nSMM are 11.75 and 11.52 wt%, respectively. The values of number average molecular weight (M_n) and weight average molecular weight (M_w) of the nSMM are 12.8 and 27.1 kD, respectively. The glass transition temperature (T_g) of the nSMM is above 280 °C. The T_g of PES is 221.4 °C. The n, m and p are the numbers of repeat units of Siloxane, prepolymer polyurea and difluoro methane, respectively (Figure 4.1). The value of subscript "*p*" is 7.58 which was calculated from the molecular weight of OFA. The value of "*n*" calculated from the average molecular weight of PDMS is 9.81. Based on the stoichiometry of the synthesis and number average molecular weight of polymer, "*m*" has been calculated, which is 10.14 for nSMM. The assumption of all the reactants consumed in the reaction is considered. The characteristic peaks of the ^1H NMR are displayed in Figure 4.2 and summarized in Table 4.2.

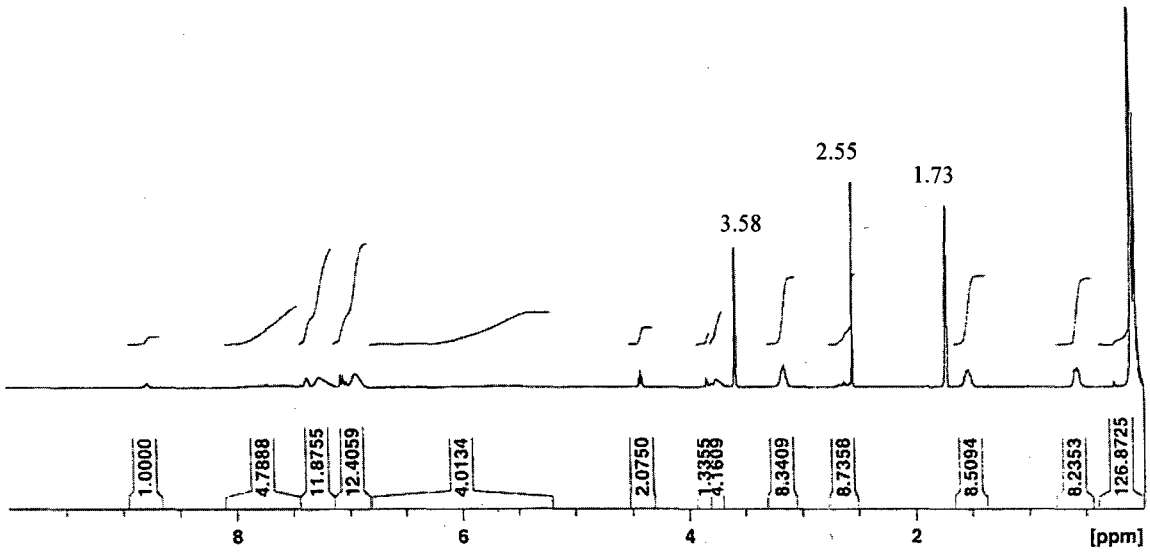

Figure 4.2. NMR spectrum of nSMM

Table 4.2 The assignments of 1H NMR characteristic peaks of nSMM

Assignment	ppm
CH_3 (PDMS)	0.11
CH_2 (PDMS) adjacent to the Si bond	0.58
CH_2 (PDMS) middle of n-propyl group	1.53
CH_2 (OFA) adjacent to the CF_2 bond	2.62
CH_2 (PDMS) adjacent to the urea bond	3.16
CH_2 between the phenyl groups of MDI	3.68 - 3.76
CH_2 (OFA) adjacent to the urethane bond	4.42
Urea NH	5.80, 7.72
Aromatic hydrogen (MDI)	6.94 - 7.39
Urethane NH	8.78

Note: 3.58 and 1.73 ppm peaks are due to THF-d_8 (C_4D_8O); 2.55 ppm peak is due to the solvent DMAc.

The functional groups listed in Table 4.2 were corresponding to the peaks in Figure 4.2 going from right to left. Those characteristic peaks confirm the available types of linkages within the nSMM.

4.4.2 FTIR analysis

The presence of functional groups at the surfaces of the asymmetric membrane was examined by FTIR-ATR spectroscopy. The FTIR spectra of both top and bottom surfaces of the membranes with and without nSMM are shown in Figure 4.3a. The spectrum of the base PES membrane shows the peaks at 1571 and 1486 cm^{-1}, which are for aromatic bands. The sharp adsorption peaks at 1323 and 1151 cm^{-1} are attributed to the asymmetric and symmetric stretching vibration of sulfone (O=S=O) group. The sharp adsorption peak at 1241 cm^{-1} is due to stretching vibration of ether (Ar—O—Ar) linkage. The top and bottom surface of PES membrane without nSMM are the same (Figure 4.3a A and B).

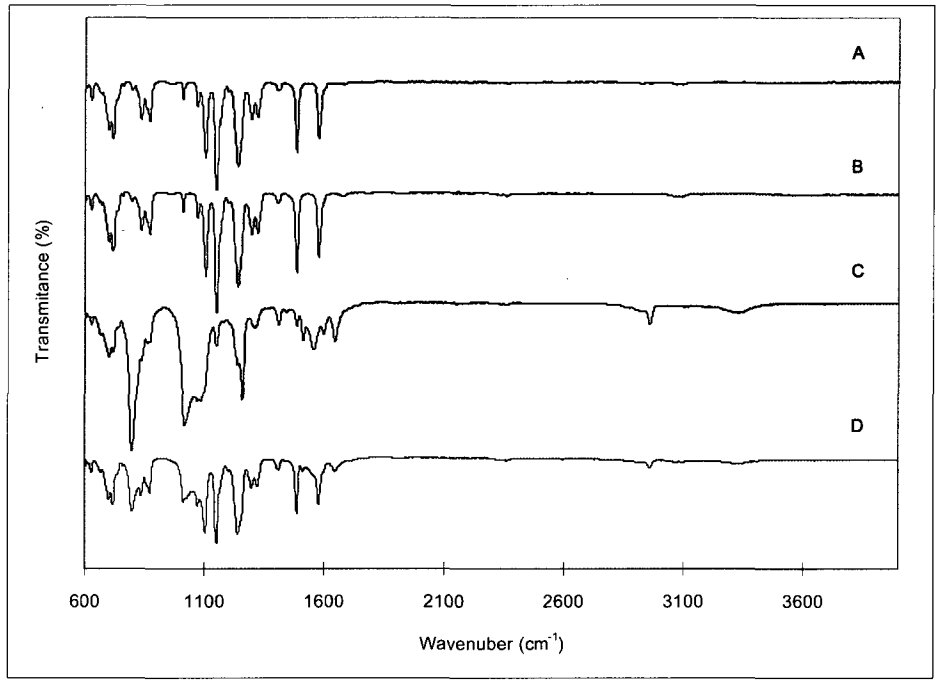

Figure 4.3a. FTIR spectra consists of (A) top surface of PES membrane without nSMM (B) bottom surface of PES membrane without nSMM (C) top surface of PES membrane with 4.5 % nSMM and (D) bottom surface of PES membrane with 4.5% nSMM

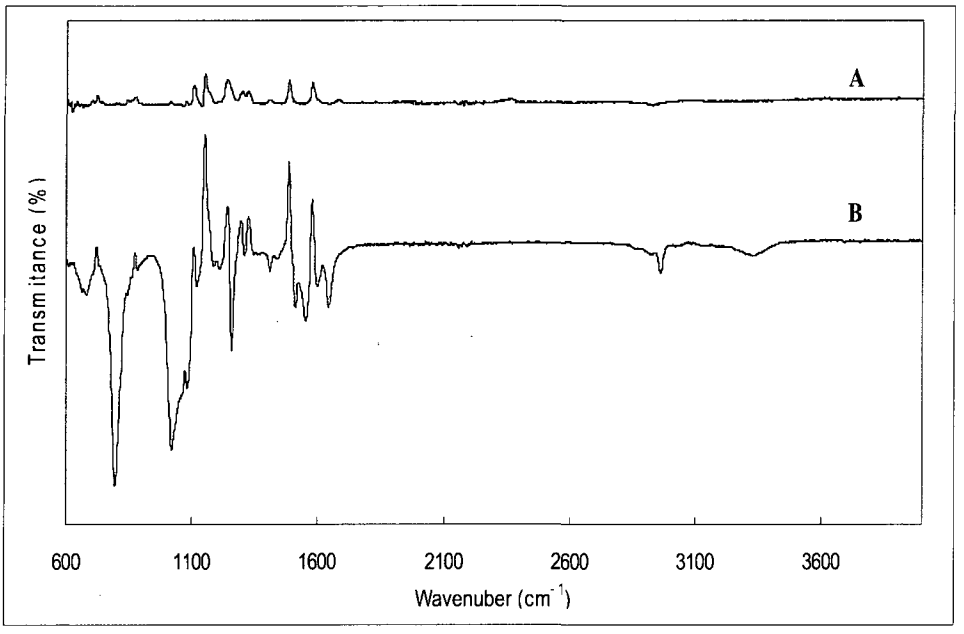

Figure 4.3b. FTIR substract spectra consists of (A) top surface minus bottom surface of PES membrane (B) top surface minus bottom surface of PES membrane with 4.5 wt% nSMM

As for the membrane in which nSMM is blended the broad peak appeared at ~3331 cm^{-1} due to the N—H stretching. Peaks appeared at 2961, 1645, 1258, 1085, 1020, and 796 cm^{-1} which can be corresponded to C—H (CH_3, CH_2 vibration) stretching, C=O (urea and urethane) stretching, Si—CH_3 (δ stretching), CF_2 stretching, Si—O—Si stretching, Si—CH_3 (γ stretching) of nSMM. The peak intensity of nSMM at the top surface (Figure 4.3a C) is much higher than the bottom surface (Figure 4.3a D). However, the clear indication of N—H stretching, C—H stretching, Si—CH_3 (γ and δ stretching), Si—O—Si stretching, etc, demonstrated that the bottom surface also contained nSMM. The FTIR subtract spectra (top surface minus bottom surface) are shown in Figure 4.3b for the membranes without and with nSMM. As expected, peaks are very small for the PES membrane without nSMM, whereas much larger peaks were obtained from the PES membrane with nSMM. These results confirm the migration of nSMM to the top surface.

4.4.3 SEM of different modified nSMM membranes

Since nSMM migrates quite fast to the surface because of its high hydrophobicity, it alters significantly the surface chemistry and morphology of membranes [20].

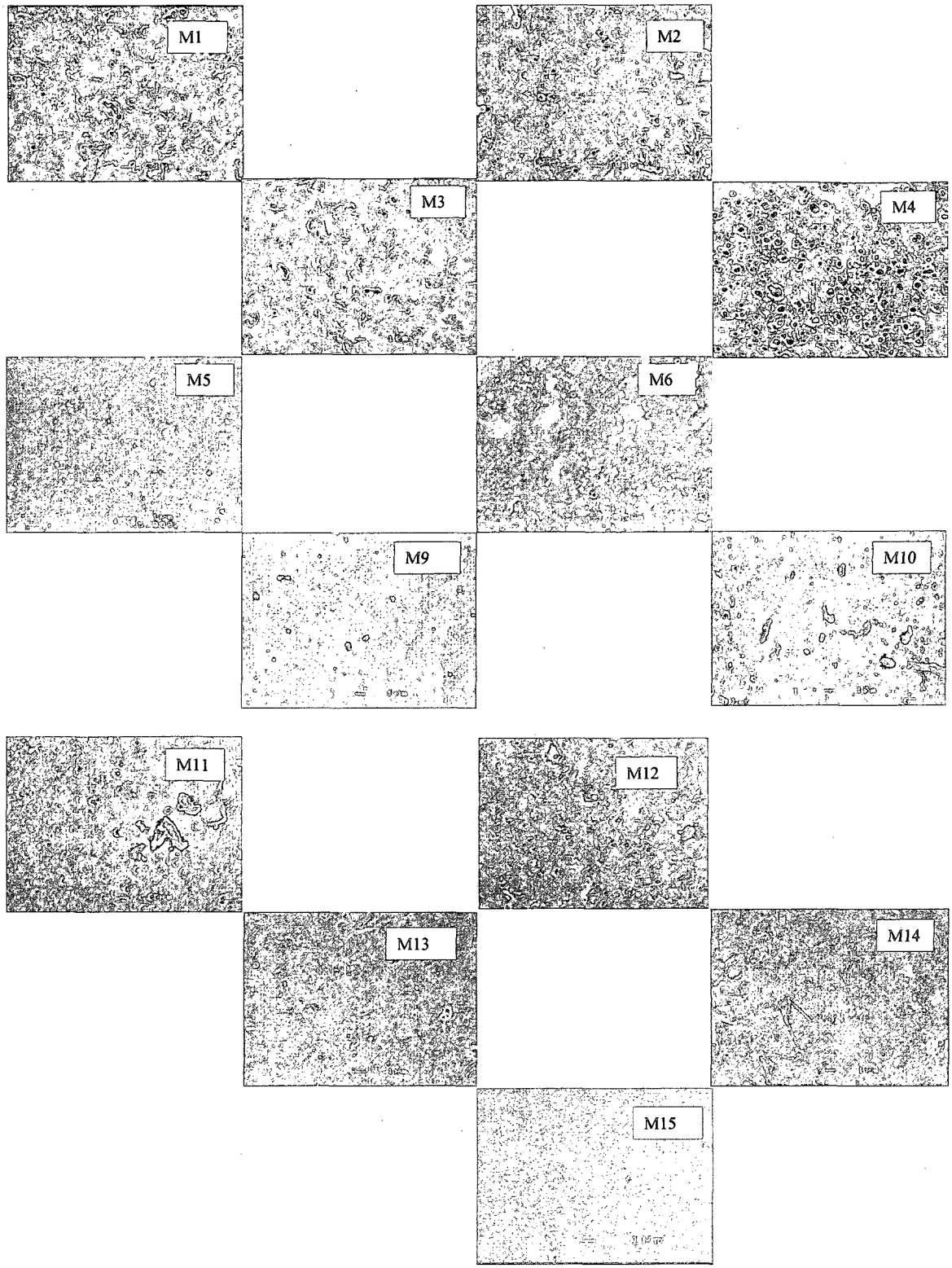

Figure 4.4. SEM of membranes with different nSMM contents
(For membrane codes, refer to Table 4.1)

Figure 4.4 presents the SEM images of 13 membrane samples evaluated (refers to Table 4.1 for their compositions). SEM images of membranes 7 and 8 are not sharp so they are not included in the figure. Compared with the control PES membranes (M15), the nSMM membranes seem to have rougher surfaces. This shows evidence of nSMM migration to the modified membrane surfaces. Nevertheless, the evidence is not clear with various additive concentrations, PES concentrations or casting speeds.

It is worth noting that when we added more nSMM additive, the solutions became less viscous (i.e., viscosity of 3 wt% nSMM+18 wt% PES is 622 cP while for the 4.5 wt% nSMM+18 wt% PES, viscosity is 573 cP). Compared with the control PES solution (viscosity of 410 cP), blending nSMM additive made the solution more viscous. The membrane surfaces are not shiny or smooth as for the control PES membranes- M15 (Figure 4.4) but rough and dry with colonies of small mound, possibly from polymer aggregation, even with a small amount of nSMM was added (0.5 or 1.0 wt%) as observed on the surfaces of M13 and M14 membranes. The surfaces are however very hydrophobic with a contact angle of 91o while that of the control PES (M15) is about 70o. Increasing the evaporation time can result in contact angles of more than 120o [21]. It is interesting that higher percentage of nSMM does not guarantee more hydrophobic nature, as confirmed in several previous studies [13, 22, 23].

4.4.4. Key factors controlling hydrophobic membrane modification

Impacts of five main factors including base polymer concentration, nSMM concentration, thickness of the cast film, the casting speed and the post treatment on the membrane responsive characteristics and performance were evaluated.

Effect of base polymer concentration

Figure 4.5 reveals the correlation between volume throughput (cumulative permeate) and DOC rejection over 50 hour filtration test for different PES concentrations (nSMM concentration was kept consistently at 4.5 wt%). Note that the natural organic matter (NOM) in Ottawa River Water (ORW) was quantified in term of DOC and ORW with a DOC of 6.8 mg/L was used a feed in the filtration tests. Membranes M2 (18 wt% of PES) exhibited quite low cumulative permeate, while membrane M6 (14 wt% of PES) yielded highest volume throughput. As a trade-off law, M6 had quite low DOC removal

(maximum about 30%). Membrane M5 with 16 wt% PES compromises this law with average volume throughput and high DOC removal (initially close to 90%). It seems that adding more base polymer delayed the demixing process, leading to less porous membranes, i.e., lower water production.

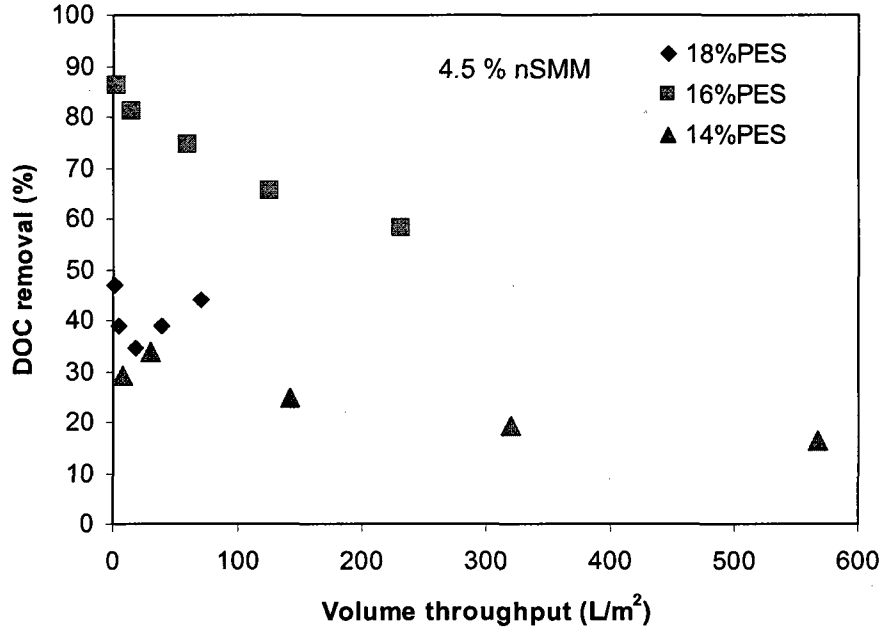

Figure 4.5. Volume throughput and DOC correlation

Membranes: M2 (18 wt% PES), M5 (16 wt% PES) and M6 (14 wt% PES); nSMM concentration, 4.5 wt%; cast film thickness, 0.2mm; casting speed, 1.5 cm/s

When the membranes were subjected to visual inspection after the filtration experiments, deposition of natural organic matter (NOM) was observed in a very limited area leaving most of the membrane surface without contamination. This means that instead of depositing on the membrane surface, most of NOMs went into the pores, some trapped inside the pores and some were transported through the pores under the hydraulic pressure.

Figure 4.6 shows surface free energy (correlated to contact angles and tabulated using SE-2500 software, which accompanies VCA Optima goniometer) and water content for the above three membranes (M2, M5 and M6). No significant difference was observed. This was consistent with earlier observation [23] that the contact angle did not statistically change with the change in the host PEI (polyetherimide) concentration.

However, higher base polymer content in casting solution led to an increase in the mechanical strength of that membrane [24].

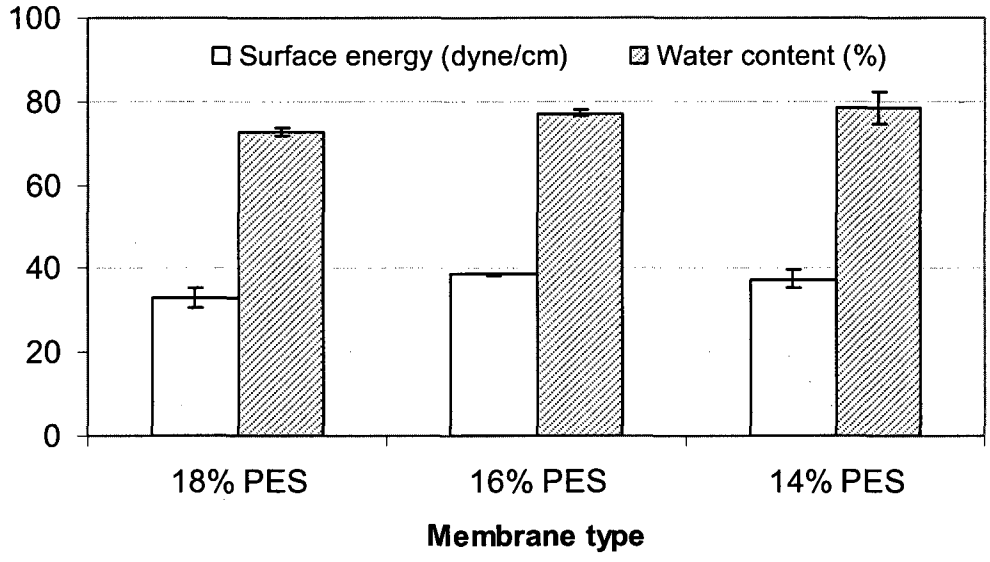

Figure 4.6. Surface energy and water content.

Membranes: M2 (18 wt% PES), M5 (16 wt% PES) and M6 (14 wt% PES) nSMM concentration, 4.5 wt%; cast film thickness, 0.2mm; casting speed, 1.5 cm/s

Effect of additive concentration

When the PES concentration was fixed at 18 wt%, homogeneous casting solutions could not be obtained even by vigorous mixing for nSMM concentrations of more than 5%. At the nSMM concentration of 1%, the solution looked homogeneous in the beginning, but phase separation took place after a few hours. This is in accordance with the earlier study where the phase separation was observed at the nSMM concentration of 2% [22]. However, casting the polymeric solution was still possible after remixing if the nSMM concentration was below 5%. Likewise, high percentage of nSMM did not guarantee a more hydrophobic surface i.e., the contact angles were statistically the same with the increasing nSMM dosage, even though their contact angles were always higher than those of the control PES membrane by 15^{o} to 20^{o}.

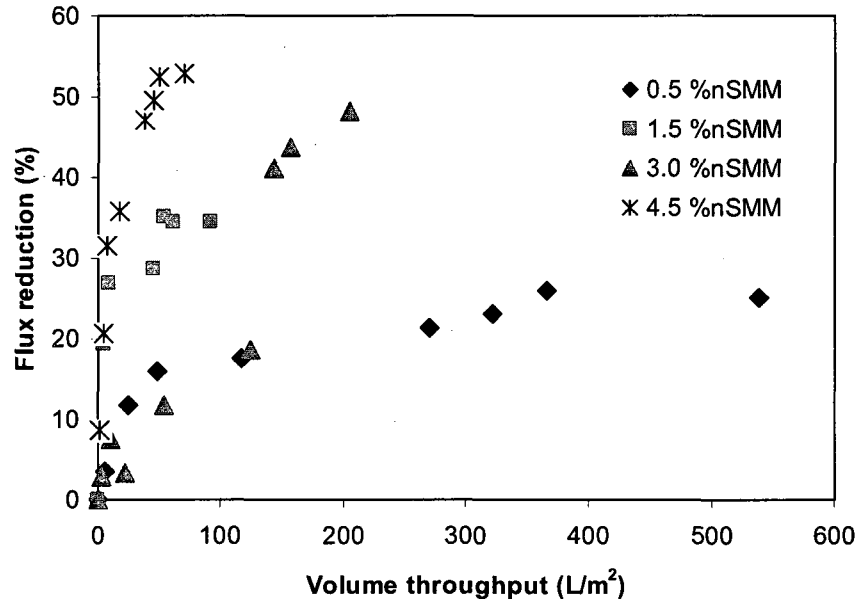

Figure 4.7. Flux reduction versus volume throughput
Membranes: M2 (4.5% nSMM), M8 (3.0% nSMM), M10 (1.5% nSMM) and M13 (0.5% nSMM); PES concentration, 18%; film thickness, 0.2mm; casting speed, 1. 5 cm/s

Figure 4.7 shows flux reduction versus volume throughput (cumulative permeate) for the membranes prepared from the casting solutions with different amounts of nSMM. Flux reduction was determined by following equation:

$$Flux\ reduction\ (\%) = \frac{J_{wi} - J_{wf}}{J_{wi}} \times 100 \qquad [4.1]$$

Where J_{wi}: initial flux during the fouling test with ORW ($L/m^2/h$)

J_{wf}: final flux during the fouling test with ORW ($L/m^2/h$)

It is obvious that the flux reduction increases with the increasing dose of nSMM. Membrane M2 with 4.5 wt% nSMM had lowest cumulative water production and highest flux resistance. It is understandable because the additive is hydrophobic. For this reason, 0.5 wt% of nSMM was chosen as the best dose in manufacturing this type of membranes for cleaning evaluation to be done in the next study.

To represent the degree of fouling, another parameter, called fouling resistance, R_f, was calculated to see the capacity of these membranes upon being fouled with contaminants, i.e., NOM. R_f was subtracted from the following two equations:

$$J_{wo} = \frac{\Delta P}{\mu \times R_m} \quad [4.2]$$

$$J_{wf} = \frac{\Delta P}{\mu \times (R_m + R_f)} \quad [4.3]$$

where J_{wo} and J_{wf} (L/m^2h) are the flux after 50-hrs filtration with pure water (Milli-Q water) and final flux after 50-hrs filtration with NOM-containing water (ORW), respectively. R_m and R_f (1/m) are membrane resistance and fouling resistance parameters, respectively. μ (Ns/m^2) is the fluid viscosity and ΔP (N/m^2) is trans-membrane pressure difference.

Based on Figure 4.8, membrane M13 (0.5% nSMM) has the smallest and membrane M2 (4.5% nSMM) the largest fouling resistance. Through visual inspection after opening the test cell, it was found that membrane M13 (0.5% nSMM) had the largest degree of NOM deposition, which made the membrane surface look slightly brown. On the other hand, the surfaces of membrane M2 (4.5% nSMM) and M10 (1.5% nSMM) remained clean and white. Another observation was that the DOC removals by membranes M8 (3.0% nSMM) and M13 (0.5% nSMM) were lower than that of M2 (4.5% nSMM). One interesting conclusion could be drawn here that with the exception of 3.0 wt% nSMM, the more nSMM is added, the higher fouling resistance and the lower DOC removal (data not shown) the modified membranes can achieve. It might be due to the interaction between the hydrophobic chains (i.e., fluoro-hydrocarbon chains) on membrane surface and the hydrophobic fraction in NOM [18]. Charge repulsion can not be the cause for this phenomenon since NOM is normally negatively charged while the surface of PES-nSMM membranes (containing fluoro-hydrocarbon chains on the surface) could probably be neutral or even positive. If that was the case, higher nSMM concentration (assumingly more neutral) would attract NOM better. Nevertheless, lowest nSMM concentration (0.5 wt%) attracted more NOM on and through membranes, proving via its lowest fouling resistance.

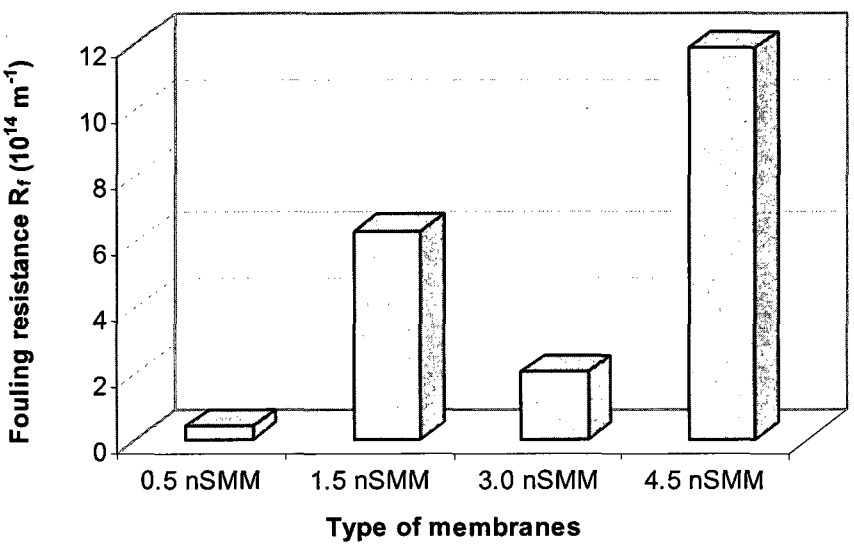

Figure 4.8. Fouling layer resistance after 50 hours of filtration Membranes:M2 (4.5 wt% nSMM), M8 (3.0 wt% nSMM), M10 (1.5 wt% nSMM) and M13 (0.5% nSMM); PES concentration, 18%; film thickness, 0.2mm; casting speed, 1. 5 cm/s

Effect of casting speed

The pure water permeation flux (PWP) and the initial DOC rejection (after 15min) at two casting speeds of 0.25 (slow) and 1.5 cm/s (fast) were presented in Figure 4.9. Three nSMM concentrations (1.5 wt%, 3.0 wt%, 4.5 wt%) in the casting solutions were used. For each nSMM concentration, both PWP and initial DOC rejection increased as the casting speed was increased. This result is consistent with the study of Ismail et al. [25] using polysulfone membranes for gas separation. They found that the asymmetric membranes made under high shear rates tended to exhibit higher pressure-normalized flux and selectivity. They have attributed this to the greater molecular orientation in the skin layer. In our study, higher casting speed was proportional to the higher shear rate, leading to greater molecular orientation and leaving bigger gaps (pores) between two aligned macromolecular nodules. When the casting speed slower and the shear rate was not as strong, the alignment of nodules was less and the gaps (pores) were smaller, resulting in smaller pores or lower MWCO. The casting speed had no effects on the apparent roughness of membranes (See M1 versus M2, M3 versus M4, etc in Figure 4.4).

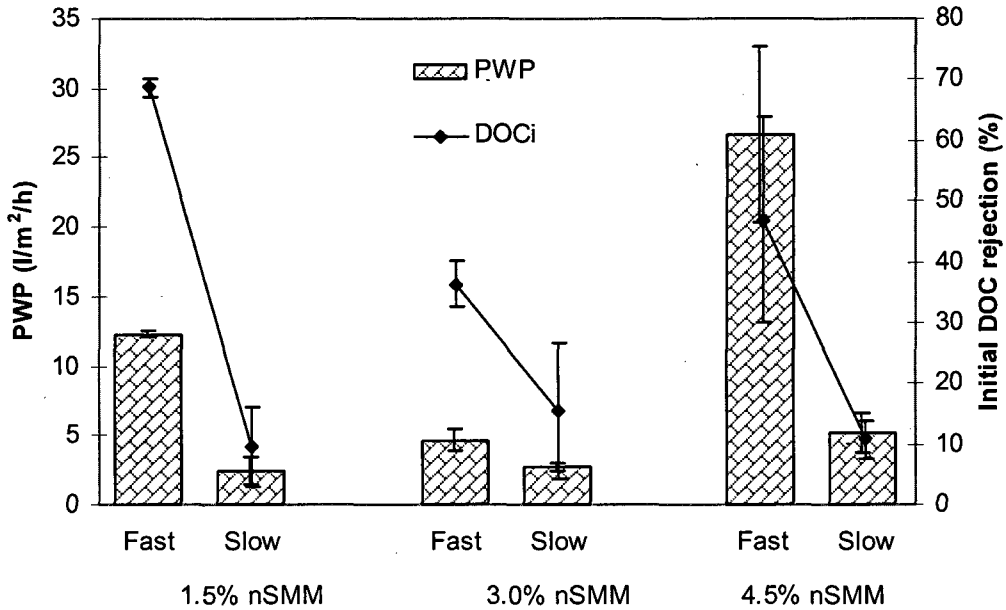

Figure 4.9. PWP and initial DOC rejection
Membranes: M10 (1.5 cm/s, 1.5% nSMM), M9 (0.25 cm/s, 1.5% nSMM), M8 (1.5 cm/s, 3.0% nSMM), M7 (0.25 cm/s, 3.0% nSMM), M2 (1.5 cm/s, 4.5% nSMM) and M1 (0.25 cm/s, 4.5% nSMM); PES concentration, 18%; cast film thickness, 0.2 mm.

Effect of membrane thickness

Figure 4.10 shows molecular weight cut-off (MWCO, molecular weight that yields 90% solute separation) and mean pore size data for two different thicknesses of the cast films. Two nSMM concentrations in the casting solutions were investigated. The data reveals that both MWCO and the mean pore size decreased as the thickness increased. The effect of film thickness has been reported by several researchers [24, 26]. Suk et al. [24] rendered that the reduced membrane thickness would lower the surface energy with higher content of fluorine. Contact angles increased from 80 ° to 106° for the thinnest membranes. In Veerapur's study [26], they found that increase in the membrane thickness resulted in a decrease in flux with a somewhat lesser profound effect on the selectivity of the membranes in their pervaporation study. It is noted that the Veerapur's study was for hydrophilic membranes. Even though no proper elucidation has been reported before, in our case, the explanation again may lie on the shear stress during the film casting. Since the shear stress is directly proportional to casting velocity and inversely proportional to

film thickness (Shear stress = (viscosity)*(velocity/thickness)), the shear stress increases by either increasing the casting velocity or by decreasing the thickness. Therefore, decreasing the thickness has the same effect on shear stress as increasing the casting speed. As discussed in the effect of casting speed, the increased shear stress presumably led to larger pore size as a result of the better alignment of the polymer nodules. Thus the thinner membrane films had a larger mean pore size or MWCO.

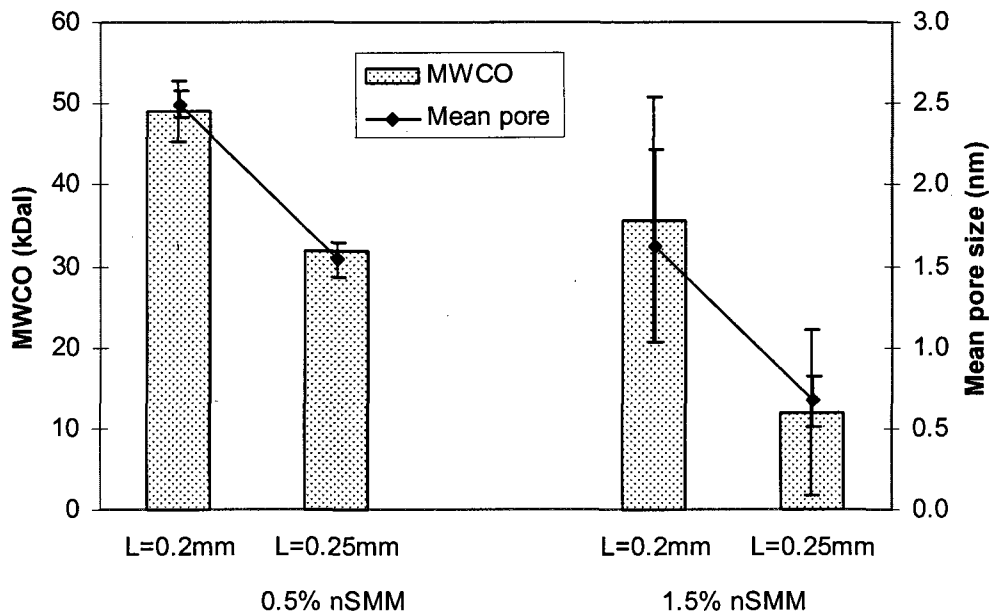

Figure 4.10. Pore characteristics
Membranes: M13 (0.2mm thickness, 0.5% nSMM), M14 (0.25mm thickness, 0.5% nSMM), M10 (0.2mm thickness, 1.5% nSMM), M12 (0.25mm thickness, 1.5% nSMM); PES concentration, 18%; casting speed, 1.5 mm.

Effect of post treatment

The nSMM membranes were post treated by immersing them in 0.1 M sodium hydroxide solution for 24 hrs to make the membrane surface more hydrophilic (due to the OH^- group sorption). The comparison of performance without and with post treatment is made in Table 4.3 for membrane M13. Increase in PWP, final flux and DOC rejection are noticeable from the Table 4.3. Thus, post-treatment by aqueous NaOH solution proved to be desirable. Probably, this resulted from the hydrophilization of the membrane surface by breaking down the fluorohydrocarbon chain or the backbone of PES. In fact, the

contact angles for M7 (3.0 wt% nSMM + 18 wt% PES) were decreased from 85 ± 4.4° to 69 ± 2.0° without and with NaOH post treatment, respectively.

Table 4.3 Performance of M13 (0.5 wt% nSMM + 18 wt% PES) membranes with and without NaOH post treatment

Condition	PWP (l/m^2h)	Final flux (l/m^2h)	Final DOC rejection (after 50 hours) (%)	Initial DOC rejection (after 15min) (%)	Volume treated (l/m^2)*
Without Post	13.19 (2.91)**	10.86 (4.82)	69.73 (14.06)	69.93 (8.66)	391.31 (10.31)
With Post	24.59 (5.35)	20.16 (5.71)	79.50 (0.36)	78.42 (2.15)	1100.57 (274.9)

** Volume of water treated was accumulated after 50-hrs fouling test*

*** Values in bracket are standard deviation*

Post treatment using sodium hypochlorite, ammonium persulphate [27], sodium hydroxide, potassium hydroxide, ethanolamine [6, 28] has been reported modifying membranes to some extent. Wan et al. [27] concluded that post treatment by ammonium persulphate made the pores become bigger, so the solute rejection was zero. Jung et al. [28] observed the opposite in which the surface became smoother with the post treatment of sodium hypochlorite due to the decomposition of PVP by sodium hypochlorite. The difference may be due to different types of membranes studied. Increase in flux was achieved more effectively for inorganic based sodium hydroxide/hydrochloric acid post treatment via 30 min circulation at 30°C [6].

To test if the effects of the five variables involved in the membrane casting are statistically significant, a one-way ANOVA test was conducted using Minitab 15 statistical software (Minitab Inc. State College PA). The null hypothesis (H_0), in which the effect of any particular independent variable on each of the response variables does not exist, was rejected if P-value ≤ 0.05 ($\alpha = 0.05$ or 5%). Therefore, for the P-values to be statistically significant they should be ≤ 0.05. Table 4.4 summarizes the results of the statistical analysis. Apparently, only additive concentration had significant impacts on the DOC removal, flux reduction and final flux. It is worth noting that these changes in performance because of different additive concentrations were not accompanied by

statistically significant changes in contact angles. Post treatment has impact solely on the flux reduction.

Table 4.4 P-values of the independent variables obtained from the analysis of variance (one-way ANOVA) for the performance variables

Source of variation	P-values		
	Solute rejection	Flux reduction	Final Flux
PES concentration (wt%)	0.07 – NO	0.744- NO	0.207 - NO
nSMM concentration (wt%)	0.014 - YES	0.004 – YES	0.041 - YES
Casting speed (m/s)	0.167 - NO	0.385 – NO	0.097 - NO
Thickness of membrane film (mm)	0.684 - NO	0.400 – NO	0.091 - NO
Post treatment	0.429 - NO	0.039 – YES	0.220 - NO

4.4.5 Modeling

This section is concerned with the fouling mechanism for membranes of different nSMM loading. To study the mechanisms leading to membrane fouling, the common practice consists of assuming that one of the four fouling mechanisms (e.g., cake formation, intermediate blocking, pore constriction (standard blocking) and complete blocking) takes place. The differential rate laws corresponding to all possible fouling mechanisms were proposed by Hermia (1982) [29] for dead-end filtration under constant applied pressure:

$$\frac{dJ}{dt} = kJ(J)^{2-n} \qquad [4.4]$$

where k is a fouling coefficient and n is a dimensionless filtration constant, which depends on the type of filtration. The constant n has values of 0, 1, 1.5 and 2 for cake filtration, intermediate blocking, standard blocking and complete blocking, respectively. The filtration experiments in this study however used cross-flow mode. Cross-flow mode has been claimed to enhance mass transfer processes that induce back transport from the membrane surface, leading to lower net flux of foulant to the membrane surface [30]. The unifying equation for cross-flow filtration applied in this study was:

$$\frac{dJ}{dt} = -k(J - J^*)(J)^{2-n} \qquad [4.5]$$

where J* is a critical flux (L/m2/h) and n can take the same values as in equation [4.4]. Determination of k, J* with corresponding n was performed using MATLAB 7.0 (Math Works, Natick, MA).

Table 4.5 presents the regressed model coefficients as well as mean square roots - MSR. Figure 4.11 shows the experimental data (circles) and simulated data (lines) for different fouling mechanisms (n values). Membrane M2 (4.5% nSMM) was taken as an example. It appears that the best fitted (i.e., has the lowest MSR) mechanism varies for every single case. Increasing concentration of nSMM affected the fouling mechanism since the best fit model changed. Intermediate blocking (n=1) best described the fouling of 0.5 wt% nSMM membranes while complete blocking (n=2) was the main fouling mechanisms for 1.5, 3.0 and for 4.5 wt% nSMM membranes, the MRS values are too close to distinguish among the various mechanisms.

Table 4.5 Fitting parameters and mean square residuals for membranes of different nSMM loading

Membranes	n (dimensionless)	k (dimensionless)	J* (L/m2/h)	MSR
M13 (0.5 wt% of nSMM)				
	0.0	0.0003	6.3364	1.0663
	1.0	-0.0211	10.5017	0.5231
	1.5	-0.0185	10.6172	0.9807
	2.0	-0.2672	10.5195	0.5843
M10 (1.5 wt% of nSMM)				
	0.0	0.2957	1.6436	0.4681
	1.0	0.0045	3.4272	0.6870
	1.5	-0.0612	1.5849	0.3584
	2.0	-0.5279	1.7952	0.0515
M8 (3.0 wt% of nSMM)				
	0.0	0.0052	2.8620	2.0494
	1.0	-0.0067	2.1613	1.9776
	1.5	-0.0566	2.4426	2.8842
	2.0	-0.0157	0.0952	1.3758
M2 (4.5 wt% of nSMM)				
	0.0	0.1062	1.2006	0.0114
	1.0	-0.0838	1.2260	0.0067
	1.5	-0.1141	1.3028	0.0089
	2.0	-0.1632	1.2480	0.0089

Noted that the MWCOs of 3.0 and 4.5 wt% PES-nSMM membranes were from 3.5-5 kDal with mean pore sizes are less than 0.5nm. The loose NF membranes often have MWCOs ranging from less than 1 kDal to several kDal for the treatment of drinking water [31]. So they can be considered as loose nanofiltration (NF) membranes, for which the major fouling mechanism was found to be intermediate or complete blocking [32].

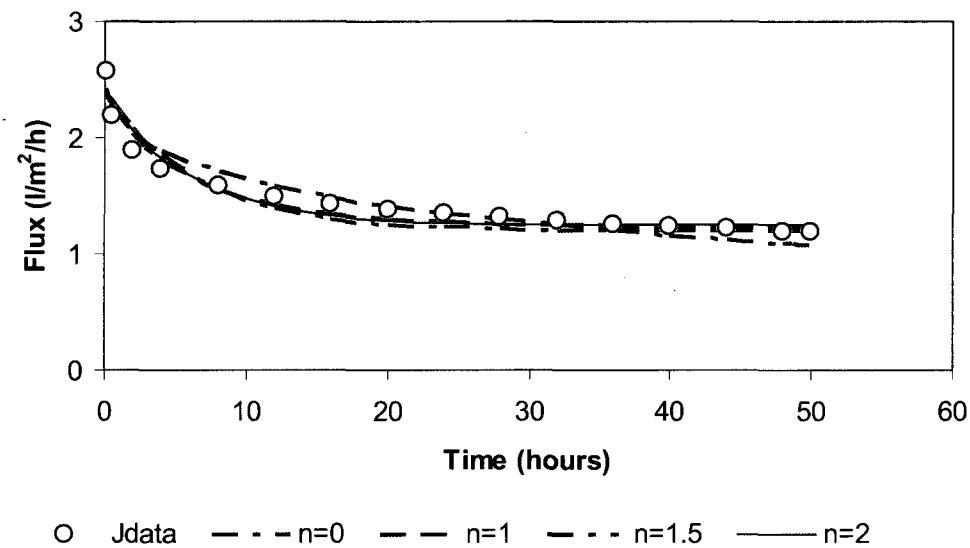

Figure 4.11. Fitting of experimental data (open circle) by different n values for M2 (4.5 wt% nSMM) membranes

Mosqueda et al., [15] found in their study that cake formation was the best fitted model which was definitely not the case for this study. The difference may be ascribed to different membranes and testing protocols even though a similar feed (NOM containing water) was used. It is worth noting that the values of J*, the critical flux, were close to the final fluxes after 50-hour testing period. In addition, when the degree of fouling became more serious (from n=0 to n=2), the fluxes often decreased more slowly and k showed larger negative values. In other words, smaller values of k represent less dramatic flux decline. It was consistent with several studies [18, 29].

The single mechanism modeling in some cases does not fit well the experimental data due to the possible fact that more than one mechanism affecting membrane fouling. A combined cake formation and pore constriction model developed by Kilduff et al. [30] for cross-flow filtration mode was therefore introduced.

The area of open pores was expressed as:

$$A_{open} = A_T \exp\left[-\alpha C_b t\left(\frac{\Delta P}{\mu R_m} - J^*\right)\right] \quad [4.6]$$

Where A_T (=A_{open} + $A_{blocked}$) is the nominal membrane area (m^2); A_{open}: area of unblocked or open pores (m^2); $A_{blocked}$: area of membrane blocked by foulant (m^2); α: pore blockage parameter (m^2/kg); C_b: bulk concentration of the solute (kg/m^3); ΔP: applied pressure (Pa); μ: solution viscosity (kg/m/s); R_m: membrane resistance (m^{-1}).

The rate of cake resistance, which is assumed to be equal to the mass of solute transported to the surface, was integrated analytically from $R_{c,0}$ to R_c:

$$\frac{dR_c}{dt} = \alpha_c (A_T - A_{open}) C_b \left(\frac{\Delta P}{\mu(R_m + R_c)} - J^*\right) \quad [4.7]$$

Where α_c: specific resistance of the cake ($m^{-1}kg^{-1}$) and $R_{c,0}$: resistance of the initial deposit (m^{-1})

Finally the modeled flux was calculated with the equation:

$$J_T = \frac{A_{open}\Delta P}{\mu R_m} + \frac{(A_T - A_{open})\Delta P}{\mu(R_m + R_c)} \quad [4.8]$$

Parameters such as α, αc, Rc and J* were optimized using Microsoft Excel Solver and MATLAB 7.0 (Math Works, Natick, MA). Mosqueda et al. [15] found that the combined mechanism fitted the experimental data better than the single one with a smaller mean square error (MSR). It is confirmed again by this study (Figure 4.12).

The MSR of combined-mechanism model are all smaller than those of single mechanism model (Table 4.5), proving the combined simulates better the fouling mechanism. Autopsy of fouled membranes suggested that the irreversible fouling layer was initially formed by pore blocking of small particles followed by strong interaction of fouling layer with mainly dissolved materials and by fouling layer compaction due to permeation drag [33].

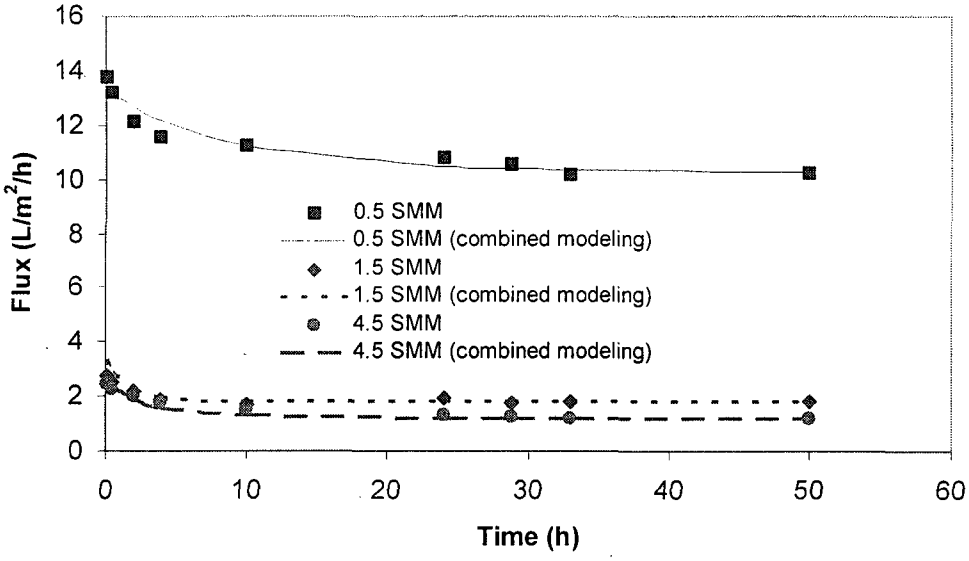

Figure 4.12. Flux reduction with time for combined-mechanism model for different types of membranes

Table 4.6: Fitting parameters for combined fouling mechanism model

Membranes	α	α_c	$R_{c,0}$	J*	MSR	MSR (Single)$^+$
0.5 SMM	0.3020	1.05E+20	1.01E+17	10.255	0.011	0.523
1.5 SMM	0.3885	1.50E+22	3.89E+17	1.795	0.006	0.052
3.0 SMM	0.1885	1.50E+19	3.69E+17	2.690	0.202	1.376
4.5 SMM	0.5619	1.50E+22	5.05E+17	1.182	0.001	0.007

$^+$: *the smallest MSR obtained from single model.*

Again, for the case of 3.0 SMM, since the data was not smooth, the simulated flux did not fit well. Its MSR was small because the values of fluxes were small, so the difference was not significant. Regardless to the case of 3.0 SMM, the specific cake resistance parameter α_c, pore block parameter α and the resistance of the initial fouling layer $R_{c,0}$ seem to be slightly affected with the increasing concentration of SMM. Moreover, the higher the flux permeation was, the lower was the resistance. This agrees with the fact that higher SMM concentration membranes had very little NOM deposition on the surface at the end of the experiment (membranes were almost clean).

4.5 Conclusions

Several conclusions can be drawn from observing the results of this study as follows:

1. The synthesis of nSMM was successful. Characterization of nSMM was performed by NMR, GPC, DSC and elemental analysis. FTIR results confirmed the enrichment of nSMM at the top surface through migration during the cast process.
2. Among the five affecting factors studied in this research (polymer concentration, additive concentration, casting speed, thickness and post-treatment), only the additive concentration impacted the membrane performance (i.e., DOC removal and flux reduction) to a statistically significant level. This was confirmed by one-way ANOVA statistical analysis. Even though other factors such as membrane thickness may alter the pore characteristic, their effect on membrane performance was marginal.
3. Single fouling mechanism modeling suggested that the fouling by NOM of these hydrophobic membranes behaved like loose nanofiltration membranes which involved in mostly intermediate or complete pore blocking. A combined cake formation and pore constriction model simulated even better the fouling mechanism for those membranes.
4. During the filtration with NOM-containing river water most of NOM penetrated through the membrane to the permeate side probably due to the morphology of PES-nSMM membranes. They were rougher with deeper and bigger features which were more likely to deform under pressure.

4.6 Acknowledgement

The authors gratefully acknowledge Vietnam Government (Vietnamese Overseas Scholarship Programs -VOSP), Natural Sciences and Engineering Research Council of Canada (NSERC), and Ministry of the Environment (MOE), Ontario, Canada, for their financial support.

4.7 References

[1] R.E. Kesting, Synthetic Polymeric Membranes, McGraw-Hill Book Company, New

York, NY, 1971.

[2] T. Matsuura, Synthetic Membranes and Membrane Separation Processes, CRC Press, Boca Raton, FL, 1994.

[3] I. Pinnau, B.D. Freeman, Membrane formation and modification overview, in: I. Pinnau, B.D. Freeman (Eds), Membrane Formation and Modification, ACS Symposium Series 744, American Chemical Society, Washington, DC, 2000, pp. 1-22.

[4] L.Y. Lafrenière, F.D.F. Talbot, T. Matsuura, S. Sourirajan, Ind. Eng. Chem. Res. 26 (1987) 2385-2389.

[5] W.R. Bowen, T.A. Doneva, H.B. Yin, J. Membr. Sci. 181 (2001) 253-263.

[6] H.R. Lokhare, S.C. Kumbharkar, Y.S. Bhole, U.K. Kharul, J. Appl. Polym. Sci. 101 (2005) 4378-4385.

[7] A. Idris, N.M. Zain, M.Y. Noordin, Desalination 207 (2007) 324-339.

[8] G. Arthannareeswaran, D. Mohan, M. Raajenthiren, Appl. Surf. Sci. 253 (2007) 8705-8712.

[9] J. Wang, Y. Xu, L. Zhu, J. Li, B. Zhu, Polymer 49 (2008) 3256-3264.

[10] A. Rahimpour, S.S. Madaeni, S. Mehdipour-Ataei, J. Membr. Sci. 311 (2008) 349-359.

[11] A. Rahimpour, S.S. Madaeni, A.H. Taheri, Y. Mansourpanah, J. Membr. Sci. 313 (2008) 158-169.

[12] Y. Su, C. Li, W. Zhao, Q. Shi, H. Wang, Z. Jiang, S. Zhu, J. Membr. Sci. 322 (2008) 171-177.

[13] D.B. Mosqueda-Jimenez, R.M. Narbaitz, T. Matsuura, Sep. Purif. Technol. 37 (2004) 51-67.

[14] D.B. Mosqueda-Jimenez, R.M. Narbaitz, T. Matsuura, G. Chowdhury, G. Pleizier, J.P. Santerre, J. Membr. Sci. 231 (2004) 209-224.

[15] D.B. Mosqueda-Jimenez, R.M. Narbaitz, T. Matsuura, J. Appl. Polym. Sci. 99 (2006) 2978-2988.

[16] D.E. Suk, T. Matsuura, H.B. Park, Y.M. Lee, J. Membr. Sci. 277 (2006) 177-185.

[17] M. Mulder, Basic Principles of Membrane Technology, Kluwer Academic Publishers, Dordrecht, The Netherlands, 1996.

[18] H.T. Dang, C. Amelot, D. Rana, R.M. Narbaitz, T. Matsuura, J. Appl. Polym. Sci. (2008) communicated.

[19] H.T. Dang, R.M. Narbaitz, T. Matsuura, J. Membr. Sci. 323 (2008) 45-52.

[20] M. Khayet, D.E. Suk, R.M. Narbaitz, J.P. Santerre, T. Matsuura, J. Appl. Polym. Sci. 89 (2003) 2902-2916.

[21] L. Zhang, G. Chowdhury, C. Feng, T. Matsuura, R.M. Narbaitz, J. Appl. Polym. Sci. 88 (2003) 3132-3138.

[22] V.A. Pham, J.P. Santerre, T. Matsuura, R.M. Narbaitz, J. Appl. Polym. Sci. 73 (1999) 1363-1378.

[23] M. Khayet, C.Y. Feng, T. Matsuura, J. Membr. Sci. 213 (2003) 159-180.

[24] D.E. Suk, G. Chowdhury, T. Matsuura, R.M. Narbaitz, P. Santerre, G. Pleizier, Y. Deslandes, Macromolecules 35 (2002) 3017-3021.

[25] A.F. Ismail, B.C. Ng, W.A.W.A. Rahman, Sep. Purif. Technol. 33 (2003) 255-272.

[26] R.S. Veerapur, K.B. Gudasi, T.M. Aminabhavi, J. Membr. Sci. 304 (2007) 102-111.

[27] L.-S. Wan, Z.-K. Xu, X.-J. Huang, A.-F. Che, Z.-G. Wang, J. Membr. Sci. 277 (2006) 157-164.

[28] B. Jung, J.K. Yoon, B. Kim, H.-W. Rhee, J. Membr. Sci. 243 (2004) 45-57.

[29] J. Hermia, J. Trans. Inst. Chem. Eng., 60 (1982) 183-187.

[30] J. E. Kilduff, S. Mattaraj, J. Sensibaugh, J. P. Pieracci, Y. Yuan, G. Belfort. Env. Eng. Sci., 19(2002) 477-495.

[31] X.-L. Wang, W.-J. Shang, D.-X. Wang, L. Wu, C.-H. Tu, Desalination, 236 (2009) 316-326.

[32] M. Bodzeka, A. Waniek, K. Konieczny, Desalination 147 (2002) 101-107.

[33] H. Choi, K. Zhang, D. D. Dionysiou, D. B. Oerther, G. A. Sorial, Sep. Puri. Technol. 45 (2005) 68-78.

Abbreviations: ANOVA, analysis of variance; ATR, attenuated total reflection; DMAc, N,N-dimethyl acetamide; DOC; dissolved organic carbon; DSC, differential scanning calorimeter; FTIR, Fourier transform infrared; GPC, gel permeation chromatography; ICP-AES, inductively coupled plasma - atomic emission spectrometry; nSMM, hydrophobic SMM; LSMM, hydrophilic SMM; MDI, diphenylmethane diisocyanate;

MF, microfiltration ; MPC, methacryloyloxyethylphosphorylcholine ; MWCO, molecular weight cut-off; NF, nanofiltration ; NMP, N-methyl pyrrolidinone; NMR, nuclear magnetic resonance; NOM, natural organic matter; OFA, oligomeric fluoro-alcohol; ORW, Ottawa river water; PAI, poly(amide imide); PDMS, α,ω-aminopropyl poly(dimethyl siloxane); PEG, poly(ethylene glycol); PES, poly(ether sulfone); PPG, poly(propylene glycol); PVP, poly(vinyl pyrrolidone); PWP, pure water permeation; SEM, scanning electron microscopy; SMM, surface modifying macromolecule; THF, tetrahydrofuran; UF, ultrafiltration;

Nomenclature

$J_{pure\ water}$	flux of pure water ($L/m^2/h$)
$J_{fouled\ water}$	flux of fouled water ($L/m^2/h$)
M_n	number average molecular weight
M_w	weight average molecular weight
T_g	glass transition temperature (^oC)
R_c	fouling resistance (m^{-1})
R_m	resistance of membrane (m^{-1})
$R_{c,0}$	resistance of the initial deposit (m^{-1})
A_{open}	area of unblocked or open pores (m^2)
$A_{blocked}$	area of membrane blocked by foulant (m^2)
C_b	bulk concentration of the solute (kg/m^3)
Greek letter	
ΔP	trans-membrane pressure (Pa)
μ	fluid viscosity (kg/m/s)
Δp	threshold value of pressure (Pa),
σ	surface tension of the feed solution (mJ/m^2)
r	pore radius (mm)
α	pore blockage parameter (m^2/kg)
α_c	specific resistance of the cake ($m^{-1}kg^{-1}$)

CHAPTER 5

DOUBLE-PASS CASTING: A NOVEL TECHNIQUE FOR DEVELOPING HIGH PERFORMANCE ULTRAFILTRATION MEMBRANES

Huyen T. Dang[1], Roberto M. Narbaitz[1], Takeshi Matsuura[2],

[1]*Dept. of Civil Engineering, Univ. of Ottawa, 161 Louis Pasteur St., Ottawa, K1N 6N5, Canada*

[2]*Dept. of Chemical and Biological Engineering,, Univ. of Ottawa, 161 Louis Pasteur St., Ottawa, K1N 6N5, Canada*

5.1. Abstract

Double-pass casting was evaluated as a technique to overcome hard-to-cast membranes or hard-to-mix solutions. Two types of polyethersulfone (PES) membranes were tested, one incorporating a hydrophilic surface modifying additive and the other with a hydrophobic one. It was found that the morphological improvement was more obvious for hydrophobic membranes since their solutions were not completely homogenous and hard-to-cast. The double-pass hydrophobic membranes had smoother surfaces and more porous support layers, resulting in higher fluxes, higher volume of treated water (67.4% increase) but decreased natural organic matters (NOM) rejection. The new casting approach produced hydrophilic membranes having a spongy structure (as opposed to finger-like cavities), yet they had similar NOM rejection, a 12.4% higher flux than the single-pass membranes prepared from the same dope. This is attributed to the quite homogenous hydrophilic casting solutions and to the performance of the original hydrophilic membranes (single-pass casting) that was relatively good.

Key words: PES-based ultrafiltration membranes, double-pass casting method, membrane surface characterization, flux performance.

5.2. Introduction

Surface modification of membranes by blending surface modifying additives has been proved successful for fouling mitigation in membrane technology. The additives could be hydrophobic [1-4], hydrophilic [5-7] or charged polymers [8-9]. However, problems may arise in mixing the principal polymers used to prepare a film with polymeric additives and solvents. These solutions may mix well but easily become heterogeneous and separate into phases when they are put into the dessicator for degassing. The bubbles produced during dope filtering (prior to casting) are sometimes hard to remove.

The phase inversion technique which is commonly used for the fabrication of ultrafiltration membranes involves a single casting step, forming one layer. If the solution has bubbles, numerous random holes will certainly be found in the resulting membranes. The hypothesis of this study is that many of these problems may be overcome by using a double-pass casting method. Basically, the second casting motion will cover the holes and/or valleys created during the nucleation of polymer-lean phase (de-mixing) after the first casting movement. As a result, the membranes produced via the double casting method are hypothesized to be smoother and hole-free. According to mixing theory, the compositions that lie in the miscible region of the phase diagram are normally chosen to prepare a casting dope to avoid the formation of heterogeneity in the membranes. The novel double-pass casting method enables successful casting of the dope that consists of a polymer blend, in which a minor polymeric component is mixed with a host polymer, even when the composition lies in the immiscible region. By employing this way of making membranes, it may no longer be necessary for researchers to be as concerned about the properties of casting solutions (viscosity, bubble content and even phase separation).

This idea of making membrane is unique and diverse from previous studies that employed two-layer casting solutions or cast two or more polymer solutions at the same time to produce membranes of multilayered structure [10, 11]. In this study, only one solution was employed and mixed completely before being cast. Likewise, the new double casting technique is not used to form two-layer membranes but hole-free and smooth membranes.

This study aims to test membranes created with and without the application of new casting method, and to compare the membrane characteristics and their performance in terms of fluxes, and solute removal.

5.3. Materials and Methods

5.3.1 Water source

Ottawa River water (ORW) collected from the intake of the Britannia Water Treatment Plant (Ottawa, Ontario) in April 2007 was used as feed water for the fouling tests. The raw water was clear and had low alkalinity (44 mg $CaCO_3$/L), low hardness (46 mg $CaCO_3$/L), low turbidity (7.57 ± 0.002 NTU), low conductivity (0.11 mS/cm), pH of 7.5 but was highly colored (50 Pt/Co color unit). Dissolved organic carbon (DOC) concentration and ultra violet absorbance at 254nm wave length (UVA_{254}) were 6.78±0.01 mg/l and 0.308m^{-1} respectively. All the characterization methods followed the Standard Methods [12]. ORW was considered typical northern river water [13].

5.3.2 Chemicals

Deionised ultra pure water from a Milli-Q Water System (Millipore, Bedford, MA) was used for the preparation of all probe solutions and water permeation tests. Polyethersulfone (PES) (Victrex 4100P, ICI Advanced Materials, Billingham, UK) and N-methyl-2-pyrrolidone (NMP) (Aldrich Chemical Company, Inc., Milwaukee, WI) were used as the casting solution's base polymer and solvent, respectively. PES has molecular weight of 31 kDal and polydispersity of 1.52. The probe solute for the solute transport method was either polyethylene glycol (PEG) (Sigma Chemical, St. Louis, MO), or polyethylene oxide (PEO) (Aldrich Chemical, Milwaukee, WI). These polymers exhibit low membrane-solute interactions; hence they are ideal as probe solutes [14]. The molecular weight of the different PEG solutes ranged from 6 to 35 kDalton, while that of PEO was 100 kDalton. The additives, also called as surface modifying macromolecules (SMM), were the hydrophilic LSMM6 [15] and the hydrophobic nSMM [16]. They were added in the casting solutions to modify the surface characteristics of the membranes (i.e., more hydrophilic or hydrophobic). These are tailor made polymers synthesized via a

two-step procedure: The initial step involved the reaction of methylene bis-ρ-phenyl diisocyanate (MDI) with polypropylene glycol (PPG), in a common solvent of N,N-Dimethylacetamide (DMAc) to form a urethane prepolymer. The reaction was then terminated by the addition of PEG (molecular weight 600 Dal) resulting in hydrophilic surface modifying macromolecules (LSMM6). In case of nSMM, the MDI and polydimethylsiloxane (PDMS) were dissolved in a solvent of tetrahydrofurane (THF) to produce prepolymer, then end-capped with Zonyl BA-L. Details about the chemical structures and characteristics of the additives can be found in the above studies.

5.3.3 Membrane tested

Four sets of membranes were prepared using two different solutions and two casting methods. Details of these membranes are presented in Table 5.1. The PES-HO membranes were cast from a solution of 18% wt PES (as the base polymer) blended with 3% wt of hydrophobic additives and dissolved in 79% wt NMP (as the solvent). The solution viscosity (measured by rotational viscometer LVT C2443 (Brookfield co., Middleboro, MA) was 671.4 cP and 622 cP for PES-LSMM and PES-SMM respectively. These data were obtained by multipling the dial reading number (corresponding to the torque required to rotate a spindle at constant speed) with the spindle factor. The surface tensions of these solutions were analyzed based on the principle of the Pendant drop method using the VCA Optima goniometer. They were 13.43 ± 0.59 (mJ/m^2) for PES-SMM solution and 19.194 ± 0.38 (mJ/m^2) for PES-LSMM solution.

The solutions were cast via the phase inversion technique in which the casting solution was poured onto a dust-free glass plate and spread using a single pass of casting bar with a 0.2mm gap. The casting speed (i.e., the speed at which the casting bar is manually moved) was evaluated as 1.5 cm/s to create a 11-cm wide and 15-cm long membrane film. The Double PES-HO membranes employed the same casting solution but were fabricated using the double-pass casting method. Upon finishing the first regular casting movement (Step 1 and 2 in Figure 5.1a, about ten seconds), the casting bar was immediately (zero time delay) moved in the opposite direction back to its original position and during the process (Step 3 Figure 5.1b, another ten seconds), the solution was spread again. The steps of the new casting method and the hypothesized impact on

membrane morphology are depicted in Figure 5.1. After casting, the support plates with the cast solutions were submerged in a four-degree centigrade water coagulation bath until polymer solidification was completed. Both membranes were the same nominal thickness and prepared under the same conditions i.e., dust-free support material, casting bar (0.2 mm gap, 66° wettability), fume hood (8% humidity, 22±0.5 °C) and coagulation bath. The PES-HI and Double PES-HI membranes were made under a similar mode but using a casting solution containing hydrophilic additive LSMM6 instead of the hydrophobic nSMM. The new casting method was again followed to make Double PES-HI membranes from the above solution. The thickness of films measured by a Digimatic caliper (Mitutoyo Corporation, Japan) either slightly increased or decreased for the double casting films. The contact angles created by the casting knife and the glass plates were 27.6 (±0.95) and 24.95 (±0.49) degrees for PES-LSMM and PES-SMM solutions respectively. There seems to be a slight difference for the contact angles. This agrees with the slight difference in viscosities of these solutions. The hydrophobic solution's viscosity (622 cP) is a bit smaller than that of the hydrophilic (671.4 cP). Since PES-SMM was less viscous, the solution was easier to be spread under the stress of casting knife and moved by itself after that. In addition, the shear-stress onto the liquid films from those different solutions during the single or double casting was almost similar due to the same casting speed, shear rate and just slightly different viscosity.

Table 5.1 Membrane description

Membranes	Components	Casting method	Surface characteristics
PES-HI	**PES**-NMP-**H**ydroph**I**lic additives	Single-pass cast	Hydrophilic
Double PES-HI	**PES**-NMP-**H**ydroph**I**lic additives	Double-pass cast	Hydrophilic
PES-HO	**PES**-NMP-**H**ydroph**O**bic additives	Single-pass cast	Hydrophobic
Double PES-HO	**PES**-NMP-**H**ydroph**O**bic additives	Double-pass cast	Hydrophobic

The performance of the hydrophobic and hydrophilic membranes will be evaluated in more detail in our later studies. It is worth noting that all the solutions were mixed overnight in an incubator shaker at 35°C, then filtered and finally degassed in a

dessicator. However, the bubbles created during the filtration and long-term storage caused the visible holes throughout the membranes or caused wrinkled surfaces. As discussed above, the double-pass casting method will be evaluated in an attempt to produce smoother and hole-free membranes.

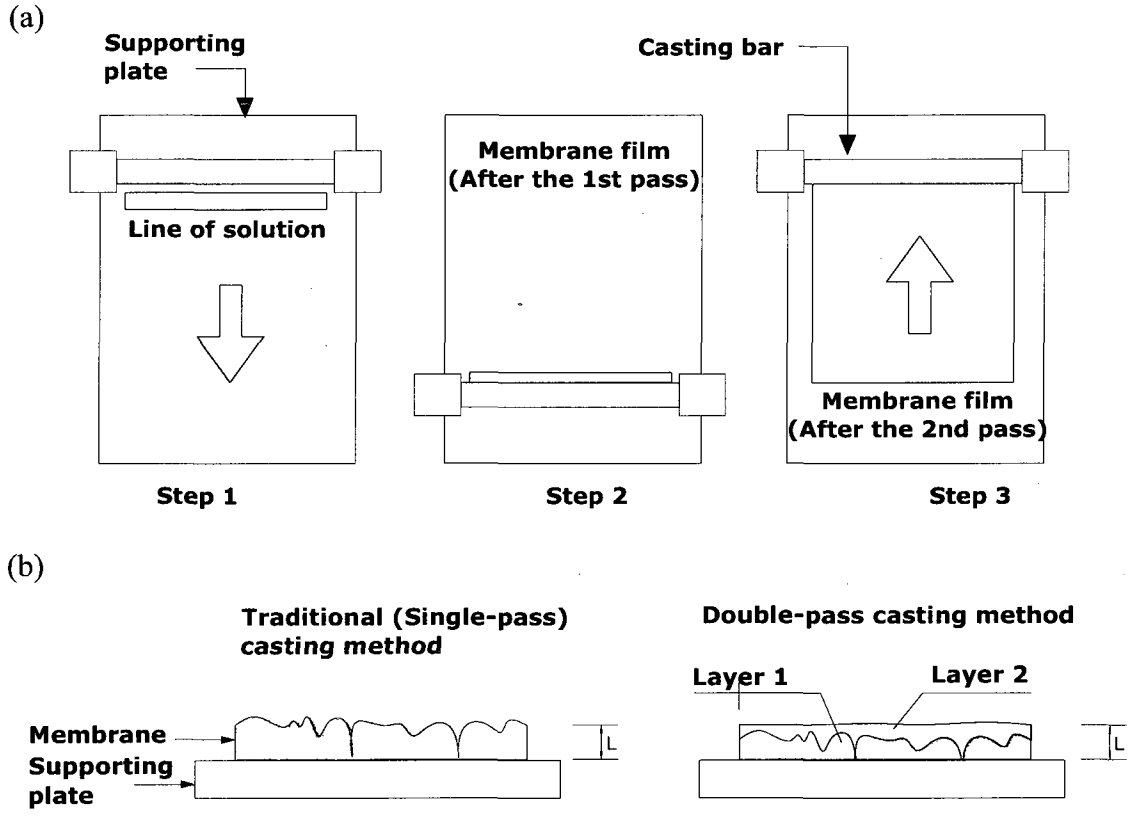

Figure 5.1. (a) Schematic representation of casting steps and (b) Hypothesized impact on the membrane cross-section

5.3.4 Testing protocol

The ultrafiltration apparatus consists of six cells in a series ultrafiltration system, each cell being used to test one 52 mm diameter flat sheet membrane coupon. The existence of a possible cell order effect within a series system was disproved using an analysis of variance (ANOVA) test of a greaco-latin square type of design [3]. Membranes were pre-compacted for one hour at 552 kPa (80 psig) and room temperature. This was followed by 50 hours of pure water permeation (PWP) monitoring, i.e. ultra-pure water filtration at 345 kPa (50 psig), 1.1 Lpm flowrate and at room temperature, then followed by the PEG/PEO solute transport quantification and completed by a 144-hour long

filtration/fouling test using Ottawa River water (with the same feed flow rate and pressure). Fluxes and DOC concentrations in the feed and permeate were monitored to evaluate the flux and NOM rejection performance. The entire filtration test was conducted in replicate.

5.3.5 Analytical methods

In order to elucidate the impact of this new casting method on membrane characteristics and performances, several analyses were performed. A model JSM-6400 JEOL (Japan Electron Optics Limited, Japan) SEM was employed to observe the surface and cross-sectional area of the dry membranes. The hydrophobicity of the membranes was explored using a goniometer (VCA Optima, AST Products, Inc., Billerica, MA). The samples were dried naturally by putting between filter papers for seven days. Dry membranes were cut into 5 x 25mm pieces and fixed onto 25 x 75 x 1mm superfrost micro slides (VWR., Mississauga, ON) using electrical tapes. Advancing contact angles were measured by placing 0.25 to 2.25 μL water droplets on the membrane coupon, the values reported are the average of ten measurements. Porosity, pore density, mean pore size and molecular weight cut-off (MWCO) were obtained through the solute transport method [17]. This is essentially a continuation of the ultrafiltration test in which the feed is changed to solutions of different known molecular weight solutes for one-hour periods. The detailed procedure was described in a previous study [18].

5.4. Results and discussion

5.4.1 SEM images of new membranes

The impact of the new casting method on the morphology of the double-pass casting ultrafiltration membranes was investigated. SEM micrographs presenting the surfaces and cross-sections of the samples are depicted in Figure 5.5.1. All the images were captured at a magnification of 1000.

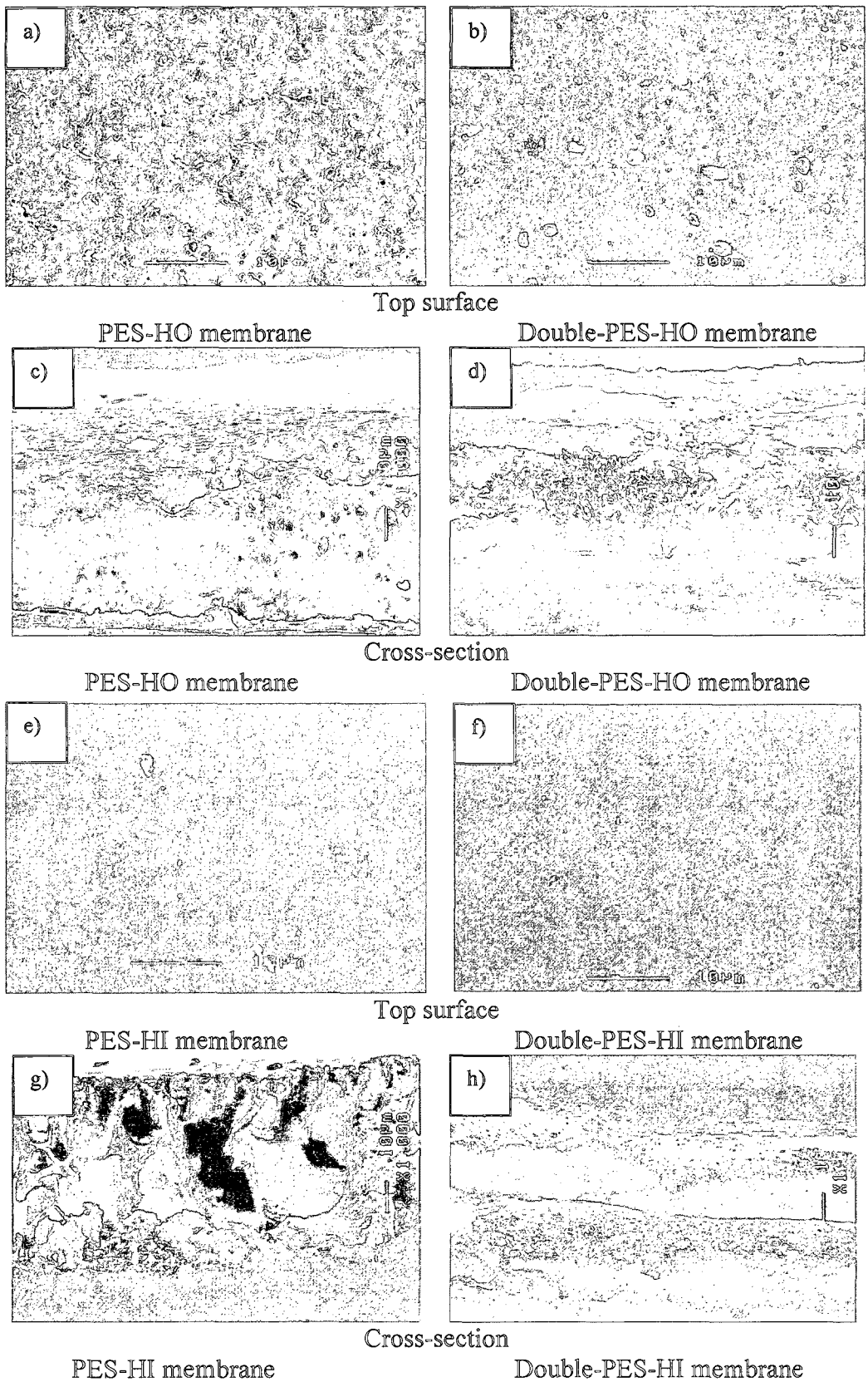

Figure 5.2. SEM images of membranes

The morphologies of the PES-HO and Double PES-HO membranes were very different. The surface changes significantly from rough (Figure 5.2a) with many valleys, ridges and holes to smooth (Figure 5.2b). However, the new surface still has some bumps of aggregated polymers generated during the process of membrane formation. The cross-section of these membranes revealed a big transformation. The apparently spongy form of the PES-HO membrane (Figure 5.2c) is replaced by a mixture of porous structure of the Double PES-HO membranes (Figure 5.2d).

There seems to be no appreciable surface variations between PES-HI and Double PES-HI membranes (Figures 5.2e and 5.2f). Only in the cross-section micrographs, did a two-layer spongy structure appear for the new casting method (Figures 5.2g and 5.2h). This is something expected as the second casting motion was done on top of the surface generated by the first casting motion. The gap between two layers (Figure 5.1h) may lead to some positive changes in membrane characteristics and performance, since the single cast PES-HI membrane very clearly exhibits large finger like cavities. These macro voids should be avoided whenever possible since they may rupture quickly or they are more susceptible to compaction under a high pressure [19]. Although the macro voids do not exist in the new Double PES-HI membranes, a larger portion of the cross-section seems to have more solid structure. The effect of the presence of the gap between two solid layers on the membrane performance is still unknown.

5.4.2 Response characteristics

Since the method of making membranes is significantly different, it is important to assess the response impact of their characteristics in terms of pore properties and contact angles.

5.4.2.1 Pore properties

Pore density, mean pore size and molecular weight cut-off (MWCO, a molecular weight that yields 90% solute separation) were obtained through the solute transport method as stated in section 2.5. Although SEM images seem to show no change on the surface of membranes for the two types of PES-HI membranes, the change in the cross-sectional view may be detected by the change in pore characteristics and MWCO.

Table 5.2 Pore characterization

Membranes	MWCO (kDal)	Mean pore size (nm)	Pore density (# of pore/m^2)
PES-HI	91.40 (3.93)	5.33 (0.63)	5.26 (0.45)
Double PES-HI	81.21 (2.05)	5.13 (0.07)	6.33 (0.17)
PES-HO	4.65 (0.61)	< 1.00 (0.06)	55.17 (11.73)
Double PES-HO	21.35 (3.13)	2.48 (0.41)	39.17 (3.28)

Note: Numbers in the brackets are standard deviations

For the PES-HI membranes, the double pass caused a reduction in MWCO from 91 kDal to 81 kDal. As observed in the SEM image, the Double PES-HI membrane has two layers of spongy structure, which may be the reason for the smaller mean pore sizes and MWCOs. As for the PES-HO membranes, their MWCOs were quite low, approaching those of nanofiltration membranes. The Double PES-HO membranes were however in the range of UF membranes. It is noted that even though the surface micro-image of the Double-PES-HO membrane looks smoother, the mean pore sizes of the Double PES-HO membranes were generally larger. Thus, the structure revealed by the cross-sectional images corresponded better to the performance. The larger pores may help increase the flux performance which will be discussed later.

It is worth noting that the hydrophobic casting solution was harder to cast than was the hydrophilic one. The solution for the hydrophobic PES-HO membranes was phase-separated and thus, required remixing before casting. In the case of PES-HI, the solution was quite homogenous and no phase separation was visible. The double casting method, hence, seems to have a stronger impact on the morphology and porosity of hard-to-cast PES-HO membranes. The impact on porosity can be seen in the probability density function plot (Figure 5.3), which provides the pore size distribution of all membranes.

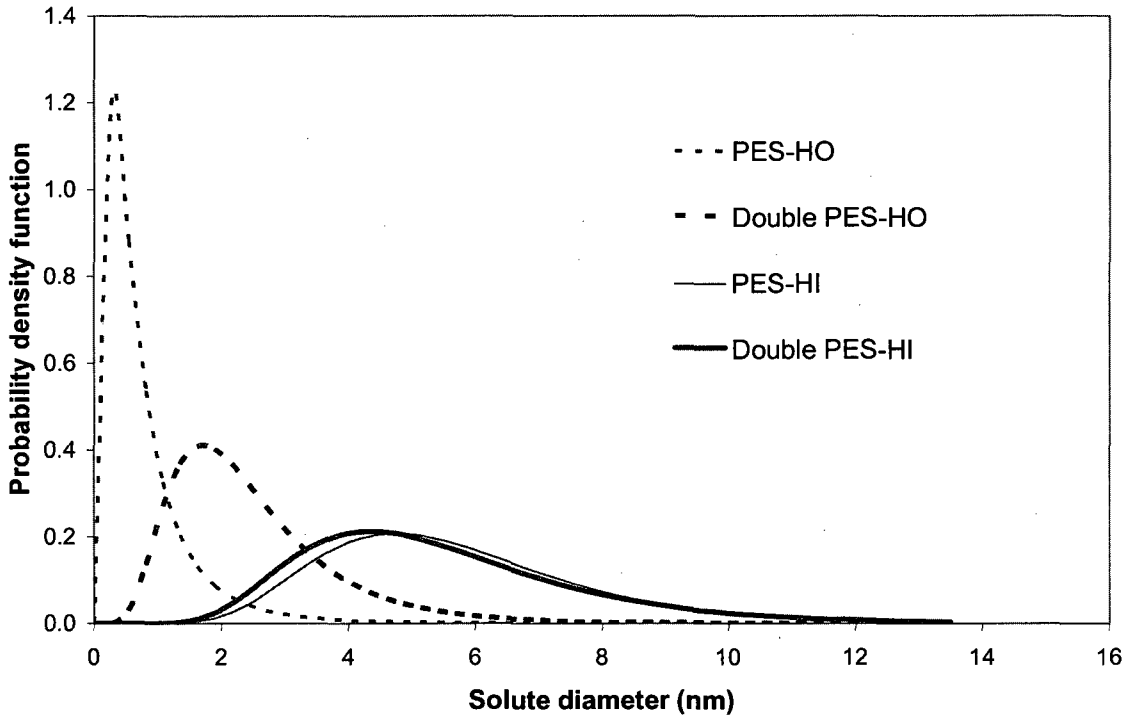

Figure 5.3. Membrane pore size distribution

It is observed that the most probable size of the pores (mode, maximum in the probability density function curves) is changed considerably from 0.5 nm for the PES-HO to nearly 2nm for the Double PES-HO while it is almost the same within the PES-HI group (slightly above 4 nm) . Table 5.2 also shows that the mean pore sizes are slightly more than 5 nm for the PES-HI membrane group. However, the pore distributions of these membranes are wider (diameters ranging from 1.8 nm to 11nm) than those of the hydrophobic membranes, especially the PES-HO. It is worth noting that the log-normal probability model represents just an approximation of the actual pore size distributions, particularly for pore sizes of less than 2nm, where the conditions are not purely steric and hydrodynamic interaction between solute and pores may not be ignored [17]. Nevertheless, the pore size and pore size distribution presented above display correctly the changes caused by the different modes of dope casting.

5.4.2.2. Contact angles

The advancing contact angles and contact angles as a function of time or drop age are shown for all the tested membranes in Figure 5.4. According to the small figure showing advancing contact angles, there is an obvious decrease in contact angle from the PES-HO

group to the PES-HI group, which is quite expected since the surface hydrophilicity should increase from PES-HO to PES-HI membranes. In particular, the order in the contact angle is PES-HO (averagely 85.5°) > PES control (about 70°) [5] > PES-HI (averagely 67.6°), which clearly shows the impact of blending either hydrophobic or hydrophilic additives.

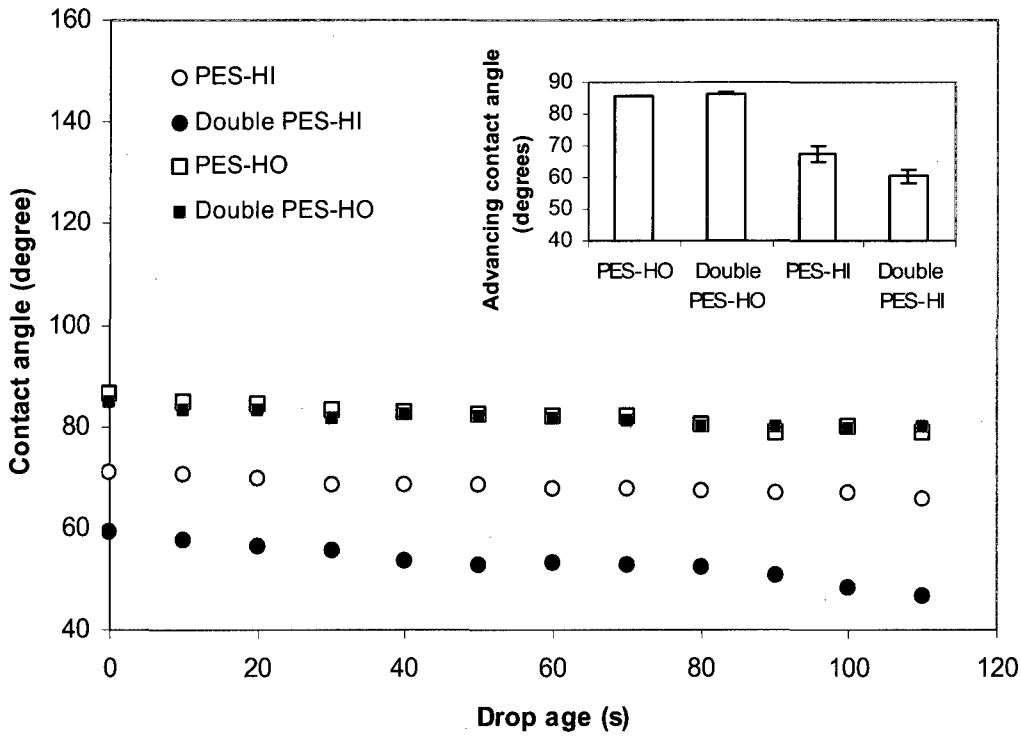

Figure 5.4. Contact angles measurement

The effect of the casting mode is not very clear. While the advancing contact angle remains almost the same for the PES-HO group (less than one degree difference), a significant decrease in the average advancing contact angle was observed from single-pass to double-pass casting for the PES-HI group (almost four-degree decrease). Furthermore, when the contact angles were monitored as a function of drop age (main figure), it is obvious that the trend observed in the advancing contact angle data is not an arbitrary or isolated phenomena. Figure 5.4 shows that as the initial advancing contact angle decreases, a stronger downward trend appears as a function of time. For example, while the decrease in the contact angle was limited to 6° within 110 s of the drop age for PES-OH and Double-PES-OH, it was about 15° for the Double PES-HI (advancing contact angle 60°). Apparently, the surface of the Double-PES-HI is more hydrophilic

and tends to draw more water into the membrane pores as the time passes (slope of -0.098). The PES-HI, on the other hand, showed a slower downward trend (slope of -0.043), similar to those for the PES-OH (slope of -0.063) and Double PES-OH membranes (slope of -0.041). The effect of the casting mode on the contact angle might be explained by the rate of SMM migration to the membrane surface. The hydrophobic n-SMM has been known to migrate to the membrane surface almost instantaneously upon membrane casting [16] due to its high incompatibility with the host PES polymer. The stronger surface instability observed when n-SMM was blended to the host PES was a clear evidence of the incompatibility. The surface hydrophobicity did not increase with time as the migration was completed within a first few seconds. On the other hand, the surface migration of hydrophilic SMM might take longer since they are more compatible with the host PES. When the membrane casting period was doubled, more hydrophilic SMMs would migrate to the membrane surface, lowering the hydrophilicity, and thereby enhancing the contact angles.

To test if the effect of the variables involved in the membrane casting is statistically significant, the ANOVA test was employed and the results presented in Table 5.3.

Table 5.3 P-values of the independent variables obtained from the analysis of variance (ANOVA) for the characteristic variables ($\alpha = 0.05$)

Source of variation	MWCO[a]	Mean pore size	Pore density	Contact angles
MAIN EFFECTS				
A: SMM type	**0.000**[b]	**0.000**	**0.001**	**0.000**
B: Casting method	0.216	**0.036**	0.160	**0.050**
INTERACTIONS				
AB	**0.002**	**0.016**	0.117	**0.024**

[a] *MWCO = Molecular weight cut-off*

[b] *If P-value ≤ 0.05 the effect is statistically significant and are shown in bold*

The null hypothesis (H_0), in which the effect of any particular independent variable on each of the response variables does not exist, was rejected if P-value ≤ 0.05 ($\alpha = 0.05$ or 5%). Therefore, for the P-values to be statistically significant they should be ≤ 0.05. The SMM type (hydrophobic versus hydrophilic) and the casting method (single-pass versus

double-pass) were chosen as the independent variables, while the response variables were given in terms of characteristics and performance. Results of Table 5.3 indicate that at a significance level of $\alpha = 0.05$, there is significant evidence for all main effects and for a two-factor interaction: membrane type × casting method. These results have been illustrated through Figures 3 and 4 which displayed clearly the presence of significant interaction effects. According to ANOVA interpretation, if the interaction is significant, any main effects involving terms of the significant interaction are not considered meaningful. Based on Table 5.3, the MWCO, mean pore size and contact angles all depend on both the type of polymeric additives and the casting method.

5.4.3 Response performance

The single- and double-pass scanning membranes were compared in terms of flux performance (long term flux behavior, volume of treated water) and NOM rejection based on the results obtained from filtration experiments with high colored river water.

5.4.3.1. Flux performance

The filtration protocol had four stages: precompaction (one hour), PWP (50 hours), solute transport (only shown as the vertical line) and ORW filtration test (50 hours). Figure 5.5 presents solely the long term flux performance in two key stages: PWP and filtration of ORW. The effect of the new casting method was displayed visually for hydrophobic membranes (solid squares compared with empty squares). The higher fluxes of the Double pass PES-HO were not surprising given the higher MWCO and mean pore size than the single pass PES-HO. The fluxes of hydrophilic membranes however do not show much difference during the initial 80 hours. This is because the pore structures of these membranes are almost the same. Interestingly, however, the flux of the double-pass membrane (Double PES-HI) improved by about 25% relative to that of the single-pass membrane during the last 20 h of operation. The flux of the Double PES-HI membranes seems to stabilize while the flux of the single-pass casting PES-HI membranes continues to decrease. This may be due to the higher mechanical stability of the Double PES-HI, which indeed exhibited a more solid cross-sectional structure (Figures 2h and 2g). Overall, the double-pass casting membranes showed higher final fluxes or also higher fouling resistance.

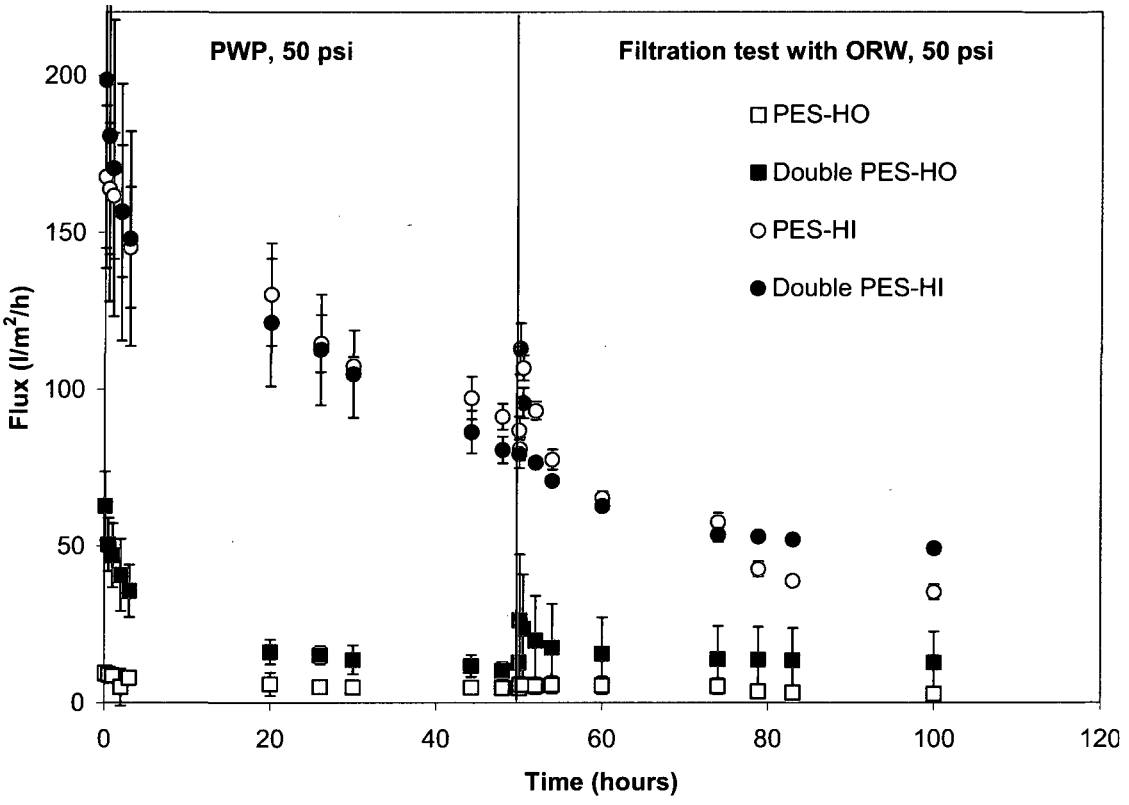

Figure 5.5. Flux performance upon 100 hours filtration

This study also considers the water production (l/m^2) by these membranes after 50 hours of filtering surface water. This index is quite important for membrane selection since it reflects the volume of water treated by membranes. Certainly, it is expected that a good membrane should produce a large volume of water. The hydrophilic PES-HI membranes can produce much greater amounts of treated water than can the hydrophobic ones (Figure 5.6). Water production increased by exercising double-pass casting on both the PES- HO and PES-HI groups, however, it was more significant for PES-HO membranes (by 67.4% or by 494 l/m^2) than that for the PES-HI ones (by 12.4% or by 334.6 l/m^2). Again, the structural changes as observed in the SEM images did impact the membrane performance, especially the flux and amount of water treated. According to Figure 5.6, PES-HI membranes performed better although the increase in water production of PES-HO membranes was higher.

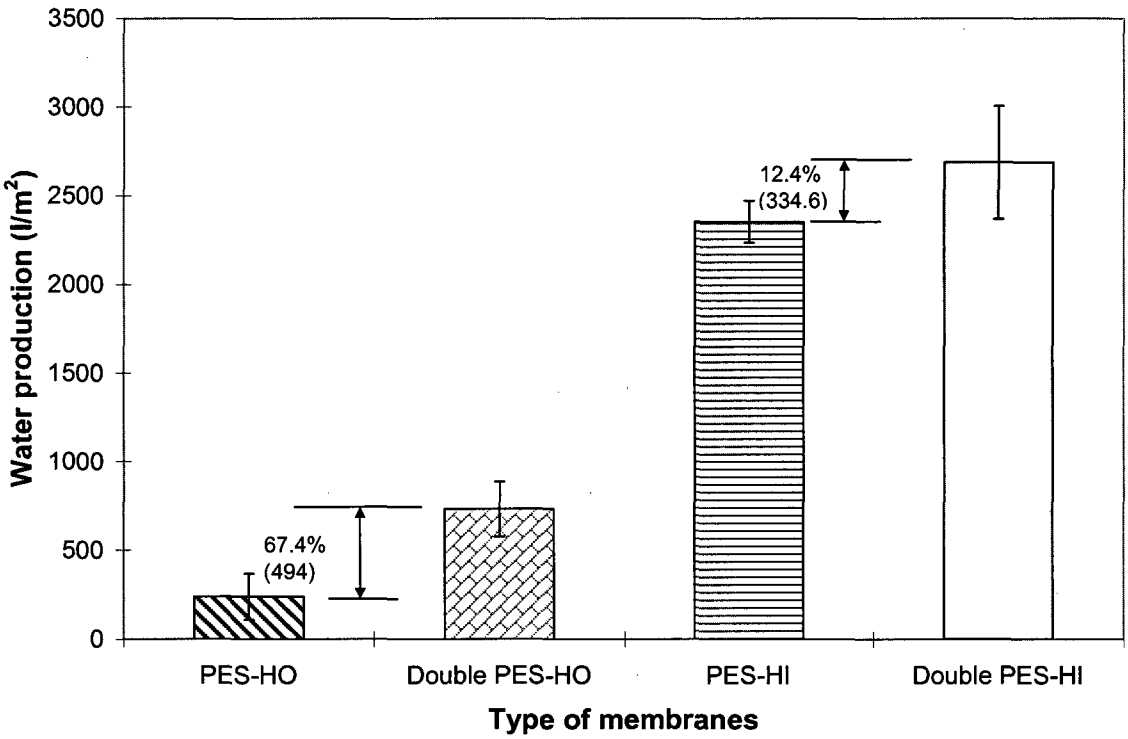

Figure 5.6. Specific treated volume (after 50 hours of surface water filtration)

5.4.3.2. NOM rejection

The NOM rejection was evaluated during the fourth phase of the test which is the filtration of surface water. The results are shown in Figure 5.7. Combining the flux data shown in Figure 5.5 and the MWCO and the mean pore size data shown in Table 5.2, several interesting observations can be made.

1) Comparing the PES-HO and PES-HI groups, NOM rejections of the membranes belonging to the PES-HI group are higher than those of the PES-HO group (Figure 5.7), despite the fact that the fluxes of the former membranes are higher than the latter membranes (Figure 5.5). This violates the trade-off law, which dictates a lower flux corresponding to a higher rejection. According to Table 5.2, the MWCOs and the mean pore sizes of the membranes for the PES-HI group are greater than those of the PES-HO group. If the NOMs are rejected by the sieving mechanism alone, the NOM rejections by the membranes of the PES-HI group should be less than those of the PES-HO group. The experimental results contradict the above expectation, indicating that the mechanism involved

in the NOM rejection is not sieving alone. In addition, the NOM removal values are quite small compared with those of other hydrophobic membranes made by our co-workers [4]. Different experimental protocol (much longer pre-compaction time and different batch of ORW) and different hydrophobic additives may explain this difference. For the PES-HI membrane group, the high final DOC removal was likely due to the formation of a gel/cake layer given the higher volume of water treated.

2) Comparing the single-pass and double-pass casting, the NOM rejection of PES-HO is higher than that of Double PES-HO (Figure 5.7). Since the flux increased for the double-pass casting (Figure 5.5), these results follow the trade-off effect. MWCO and the mean pore size also increased when the double-pass casting was applied (Table 5.2). The effect of the double-pass casting can therefore be explained as an increase in the pore size. With respect to the PES-HI and Double PES-HI membranes, the NOM rejection and the flux are similar for both membranes. This is understandable since the MWCO and the mean pore size did not change significantly.

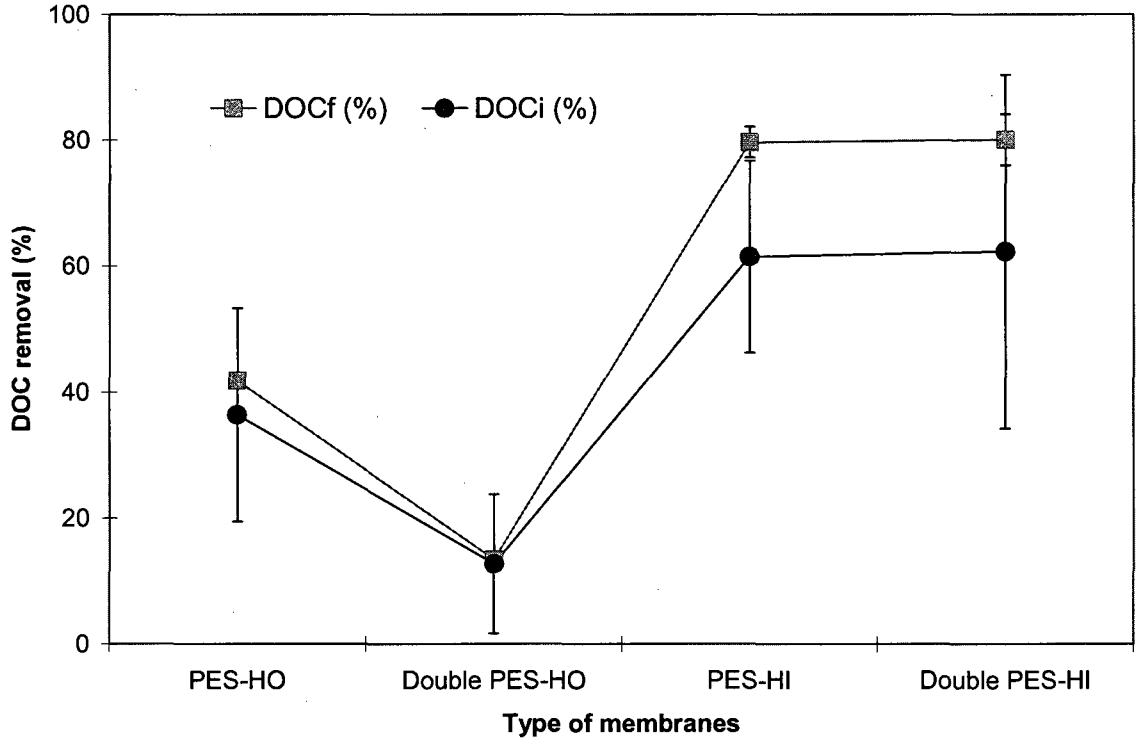

Figure 5.7. Initial and final DOC rejection

The change in the membrane performance as a result of double-pass casting is quite understandable, while the change from the hydrophobic to hydrophilic surface contradicts our expectation in several ways. This seems due to the significant change in the surface hydro-phobicity/-philicity occurring when different SMMs are blended. Considering the higher flux and flux stability, the Double PES-HI membrane is obviously the membrane of choice.

An ANOVA test was conducted to determine the effects of the independent variables involved in the membrane casting on the membrane performance. The results are shown in Table 5.4. From the table, the new casting method impacts less on membrane performance than it does on membrane characteristics (Table 5.3). The double-pass casting method only helped the pure water filtration rate increase while it made no difference statistically for other performance variables. The SMM type, on the other hand, exhibited significant effects on all performance variables.

Table 5.4 P-values of the independent variables obtained from the analysis of variance (ANOVA) for the performance variables ($\alpha = 0.05$)

Source of variation	DOCi Removal	PWP	Final flux	Volume treated
MAIN EFFECTS				
A: SMM type	**0.020**	**0.000**	**0.003**	**0.010**
B: Casting method	0.059	**0.023**	0.181	0.529
INTERACTIONS				
AB	0.092	0.150	0.693	0.351

* *If P-value ≤ 0.05 the effect is statistically significant)*

5.5. Conclusions

Based on the study of new casting method on two types of membranes (more hydrophobic and more hydrophilic ones), some conclusions can be drawn as follows:

1. The double-pass casting had a significant effect on membrane morphology (smoothness of the surfaces and cross-sectional structure), especially when hydrophobic SMM was blended. When hydrophilic SMM was added the change

was noticed in the decrease in contact angle. The ANOVA analysis demonstrated that the novel casting method had a considerable impact on the contact angles and the mean pore sizes.

2. The new casting method helped increase the permeate flux and the water production but DOC rejection was lowered when hydrophobic SMM was blended. On the other hand the effect of the double pass casting on the membrane flux was only marginal when the hydrophilic SMM was blended because the performance of the membrane prepared by single-pass casting was already high.
3. The impacts of new double pass casting method were more obvious for the PES-HO membranes since their casting solution was phase-separated. In the case of PES-HI, the solution was quite homogenous and no phase separation was visibly observed. Therefore, the impact of the double pass casting was not strong.
4. The double-pass casting method may be desirable for the following types of casting solutions: (i) highly viscous solutions; (ii) easily-demixed (phase separated) solutions and (iii) bubble-containing solutions. The testing of new method has been solely conducted for PES-based membranes. Future study would involve in the valuation of this new technique for different casting solutions.

5.6. Acknowledgement

The authors gratefully acknowledge Vietnam Government (Vietnamese Overseas Scholarship Programs -VOSP), Natural Sciences and Engineering Research Council of Canada (NSERC) and University of Ottawa for their financial support. We also thank Britannia Water Purification Plant for the water sampling.

5.7. References

[1] J.Y.C. Ho, T. Matsuura and J.P. Santerre, The effect of fluorinated surface modifying macromolecules on polyethersulfone membranes. J. Biomater. Sci. Polym., 11 (2000) 1085.

[2] D.E. Suk, G. Chowdhury, T. Matsuura, R.M. Narbaitz, P. Santerre, G. Pleizier and Y. Deslandes, Study on the kinetics of surface migration of surface modifying macromolecules in membrane preparation, Macromolecules, 35 (2002) 3017.

[3] D.B. Mosqueda-Jimenez, R.M. Narbaitz and T. Matsuura, Membrane fouling test: apparatus evaluation. J. Environ. Eng., 130 (2004a) 90.

[4] D.B. Mosqueda-Jimenez, R.M. Narbaitz and T. Matsuura, Manufacturing conditions of surface-modified membranes: effects on ultrafiltration performance, Sep. and Puri. Technol., 37 (2004b) 51.

[5] A.H Nguyen., R.M. Narbaitz and T. Matsuura, Impacts of Hydrophilic Membrane Additives on the Ultrafiltration of River Water, J. Env. Eng., 133 (2007) 515.

[6] D. Rana, T. Matsuura, R.M. Narbaitz, and C. Feng, Development and characterization of novel hydrophilic surface modifying macromolecule for polymeric membranes, J. Membr. Sci., 249 (2005) 103.

[7] Y.H. Zhao, B.K. Zhu, L. Kong and Y.Y. Xu, Improving hydrophilicity and protein resistance of poly(vinylidene fluoride) membranes by blending with amphiphilic hyperbranched-star polymer, Langmuir, 23 (2007) 5779.

[8] W.R. Bowen, T.A. Doneva and H.B. Yin, Separation of humic acid from a model surface water with PSU/SPEEK blend UF/NF membranes, J. Membr. Sci. 206 (2002) 417.

[9] L.Q. Shen, Z.K. Xu, Z.M. Liu and Y.Y. Xu, Ultrafiltration hollow fiber membranes of sulfonated polyetherimide/polyetherimide blends: preparation, morphologies and anti-fouling properties, J. Membr. Sci. 218 (2003) 279.

[10] C.C. Pereira, R. Nobrega, and C.P. Borges, Membranes obtained by simultaneous casting of two polymer solutions, J. Membr. Sci., 192 (1), 11-26 (2001)

[11] K. Willem, Process of forming multilayered structures, U.S. Pat. No. 7208200 (2006)

[12] S.C. Lenore, E.G Arnold, D.E Andrew, Standard methods for the examination of water and wastewater, APHA, AWWA, Washington DC., (1999)

[13] T. Thorsen, Membrane filtration of humic substances –state of the art. Wat. Sci. Tech., 40 (1999) 105.

[14] C.M. Tam, S. Singh, K.C. Khulbe, T. Matsuura and P. Ramamurthy, Membrane characterization by solute transport and atomic force microscopy. J. Membr. Sci. 142 (1998) 111.

[15] D. Rana, T. Matsuura and R.M. Narbaitz, Novel hydrophilic surface modifying macromolecules for polymeric membranes: Polyurethane ends capped by hydroxy group, J. Membr. Sci., 282 (2006) 205.

[16] D.E. Suk, T. Matsuura, H.B. Park and Y.M. Lee, Synthesis of a new type of surface modifying macromolecules (nSMM) and characterization and testing of nSMM blended membranes for membrane distillation, J. Membr. Sci., 277 (2006) 177.

[17] S. Singh, K.C. Khulbe, T. Matsuura and P. Ramamurthy, Membrane characterization by solute transport and atomic force microscopy, J. Membr. Sci., 142 (1998) 111.

[18] H.T. Dang, R.M. Narbaitz, T. Matsuura and C.K. Khulbe, A comparison of commercial and experimental ultrafiltration membranes via surface property analysis and fouling tests, Water Quality Res. J. of Canada, 41 (2006) 84.

[19] R.E. Kesting, Synthetic polymeric membranes: A structural perspective, John Wiley & Sons, New York, NY, (1985).

CHAPTER 6

A COMPARISON OF COMMERCIAL AND EXPERIMENTAL ULTRAFILTRATION MEMBRANES VIA SURFACE PROPERTY ANALYSIS AND FOULING TESTS

Huyen T. Dang[1], Roberto M. Narbaitz[1], Takeshi Matsuura[2], Kailash.C. Khulbe [2]
[1]*Dept. of Civil Engineering, Univ. of Ottawa, 161 Louis Pasteur St., Ottawa, K1N 6N5, Canada*
[2]*Dept. of Chemical Eng., Univ. of Ottawa, 161 Louis Pasteur St., Ottawa, K1N 6N5, Canada*

6.1 Abstract

Surface modified polyethersulfone (PES) membranes via the addition of different hydrophiLic Surface Modifying Macromolecules (LSMMs) have been developed by Matsuura, Narbaitz and co-workers. This study compares the performance of the best PES-LSMM membrane with nine commercial ultrafiltration membranes manufactured using five different types of base polymers (polyethersulfone, polysulfone, celluloseacetate, polyacrylonitrile and cellulose) in the same range of molecular weight cutoff- MWCO (from 40 to 120 kDal). All membranes were characterized by using atomic force microscopy, contact angle measurements, solute transport analysis and then evaluated through fouling tests with Ottawa River water (ORW). While PES-LSMM membranes had much lower initial flux than cellulose acetate or cellulose membranes, they had the highest Total Organic Carbon (TOC) rejection (80%) and the lowest flux reduction (62%). For the commercial membranes, the range of TOC rejections and flux reductions were 62-80% and 68-80%, respectively. Given their high TOC rejection and relatively high foulant deposition, fouling of the PES-LSMM membranes appears to be controlled by a surface gel.

Key words: Ultrafiltration membranes, surface water, membrane surface characterization, fouling, humic substances.

Notations

R_m	membrane resistance (m^{-1})
R_a	mean roughness (nm)
ΔP_T	transmembrane pressure (N/m^2)
J	pure water permeation flux ($m^3/m^2.s$)
μ	viscosity (Ns/m^2)
$PR_{(t)}$	permeate flux after fouling test ($l/m^2.h$)
PWP	pure water permeation ($l/m^2.h$)
TOC_f	total organic carbon in the feed (mg/l)
TOC_p	total organic carbon in the permeate (mg/l)

Abbreviations

AFM	Atomic Force Microscopy
C	Cellulose
CA	Cellulose acetate
DMAc	N,N-dimethylacetamide
LSMMs	HydrophiLic Surface Modifying Macromolecules
MDI	Methylene bis-*p*-phenyl diisocyanate
MWCO	Molecular weight cutoff (kDal)
NMP	N-methyl pyrrolidone
NOM	Natural organic matter
ORW	Ottawa River Water
PAN	Polyacrylonitrile
PEG	Polyethylene glycol
PEO	Polyethylene oxide
PES	Polyethersulfone
PPG	poly(propylene glycol)
PS	Polysulfone
PVDF	Poly(vinylidene-fluoroethylene)
UF	Ultrafiltration

6.2 Introduction

Fouling, i.e., flux reduction with time, is one of the most serious concerns in the application of membrane processes. This phenomenon depends on many factors, including feed characteristics, membrane apparatus type, membrane characteristics and operational procedures. Many approaches have been examined to minimize the impact of membrane fouling. Among others, Matsuura, Narbaitz and co-workers (Pham, 1995; Ho et al., 2000; Suk et al., 2002) have concentrated on developing membranes whose surfaces are modified by blending tailor-made surface active polymers into polyethersulfone (PES) solutions. During the casting process the surface active additives migrate to the membrane surface, thus creating asymmetric membranes with modified surfaces via a single manufacturing step. Initial work with hydrophobic tailor-made additives produced only marginally better performance in river water filtration (Mosqueda-Jimenez et al. 2004b,c,d). Recently, Rana et al. (2005) developed several different tailor-made hydrophi**L**ic **S**urface **M**odifying **M**acromolecules (LSMMs) and Nguyen et al. (2007) demonstrated LSMM addition had positive impacts on PES membrane performance, i.e., higher TOC removals and final fluxes than PES membranes without LSMM addition.

The objective of this study was to compare the surface characteristics and performance of the best PES-LSMM membrane (as identified by Nguyen, 2005) with nine commercial ultrafiltration (UF) membranes. The key features of this study were to (i) prepare the optimum PES-LSMM membrane based on the previous work; (ii) characterize the properties of the experimental PES-LSMM and commercial UF membranes via solute transport tests, contact angle and surface roughness measurements; (iii) test the fouling characteristics of the membranes via filtration tests using highly colored river water and (iv) finally compare their performance to assess the effectiveness of PES-LSMM membranes. The performance was assessed in terms of long term flux rates, flux reduction, and TOC rejection.

6.3 Materials and methods

6.3.1 Materials

Nine commercial membranes prepared using five different base polymers (polyethersulfone (PES), polysulfone (PS), cellulose acetate (CA), polyacrylonitrile (PAN) and cellulose) were selected for testing. Details of these membranes are presented in Table 6.1.

Table 6.1 Description of commercial membranes

Type of Membrane	Manufacturer	Materials
XM50	Millipore	Regenerated Cellulose
Mil100	Millipore	PES
FO100	Millipore	Modified PS
FO50	Millipore	Modified PS
PAN100	GE Osmonics	PAN
PX150	GE Osmonics	PES
PU40	GE Osmonics	PES
EWH70	GE Osmonics	PS
CQ40	GE Osmonics	CA

The optimum tailor-made PES-LSMM membrane as identified by Nguyen et al. (2005) was prepared using PES (Victrex 4100P, ICI Advanced Materials, Billingham, UK, molecular weight ~ 17-19 kDal) and the LSMM-600 developed by Rana et al. (2005). The LSMM-600 was synthesized using a two-step solution polymerization method: the initial step involved the reaction of methylene bis-*p*-phenyl diisocyanate (MDI) with poly(propylene glycol) (PPG) in a common solvent of N,N-dimethylacetamide (DMAc), then it was terminated by the addition of poly(ethylene glycol) (PEG) with MW of 600 Daltons. LSMMs are surface-active polymeric additives, which are blended into the casting solution containing the base polymer PES and a solvent. During the casting, LSMM molecules diffuse and migrate to the surface of membrane to a certain extent. As a result, the modified membrane surface becomes more hydrophilic. Reagent grade N-

methyl-2-pyrrolidone (NMP) (Aldrich Chemical Company, Inc., Milwaukee, WI) was used as solvent for casting membranes. Polyethylene glycol (PEG) and polyethylene oxide (PEO) (Aldrich Chemical, Milwaukee, WI) were used as probe solutes for the solute transport tests in molecular weight cut-off (MWCO) determinations. The molecular weight of the PEG used were 10, 20 and 35 kDal and for PEO the molecular weight was 100 kDal. Ultra pure water was prepared with a Milli-Q Water System (Millipore, Bedford, MA).

Ottawa River water collected at the intake of the Britannia Water Treatment Plant on May 8th, 2004 was used as feed water for the fouling tests. This water was selected because it is highly colored and had a TOC of about 6mg/L, thus it should cause substantial natural organic matter (NOM) fouling of the membranes.

6.3.2 Preparation of membranes

The experimental PES-LSMM ultrafiltration membrane evaluated in this study was prepared with a casting solution of 18 wt % PES, 4.5 wt % LSMM 600 and 77.5 wt % solvent NMP (Nguyen, 2005). PES, NMP and LSMM 600 were completely mixed for 24 hours in an incubator shaker (New Brunswick Scientific Co., Edison, N.J.), filtered in a nitrogen gas-driven filter using 47-mm white mitex filter media (Milipore Corp., Bedford, MA). The solution was then degassed via a vacuum desiccator (VWR, Mississauga, ON) for several hours. Casting of the PES-LSMM membrane was conducted according to the procedures described by Mosqueda-Jimenez et al. (2004b). After casting, the flat sheet membranes were stored in ultra pure water until they were tested. For commercial membranes, since they were coated with glycerine as a preservative to prevent them from drying and cracking, they were soaked in water for rinse for three to six hours prior to use according to manufacturer' recommendations. All membranes were cut into 52-mm diameter coupons for testing in the ultrafiltration system. For the measurement of the contact angles, the membranes were dried naturally by putting them between filter papers instead of using the ethanol solvent exchange method (Matsuura, 1994) that is more complicated. Also, this air-drying method was selected to guarantee a fair comparison since ethanol solvent exchange may alter the commercial membranes, which might already be dried by other methods.

6.3.3 Methods of analysis

Atomic force microscopy. Atomic force microscopy (AFM) is an advanced analysis technique that can produce three-dimensional images of solid surfaces at very high resolution (Chan, 1994). The advantage of using AFM is that it can image non-conducting samples, such as polymers. In contrast to scanning electron microscopy (SEM), which requires a high vacuum both during heavy metal coating and during examination, AFM can be performed on wet ultrafiltration membranes (Fritzsche et al., 1992) so it is less destructive and more representative of "natural" conditions. The AFM studies were conducted in a tapping mode using a Nanoscope III equipped with a 1533D scanner (Digital Instruments, Gainesville, FL). Pieces of flat-sheet membranes were cut and fixed over magnetic disks with two-sided adhesive tape. The laser beam of the AFM was focused on a pre-selected spot of the surface prior to the engagement of the cantilever (Khayet et al., 2002). A tapping mode, AFM, in air was used to generate the AFM images. Based on the data, the roughness was obtained. For more detailed information refer to Appendix N.

Contact angle measurement. Contact angle is considered the most convenient index of membrane hydrophilicity if measuring methods and times are carefully kept consistent (Amy et al., 2001), the surface of the solid is smooth, chemically homogenous and rigid (Chan, 1994), and water is used as a testing liquid. The sessile drop method, which is based on the principle of the three-phase equilibrium that occurs at the solid/liquid/air interface, was used in this study. The dry membranes were cut into 5 x 25mm pieces and fixed onto 25 x 75 x 1mm superfrost micro slides (VWR., Mississauga, ON) using invisible tape. Advancing contact angles were determined via a goniometer (C860 701, Sherr Tumico, Germany). Water was continuously added using a 100-µm syringe at a very slow rate until the drop moved. The water drop volume ranged from 1.6 to 2.4 µl. The contact angle was measured immediately after the sudden movement of the water drop using the goniometer. The reported contact angles are the average of five or six measurements. According to the manufacturer, the accuracy of this analyzer is ± 2 degrees.

Ultrafiltration testing protocol. The ultrafiltration testing protocol consisted of several stages: pre-compaction, pure water permeation (PWP) rate determinations, solute transport evaluations and river water fouling tests. The ultrafiltration apparatus consists of the six cells in series ultrafiltration system described by Mosqueda-Jimenez et al. (2004a), each cell is used to test one 52 mm diameter flat sheet membrane coupon. The filtration test protocol followed was that described in Nguyen (2005).

Membranes were pre-compacted for one hour at 552 kPa (80 psig) and room temperature. The purpose of pre-compaction is to minimize flux reduction due to membrane compaction while avoiding a significant impact on membranes pore structure. This was followed by 50 hours of PWP monitoring, i.e., ultra-pure water filtration at 345 kPa (50 psig) and room temperature. The pure water permeation rate was checked by measuring the volume of permeate collected over specific time intervals.

Solute transport. Solute transport was evaluated following the procedure described by Mosqueda-Jimenez (2004b). It is essentially a continuation of the ultrafiltration test in which the feed is changed to solutions of different known molecular weight solutes for one-hour periods. The feed solutions were solutions of PEG with molecular weights of 10, 20, 35 kDal and PEO with molecular weight of 100 kDal. The tests were run at 345 kPa (50 psig) pressure and room temperature (23±0.2°C). The membrane system was flushed with ultra-pure water for one hour after each PEG/PEO solution circulation. At the end of the hour the PWP rate was re-measured to corroborate that the solute transport tests had not altered the flux (i.e., fouled the membrane). The feed and permeate samples were collected and analyzed for total organic carbon (TOC) concentrations using a UV-persulfate oxidation based TOC analyzer (Phoenix8000, Teledyne-Tekmar, Mason, OH). The solute feed concentrations were 100 mg/L and the samples were diluted prior to analysis due to the concentration range measurable by the above analyzer. The MWCO, which is the molecular weight that would yield 90% solute separation, was determined based on the solute transport tests. These results were used to determine the pore distribution, pore density and surface porosity of each membrane following the approach of Singh et al. (1998) (see Appendix M).

Fouling test. After the solute transport analysis, the fouling test was conducted using the same experimental set-up and switching the feed to Ottawa River water (ORW). ORW was used as a feed because of its relatively high color and NOM content, and this makes it a good challenge water for the fouling tests. The system was operated at room temperature and the pressure was controlled manually using two valves and pressure gauges (MIX3, France). The 144-hour test duration allowed the permeate flux to reach a pseudo-steady state. The permeate flux was determined by weighing the mass of the permeate collected during predetermined times or measuring the volume of permeate with higher permeability membranes. The feed flow was set at 1.1 Lpm to allow the operation of two systems (six cells per each) in series with a pressure drop of less than 14 kPa (2 psig) while creating turbulent flow conditions so as to avoid concentration polarization (Mosqueda-Jimenez, 2003). The NOM rejection was quantified using the feed and permeate total organic carbon (TOC) concentrations. At the end of the fouling test, the diameter of the fouled membrane surface area was measured to permit accurate calculation of the fluxes. In addition, the mass of foulant was quantified by the technique suggested by Hong and Elimelech (1997). The NOM-fouled membranes were immersed in 25 mL of 0.1 M NaOH within pre-weighed beakers. After the NOM was completely removed from the membrane coupons, all the coupons were removed from the beakers. The beakers were placed in an air-circulating oven at 105°C for 24 h to evaporate the water and then reweighed. The mass of NOM calculated by the difference between the dry weight of the beakers containers containing NOM and NaOH and that of the controls (containing just NaOH).

6.4 Results and discussion

6.4.1 Ultrafiltration membranes' performance and comparison

Pure Water Permeation and Membrane Resistance. The intrinsic membrane resistance, determined using pure water as a feed, is not only useful for modeling purposes, but also for evaluating the stability of the membrane (Cheryan, 1986). This resistance R_m (or hydraulic resistance of clean membranes-m^{-1}) can be expressed as:

$$R_m = \frac{\Delta P_T}{J\mu} \qquad [6.1]$$

where ΔP_T is the transmembrane pressure (N/m^2), J is the pure water permeation flux ($m^3/m^2.s$) and μ is the viscosity of water (Ns/m^2).

This value was evaluated after one-hour precompaction and 50-hour permeation using ultra-pure water. From Figure1, it was obvious that the resistance was similar for all membranes, ranging from 9 to 13 m^{-1}. The experimental membrane, PES-LSMM, had the highest hydraulic resistance. The hydraulic resistance is inversely proportional to the flux, hence, the permeation rate after 50-hour test of PES-LSMM membrane was not as high as the commercial membranes. Cellulose membranes had the lowest resistance or highest permeation rate. This can be explained based on the differences in polymer structure. In addition to differences in pore sizes and porosity, cellulose membranes have a continuous sponge-like structure that makes them less susceptible to compaction and obtains higher flux while PES membranes have a structure with macrovoids below the thin separation layer (Persson et al., 1995).

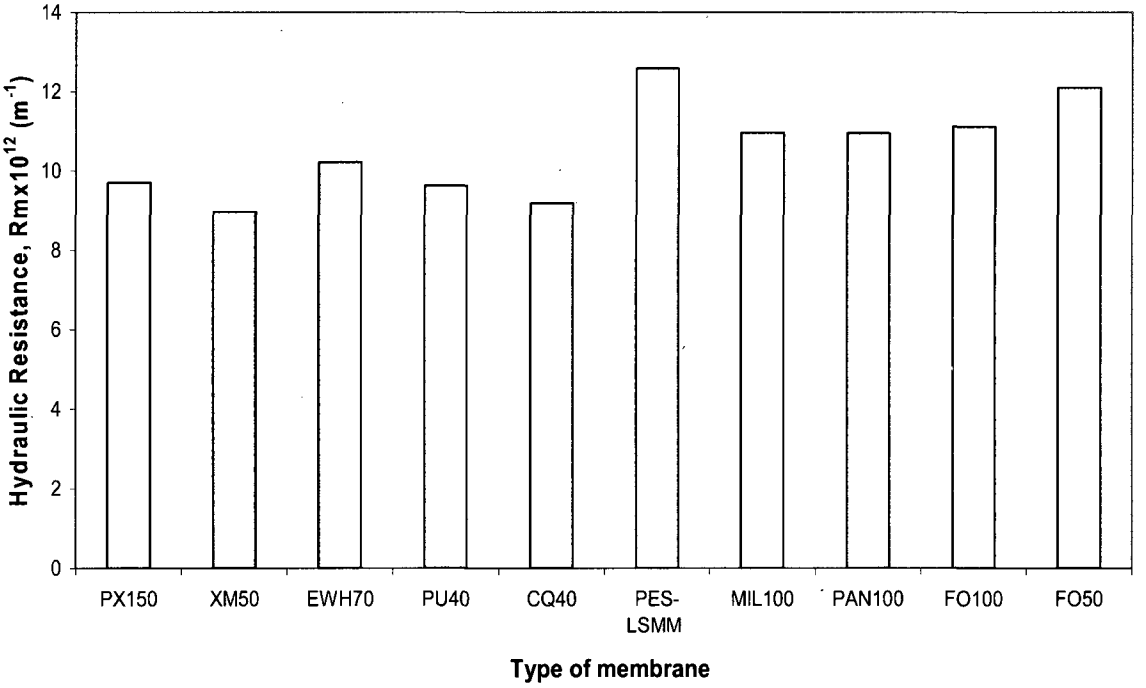

Figure 6.1. Hydraulic resistance of the various membranes (after 50-hour test)

Long-term fouling test. Figure 6.2 illustrates the flux over the various stages of the ultrafiltration protocol: precompaction, PWP, solute transport (only shown as the vertical line) and ORW fouling test. Although commercial membranes such as FO50, MIL100 or XM50 had high permeation rates at the start-up, their fluxes quickly dropped in the first six hours and gradually reached a pseudo-steady state after 80 hours. The flux decline at the beginning of filtration test might be due to the characteristics of the pore structures of the membranes which allowed large amount of humic substances to pass through and thus were more vulnerable to pore blocking (Nguyen, 2005). The flux of the PES-LSMM membrane did not decline as significantlyas the other membranes particularly during the stages of each cycle.

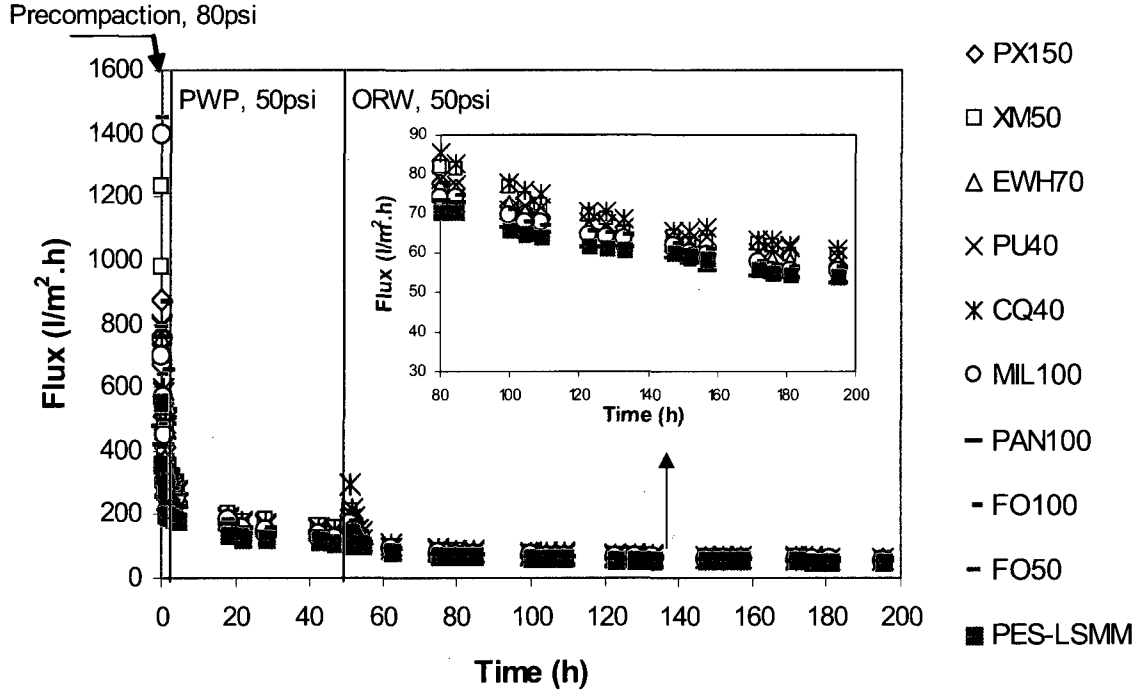

Figure 6.2. Filtration flux versus time

Flux reduction, which is an indicator of fouling, was calculated as below:

$$\text{Flux reduction}_{(t)}\ (\%) = 100\left(1 - \frac{PR_{ORW}}{PWP}\right) \qquad [6.2]$$

where PR_{ORW} is the permeate flux after the 6-day fouling test with Ottawa River water (L/m2/h) and PWP is the stable pure water permeation rate (L/m2/h).

The flux reductions during the six-day ORW filtration test are presented in Figure 6.3. The initial fluxes of commercial membranes were relatively high compared to the modified membrane but the final fluxes were similar (from 52.10 L/m^2.h to 60.68 L/m^2.h) after the long-term filtration test. Therefore, the flux reduction of the modified membrane was lower since its initial flux was not competitive. One interesting conclusion drawn from the above results was that the flux stability of PES-LSMM membrane was better than others. The lower flux reduction also implied less susceptible to fouling. This is probably due to the rather small values of mean pore sizes, which are discussed in later section.

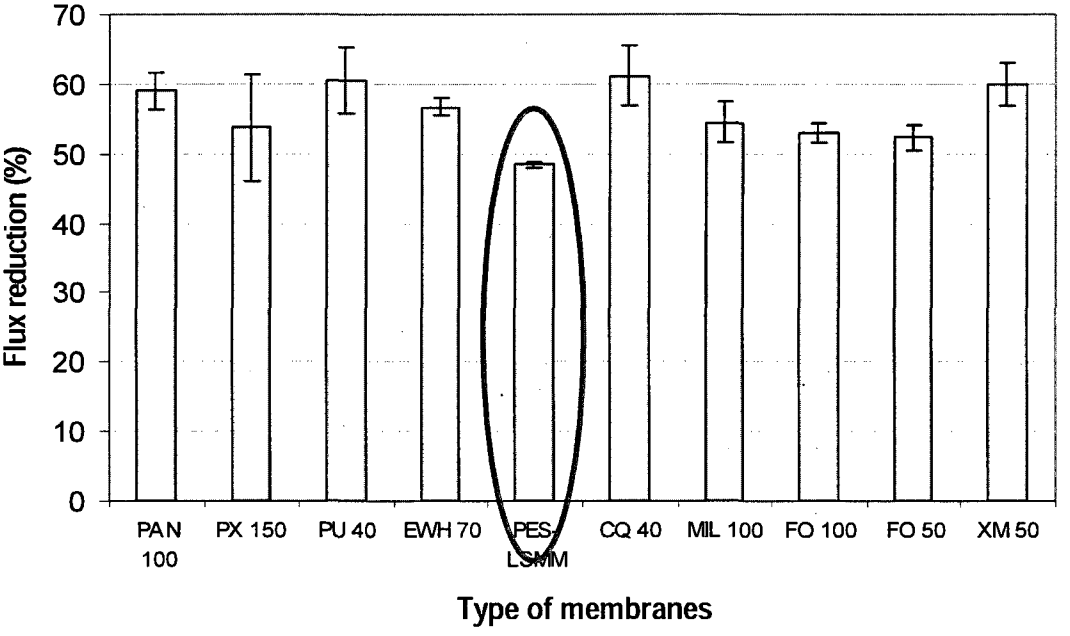

Figure 6.3. Flux reduction after filtration test (144 hours)

Humic substances deposition and TOC rejection. Removal of NOM, or more specifically humic substances, is important in water treatment primarily because they react with chlorine to form harmful disinfection by-products (DBPs). In membrane technology, the amount of humic substances deposited on membrane surfaces was studied since it is related to the cleaning frequency. This deposition layer is known as the fouling layer. The more quickly the fouling layer grows, the greater the frequency of cleaning required. The amount of chemicals used for cleaning the membranes with highly accumulated NOM is typically greater than those having less NOM deposition.

It is also important to quantify TOC rejection, which was calculated via the following equation:

$$\text{TOC rejection}(\%) = 100 \times \left(1 - \frac{TOC_p}{TOC_f}\right) \qquad [6.3]$$

where TOC_f and TOC_p are total organic carbon concentration (mg/l) in the feed and permeate, respectively.

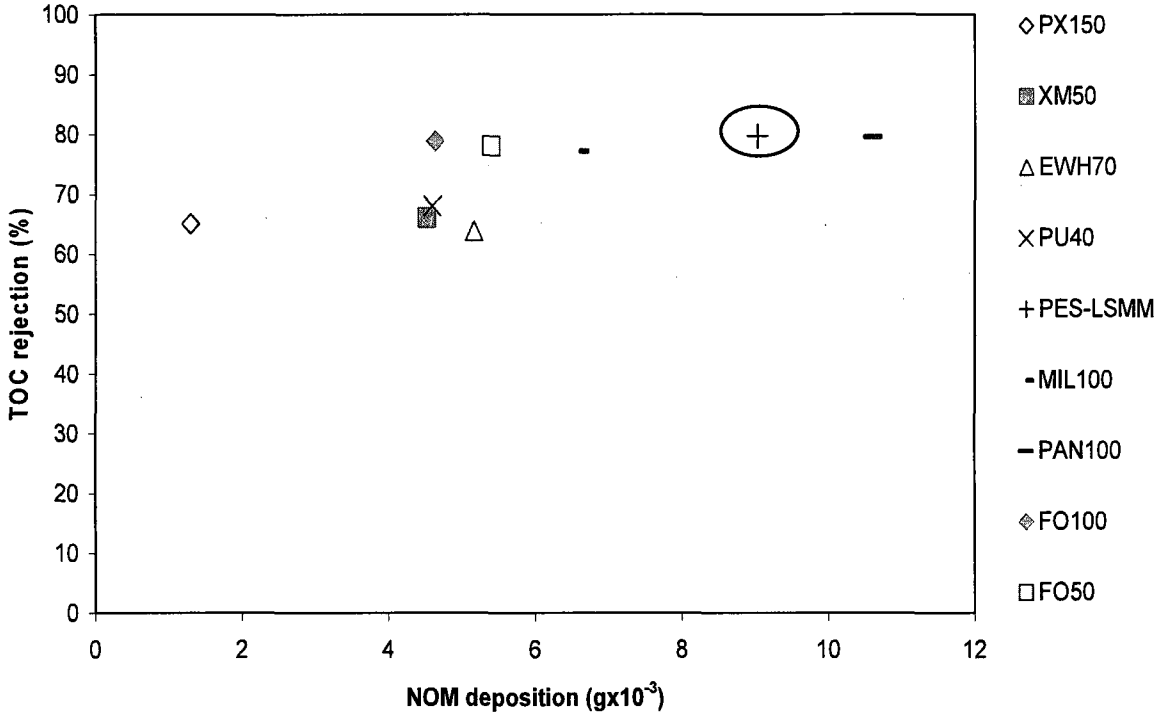

Figure 6.4. TOC rejection vs NOM deposition

Small amounts of NOM deposition and high TOC rejection suggests that there is more internal fouling, i.e., more humic substances penetrate into the pores and plug them. Internal fouling is generally irreversible and requires more expensive and complex cleaning procedures. High amounts of NOM deposition accompanied by high TOC removals, on the other hand, indicate that surface fouling is dominant. This fouling layer is generally reversible and can be easily controlled by high turbulence, regular cleaning and using hydrophilic or charged membranes to minimize adhesion to the membrane surface (Baker, 2004). Ideally, the membranes that foul predominantly on the surface are preferred since they are easier to clean and maintain. The experimental PES-LSMM

membrane (circled in Figure 6.4) has the highest TOC rejection and the relatively high NOM deposition ($9.03x10^{-3}$g). Thus it is hypothesized that for the apparatus, test conditions and water tested, the modified PES-LSMM membranes the dominant fouling mechanism was surface fouling. The percentage of TOC removal by the experimental membrane was significant. Its initial TOC rejection (72%) was the highest and increased to 80% by the end of the six-day filtration test. This value was higher than those reported in the literature (Nguyen et al., 2005, Rana et al., 2005) for membranes prepared in a similar fashion. The initial TOC rejections of the commercial membranes ranged from 34% to 61%, while the long-term rejections of these membranes ranged from 64% to 70%. These above values are considerably higher than the values of 20%-40% reported in other studies for commercial UF membranes (Mosqueda-Jimenez, 2003). This may be attributed to the characteristics of the fouling test apparatus, the characteristics of the test water (which in this case was a raw river water), the duration of the fouling test, etc. To understand further the impact of surface gel, the percentages of initial and final TOC rejection were assessed in this study (Figure 6.5).

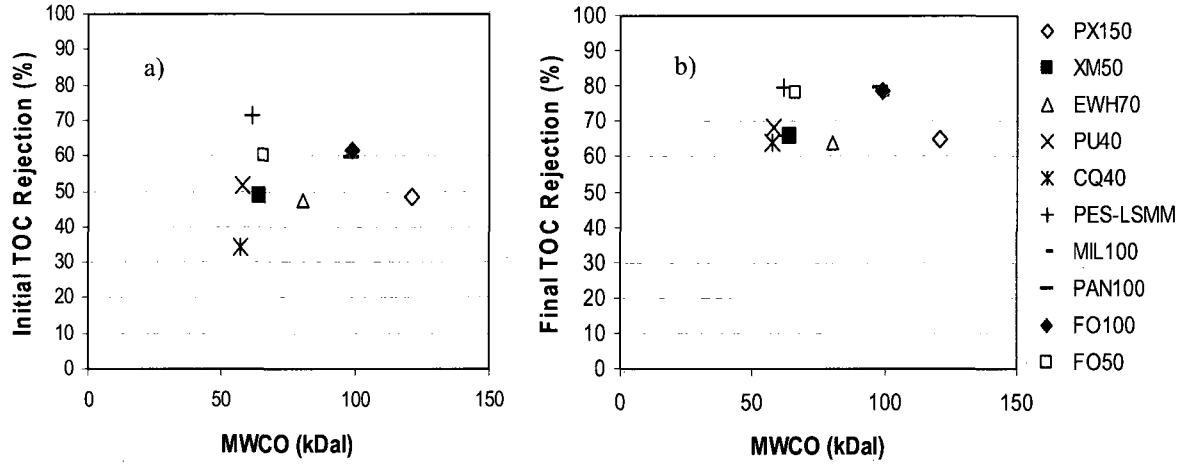

Figure 6.5. Impact of surface gel through (a) initial TOC rejection and (b) final TOC rejection (after the fouling test with Ottawa River Water)

The initial TOC rejection usually reflects the rejection of membrane without the impact of fouling layer. Gradually, NOM deposition layer increases and results in the increasing selectivity of the membranes. The final TOC rejection, therefore, can be higher than the initial one. Comparing the maximum values in the initial and the final rejections of the PES-LSMM membrane, the difference was not very significant (from over 70% to

approximately 80%). It proved that for the experimental membrane TOC rejection by surface gel to some extent was not so significant. Evaluation of the membrane retention would be possibly reliable based on the initial percentage of rejection since fouling layer may be controlling in many cases but not all cases.

6.4.2 Correlation between surface properties and fouling phenomenon

Hydrophilicity. Advancing contact angles of all membranes were less than 53° (see Table 6.2) demonstrating that they are all hydrophilic membranes. The tailor-made membrane with a contact angle of 52.5° was the least hydrophilic one. This value of contact angle was approximately 20° smaller than that reported by Nguyen (2005). This could be attributed to the membrane drying method. In this study, the membranes were dried naturally by placing them between filter papers while the membranes developed by Nguyen (2005) were dried with traditional ethanol solution. The impacts of different drying methods require further study. In addition, Nguyen (2005) used a more sophisticated goniometer which may have contributed to the observed differences to some extent.

Table 6.2 Contact angle measurements before and after the fouling test

Membranes	Before the fouling test		After the fouling test	
	Mean contact angle (°)	Standard deviation	Mean contact angle (°)	Standard deviation
PX150	50.17	0.62	46.58	2.18
XM50	16.50	2.65	44.70	3.04
EWH70	54.75	2.73	35.97	1.63
PU40	46.33	1.95	51.80	3.62
CQ40	29.36	2.72	40.17	0.29
PES-LSMM	52.47	1.17	50.97	1.90
MIL100	47.67	1.21	48.95	1.28
PAN100	34.53	0.41	35.08	1.83
FO100	51.00	2.02	46.72	2.03
FO50	50.28	1.24	46.50	3.91

Upon completing the test with Ottawa River water, the fouled membranes were submerged in 0.1M NaOH solution for one hour for cleaning, and then rinsed by immerging in ultra-pure (MQ) water for 48 hours prior to being dried naturally. The contact angles of these membranes were measured after drying them for five days and compared with the contact angles of clean membranes. The hydrophobicity of almost all membranes was found to either increase or decrease after the filtration test. This maybe depends on the NOM characteristics and membrane types. No satisfactory explanation of this phenomenon was given in the literature. More sophisticated tests are required to have a better understanding of these seemingly inconsistent results. However, it is worth noting that the contact angles of all membranes after fouling became more uniform. The difference between the lowest and the highest membrane contact angles decreased from 36 degree to 16.7 degree due to the filtration test. This suggests that some foulants penetrated into and stayed in the membrane pores or on surface without being removed by NaOH cleaning.

Pore characteristics. The pores of all tested membranes were characterized by the solute transport method and the results are summarized in Table 6.3.

Table 6.3 Pore characteristics and MWCO of tested membranes

Membranes	Nominal MWCO (kDal)	Measured MWCO (kDal)	Pore density (# of pores/m^2)	Surface Porosity (%)	Mean Pore size (nm)
PX150	150	120.87	4.52	0.0008	6.83
XM50	50	64.13	15.14	0.0017	5.43
EWH70	70	80.39	9.41	0.0012	5.90
PU40	40	58.06	19.90	0.0018	4.80
CQ40	40	57.59	19.55	0.0019	5.14
PES-LSMM	60	*61.64*	*15.79*	*0.0016*	*5.05*
MIL100	100	98.52	6.63	0.0010	6.19
PAN100	100	98.21	7.52	0.0009	5.40
FO100	100	98.91	6.51	0.0010	6.33
FO50	50	66.01	13.42	0.0014	5.12

Efficient membranes should have small pore sizes, high pore density and high surface porosity (Alsari et al., 2001) so that they can remove more contaminants such as humic substances from water, and yet achieve high permeation fluxes. Based on the data in Table 6.3, CQ40 and PU40 seemed to best satisfy these requirements, followed by XM 50 and PES-LSMM membranes.

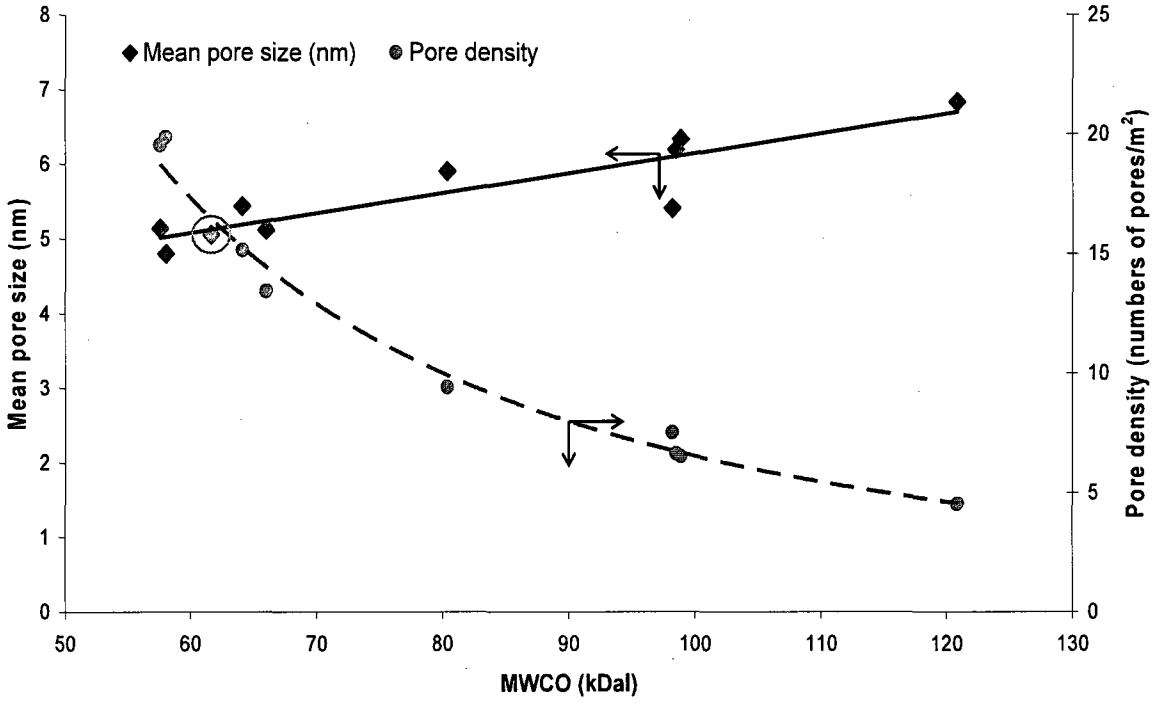

Figure 6.6. Correlation of MWCO and pore characteristics (Red circle locates the data points of PES-LSMM)

Figure 6.6 presents the correlation between pore characteristics and molecular weight cut off (MWCO). There was a clear trend that as MWCO increased, the mean pore size increased. It completely follows the logical concept of membrane technology since MWCO is defined as the molecular weight that yields 90% solute separation and smaller MWCO values are only obtained for membranes having smaller pore sizes. MWCO of the commercial membranes determined by solute transport method in this study differed somewhat from the estimated values provided by the suppliers. The reasons may be due to different characterization methods and different histories of membranes (i.e., length of the storage period prior to use). Cho et al. (2002) also reported that an effective MWCO is not usually the same as a nominal MWCO provided by the manufacturer. From Figure

6.6, the pore density significantly decreased with the increasing MWCO. It may be explained by the fact that to yield similar fluxes, membranes with smaller pores (smaller MWCO) often have higher pore densities. The tailor-made membranes, which had MWCO of approximately 62 kDal, had a low MWCO, small mean pore size and high pore density. The fractionation study of Ottawa River water showed that 99% of NOM had molecular weights less than 30 kDa. On the other hand, the maximum NOM rejection of about 80% was achieved with the membranes whose MWCO were above 50 kDal. Hence, it is proved that the effective MWCO of the membranes was much lower than the MWCOs measured in this work or those supplied by the manufacturers. The effects of electrostatic repulsion and hydrodynamic operating conditions are potential reasons for this discrepancy (Cho et al., 2000). MWCO therefore is not truly a precise indicator for membrane performance evaluation.

Roughness. Surface morphology may be an important factor affecting the performance of membranes. Membrane morphology can be examined through AFM measurements such as the mean roughness, Ra, which represents the mean value of surface relative to the center plane for which the volume enclosed by the images above and below this plane are equal. The three-dimensional images of all membrane surfaces showed that most membranes were not as smooth as cellulose acetate (CQ40) and polyethersulfone (PU40) membranes. The PES-LSMM membrane had a rather high roughness value.

Surface roughness is usually related to many other parameters. Singh et al. (1998) found that roughness became higher when MWCO increased since high MWCO had less tightly packed nodules/aggregates in the skin layer. The same trend was observed by many other researchers (Fritzsche et al., 1992; Bessieres et al., 1996). It was confirmed again in this study that PU40 and XM40 membranes, which had lowest values of MWCO, showed the smoothest surfaces. Hirose et al. (1996) found that an increase in surface roughness resulted in a higher water permeation flux. For PVDF membranes, Khayet et al. (2004) observed that the measured pure water flux increased with the increase of roughness and the roughness parameter was higher for membranes having larger pore sizes and nodule sizes as well as higher surface porosity.

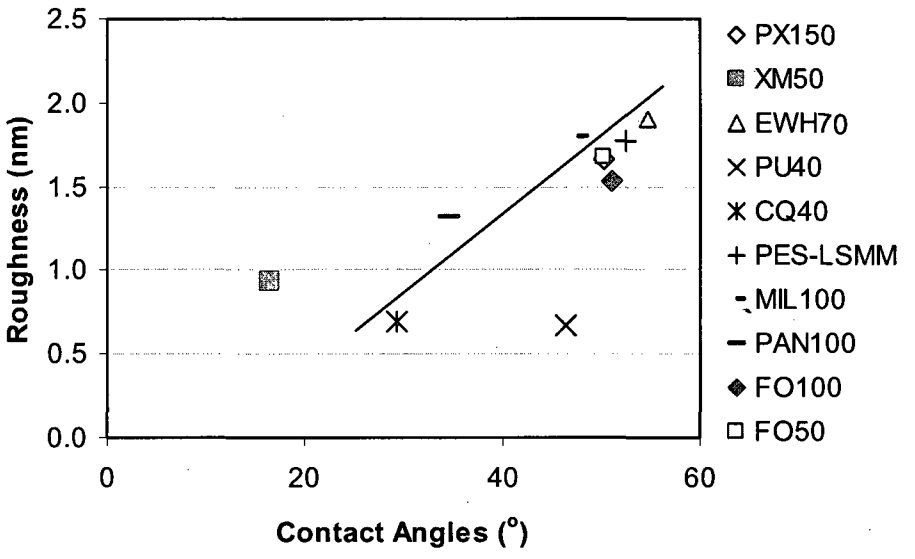

Figure 6.7. Relation of Hydrophilicity and Roughness

Figure 6.7 shows that roughness increased with an increase in the contact angles except for XM50. The water permeation rate will increase with a decrease in the contact angle, which means an increase in hydrophilicity. In fact, both cellulose (XM50) and cellulose acetate (CQ40) membranes that correspond to the lowest contact angles showed the highest PWP values (see Figure 6.1 where the hydraulic resistance of the membranes is given). Then, from the trend shown in Figure 6.7, it is concluded that the smoother membranes will have higher values of PWP. This seems contradictory to the results reported by Khayet et al. (2004) and Hirose et al., (1996). It should, however, be noted that the results presented in Figure 6.7 involves membranes made of many different materials. On the other hand the data shown by Khayet et al. (2004) and Hirose et al. (1996) were obtained from membranes prepared from the same base polymeric material. It should also be emphasized that cellulose and cellulose acetate membranes were the smoothest and the most hydrophilic among the tested membranes.

The impact of roughness on foulant deposition is also a topic of interest. Assuming no other factors are at play, membranes that have higher roughness should retain more foulants since it is easier for them to accumulate in the valleys within the rough membrane surfaces. Roughness can impact the interactions between particles and membrane surface resulting in enhanced attachment of particles onto the surface and

hence more severe fouling (Elimelech et al., 1997). Figure 6.8 shows the correlation of roughness and fouling phenomenon in term of flux reduction. Statistical analysis showed that no clear trend could be found with increasing roughness for the conditions tested. Again, the reason might be attributed to different base polymer membranes.

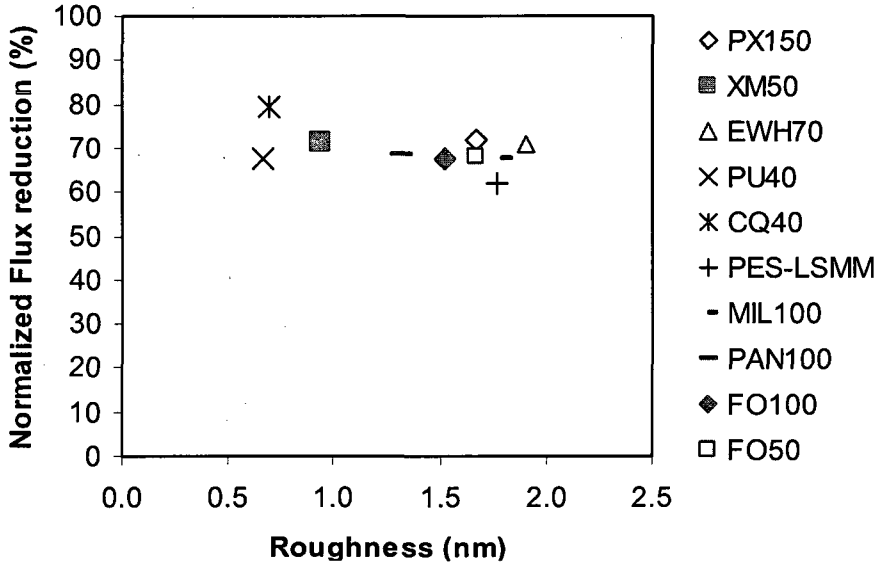

Figure 6.8. Impact of surface roughness on membrane fouling

6.5 Conclusions

The characteristics and performance of nine commercial ultrafiltration membranes were compared with those of an experimental membrane. The PES-LSMM experimental membrane had the highest flux resistance due to its low initial PWP flux and comparable long term fluxes to those of the other commercial membranes. Based on the pore characterization and roughness measurement, the modified cellulose acetate (CQ40) and polyethersulfone (PU40) membranes appeared to be the most promising in terms of fluxes and fouling potentials. Considering the MWCO of membranes, molecular weight distribution of NOM and NOM rejection, it is noted that MWCO as measured by PEG was not a good predictor of NOM rejection. The experiments showed that the membrane with the highest NOM rejection (PES-LSMM) was not the one having the lowest MWCO. The highest TOC rejection (approximately 80%) was achieved by the tight, tailor-made PES-LSMM membrane. This TOC rejection was relatively high compared with the 20% to 40% reported in the literature. Thus, LSMM was proved to have a

positive impact on membrane modification. Future researches on fabrication of LSMM hollow fiber UF membranes as well as the impact of cleaning on their performance should be implemented to obtain the full understanding of the effects of these surface active molecules.

6.6 Acknowledgement

The authors gratefully acknowledge the financial support from the Vietnam Government (Vietnamese Overseas Scholarship Programs -VOSP) and Materials and Manufacturing Ontario (MMO) for this research. Sincere thanks to Dr. Dipak Rana of the Industrial Membrane Research Institute, Department of Chemical Engineering, University of Ottawa for his cooperation in the LSMM synthesis.

6.7 References

Alsari AM, Khulbe KC, Matsuura T. 2001. The effect of sodium dodecyl sulfate solutions as gelation media on the formation of PES membranes. J. Membr. Sci. 188: 279-293

Amy G, Clark M, Pellegrino J. 2001. NOM rejection by, and fouling of, NF and UF membranes. Project #390, AWWA Research Foundation, Denver, CO.

Baker RW. 2004. Membrane Technology and Applications. John Wiley & Sons, Ltd. Hoboken. NJ

Bessieres A, Meireles M, Coratger R, Beauvillain J, Sanchez V. 1996. Investigations of surface properties of polymer membranes by near field microscopy. J. Membr. Sci.109: 271-284

Chan C.M. 1994. Polymer Surface Modification and Characterzation. Hanser Publishers. New York, NY

Cheryan M. 1986. Ultrafiltration Handbook. Technomic Publishing Co., Lancaster, PA

Cho J, Amy G, Pellegrino J. 2000. Membrane filtration of natural organic matter: comparison of flux decline, NOM rejection, and foulants during filtration with three UF membranes. Desalination, 127: 283-298

Cho J, Sohn J, Choi H, Kim IS, Amy G. 2002. Effects of molecular weight cutoff, f/k ratio (a hydrodynamic condition), and hydrophobic interactions on natural organic

matter rejection and fouling in Membranes. J. Water Supp. Res. Technol.—AQUA. 51.2:109-123

Elimelech M, Xiaohua Z, Childress AE, Seungkwan H. 1997. Role of membrane surface morphology in colloidal fouling of cellulose acetate and composite aromatic polyamide reverse osmosis membranes. J. Membr. Sci. 127:101-109

Fritzsche K, Arevalo AR, Connolly AF, Moore MD, Elings V, Wu CM. 1992. The structure and morphology of the skin of polyethersulfone ultrafiltration membranes: A comparative atomic force microscope and scanning electron microscope study. J. Appl. Polym. Sci. 45: 1945-1956

Hirose M, Itoh H, Minamizaki Y, Kamiyama Y. 1996. Proceedings of International Congress on Membranes and Membrane Processes, Yokohama, 178-179

Ho JYC, Matsuura T, Santerre JP. 2000. The effect of fluorinated surface modifying macromolecules on polyethersulfone membranes. J. Biomater. Sci. Polym. 11: 1085-1104

Hong S, Elimelech M. 1997. Chemical and physical aspects of natural organic matter (NOM) fouling of nanofiltration membranes. J. Membr. Sci. 132: 159-181

Khayet M, Suk DE, Narbaitz RM, Santerre JP, Matsuura T. 2002. Study on surface modification by surface-modifying macromolecules and its application in membrane separation processes. J. Appl. Polym. Sci. 89: 2902-2916

Khayet M, Khulbe KC, Matsuura T. 2004. Characterization of membranes for membrane distillation by atomic force microscopy and estimation of their water vapor transfer coefficients in vacuum membrane distillation process. J. Membr. Sci. 238: 199–211

Matsuura T. 1994. Synthetic membranes and membrane separation processes. CRC Press. Boca Raton. FL.

Mosqueda-Jimenez DB, Narbaitz RM, Matsuura T. 2004a. Membrane fouling test: apparatus evaluation. J. Environ. Eng. 130: 90-99

Mosqueda-Jimenez DB, Narbaitz RM, Matsuura T. 2004b. Impact of the membrane surface modification on the treatment of surface water. J. Environ. Eng. 130: 1450-1459

Mosqueda-Jimenez DB, Narbaitz RM, Matsuura T, Chowdhury G, Pleizier G, Santerre JP. 2004c. Influence of processing conditions on the properties of ultrafiltration membranes. J. Membr. Sci. 231: 209-224

Mosqueda-Jimenez DB, Narbaitz RM, Matsuura T. 2004d. Manufacturing conditions of surface-modified membranes: effects on ultrafiltration performance. Sep. and Puri. Technol. 37: 51-67

Mosqueda-Jimenez DB. 2003. Impact of manufacturing conditions of polyethersulfone membranes on final characteristics and fouling reduction. Ph.D. thesis. University of Ottawa, Ottawa, ON

Nguyen HA. 2005. Membrane fouling reduction by the incorporation of hydrophilic surface modifying macromolecules in ultrafiltration membrane manufacturing. M.A.Sc thesis. University of Ottawa, Ottawa, ON

Nguyen HA, Narbaitz RM, Matsuura T. 2007. Impacts of hydrophilic membrane additives on the ultrafiltration of river water", J Environ Eng, 133, 515-524

Persson KM, Gekas V, Trägårdh G. 1995. Study of membrane compaction and its influence on ultrafiltration water permeability. J. Membr. Sci. 100:155-162

Pham VA. 1995. Surface modifying macromolecules for enhancement of polyethersulfone pervaporation membrane performance. M.A.Sc. thesis. University of Ottawa, Ottawa, ON

Rana D, Matsuura T, Narbaitz RM, Feng C. 2005. Development and characterization of novel hydrophilic surface modifying macromolecule for polymeric membranes. J. Membr. Sci. 249: 103-112

Singh S, Khulbe KC, Matsuura T, Ramamurthy P. 1998. Membrane characterization by solute transport and atomic force microscopy. J. Membr. Sci. 142: 111-127

Suk DE, Chowdhury G, Matsuura T, Narbaitz RM, Santerre P, Pleizier G, Deslandes Y. 2002. Study on the kinetics of surface migration of surface modifying macromolecules in membrane preparation. Macromolecules. 35: 3017-3021

CHAPTER 7

EVALUATION OF APPARATUSES FOR MEMBRANE CLEANING TESTS

Huyen T. Dang[1], Roberto M. Narbaitz[1], Takeshi Matsuura[2]

[1]*Dept. of Civil Engineering, Univ. of Ottawa, 161 Louis Pasteur St., Ottawa, K1N 6N5, Canada*
[2]*Dept. of Chemical and Biological Engineering, Univ. of Ottawa, 161 Louis Pasteur St., Ottawa, K1N 6N5, Canada*

7.1 Abstract

Membrane cleaning is critical part of the operation of membrane processes. This paper studies the impact of four different types of bench-scale membrane systems on evaluating the effectiveness of different cleaning steps. The systems are a stirred ultrafiltration (UF) cell, a SEPA cell, a cross-flow (CF) cell and a six-CF cells-in-parallel system. The effect of cleaning frequency (every four hours, two hours and 30 min) also was investigated. The comparison was implemented in terms of flux recovery, solute removal, solute resistance removal and changes of contact angles. The stirred UF cell was only reliable and comparable in terms of flux. The flux behavior of six-cells-in parallel system was far different with the factor of two compared with that of single cells. However at short cleaning interval (i.e., 30 min), the cleaning efficiency of membranes was not altered significantly for those CF systems. The cleaning interval did not statistically affect the flux recovery when stirred UF cell and SEPA cells were used. NOM from Ottawa River water fouled the membranes irreversibly; they could not be restored completely by clean-in-place method even with rigorous chemicals. Only ex-situ cleaning with a sponge could remove up to 99% of the fouling layer.

Keyword: membrane cleaning, test apparatuses, surface modification, flux recovery, solute resistance removal.

7.2 Introduction

In water and wastewater treatment applications of membrane technology, cleaning is a vital part of operations and has significant economic and technical impacts. Even though cleaning will gradually change the membrane integrity and properties [1], the increased water production is of greater interest. The degradation of membrane quality due to cleaning is minimal as membranes can last seven or more years with frequent cleaning. Research into the effectiveness of the cleaning process has studied the impact of cleaning frequency and duration, types of cleaning (physical versus chemical), cleaning mechanisms, types and concentration of cleaning chemicals. The optimum conditions depend on the types of foulant(s), membranes and operational conditions (temperature, pH, velocity, pressure). Nevertheless, so far there has not been a study on the impact of the membrane filtration apparatus type on cleaning efficiency. Thus, this paper would look at the cleaning efficiency as a function of the type of lab-scale apparatus utilized. A variety of bench-scale apparatuses have been employed to investigate membrane cleaning. By far, the most widely used for flat sheet membranes is stirred batch UF cell with different volumes [1-4]. Crossflow (CF) cells have also been utilized in fouling and cleaning evaluations, especially the ones from Nitto Denko Corporation [5, 6] and the SEPA CF cell from GE Osmonics [7]. The cleaning can be as simple as soaking in glass tubes of chemical solutions for a day [8]. Certainly these apparatuses are standardized cells (except for the last method) which can be used to examine the behavior of flat sheet membranes. In this study, besides the above apparatuses, another CF cell which was designated according to the principle described by Matsuura [9] will be tried for cleaning purpose. This type of CF cell has been used for permeation tests [10-13].

Our main objective is to compare systematically the behavior of cleaning efficiency using four different lab-scale membrane filtration apparatuses (Stirred UF cell, SEPA cell, single CF cell and six CF cells in parallel). In addition, two related topics are also investigated: (a) impact of cleaning frequency (every four hours, two hours or 30 min); and b) the impact of membrane surface modification on cleaning. The experimental membranes used in this study were blended with hydrophilic additives. Details of this modifying additive will be given in a later section.

7.3 Experimental methods and analysis

7.3.1 Water characteristics

The cleaning was conducted on membranes that became fouled by filtering raw Ottawa River water (ORW) collected from the intake of the Britannia Water Treatment Plant (Ottawa, Ontario) in April 2007. Water quality is presented in Table 7.1. Ottawa River water (ORW) is considered to be as typical of northern rivers with brown color, relatively high natural organic matter (NOM) content, low turbidity and hardness. The test results reported in Table 7.1 were conducted following the procedures outlined in Standard methods for Water and Wastewater Examination [14]. Raw water was utilized to accelerate the fouling. A ultrafiltration water treatment plant would likely include a coagulation pre-treatment step.

Table 7.1 Characteristics of Ottawa River water (ORW)

Parameter	Unit	Analyzed data
TOC[a]	mg/L	6.78 ± 0.012
UVA^{b}_{254}	m^{-1}	0.308
SUVA[c]	L/mg.cm	4.54
pH		7.65
Conductivity	mS/cm	0.118
Colour		50
Turbidity	NTU	7.57 ± 0.002
Alkalinity	mg $CaCO_3$/L	44
Acidity	mg/L	80
Total Hardness	mg $CaCO_3$/L	45.65
Calcium Hardness	mg $CaCO_3$/L	43.48

[a] *TOC: Total organic carbon*

[b] *UVA_{254}: Ultraviolet absorbance at 254 nm*

[c] *SUVA: UVA_{254}/TOC*

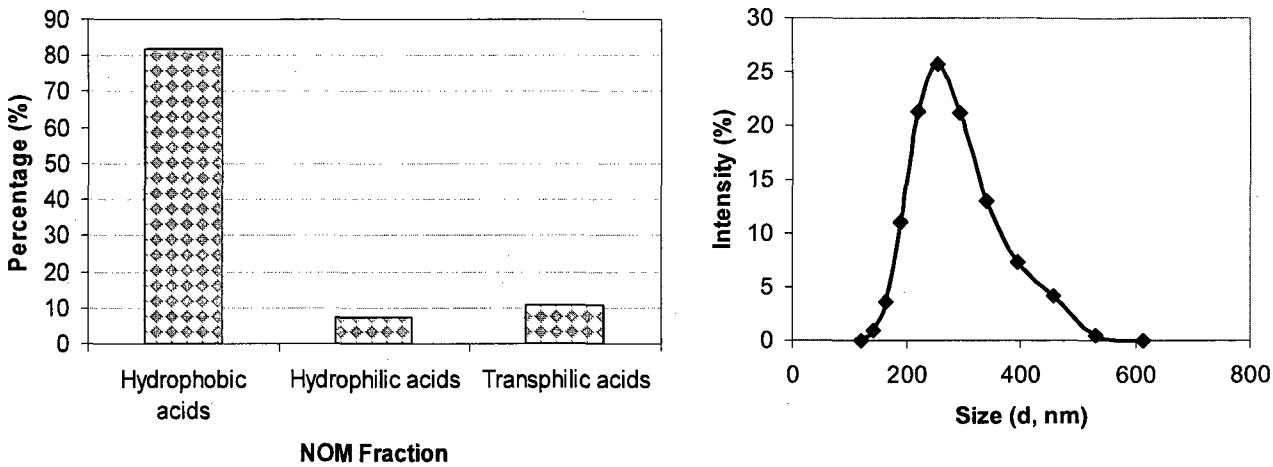

Figure 7.1. NOM fractions (a) and size distribution (b)

The NOM in ORW was isolated using XAD8/XAD4 resin into hydrophobic, hydrophilic and transphilic fractions [15]. ORW contains mostly hydrophobic organics (Figure 7.1a), NOM (natural organic matter) size distribution was analyzed by Zetasizer Nano series particle size analyzer. This equipment performs size measurement using a process called Static Light Scattering (SLS) and combining with Debye plot. The average NOM size was found approximately 290 nm and most of the particles are between 200 and 400 nm in size.

7.3.2 Membranes

Three types of PES membranes were employed in this study. The first two were laboratory-made PES and PES-LSMM membranes. They are fabricated by the phase inversion technique using polyethersulfone (PES) as the base polymer (Victrex 4100P, Powder, ICI Advanced Materials, Billingham, England) with or without blending hydrophiLic Surface Modifying Macromolecule (LSMM) and 1-methyl-2-pyrrolidinone (NMP) as the solvent. Details of LSMM can be found elsewhere [12, 16]. For the PES-LSMM membranes, the additive LSMM was incorporated in the casting solution. The flux enhancement achieved by blending LSMM was reported in our previous work [11, 12, 16]. The third membrane type tested was a commercial PES-PU membrane from GE Osmonics. The characteristics of these membranes as determined in earlier studies [16, 17] are presented in Table 7.2.

Table 7.2 Membrane characteristics

Membrane type	MWCO (kDal)	Mean pore size (nm)	Contact angle (°)	Surface charge (mV)	Roughness (nm)	Water content (g/m^2)
PES	72	4.6	71.6	-6	1.27	126.84
PES-LSMM	70	4.35	70.1	-3	1.72	126.94
PES-PU	58	4.8	64.2	-3.3	0.67	-

Obviously, the commercial PES PU membranes are more hydrophilic and smoother than the laboratory-made membranes. The commercial membranes were rinsed thoroughly with distilled de-ionized water and stored in 10% ethanol solution before testing.

7.3.3 Test cells

Four systems were evaluated including an Amicon stirred UF cell 8400 (Fisher Scientific, Hampton, NH), an Osmonics' SEPA cell (GE Osmonics Labstore, Minnetonka, MN), a single CF cell and a six-CF cells-in-parallel system (Fig. 2). As mentioned previously, the stirred UF cell (Figure 7.2a) was chosen since it has been widely used for not only permeation tests but also cleaning studies. The cell is made of polysulfone and has a volume capacity of 400ml. The minimum working volume is 10 ml. The SEPA cell was chosen because it has been recommended by Osmonics® for simulating the flow dynamics of larger commercially spiral-wound membrane elements [18]. The CF cells, fabricated at our machine shop according to the design described by Sourirajan and Matsuura [19], were used in the last two systems (Figures 7.2c and 7.2d). The cell is made of 316 stainless steel, having a relatively large cross-sectional area for fluid flow at the entrance and the exit, thus the pressure drop across the cell is less than 7 kPa gauge (1 psig) per cell. The CF cell also has a thin channel flow design above the membrane surface (Table 7.3), which allows a relatively high fluid velocity parallel to the membrane surface. The volume in this channel and the inlet and outlet openings were approximately the same [18]. The smaller membrane area of the CF cells is advantageous in testing experimental membranes because defect-free membrane coupons of a large size may be difficult to produce. The six-cells-in-parallel setup was constructed to be able to test six

membrane coupons simultaneously and shorten the duration of the study. The multiple cells can be used to test replicates, increasing the membrane area tested, or to test different types of membranes. To maintain even flow rate and pressure distribution among the cells, pressure gauges and valves were installed for each cell (Figure 7.2d) and the flow-meters were installed before and after the cells to check the flowrate apiece. The discrepancy among the cells was less than 6% and 5% for pressure and flow rate, respectively. Previous study on filtration of NOM using these apparatus found after six-day continuous flow tests that the SEPA cell and the CF cells yielded very similar dissolved organic carbon removals and flux decline, despite SEPA cell using membrane coupons eight times larger than CF cells [18]. This study would disclose if the cleaning efficiency is similar for the four membrane filtration set-ups.

Table 7.3 Detailed descriptions of test cells

Test Cell	Manufacturer	Pressure (kPa)	Membrane dimension (cm)	Effective membrane area (cm^2)	Cell parameters (cm)
Stirred UF cell 8400	Amicon	345 (517.5)[1]	D=7.6	41.8	Working V=10-400ml
SEPA cell	Osmonics	345 (6900)[1]	LxW= 19.1 x 14.0	155	$W_{membrane}$ = 8 δ_{spacer} = 0.086 L x W x H ($_{channel}$) =7.7 x 2.6 x 0.3
CF cell	Civil Engineering machine shop	345 (1380)[1]	D=5.2	19.5	r_1=0.3175; r_2=2.55 $\theta = 4.5^{o}$, h_{gap}= 0.06

- *pH = 2-10*
- *Temperature: 20-25°C*
- [1] *Operating pressure (max pressure)*

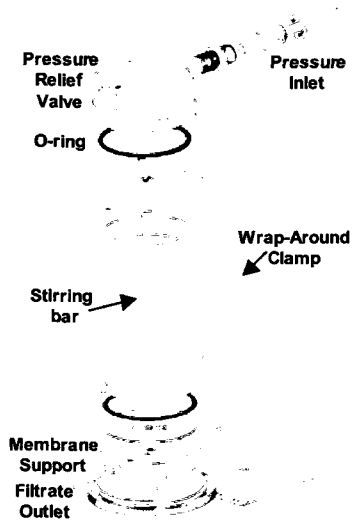

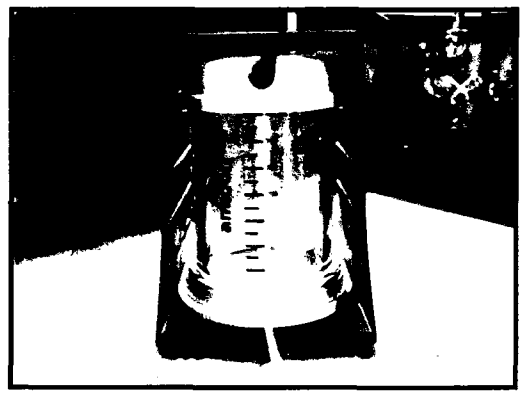

(a) Stirred cell (Amicon)

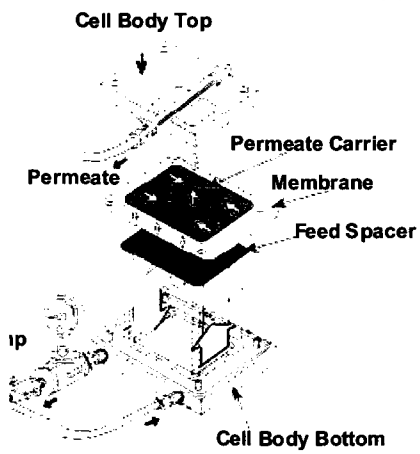

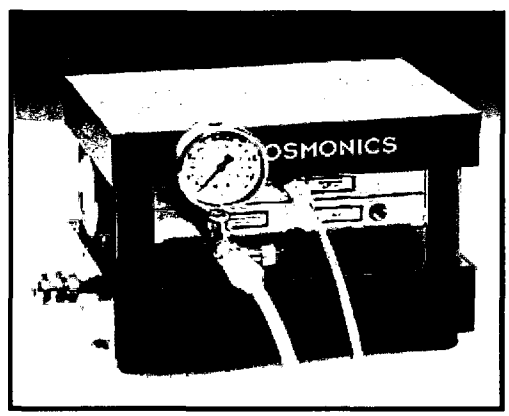

(b) SEPA cell (Osmonics)

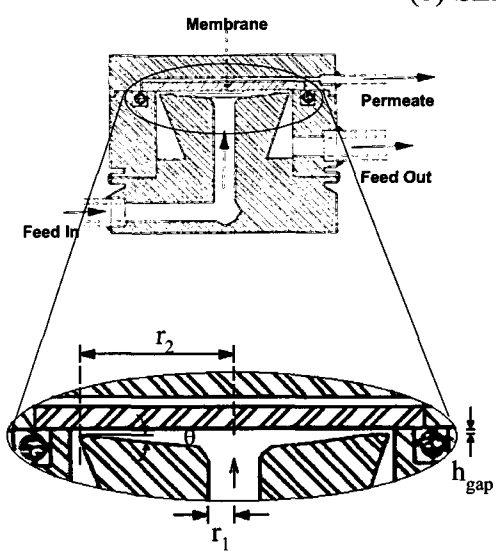

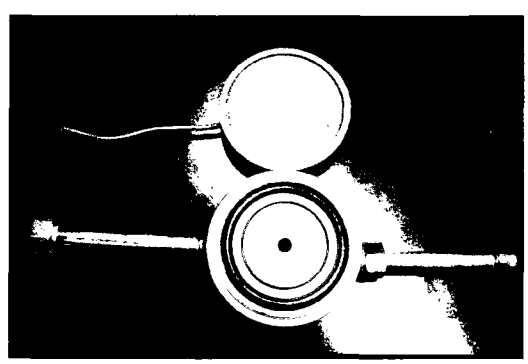

(c) CF cell

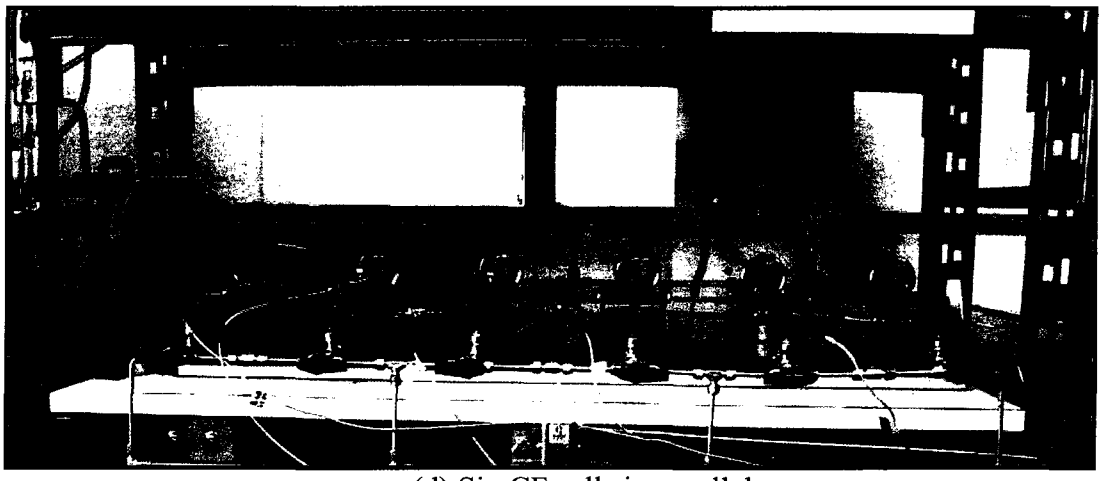

(d) Six CF cells in parallel

Figure 7.2. Cleaning apparatuses

7.3.4 Experimental protocol

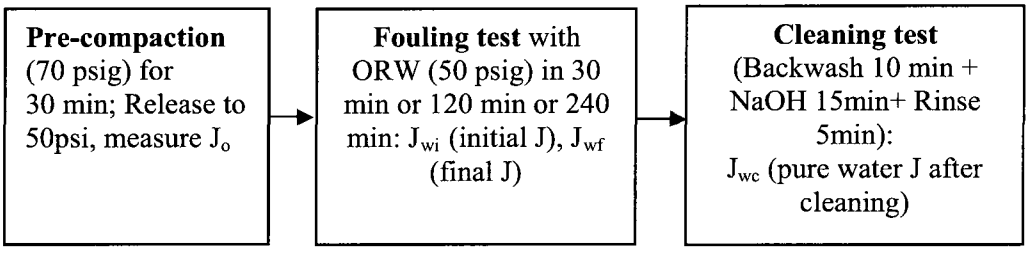

Figure 7.3. Fouling and cleaning protocol

The protocol for fouling and cleaning is outlined by Figure 7.3. This protocol was used for both dead-end cell (stirred UF cell) and the three types of crossflow cells. The membranes were first pre-compacted with deionized water for 30 min at 483 kPa (70 psig), followed by a filtering step with ORW (i.e., fouling) under an operating pressure of 345 kPa gauge (50 psig) and at a feed flow rate of 0.4 Lpm. Deionised ultra pure water from a Milli-Q Water System (Millipore, Bedford, MA) (hereafter called MQ water) was used for water permeation, backwashing and rising test. The duration of the fouling run was varied from 30 min, 120 min or 240 min to investigate the effect of the cleaning interval. The fluxes J_{wi} and J_{wf} were measured in the beginning and at the end of the fouling run. After cleaning test (backwashing and chemical cleaning), flux with pure water was recorded as J_{wc} to compare with J_o. It should be noted that the feed flowrate of 0.4 Lpm was chosen to create a mean crossflow velocity (U_c) of about 0.1 m/s which is within a common range of crossflow velocity used in bench-scale operation of UF

membrane elements [20]. The mean crossflow velocity of both CF cell and SEPA cell was calculated based on equations provided elsewhere [18] with cell dimensions summarized in Table 7.3. It was claimed that although the mean cross-flow velocity was the same for SEPA cell and CF cell, their Re (Reynolds number) were quite different (Re_{CF}/Re_{SEPA} = 1.9). It was unsure which hydrodynamic parameter, U_c or Re, has a greater influence on the fouling since the flux reduction after long-term experiment was statistically the same [18]. Given the objective of this study is to evaluate the membrane test cells for cleaning, not to find the effect of hydrodynamic parameters on cleaning, we chose to use equal mean U_c for fouling and cleaning tests and set the feed flowrate to get U_c in the common range used in bench-scale operation of UF membrane elements.

The schematic diagram of the fouling and cleaning experimental setup for the systems with *crossflow cells* is depicted in Fig. 4. It consists of a feed tank, a permeate tank (or MQ water tank in case of backwashing since the amount of the permeate generated was not sufficient), a chemical tank (0.1M NaOH solution), a high pressure diaphragm pump (Hydra-Cell, Wanner Engineering, Inc.; Minneapolis MN), a pressure regulator, valves and the membrane test cells. ORW was used as a feed water for the fouling test (Figure 7.4a). The same cleaning protocol was used for the three systems with crossflow cells including backwashing, chemical cleaning and rinsing with ultra pure water.

During the backwashing, the MQ water was pumped from the permeate side for 10 min at the same operating pressure (50 psig). In the case of CF-cells-in-parallel system, which was not designed to accommodate backwashing, the cells were opened, the membranes were then flipped over and the cells reassembled. MQ water was pumped and detached the foulants as a normal backwashing. This method has been done else where [21].

During the chemical cleaning, 0.1M NaOH (pH=12.5) solution was circulated under no pressure for 5 min then the membranes were rinsed with MQ water for 5 min. NaOH solution was selected for cleaning because it is cheap and among the most effective reagents widely used in industrial application. After rinsing the pure water flux (J_{wc}) was measured. pH was checked to guarantee the return neutral pH conditions after the chemical cleaning.

For the stirred UF cell (*dead-end mode*), the experimental protocol is slightly different because the pressure is applied by nitrogen gas. During the fouling test, filtration was

carried out under an operating pressure of 345 kPa gauge (50 psig) supplied from a nitrogen gas cylinder. After a specific interval (30 min, 120 min or 240 min), the membranes were cleaned following the same protocol as that for the crossflow cells. Similar to the CF-cell-in-parallel system, it is impossible to backwash the membranes with stirred UF cell, the membranes were then flipped over for backwashing. For chemical cleaning, the membranes were brought into contact with 0.1 M NaOH solution by loading the feed chamber of the cell with NaOH solution. Finally, the membranes were rinsed with MQ water. During the fouling and cleaning tests, the permeation rates and TOC (total organic matter) drawn from the four apparatuses were measured at a predetermined interval.

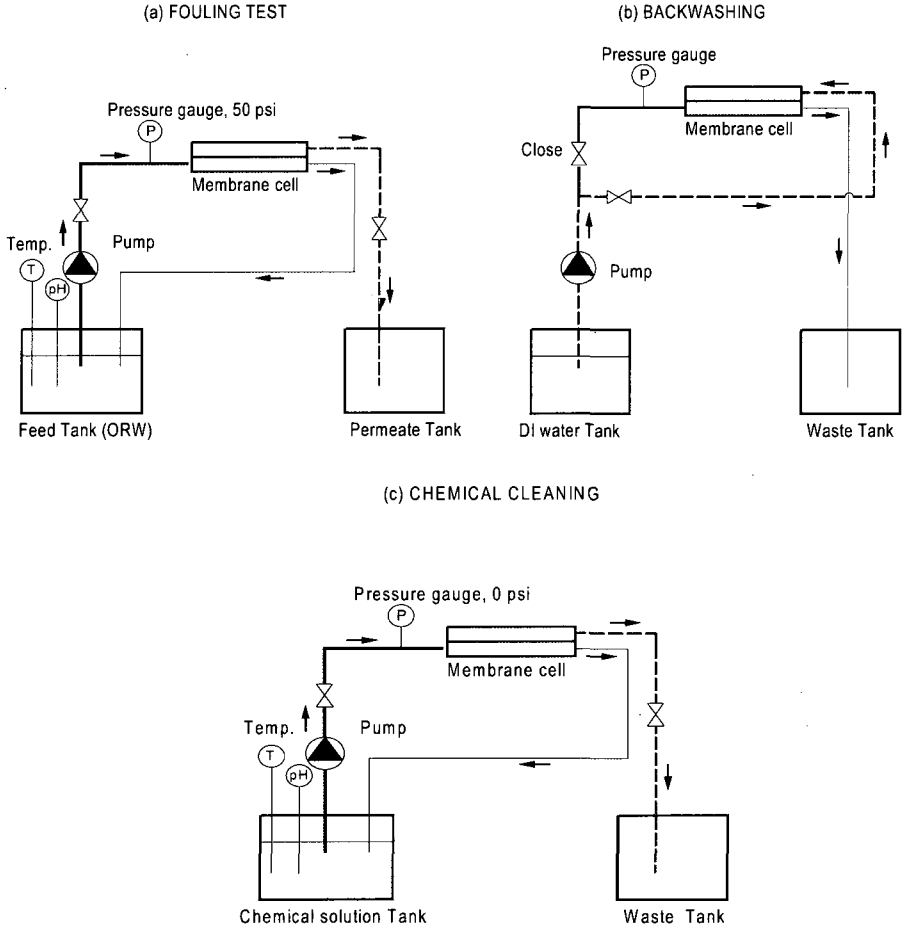

Figure 7.4. Schematic diagram of the apparatus for fouling and cleaning experiment

In all cleaning tests, care was taken to ensure the system is under the same operating conditions (pH=7±0.5, room temperature) before each test. The fouling and cleaning experiments were conducted in replicate at room temperature.

In order to interpret the discrepancy, non-destructive measures such as flux, solute retaining, contact angle and streaming potential have been used extensively [8, 21-23]. The purpose of this study is to investigate the macro-scale behavior of membranes with the same cleaning method but using different apparatuses, thus conventional parameters such as flux recovery, solute rejection (via TOC measurement) and contact angle (hydrophilicity) alternation are of the most concern to be evaluated. The contact angle was measured using a goniometer (VCA Optima Surface Analysis System, AST Products, Inc., Billerica, MA). The efficiency of membrane performance and efficiency of cleaning will be quantified by the following parameters:

$$Flux\ reduction = \frac{J_{wi} - J_{wf}}{J_{wi}} x100\% \qquad [7.1]$$

Where J_{wi}: initial flux during the fouling test with ORW (L/m2/h)

J_{wf}: final flux during the fouling test with ORW (L/m2/h)

$$Flux\ recovery\ \text{FR:}\ FR = \frac{J_{wc}}{J_{wo}} x100\% \qquad [7.2]$$

Where J_{wc}: Pure water flux after cleaning test (L/m2/h)

J_{wo}: Initial flux with pure MQ water (L/m2/h)

$$NOM\ removal = \frac{C_b - C_p}{C_b} x100\% \qquad [7.3]$$

Where C_b, C_p: concentration of NOM in the feed and permeate at the end of the fouling test (mg/L)

$$Solute\ resistance\ removal\ RR = \frac{R_{sw} - R_{sc}}{R_{sw}} x100\% \qquad [7.4]$$

$$\text{Where } R_{sw} = \frac{\Delta P}{\mu J_{wf}} - R_m : \text{Residual solute resistance of the fouled membranes} \qquad [7.5]$$

$$R_{sc} = \frac{\Delta P}{\mu J_{wc}} - R_m : \text{Residual solute resistance of the cleaned membranes} \qquad [7.6]$$

$$R_m = \frac{\Delta P}{\mu J_{wo}}$$: Hydraulic membrane resistance [7.7]

J_{wf}: flux at the end of fouling test period (L/m^{2}h)

ΔP: transmembrane pressure (N/m^2)

μ: viscosity of water at 22°C (Ns/m^2)

As recommended by Muñoz-Aguado [4], neither flux recovery nor solute resistance removal alone can be sufficiently used to characterize cleaning efficiency because large resistance removal values are often easily achieved when large amounts of foulants are deposited, but these high resistance removals do not equate with high flux recoveries.

7.4 Results and discussions

7.4.1 Effect of tested apparatuses

This section compares membrane cleaning and post-cleaning performance using the four UF systems (a stirred UF cell, a SEPA cell, a single CF cell and a six-CF cell- in parallel system) used in bench-scale membrane filtration studies. In order to minimize the variability due to membrane coupons while comparing the cleaning efficiency of the four cells, coupons of only one commercial membrane (PES PU membranes provided by Osmonics) were chosen for the analysis.

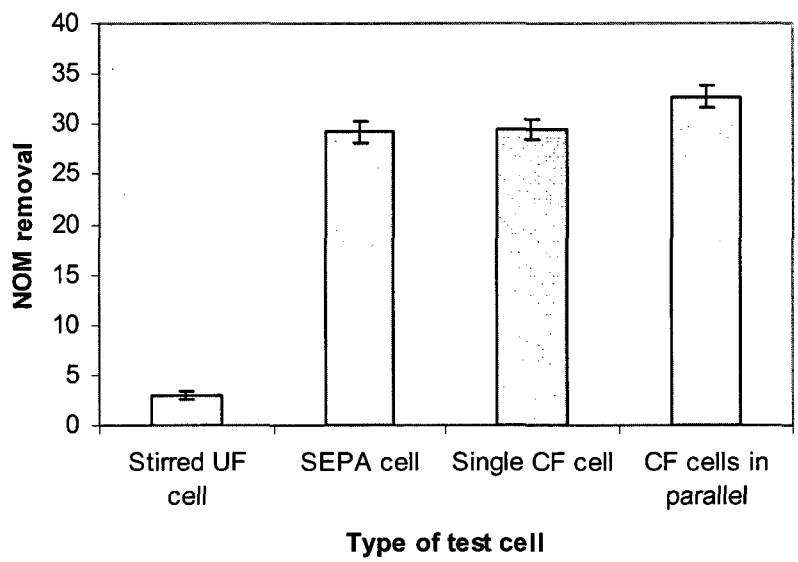

Figure 7.5. NOM removal after four-hour fouling test with ORW (using PES PU membranes only)

The stirred UF cell has been of interest because of it is compact, portable and less expensive than other cells. Since it operates in a dead-end mode, one can expect high fouling acceleration because of the increase of the bulk concentration inside the cell with time. However, its consistent low NOM removal (Figure 7.5) proved that some of NOM leaked through the membranes pores to the permeate side. Other possible explanation may lie in the higher bulk concentration with time within stirred UF cell. The NOM removal by the stirred cell was only 3% while the other cells rejected approximately 30% of the NOM during the test period. Hence for cleaning purposes, it seems inappropriate to evaluate the performance of membranes in term of NOM rejection using the stirred UF cell. Only flux monitoring before and after cleaning was used in the remaining evaluations for this cell. Secondly, since the membranes were flipped over for backwashing, pressure was applied at the most powerful mode (perpendicular to the membrane surface not tangent). Thus, some NOM foulant was even detached from inside membrane pores. The efficiency of backwashing by this module was the highest, i.e., up to 60-70% of total recovery by the combined backwashing and chemical method while for the other cells, backwashing recovered only about 50% (See Figure 7.6). Choi [25] found the same results that in the absence of tangential flow (i.e., the case of UF stirred cell), permeate flux decline was dominantly caused by reversible fouling. The reversible fouling then could be removed effectively by physical cleaning such as backwashing.

The flux curves for two cycles of cleaning are presented in Figure 7.6 (PES PU membranes, four-hour cleaning interval i.e., four hours of fouling test was followed by 10-min backwashing and 15-min chemical cleaning, then terminated with 5-min MQ water rising). It is worth noting that in some cases, cleaning led to higher water flux. Arkhangelsky [1] explained that phenomenon in term of ionization of the membrane surface. It happened due to the partial scission of the C–S bond, which was manifested in the elevated concentrations of sulfur and carbon in the upper part of the PES membrane. Kuzmenko [2] interpreted the increase of flux and faster fouling in consecutive cleaning in aspect of the nature of interactions between solutes and the membrane surface. When the membrane is pristine, the interactions were mainly electrostatic, and when it started being fouled, the bonds between solutes and membrane surface were probably covalent.

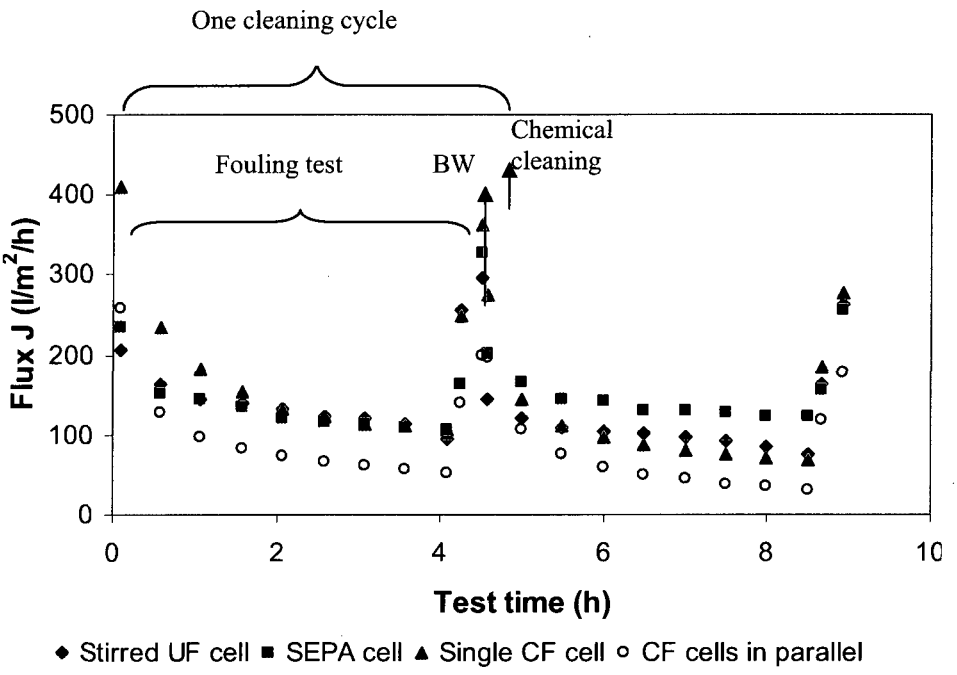

Figure 7.6. Flux path during the testing period

In the first fouling-cleaning cycle (4 hours/cycle), the single CF cell initially generated higher flux than did the SEPA cell and the stirred cell. It might be due to the very thin channel above the membrane surface which creates more turbulent flow adjacent to the membrane surface, accordingly permitting higher water mass transfer rates. However, high flux rates often led to a higher fouling tendency, thus for the last two hour of the first cycle the fluxes of the three single cells were similar. The SEPA cell has a bit greater gap (1.4 times greater) above the membrane surface due to the spacing material (feed spacer). Such plastic netting spacing materials are typically designed to facilitate mass transfer by promoting turbulence of the bulk feed flow [24]. For the stirred UF cell, the gap between stirred bar and membrane was 3mm, the pressure driven by the nitrogen gas was applied perpendicularly not tangential to the membrane, the mass transfer rate or the flux obtained was therefore comparable with the other cells. Choi [25] reported that tangential flow caused slightly higher irreversible fouling due to higher permeation drag, as compared to the case of absence of tangential flow. The flux behavior of the three single cells however was different for the consecutive cycles. It would appear that the effect of NOM fouling layer deposited on membrane surface was the main reason. The flux of the cells within the six-cells-in-parallel system was about half of that of the single test CF cell for the same membranes (Figure 7.6). The possible explanation of this result may lie in the flowrate/pressure distribution among the 6-cell system and/or the cell

design even though the discrepancy was recorded less than 6% and 5% for pressure and flowrate, respectively.

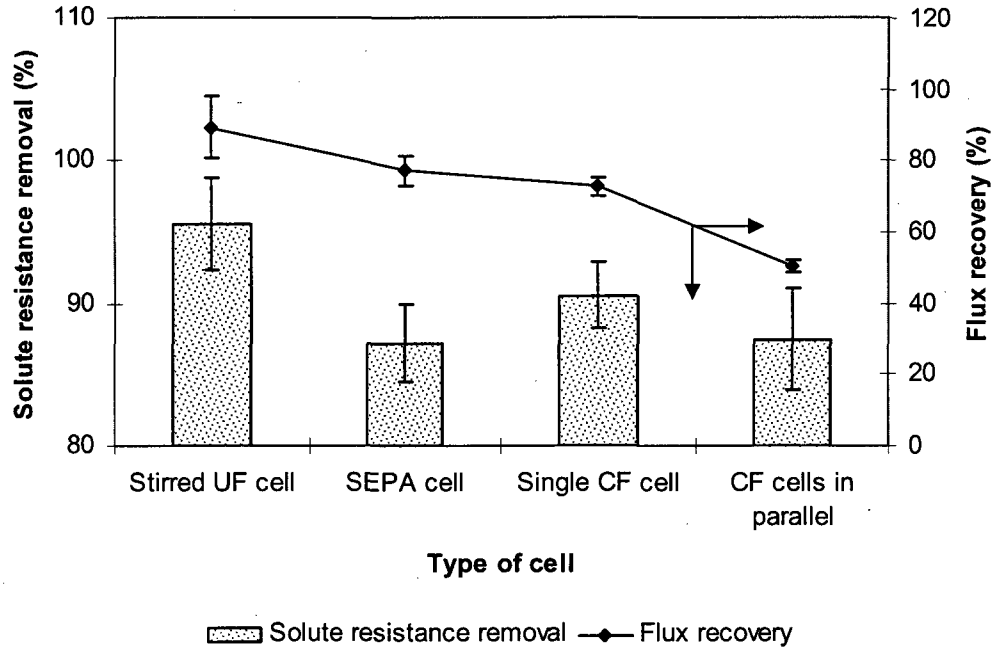

Figure 7.7. Cleaning efficiency after 4-hour fouling period

Figure 7.7 shows the cleaning efficiency of commercial PES PU membranes using different cells. The flux recovery increased from 50% for CF system to almost 90% for the stirred UF cell. The solute resistance removal was surprisingly high (averaging 90% for all cells). It is understandable for the stirred UF cell to have the highest resistance removal since most of the NOM detached during the backwashing. The solute resistance removal for the SEPA tests seemed to be a bit low. A possible explanation may fall in the cell design. As the SEPA cell had a feed spacer even with harsh chemical cleaning or backwashing, it might be still difficult to remove completely the NOM deposition hidden under or attached to the spacer net. For the stirred cell, membrane flipping-over during backwashing under perpendicular flow (dead-end operation mode) helped remove the reversible NOM at most, leading to the highest solute resistance removal for this cell. However at the 95% confidence level there was no difference in the resistance removal among the tested cells.

7.4.2 Effect of cleaning frequency

Further to the evaluation of cells for cleaning tests, this study also assessed the impact of cleaning frequency on the different cell systems. The filtration/fouling periods in the literature ranged from as short as less than one hour [2, 26-28], to several hours [22] or even several months, which usually applied to a pilot plant tests [29-31]. In most cases, short fouling durations were chosen. It is well recognized that short filtration (fouling) periods or more frequent cleaning maintain higher water production and achieve better foulant removal because the cake layer is not too thick or compact or penetrates deep inside the membrane pores under the cross flow and pressure with time. In practice, for commercial membranes, the cleaning frequency is usually recommended by the manufacturers. The most common chemical cleaning frequency is often two to three times per month. However it would be different for bench-scale experiments. The factors governing the selection of fouling period for a bench scale have not been clarified in most studies. They possibly were chosen depending on experience on fouling acceleration of tested membranes, critical fluxes of membranes or just time convenience. Kuzmenko [2] performed his fouling tests for 30 min because it was sufficient for filtration of 50 ml of the feed suspension.

In our study with ORW, the duration of the filtration (fouling) step was chosen to be 0.5h, 2 h or 4 h. Table 7.4 presents the flux recoveries for various cleaning frequency using different cell systems. In general the smaller the filtration time, the higher flux recovery for all types of test cells. Flux recovery was highest for SEPA cell, then stirred cell and CF cell showed the least recovery.

Table 7.4 Flux recoveries of the tested cells with different fouling durations for three types of membranes

Cleaning frequency	Stirred UF cell			SEPA cell			Six CF cell system		
	PES	PES PU	PES LSMM	PES	PES PU	PES LSMM	PES	PES PU	PES LSMM
4h fouling duration	**90.00** (3.22)	**89.43** (8.93)	**87.79** (8.11)	**70.15** (19.08)	**74.69** (4.33)	**82.77** (17.15)	**56.35** (13.47)	**50.58** (1.84)	**55.62** (1.87)
2h fouling duration	**97.94** (10.48)	**97.87** (6.32)	**93.63** (2.30)	**100.92** (20.81)	**87.90** (3.99)	**111.31** (16.06)	**68.22** (1.12)	**63.04** (7.12)	**66.46** (2.71)
0.5h fouling duration	**94.66** (4.88)	**99.77** (1.64)	**104.37** (10.69)	**80.81** (9.03)	**102.26** (15.03)	**100.51** (17.71)	**93.11** (14.46)	**72.53** (1.23)	**78.57** (3.16)

Since the standard deviations were not small, an one-way ANOVA statistical analysis was conducted. It revealed that at a significance level of $\alpha = 0.05$, the impact of cleaning frequency on flux recovery was only significant when using the six-CF cell-in-parallel system for all membranes types. In addition, there was significant evidence for the cell type effects at the 4-hour cleaning interval. Different cells had no impact at the 0.5-hour interval. Thus, the cleaning efficiency or cleaning evaluation would have no significant difference regardless of test cells as long as a short cleaning frequency (i.e., 30 min) is employed. Statistical analysis showed no significant difference in flux recovery for stirred UF cell and SEPA cell at long cleaning intervals (i.e., 2 hours or 4 hours). Nevertheless, to avoid the risk of difference in pressure/flowrate (as in six-CF cell system) or the impact of flow mode (as in stirred UF cell), SEPA cell would be recommended for the longer bench-scale cleaning test (several hours). The SEPA can also predict better a full-scale performance because it has permeate carrier and feed spacer as in the real spiral wound membrane modules. On the aspect of selecting cleaning interval for bench-scale testing, it would be difficult to recommend the best one since the optimized cleaning interval/frequency depends on many factors such as membrane types, test cell or type of feed water. Flux reduction can be used as an indication of time for cleaning, however, it varies with the above factors.

7.4.3 Effect of surface additive LSMM

Earlier studies showed that the increase of OH^- group on the surface of modified PES LSMM membranes made them slightly more hydrophilic and improved the flux and NOM removals to some extent [12]. For the cleaning, it has been hypothesized that since the hydrophilic membranes are often smoother and have water-like characteristic, they may increase the cleaning efficiency. According to Figure 7.8, the average flux recovery was smallest for backwashing and highest for combined backwashing+chemical cleaning method, and also slightly higher for the modified membranes. However, given the large error bars from the statistical point of view the three cleaning techniques were equally effective. In addition, the cleaning efficiency of the PES-LSMM modified membranes was not statistically better than that of the PES membranes.

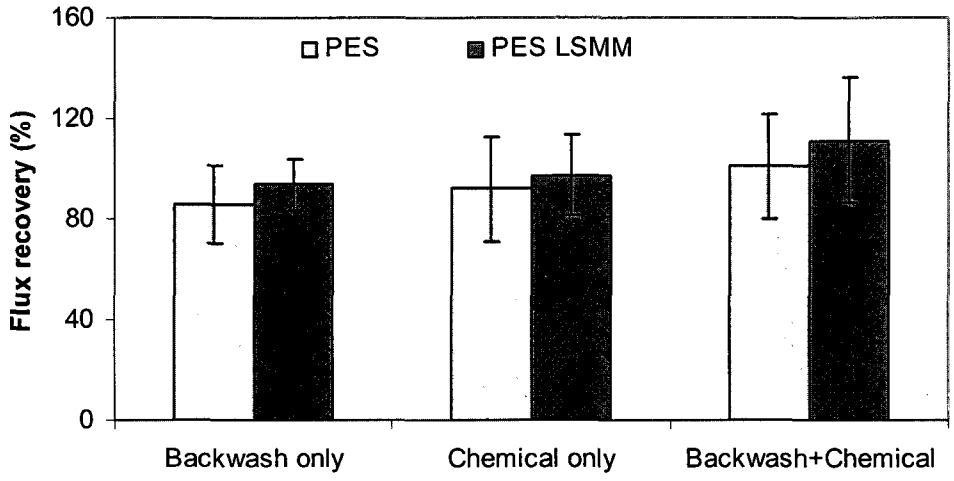

Figure 7.8. Cleaning efficiency of PES and PES LSMM (Test cell: SEPA cell)

7.4.4 Change of membrane surface

Membrane surface before and after cleaning was examined in terms of contact angles and morphological visualization. The first aspect is presented in Table 7.5.

Table 7.5 Recorded contact angles

Membrane type	Pristine membranes (°)	Fouled membranes (°)	Cleaned membrane* (°)
PES	71.6 (1.84)**	46.8 (4.62)	65.9 (3.66)
PES-LSMM	70.1 (4.08)	44.4 (3.22)	64.1 (2.72)
PES-PU	64.2 (2.95)	55.7 (7.78)	49.4 (4.54)

** Membranes after backwash and chemical cleaning*

***Values in brackets are standard deviations*

The trends of behavior of contact angles after cleaning were followed the previous observations [12] for PES LSMM but with different magnitude. This discrepancy may be due to different method of cleaning and goniometer used. The hydrophobic changes were the same for experimental membranes (PES and PES LSMM ones), i.e., they both became very hydrophilic as being fouled and came back to be less hydrophilic upon being cleaned. For the commercial PES PU, the contact angles kept decreasing during the fouling and cleaning tests. For all membranes it seems that once the membranes contact with water and solutes (during fouling period), the water molecules and solutes under

compaction are trapped inside the pores, giving membranes greater affinity to water and becoming more hydrophilic. That's why the contact angles all decreased for the tested membranes. This trend was consistent with [1] in which they found a decrease in contact angle and flux values due to the dislodgement of PVP component from the membrane matrix. However, Pontiéa [23] found an increase in the contact angle of a droplet deposited on the fouled membranes. Their contact angle measurements showed the acidic characteristic of the PES material at low pH. ANOVA analysis proved that at 95% confidence, the difference of contact angles of pristine, fouled and cleaned membranes in this study was significant.

Additionally, it was observed that all the membranes were irreversibly fouled and could not be restored completely by clean-in-place method even with rigorous chemicals (Figure 7.9). Only out-of-place cleaning with a sponge could remove up to 99% of the fouling layer. This result was obtained by examining the cleaned membranes using different cleaning methods. The coupons were taken off the cells and carefully checked. The advanced analyzed techniques such as SEM and AFM would have shown micro-images of foulants deposited on the surface. However, visual observation itself provided obvious images of changes. Membranes which were clean and white at the beginning (Figure 7.9a) became dark brown due to cake formation of NOM (Figure 7.9b) and remained yellow upon being soaked with chemicals (Figure 7.9c). Surfaces of cleaned membranes also altered (rougher) with aggregation of NOM particles on some parts compared with those of the original (pristine) ones.

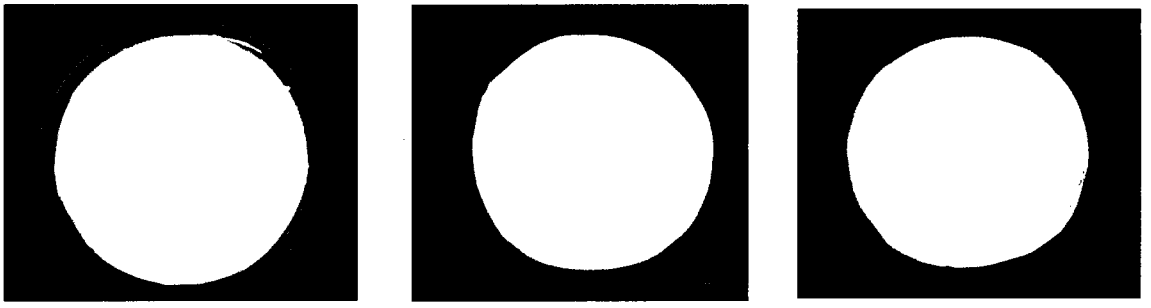

Pristine membrane Fouled membrane After-cleaned membrane

Figure 7.9. Images of pristine, fouled and after-cleaned membranes (PES membranes)

Possible method to diminish the deposition of NOM on membrane surface is a high cleaning frequency. However, high frequency of cleaning would lead to greater operation expense. In this study, two hour fouling seemed to be the best choice to compromise between the flux reproduction and operation cost.

7.4.5 Variability

The variation in feed water organic content was so slight that the characteristics of the fouling material can be assumed to remain stable during the test period. In this study, the temperature varied by less than 2°C and pH ranged from 6.5-7.5. However, the flux was observed to vary during the study. This problem has been observed in most of membrane research, some mentioned it [18, 21], some did not. The other possible reasons might be due to the difference among membrane coupons and/or test cells. It should be noted that the fourth membrane system consists of six CF cells in parallel. Those cells were built as one job by one technician using the same specifications, so there should be no difference among cells. In addition, great effort was made to adjust and even out the flowrate and pressure distribution among the cells before testing. As mentioned in the previous section, the flowrate and pressure were monitored for each cell. The discrepancies were less than 6% and 5% for pressure and flowrate, respectively. In order to reduce variability due to the test cells, the cells used to test given membranes coupons were chosen randomly and different cells were used in subsequent tests. This means that the differences arise primarily due to variations in the membrane coupons. It was confirmed by Mosqueda-Jimenez [18] that the ranking of the various cells in terms of flux varied from one set of coupons to the next. A preliminary study with six identically commercial PES PU membrane coupons also revealed that the flux behavior followed slightly dissimilar trends. It means even for commercial membranes which have been manufactured in large scale still faces this problem. To eliminate the error introduced by variation among different membrane coupons, six coupons for each type of membranes were used. After each tests, membranes were thoroughly cleaned out of place with chemicals and stored in 10% ethanol solution at 4°C and checked the permeation rate before the sequent tests to maintain the same performance. For the limited number of

replicates, the variance analysis indicated that at 95% level of confidence there was no significant difference either among the coupons or among the units [18].

7.5 Conclusions

Based on the experimental work on comparison of test cells and cleaning frequency for membrane cleaning purposes, following comments can be drawn:

(i) Four types of UF cells for membrane cleaning have been evaluated in this study including stirred UF cell, SEPA cell, single CF cell and six-CF cell- in parallel. The performance of three single cells in term of flux was similar for the first testing cycle and then deviated in subsequent cycles due to different degree of NOM deposition and the ease of cleaning corresponding with different cell geometries. The six-cell-in-parallel system behaved quite differently from the single cell CF system. The discrepancies require further investigation and as such are not currently recommended for membrane cleaning studies.

(ii) Different cells have no impacts at 0.5-hour cleaning interval for all membranes. Therefore, the cleaning efficiency at bench-scale would have no significant difference regardless of cell type as long as a short cleaning frequency (i.e., 30 min) is employed. The cleaning interval did not statistically affect the flux recovery as stirred UF cell and SEPA cells were used. However, SEPA cell would be recommended for a long-term cleaning test (several hours) since its design simulates better a real spiral wound membrane module with permeate carriers and feed spacers below and on top of membrane sheets.

(iii) For all the membranes there was some irreversible fouling could not be restored completely by clean-in-place method even with rigorous chemicals. Only out-of-place cleaning with sponge could remove up to 99% of the fouling layer.

7.6 Acknowledgement

The authors gratefully acknowledge Vietnam Government (Vietnamese Overseas Scholarship Programs -VOSP), Natural Sciences and Engineering Research Council of Canada (NSERC) and University of Ottawa for their financial support. We would like to thank to GE Osmonics for the membrane provision. We also express gratitude to

Britannia Water Purification Plant for the water sampling, Department of Chemical and Biological Engineering, University of Ottawa, for the access to lab equipments.

7.7 References

[1] E. Arkhangelsky, D. Kuzmenko, V. Gitis, J. Mem. Sci. 305 (2007) 176–184

[2] D. Kuzmenko, E. Arkhangelsky, S. Belfer, V. Freger, V. Gitis, Desalination 179 (2005) 323–333.

[3]M.H. Tran-Ha, D.E. Wiley, J. Membr. Sci. 145 (1998) 99-110.

[4] M.J. Muñoz-Aguado, D.E. Wiley, A.G. Fane, J. Membr. Sci., 117 (1996) 175-187.

[5] K. Kimura, Y. Hane, Y. Watanabe, G. Amy, N.Ohkuma, Water Research, 38 (2004) 3431-3441.

[6] H.K. Shon, P.J. Smith, S. Vigneswaran, H.H. Ngo, Desalination 202 (2007) 351-360.

[7] M. Bodzek, K. Konieczny, Sep. Purif. Technol. 14 (1998) 69-78.

[8] J.M. Arnal, B. Garcia-Fayos, J. Lora, G. Verdú, M. Sancho, Desalination 221 (2008) 331–337.

[9] T. Matsuura, Synthetic membranes and membrane separation processes, CRC Press, Boca Raton, FL, 1994.

[10] D.B. Mosqueda-Jimenez, R.M. Narbaitz, T. Matsuura, Sep. Puri. Technol. 37 (2004a) 51-67.

[11] A.H Nguyen., R.M. Narbaitz and T. Matsuura, J. Env. Eng. 133 (2007) 515-528.

[12] T.H. Dang, M.R. Narbaitz, T. Matsuura, C.K. Khulbe, Water Qual.Res. J. Canada 41 (2006a) 85-94.

[13] T.H. Dang, M.R. Narbaitz, T. Matsuura, J. Membr. Sci., 323 (2008) 45-52

[14] Standard methods for the examination of water and wastewater, APHA, AWWA, and WEF, Washington, D. C. (1995)

[15] J.S. Leenheer, J.P. Croue, S.W. Krasner, ACS Symposium, 76 (2000) 173-187.

[16] D. Rana, T. Matsuura, R.M. Narbaitz, C. Feng, J. Membr. Sci. 249 (2005) 103.

[17] T.H. Dang, M.R. Narbaitz, T. Matsuura, D. Rana, Proceedings, '07 ACE, AWWA, (2006b)

[18] D.B. Mosqueda-Jimenez, R.M. Narbaitz, T. Matsuura, J. Env. Eng., 130 (2004b) 90-99.

[19] S. Sourirajan, T. Matsuura. National Res. Council of Canada, Ottawa, Ontario (1985)

[20] J. Cho, J. Sohn, H. Choi, I.S. Kim, G. Amy, J. Water Supply: Res. and Tech.—AQUA, 51 (2002) 109-123.

[21] R. Liikanen, J. Yli-Kuivila, R. Laukkanen, J. Membr. Sci., 195 (2002) 265-276.

[22] H. Liang, W. Gong, J. Chen, G. Li, Desalination 220 (2008) 267–272.

[23] M. Pontiéa, L. Durand-Bourlier, D. Lemordant and J. M. Lainé, Sep. Purif. Technol. 14 (1998) 1-11.

[24] J. Lipnizki, G. Jonsson, Desalination, 146 (2002) 213-217.

[25] H. Choi, K. Zhang, D. D. Dionysiou, D. B. Oerther, G. A. Sorial, Sep. Puri. Technol. 45 (2005) 68-78.

[26] S. Nakatsuka, I. Nakate, T. Miyano, Desalination 106 (1996) 55-61.

[27] P. Weber, R. Knauf, Desalination 119 (1998) 335-339.

[28] A.A. Karimi, J.C. Vickers, R.F. Harasick, J. AWWA, 91 (1999) 90-103.

[29] J.H. Green, M. Tylla, Desalination119 (1998) 79-83.

[30] S. Chellam, J.G. Jacangelo, T.P. Bonacquisti, Env. Sci. Technol., 32 (1998) 75-81.

[31] J. Zhang, S.I. Padmasiri, M. Fitch, B. Norddahl, L. Raskin, E. Morgenroth, Desalination, 207 (2007) 153-166.

CHAPTER 8

PERFORMANCE OF A NEWLY-DEVELOPED HYDROPHILIC ADDITIVE BLENDED WITH DIFFERENT UF BASE POLYMERS

Huyen T. Dang[1], Camille Amelot[2], Dipak Rana[3], Roberto M. Narbaitz[1], Takeshi Matsuura[3]

[1]*Dept. of Civil Engineering, Univ. of Ottawa, 161 Louis Pasteur St., Ottawa, K1N 6N5, Canada*

[2]*École Nationale Supérieure d'Ingénieurs de Limoges, Université de Limoges, 13 Rue F. Chénieux 87031 Limoges Cedex, France*

[3]*Dept. of Chemical and Biological Eng., Univ. of Ottawa, 161 Louis Pasteur St., Ottawa, K1N 6N5, Canada*

8.1 Abstract

The capability of modifying ultrafiltration (UF) membranes with different base-polymers using a newly synthesized hydrophilic additive was investigated in this study. Five typical base-polymers were tested: cellulose acetate (CA), polyetherimide (PEI), polyethersulfone (PES), polysulfone (PS) and polyvinylidene fluoride (PVDF). The changes in characteristics and performance of the membranes were analyzed using scanning electron microscopy (SEM), atomic force microscopy (AFM), contact angle analysis, and solute transport tests. It was found that the effect of the hydrophilic additive was different for each polymer. Higher additive contents resulted in higher permeation flux. A visible effect on water content and permeability was obtained but the impact was not shown clearly in contact angles, possibly the additive's concentration was not sufficiently high at the surface. In term of flux enhancement the PES and PVDF membranes benefited the most by the addition of the hydrophilic additive.

Key words: Hydrophilic additive, surface modification, typical ultrafiltration based polymers, contact angles.

8.2 Introduction

Currently membrane surface modification is considered as important to the membrane industry as the bulk membrane material and the membrane preparation process. The key objective is to enhance the flux and retention performance beyond the trade-off line of conventional membranes, in which high flux often leads to low retention and vice versa. The techniques applied for surface modification can be blending, grafting, coating or exposure of the surface to radiation, plasma, ion beams and ultrasonic waves. Among these, blending of additives into casting solutions has been studied by many researchers recently due to its simplicity and low cost approach. Only one-single-step casting procedure is required for the blended dope while for the other modification processes at least an additional processing step is necessary [1]. In the blending technique, the additives are mixed with base polymer(s) to prepare the modified membranes with different surface hydrophilicity and surface morphology. For instance, incorporation of hydrophilic polyethylene glycol (PEG) had a significant role in determining the pore size and porosity of cellulose acetate (CA) membranes, and their permeate flux and protein rejection behavior [2]. The incorporation of PEG lowered the flux reduction in the ultrafiltration (UF) treatment of machine oil-water emulsion [3] or they could act as pore reducing agents in asymmetric polyetherimide (PEI) membranes [4]. It has also resulted in higher pure water permeation (PWP) and larger pores when membranes were prepared from higher molecular weight polyethersulfone (PES) [5]. However, increasing molecular weight of PEG additives (0.6, 2, 6, and 12 kD) in PS membranes led to the increase of water flux but decrease of PEG solute (12 and 35 kD) rejections [6]. Many studies have claimed that addition of polyvinylpyrrolidone (PVP) with various molecular weights in the casting solution of PES resulted in better permeability while the same solute retention is maintained [7]. Sometimes it led to lower rejection [8]. Charged additives such as sulfonated polyether ether ketone (SPEEK), or sulfonated polyether imide (SPEI), have improved the flux reduction of the PEI membranes [9-11] due to the presence of more negative charges on surface. The performance of these modified membranes, however, seems unstable. It is hypothesized that these additives may also be leached out after a long period of operation because they are all miscible in water.

In contrast to the above highly hydrophilic polymers, such as PEG, PVP, SPEI or SPEEK, etc. our group has been developing surface modifying macromolecules (SMMs) for over ten years. SMMs are prepared by the synthesis of a urethane prepolymer from a diisocyanate with a polyol, followed by end-capping with a surface modifying end-group.[12-14]. It was reported that these surface modifying macromolecules (SMMs) remained at the membrane surface for a much longer period due to the affinity between the central polyurethane (PU) segment and the host base polymer. The long chain of the PU stayed in the bulk polymer phase and end groups remained at the top selective layer surface, being in contact with air during the casting [14]. Three different types of SMMs have been developed: the hydrophobic SMMs [1, 8, 12-13], hydrophilic surface modifying macromolecules (LSMMs) [14-16] and charged surface modifying macromolecules (CSMMs) [17]. A key characteristic of these polymers is that they are miscible with the base (or principal) polymer, so they can readily be added into the membrane casting solution. Due to their hydrophobic or hydrophilic properties, SMMs migrate to the surface of the membrane either during the casting or the gelation process. The LSMMs are prepared using PEG as the end capping groups, and the hydrophilicity is expected to arise from the hydroxyl groups of the PEG. As a result, the membrane surface becomes different from the layers below (analogous to thin-film composite membranes). SMMs have proved to impact on membrane separation processes such as pervaporation, membrane distillation, ultrafiltration and oil/water emulsion. Studies carried out so far only investigate the effect of blending SMMs into PES [18].

The objective of this study is therefore to investigate the effect of LSMMs blending with various host polymers on the performance of UF membranes. Five polymers (CA, PEI, PES, polysulfone (PS), and polyvinylidene fluoride (PVDF)) were selected as the base polymers to cover a wide range of hydrophilicity/phobicity spectrum. This paper not only involves an evaluation of the miscibility and film formation but also assesses the migration of the SMMs to the membrane surface via contact angle measurement and water permeation tests.

8.3 Experiments

8.3.1 Materials

The chemicals used in this study are listed in Table 8.1. All polymers were dried in an oven for two hours at 105°C and dehumidified in a dessicator. The 1-methyl-2-pyrrolidinone (NMP) was used as a solvent. The LSMM was synthesized according to the method outlined by Rana et al. [15]. LSMM was synthesized by end-capping the urethane prepolymer with PEG having average molecular weight of 600 Daltons. The urethane prepolymer was formed from the reaction of methylene bis-p-phenyl isocyanate (MDI) with poly(propylene glycol) (PPG) in N,N-dimethylacetamide (DMAc) solvent (Figure 8.1). The values of the n and q were calculated from the average molecular weight of PPG and of PEG, which are 7.02 and 13.23, respectively. Based on the stoichiometry of the synthesis and the M_w, the repeat unit of m and p were calculated, which are 30.57 and 15.28, respectively. Average molecular weights (weight average molecular weight, M_w, and number average molecular weight, M_n) and polydispersity index (PDI, M_w/M_n) were measured by gel permeation chromatography (GPC) (Waters Associates, Milford, MA). The polymer molecular weights were calculated using the universal calibration curve. Average molecular weights of the LSMM were $M_n = 1.28 \times 10^4$, $M_w = 3.63 \times 10^4$.

Table 8.1 Description of chemicals

Material descriptions	CAS number	Source	Specifications
CA (Eastman 4650, Powder)	9004-35-7	Eastman Kodak Co., Rochester, NY	Mw: 41 kD; PDI: 2.71; Tg: 39.7 °C
PEI (Ultem 1000, Natural Pellet)	61128-46-9	General Electric Co., Pittsfield, MA	Specific gravity (SG): 1.27; Mw: 15 kD; Tg: 212.7 °C
PES (Victrex 4100P, Powder)	25667-42-9	ICI Advanced Materials, Billingham, England	Mw: 31 kD; PDI: 1.55; Tg: 221.4 °C
PES (E6020P, Porous Flake)	25608-63-3	BASF Aktiengesellschaft, Ludwigshafen, Germany	Mw: 58 kD; PDI: 3.6; Tg: 226.1 °C; SG: 1.40;
PS (Udel 3500, Pellet)	25135-51-7	Amoco Performance Products Inc., Atlanta, GA	Mw: 37 kD; PDI: 2.11; Tg: 184.2 °C; SG: 1.24;
PVDF (Kynar 740, Pellet)	24937-79-9	Elf Autochem Canada Inc., Oakville, ON, Canada	Mw: 254 kD Density (ρ): 1.78 g/cm3; Tg: -49.4 °C; Tm: 160.1 °C;

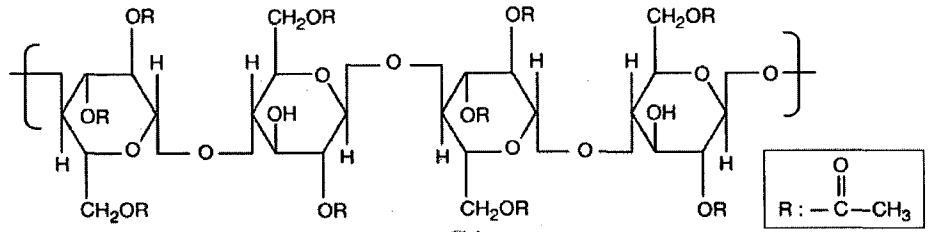

CA

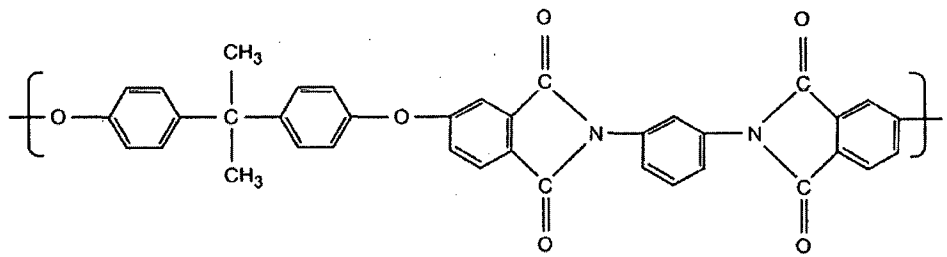

PEI

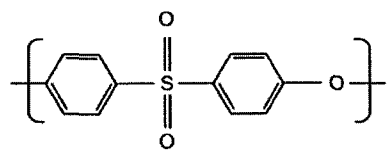

PES

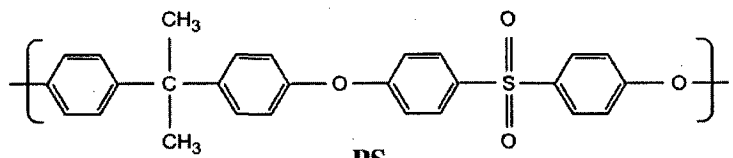

PS

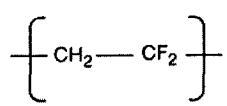

PVDF

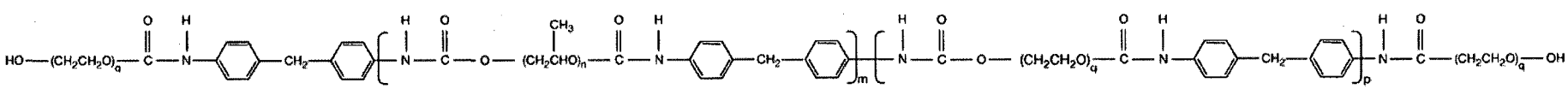

LSMM

Figure 8.1. Chemical structures of LSMM and based polymers

The T_g (glass transition temperature) was determined by a differential scanning calorimeter (DSC) equipped with an universal analysis 2000 program (DSC Q1000, TA Instruments, New Castle, DE). This equipment was also used to verify the miscibility of the additive LSMM in the different base polymers by evaluating T_g and T_m (melting temperature). The T_g of LSMM was 8.15 °C. Reagent-grade water (MQ water) was prepared with a Milli-Q Water System (Millipore Co., Bedford, MA). Detailed chemical structures of LSMM and the base polymers are shown in Figure 8.1.

8.3.2 Membrane preparation

The membranes were prepared by the following phase inversion procedure. The casting solutions with compositions shown in Table 8.2 were prepared. Note that all casting solutions contained 18 wt % of the base polymer. The LSMM concentrations were 0.0, 0.5 and 3.0 weight percent and the balance was NMP as solvent. The three components (base polymer, LSMM and solvent) were loaded in 250-ml bottles and mixed vigorously in an incubator orbital shaker (New Brunswick Scientific Co., Edison, N.J.) overnight at 35°C, and then stored in a dessicator for several hours to dissipate bubbles. The solutions were cast onto clean glass plates using a casting knife with a 0.2mm gate opening. The glass plates with the nascent membranes were immediately immersed into 4°C MQ water until they hardened. The membranes were stored in MQ water and placed in a refrigerator until they were used. It is worth noting that all the membranes were prepared under the same conditions which yield good PES membranes. These conditions (18 wt% of PES, less than 6 wt% of LSMM, zero migration or evaporation time and 4°C coagulation bath) have been optimized and proved effective from our previous studies [16, 18]. The permeation test for those membranes was described in detail elsewhere [18].

Table 8.2 Composition of the casting solutions for membrane preparation

Sample	Base Polymer (%)	LSMM (%)	NMP (%)
PVDF-0	18	0.0	82.0
PVDF-0.5	18	0.5	81.5
PVDF-3.0	18	3.0	79.0
PS-0	18	0.0	82.0
PS-0.5	18	0.5	81.5
PS-3.0	18	3.0	79.0
PEI-0	18	0.0	82.0
PEI-0.5	18	0.5	81.5
PEI-3.0	18	3.0	79.0
CA-0	18	0.0	82.0
CA-0.5	18	0.5	81.5
CA-3.0	18	3.0	79.0
PES-58-0	18	0.0	82.0
PES-58-0.5	18	0.5	81.5
PES-58-3.0	18	3.0	79.0
PES-31-0	18	0.0	82.0
PES-31-0.5	18	0.5	81.5
PES-31-3.0	18	3.0	79.0

8.3.3 Contact angle (CA) measurement

The membrane samples were cut into 5 x 25 mm pieces and fixed onto 25 x 75 x 1 mm superfrost micro slides (VWR., Mississauga, ON) using electrical tape. Advancing contact angles were determined using VCA Optima Surface Analysis System (AST Products, Inc., Billerica, MA). They are recorded as the critical angles at which the edge of contact between water drop and membrane expands. The water drop volume ranged from 2.5 to 3.0 μL. The reported contact angles are the average of ten measurements.

8.3.4 Water content

Water content defined by equation [1] was determined by gravimetric analysis.

$$W_{\%} = \frac{W_{wet} - W_{dry}}{W_{wet}} x100 \qquad [8.1]$$

Where, W_{wet} and W_{dry} are mass (g) of the wet and dry membranes, respectively. The membranes were dried by keeping them in an oven at 75°C for two days [19]. The membrane samples and trays were weighed before (W_{wet}) and after drying (W_{dry}). Three measurements were conducted for each membrane type and the average values were reported.

8.3.5 Morphology and porosity

Membranes' morphology was examined via the atomic force microscopy (AFM) and scanning electronic microscopy (SEM). A Nanosurf® easyScan 2 atomic force microscope (AFM) equipped with a software version 1.3 (Nanosurf AG, Grammmmetstrasse, Liestal, Switzerland) was used for characterization of samples. The average surface roughness (R_a) in an area of $2.52x10^{-11}$ m^2 was obtained for the top membrane surface via the AFM's software calculation. A model JSM-6400 JEOL (Japan Electron Optics Limited, Japan) SEM was employed to observe the cross-sectional area of the dry membranes. Pore property and molecular weight cut-off (MWCO) were obtained through the solute transport method [20].

8.4 Results and discussion

8.4.1 Miscibility

The LSMM was visually miscible in all the tested polymer solutions. The casting solutions had different appearances for the various base polymers (Table 8.3). There were no distinguishable differences between the solutions, as well as the membranes, of the same base polymer with and without LSMMs. Solutions with the lower LSMM concentration (0.5 wt %) were easier to cast. Whereas incorporation of a greater amount of LSMM (3.0 wt %) made the formation of membranes with good appearances more

difficult, especially for those with CA and PVDF as base polymers. It seems that the miscibility of LSMM in the latter polymers was lowered at a higher LSMM content. Their solutions were less viscous and not completely homogeneous. Nevertheless, with the same 0.5wt% LSMM content, the viscosity range was PVDF<PES<PS<PEI<CA. The CA-based membranes were fragile compared with the others.

Table 8.3 Solution and membrane appearances

Polymer	Solution appearance	Membrane appearance
PS	clear yellow and viscous	white and rigid
PEI	dark yellow and viscous	beige and flexible
PES58k and PES31k	clear yellow and fluid	white and a bit wrinkly
CA	transparent and viscous	transparent and rubbery
PVDF	transparent and fluid	transparent and very flexible

As stated above, to further verify the miscibility of the additive in the different base polymers, DSC analysis was performed for solid membrane samples. The DSC analysis showed that the amorphous LSMM mixed well with the amorphous base polymers, such as PEI and PES, as the blended membranes had only a single transition (Figure 8.2). The Tg of the LSMM blended polymeric membranes were lower than that of the corresponding base polymer (Table 8.1), which indicated that these systems were partially miscible at the molecular scale. It is worth noting that as the LSMM concentration increased, the Tg decreased. For example, the Tg values of 0.5 and 3 wt% of LSMM blended PES-58K membrane were 213.71 and 202.8 °C, respectively. Similarly, the Tg values of 0.5 and 3.0wt% of LSMM blended PEI membrane were 199.34 and 158.68 °C, respectively. Hence, based on their lower T_g the 3.0wt% LSMM blended membranes were more compatible than the 0.5 wt% LSMM blended membranes. In contrast, for the case of LSMM blended PVDF membranes, double melting peaks were observed (Figure 8.2). The melting maximum peaks were 163.9 and 168.0 °C for 0.5 wt% LSMM blended PVDF, however, 163.5 and 167.9 °C for 3.0 wt% LSMM blended PVDF membrane. This data reflected that LSMM influenced the crystallization of the PVDF chain segments since PVDF is a crystalline polymer in nature in contrast to the amorphous base polymers discussed above.

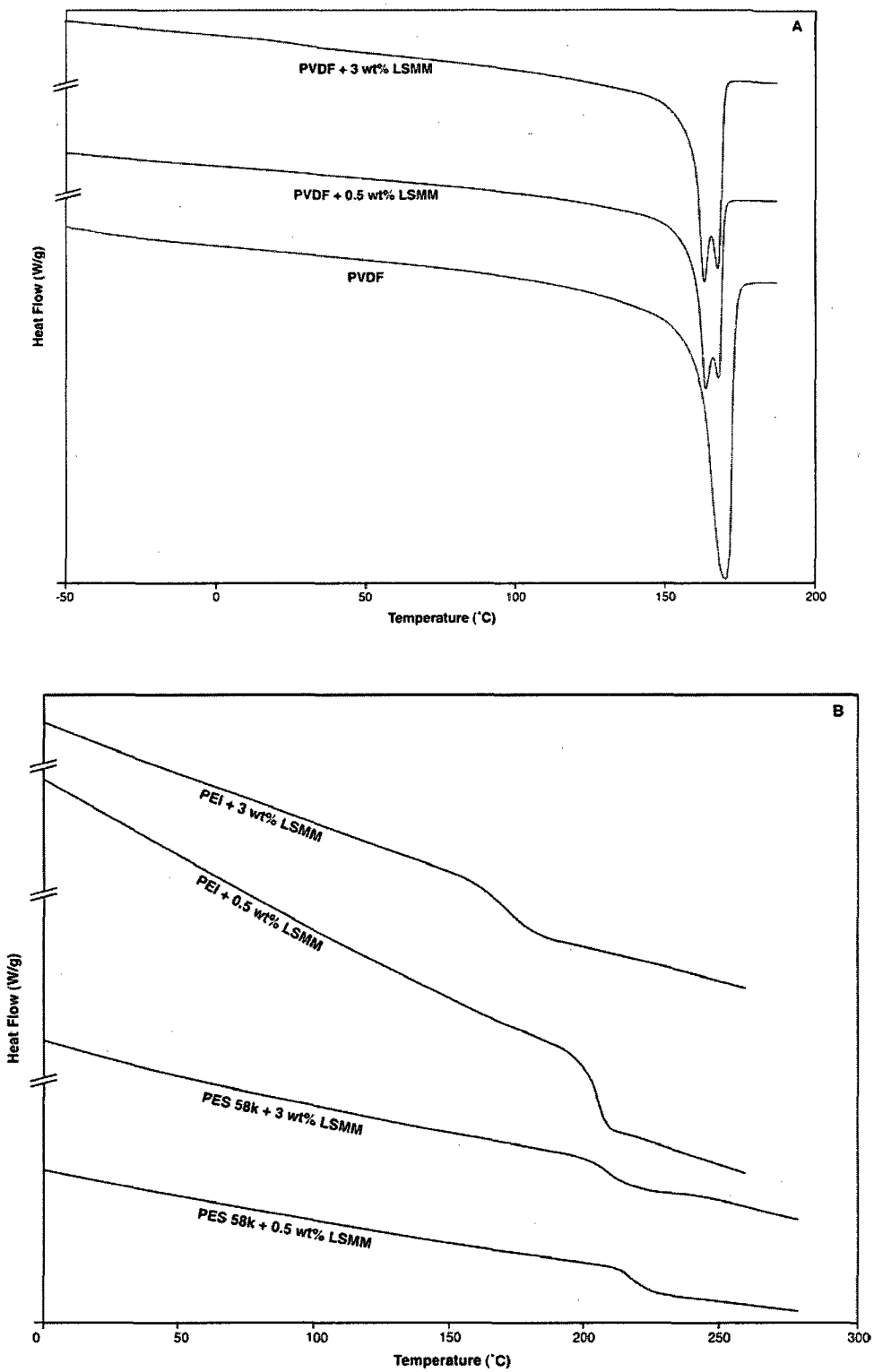

Figure 8.2. DSC response for (A) PVDF membranes with/without LSMM; (B) PEI and PES 58k membranes with LSMM

Accordingly, two different kinds of lamellae were formed. One peak represented the pure PVDF chain segments, and the other peak was the representation of the PVDF chain segments contaminated with LSMM chain segments. The response of CA-LSMM was similar to PVDF (not shown in here). While this indicates that the PVDF-LSMM and CA-LSMM membranes are likely to be ineffective, the DSC data did not become available until the filtration test was completed. Therefore, the performance and characteristics of all blended membranes including CA and PVDF based were evaluated and reported below.

8.4.2 Molecular weight cut-off (MWCO)

The MWCOs of the membranes determined by ultrafiltration experiments with PEGs and PEO as the solutes are presented in Figure 8.3. With the addition of LSMM, the MWCOs were altered in different ways depending on the base polymers. In almost all cases, however, the addition of LSMM increased the MWCOs, except for PES58k membranes where an increase in LSMM concentration from 0.5 to 3.0 wt% resulted in a smaller MWCO value.

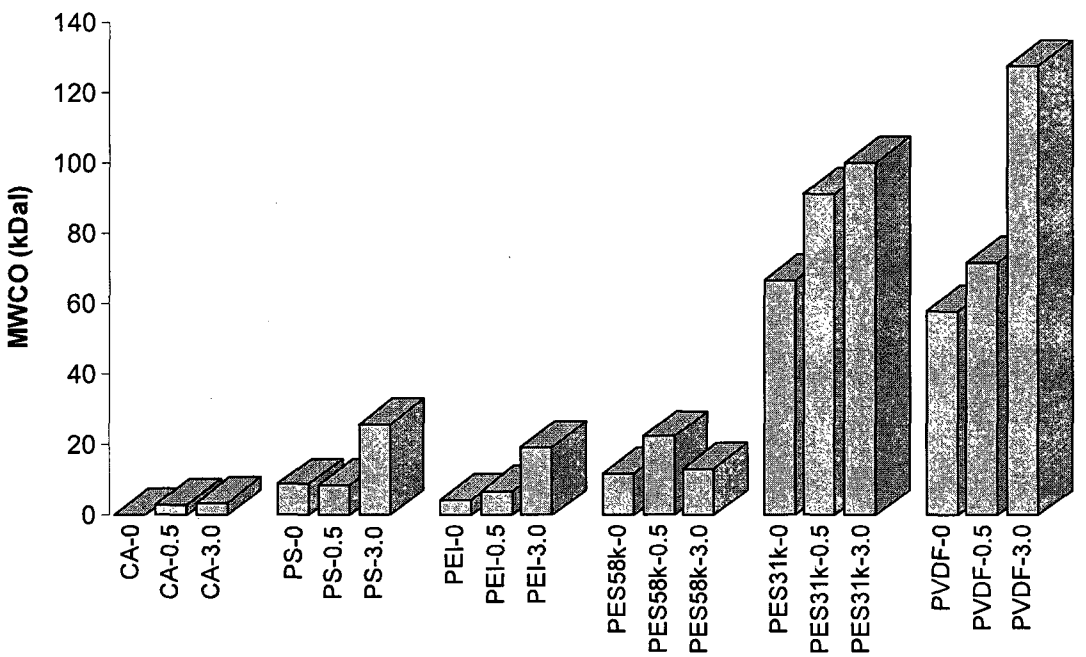

Figure 8.3. MWCO of membranes

It is noticed that the order in membrane MWCO is CA < PEI < PS< PES < PVDF, when LSMM is not blended. For convenience, polymers are classified into the following three groups to explain not only the MWCO data but also some other experimental data obtained in this work: 1) CA contains alicyclic and polar functional groups; 2) PES, PEI and PS with intermediate MW, containing aromatic and some polar functional groups; and 3) PVDF with the highest MW, containing straight an aliphatic chain and highly non-polarizable fluorine. From the above MWCO data, it is observed that MWCO increases progressively from the first to the third group of the polymers. This is consistent with the fact that CA is a polymer used for manufacturing many commercial reverse osmosis (RO) and nanofiltration (NF) membranes while PVDF is a polymer for many commercial MF membranes. Of course this trend can not be generalized since the performance of the membranes depends on many other factors involved in the membrane preparation.

The MWCO of CA and PEI were small compared with those reported in the literature [9, 21]. It is suspected that the discrepancy is due to the membrane preparation conditions used in this study, which differ from the standard ones for CA and PEI membranes. In this study, the base polymers were dissolved solely in NMP solvent to limit the variability in comparison. However, higher MWCO of CA membranes (i.e., 40 to 50 kDal) could be obtained if CA was mixed in acetone/dioxin/tetrahydrofuran (THF)/DMAc/dimethylformamide (DMF) [21]. Likewise, for PEI membranes, Bowen et al. [9] observed that the membrane pore sizes increased from undistinguishable to 3 nm when the solvent changed from NMP to Dioxan/THF. Thus, solvents other than NMP would likely produce better CA or PEI membranes.

Figure 8.3 also shows that PES molecular weights have a significant impact. Theoretically, with the same weight concentration, the polymer with a higher MW will become less viscous and slower demixing will occur, leading to a denser membrane with a lower MWCO. This expectation was not only confirmed by this experimental data but also by some previous studies [22].

8.4.3 Water Content and Hydrophobicity

Before the contact angle measurements, all the membranes were subjected to drying. Three methods of drying were compared: drying after solvent exchange with ethanol, drying in an oven at 75°C and natural drying in ambient air. The contact angles obtained

by the above three methods did not show any statistically significant differences (Figure 8.4). Hence, natural air drying was adopted. The contact angle data shown in Figure 8.4 are for four polymeric materials and for different LSMM concentrations. Compared with the contact angle data that were obtained for the dense films i.e., PVDF (~100°); PES (~105°) [1, 23], the contact angles measure here are lower without exception. This is because the membranes studied in this work are porous and the water in the membrane pores brought down the contact angle values. Another observation can be made is that blending LSMM did not change the contact angle significantly regardless of the amount of LSMM added. Rana et al. [15] and Nguyen et al. [16] both reported that the addition of LSMM only marginally changed the contact angles of PES membranes. Thus, the noticeable changes observed in MWCO are not due to the change in the contact angle.

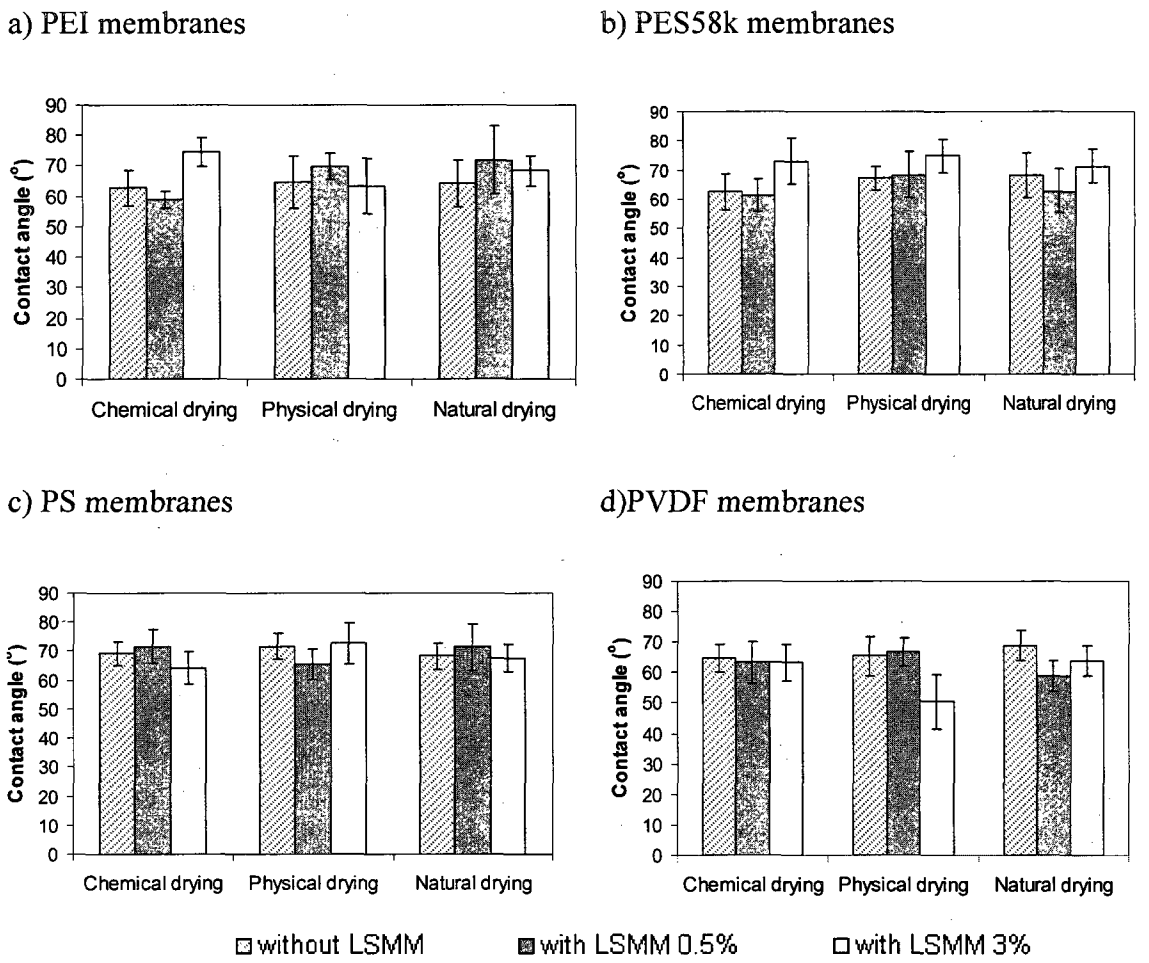

Figure 8.4. Advancing contact angle for each polymer as a function of the different drying methods

The contact angles did not change as a function of additive contents; however they may do if time for migration (prior to gelation) is incorporated. It was confirmed by statistical analysis which shows in Table 8.4.

Table 8.4 Two-way ANOVA for contact angles

Source	DF	SS	MS	F	P*
Base Polymers	4	686.6	171.7	6.73	**0.003**
%LSMM	2	136.7	68.4	2.68	0.101
Interaction	8	502.7	62.8	2.46	0.063
Error	15	382.8	25.5		
Total	29	1708.8			

**If P≤0.05, the effect is significant*

It was found that for the same drying method (chemical drying), only base polymers have impacts on contact angle and surface energy (P=0.003, ≤0.05). The percent of LSMM is statistically not important.

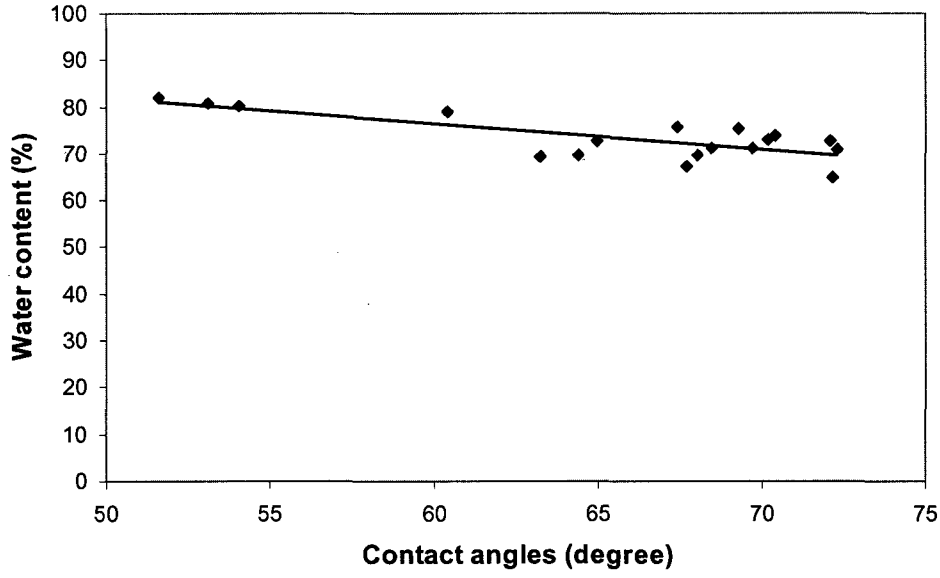

Figure 8.5. Correlation plot between water content and contact angles

Figure 8.5 shows that the water content is correlated to the contact angle. As the contact angle decreases the water content increases. This follows the natural behavior since both (contact angle decrease and water content increase) are an indication of an increase in hydrophilicity. Considering further that the contact angle is related to the surface, while

the water content is a bulk property, the above correlation implies that the surface property is affected by the bulk property and vice versa. This is logical considering that the contact angle also depends also on the presence of water in the membrane pores and hence on the morphology underneath the top surface layer.

8.4.4 Water permeation

The pure water permeation flux is given as a function of the operation period for the six membrane samples that do not contain LSMM (Figure 8.6).

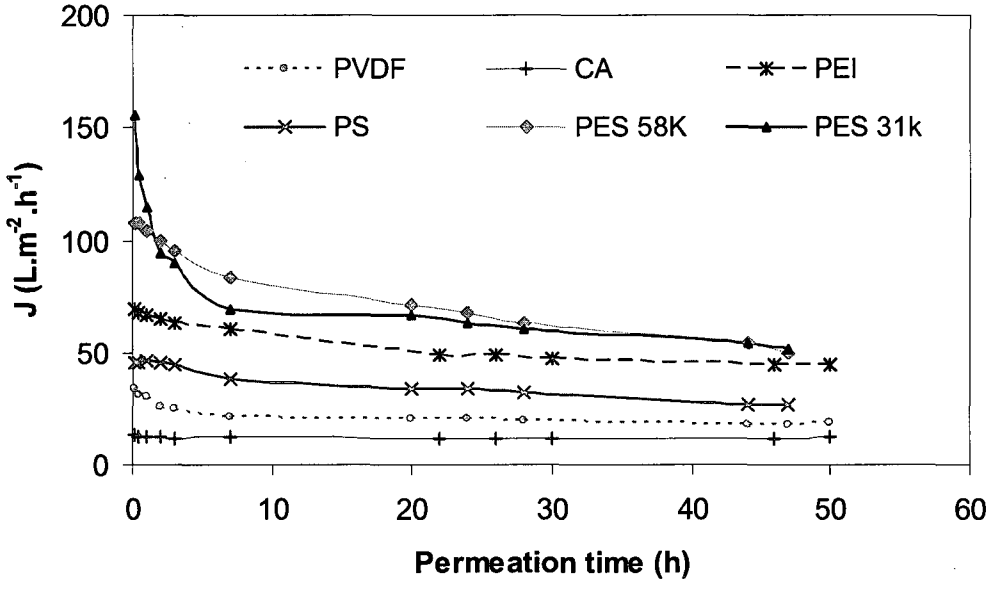

Figure 8.6. Pure water permeation flux of membrane with no addition of LSMM

Note that the flux decreases with time, which is the result of the membrane compaction. The order in the pure permeation rate is CA < (PS< PEI < PES) > PVDF. Again classifying the polymers into the groups (CA), (PES, PEI and PS) and (PVDF) with progressively increasing hydrophilicity, the permeation rate of the membrane from the first group (CA) is lower than those of the membranes belonging to the second group. This is understandable since the MWCO of the membrane from first group (CA) is lower than the second group. Interestingly, the permeation rate of the third group (PVDF) is lower than the second group despite the fact that the PVDF membrane showed the largest MWCO. This seems to be due to the higher hydrophobicity of PVDF. Penetration of water into the smaller pores is prevented by the hydrophobic property of PVDF and only

large pores are open to water flow, resulting in a high MWCO value and a low permeation rate. It should be noted that all the membranes were prepared under the same conditions (concentrations of casting solution and casting procedure), the optimality to obtain good membranes might be different for different base polymers.

The change of flux due to the incorporation of LSMM in the casting solutions is presented in Figure 8.7, where the % flux change is defined by the following equation.

$$\% \text{ Flux change} = \frac{J_{withLSMM} - J_{withoutLSMM}}{J_{withoutLSMM}} x100 \qquad [8.2]$$

Whereas $J_{withLSMM}$ ($L/m^2/h$) and $J_{withoutLSMM}$ ($L/m^2/h$) are the pure water fluxes corresponding to the membranes prepared from the same host polymer with and without LSMM blending. The figure shows the change of the above parameter as a function of operating time. The positive percentage of flux change illustrates an increase in the pure water flux by SMM blending. Furthermore, the line slopes indicate the effect of SMM blending on the membrane compaction, i.e., the upward trend indicates less compaction, horizontal line equal compaction and downward trend the stronger compaction of the membranes in which LSMM is blended.

The following observations can be made.

1) Lines for the flux change are always above zero except for the case of base polymer PES58k and 0.5 wt% LSMM.
2) The flux change increases as LSMM concentration increases from 0.5 to 3.0 wt%.
3) The three groups (CA), (PES, PEI and PS) and (PVDF) were impacted differently. The effect of SMM blending is the weakest for the first group with an average of 12% flux increase, followed by the second group with an average of 65 % and further by the third group with an average of 160%. PES58k is the exception with its small gain in the pure water flux by LSMM blending. This may be due to the high molecular weight of the polymer that makes the membrane more rigid and resistant to the pore expansion. Exceptionally for the case of CA membranes, no improvement of fluxes was observed with the addition of LSMM. Again, the reason might be due to the non-optimal solvent and concentration of components in casting solution. If cellulose nitrate/acetate polymer was dissolved

in acetone and added with 12% glycerol [24] or 20% PVP [25], pure water permeation rates would have been higher.

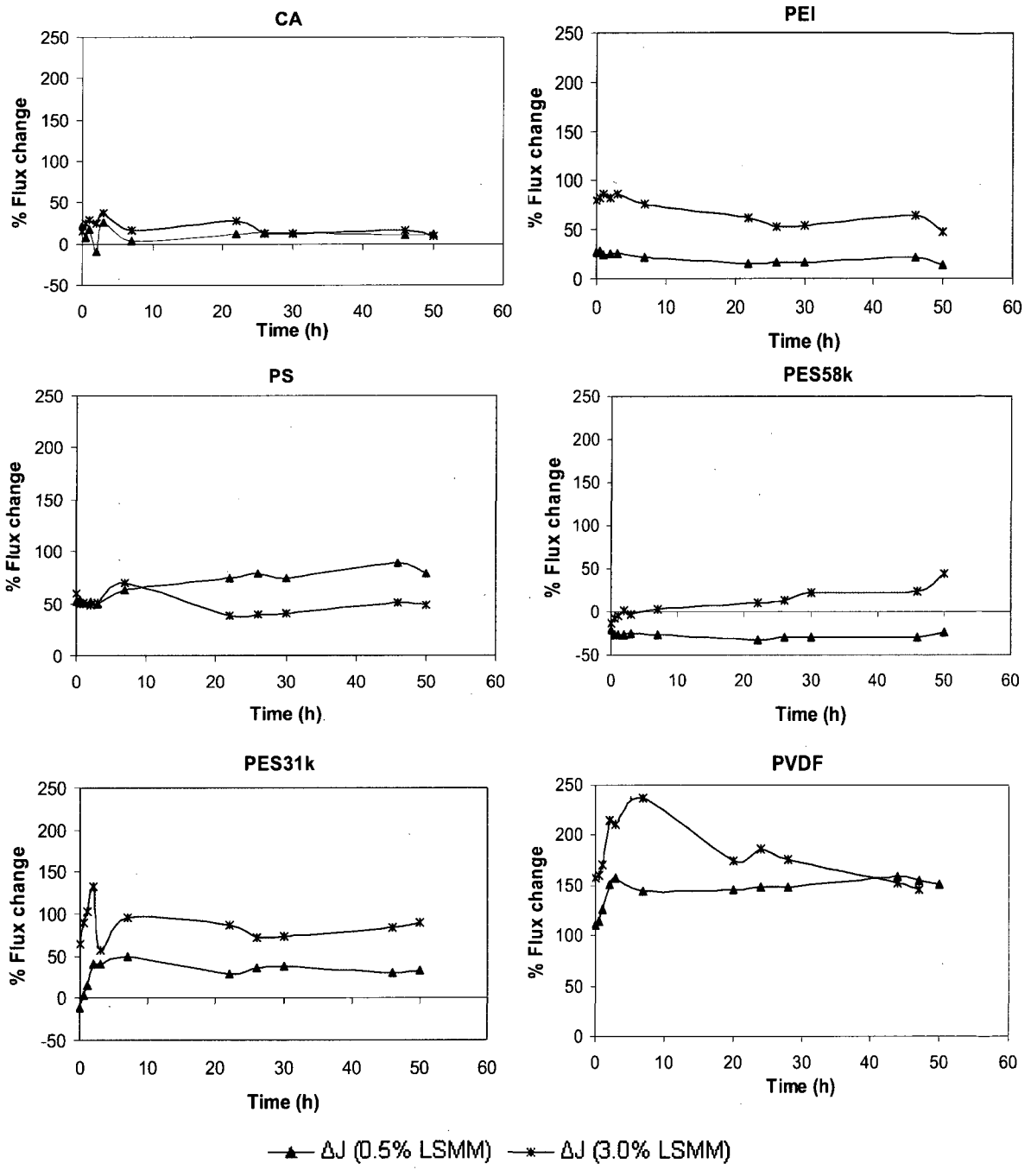

Figure 8.7. Percent of flux change as a function of filtration time

4) Except for a very obvious downward trend of PVDF with 3.0 wt% LSMM, the lines are mostly horizontal. Interestingly, there are two cases of upward trend, i.e.,

PS with 0.5 wt% LSMM and PES58k with 3.0 wt% LSMM. This means the compaction of the membranes with LSMM blending is equal to or less than the membrane without LSMM blending despite the increase in the pore size. Usually, compaction becomes more severe with an increase in the pore size when the membranes are prepared from the same polymeric material. Therefore, it can be concluded from the above results LSMM blending made the membranes mechanically stronger. Increase in mechanical strength of the membrane by blending a hydrophobic SMM was reported earlier [1].

The behavior of different membranes with 3wt% LSMM is further illustrated in Figure 8.8, indicating the relationship between the water flux and transmembrane pressure. The CA-based membranes were not included in this figure due to very low fluxes at low pressures. A steep slope indicates the high permeability. PES31k apparently had the highest fluxes at any operation pressure. Comparing the water of the unmodified membranes (Figure 8.6) and the modified membranes (Figure 8.7), the order of the permeability among membranes was almost the same except for the PES31k and PES58k. Certainly, though all the fluxes were increased with the addition of the hydrophilic additive, PES31k membranes nevertheless were proved to benefit most from the addition.

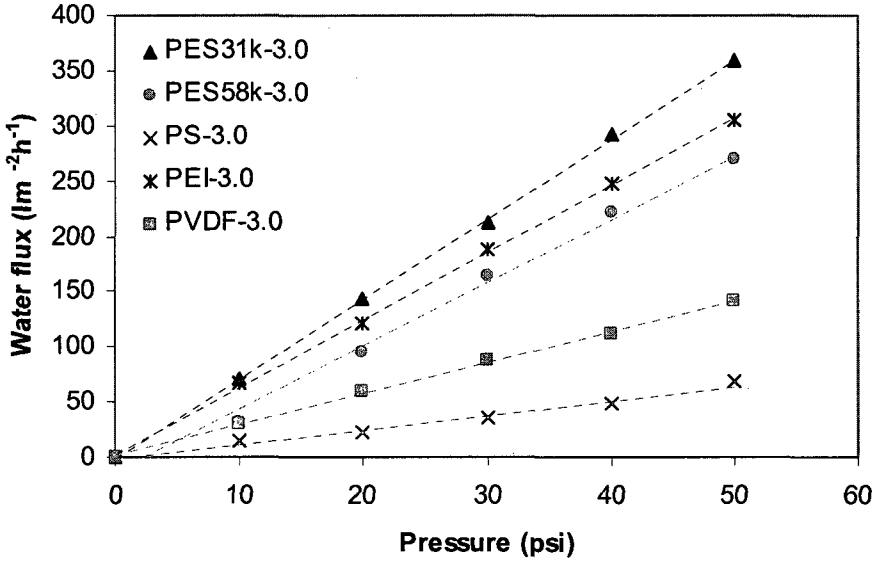

Figure 8.8. Relationship of water flux w.r.t transmembrane pressure

8.4.5 SEM images and roughness

This last section would further elucidate the impact of LSMM additives via SEM images and AFM information. Figure 8.9 presents the cross-section views of membrane surfaces with LSMM (B, D, F, H) and without LSMM (A, C, E, G). A typical asymmetrical structure consisting of a dense top layer and a finger-like porous sub-layer can be seen in most cases due to the strong affinity between NMP (used as a solvent) and water (as a coagulant) [26]. However, the distance from the top surface to the end of macro voids became shorter for CA membranes with additives, while it was larger for PVDF-3.0 membranes. For PES-58k membranes, no significant change was observed. It could be explicated based on the modification capacity of polymers, especially through their chemical structures in Figure 8.1. The PVDF polymer has a simpler structure whereas the complexity in structures increases from PES to PEI and CA polymers with increasing aromatic rings. Usually the presence of aromatic or heterocyclic groups reduces the rotation of the main chain, affecting the number of possible interaction sites between the various chains [21]. Therefore, the morphologic alteration showed clearer in cases of PVDF and PES-31k membranes in a way of being more porous. The changes of morphology may result in the changes of fluxes [27] which could be seen in the Figure 8.7.

The surface morphology in terms of roughness (Ra) would be described in Table 8.5. Apparently, the trend of roughness variation followed the classification: (i) Roughness of the control membranes increased gradually from Group 1 to Group 3; (ii) Group 1 (CA) roughness increased significantly (with the factor >15); (iii) Roughness of the Group 2 (PEI, PS and PES) membranes remained almost stable (with the factor around 2) and (iv) the roughness of the Group 3 (PVDF) membrane decreased notably by LSMM addition.

Table 8.5 Roughness

Membrane	Control (nm)	+ 0.5 wt% LSMM (nm)	+ 3 wt% LSMM (nm)
CA	0.67	1.05	1.34
PEI	2.40	1.72	2.26
PS	1.05	3.04	2.39
PES58k	0.89	1.05	1.10
PES31k	1.27	1.56	2.73
PVDF	4.32	3.46	1.64

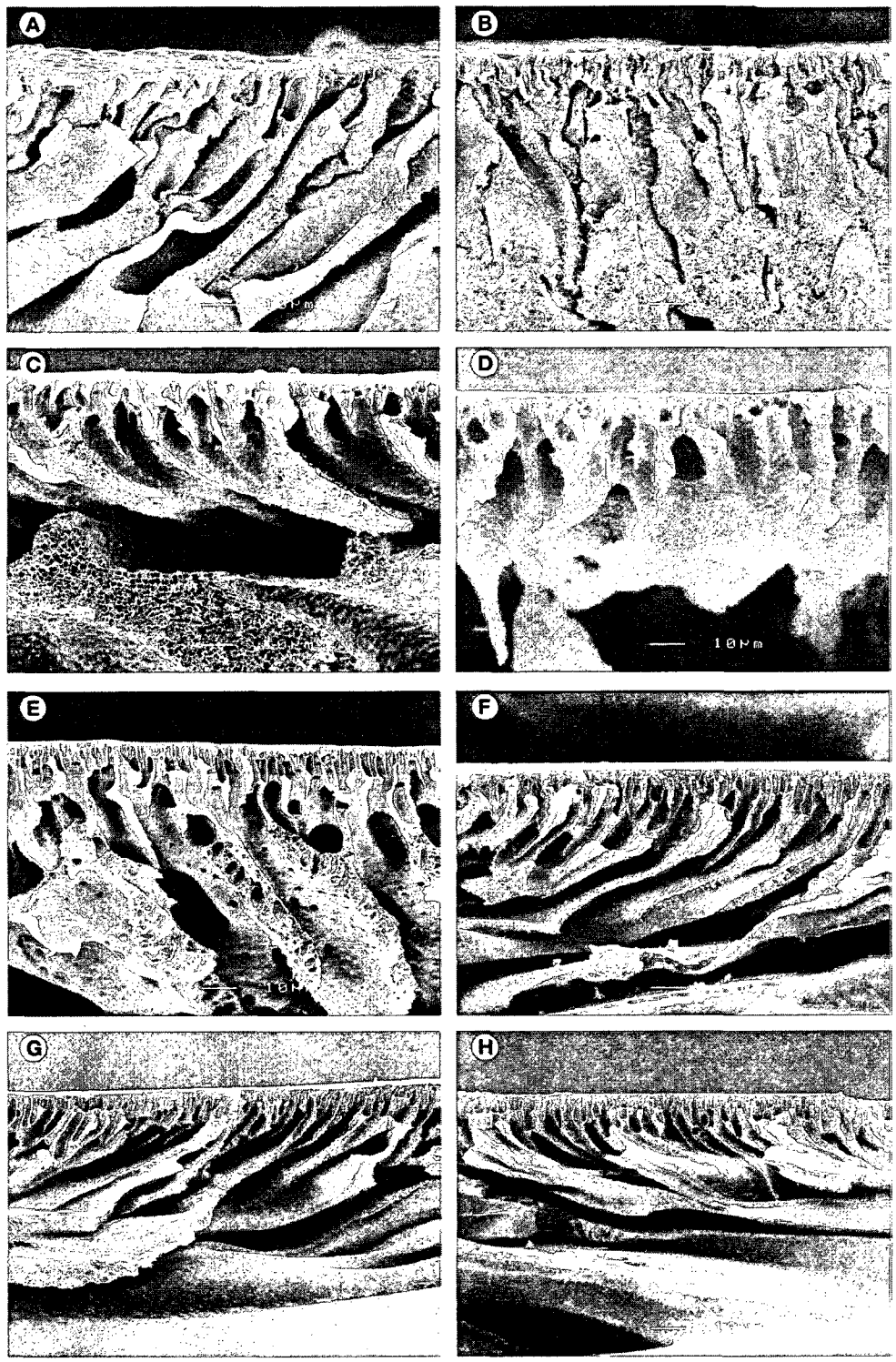

Figure 8.9. SEM photographs of the cross section surface of the membranes (A) CA; (B) CA–3.0; (C) PVDF; (D) PVDF-3.0; (E) PES31k; (F) PES31k-3.0; (G) PES58k; (H) PES58k-3.0.

The incorporation of LSMM smoothened PVDF but roughened the CA membranes. Relating to the cross-section images for those membranes (CA and PVDF), the alterations of morphology could also be seen in the first four pictures A, B, C and D. The impact of roughness on water permeation and fouling depends on many factors involved in how membranes are manufactured [18].

8.5 Conclusions

Improving membranes by using LSMM additive with five typical UF-base polymers PS, PES, CA, PEI and PVDF have been evaluated in this study. Hereafter are some critical conclusions:

1. Based on DSC analysis, LSMM did not mix well with CA and PVDF, particularly at the higher LSMM concentration. For the other polymers, which were amorphous polymers like LSMM, the casting solutions were homogenous and easy to cast.
2. The LSMM addition under the membrane making conditions, which were not optimized for the specific base polymers, did not cause a statistically significant change in contact angle. Alternative manufacturing conditions such as increasing the migration time or introducing stronger LSMM may lead to a greater impact.
3. LSMM had a visible effect on MWCO, morphology and permeability. Statistical analysis showed that membranes' responsive characteristics and performance all depended on the types of base polymers and additions of LSMM, however the first one played more important roles in those changes. Among the modified membranes, PES and PVDF membranes apparently had benefed from this hydrophilic additive with high flux changes or water production.
4. Different methods of drying membranes for contact angle measurements produced statistically the same readings, hence using the natural method is the best choice which is easiest and cheapest.

8.6 Acknowledgement

The authors gratefully acknowledge Vietnam Government (Vietnamese Overseas Scholarship Programs -VOSP) and Natural Science and Engineering Research Council of Canada (NSERC) for their financial support.

8.7 References

[1] Suk, D. E.; Chowdhury, G.; Matsuura, T.; Narbaitz, R. M.; Santerre, P.; Pleizier, G.; Deslandes, Y. Macromolecules 2002, 35, 3017.

[2] Arthanareeswaran, G.; Thanikaivelan, P.; Srinivasn, K.; Mohan, D.; Rajendran, M. Eur Polym J 2004, 40, 2153.

[3] Li, H.-J.; Cao, Y.-M.; Qin, J.-J.; Jie, X.-M.; Wang, T.-H.; Liu, J.-H.; Yuan, Q. J Membr Sci 2006, 279, 328.

[4] Kim, I. C.; Lee, K. H. J Membr Sci 2004, 230, 183.

[5] Idris, A.; Zain, N. M.; Noordin, M. Y. Desalination 2007, 203, 324.

[6] Kim, J. H.; Lee, K. H. J Membr Sci 1998, 138, 153.

[7] Ochoa, N. A.; Masuelli, M.; Marchese, J. J Membr Sci 2006, 278, 457.

[8] Mosqueda-Jimenez, D. B.; Narbaitz, R. M.; Matsuura, T. Sep Purif Technol 2004, 37, 51.

[9] Bowen, W. R.; Cheng, S. Y.; Doneva, T. A.; Oatley, D. L. J Membr Sci 2005, 250, 1.

[10] Bowen, W. R.; Doneva, T. A.; Yin, H. B. J Membr Sci 2002, 206, 417.

[11] Shen, L.-Q.; Xu, Z.-K.; Liu, Z.-M.; Xu, Y.-Y. J Membr Sci 2003, 218, 279.

[12] Pham, V. A.; Santerre, J. P.; Matsuura, T.; Narbaitz, R. M. J Appl Polym Sci 1999, 73, 1363.

[13] Ho, J. Y.; Matsuura, T.; Santerre, J. P. J Biomater Sci Polym Ed 2000, 11, 1085.

[14] Rana, D.; Matsuura, T.; Narbaitz, R. M.; Feng, C. J Membr Sci 2005, 249, 103.

[15] Rana, D.; Matsuura, T.; Narbaitz, R. M. J Membr Sci 2006, 282, 205.

[16] Nguyen, A. H.; Narbaitz, R. M.; Matsuura, T. J Environ Eng 2007, 133, 515.

[17] A.-M. Garand-Sheridan, M.A.Sc. thesis, Department of Civil Engineering, University of Ottawa, Ottawa, ON (2008).

[18] Dang, H. T.; Narbaitz, R. M.; Matsuura, T.; Khulbe, K. C. Water Quality Res J Canada 2006, 41, 84.

[19] Sivakumar, M.; Susithra, L.; Mohan, D. R.; Rangarajan, R. J Macromol Sci Pure Appl Chem 2006, 43, 1541.

[20] Singh, S.; Khulbe, K. C.; Matsuura, T.; Ramamurthy, P. J Membr Sci 1998, 142, 111.

[21] M. Mulder, Basic Principles of Membrane Technology; Kluwer Academic: Boston, 1996.

[22] Wan, L.-S.; Xu, Z.-K.; Huang, X.-J.; Che, A.-F.; Wang, Z.-G. J Membr Sci 2006, 277, 157.

[23] Khayet, M.; Matsuura, T. Desalination 2002, 148, 31.

[24] Sun, H.; Liu, S.; Gea, B.; Xing, L.; Chen, H. J Membr Sci 2007, 295, 2.

[25] Raguime, J. A.; Arthanareeswaran, G.; Thanikaivelan, P.; Mohan, D.; Raajenthiren, M. J Appl Poly Sci 2006, 104, 3042.

[26] Kim, I. C.; Yun, H. G.; Lee, K. H. J Membr Sci 2002, 199, 75.

[27] Zhu, L.-P.; Xu, L.; Zhu, B.-K.; Feng, Y.-X.; Xu, Y.-Y. J Membr Sci 2007, 294, 196

CHAPTER 9

CONCLUSIONS AND RECOMMENDATIONS

9.1 Conclusions

Based on the results of this research, the following general conclusions can be made:

1. Among the five affecting factors studied in PES membrane modification using nSMM hydrophobic additive such as polymer concentration, additive concentration, casting speed, thickness and post-treatment, only the additive concentration had a statistically significant impact on the membrane performance (i.e., DOC removal and flux reduction). The effect of remaining factors on membrane performance was marginal.

2. Although the PES-nSMM membranes had small pores, low MWCO and possibly neutral charge, they did not seem to be a good barrier for NOM. So, molecular sieving and charge repulsion are not the principal mechanisms in NOM removal by hydrophobic PES-nSMM membranes. These membranes had low water permeation rates, thus they are a poor choice for drinking water treatment. The low water permeation rates were presumably due to the membrane's more hydrophobic nature i.e., they have no affinity to water or dislike water.

3. The double-pass casting technique had a statistically significant effect on membrane morphology (smoothness of the surfaces and cross-sectional structure), especially when hydrophobic SMM was blended. It also helped increase the permeate flux and the water production, but the DOC rejection was low. The effect of the double pass casting on the membrane flux was only marginal when the hydrophilic LSMM was blended because the performance of the membrane prepared by single-pass casting was already high. The double-pass casting method may be desirable for hard-to-cast solutions including: (i) highly viscous solutions; (ii) easily-demixed (phase separated) solutions and (iii) bubble-containing solutions.

4. In comparison with nine other commercial membranes with different base polymers, the PES-LSMM membranes (i.e., membranes blended with hydrophilic

SMM additive) had the highest flux resistance due to its low initial PWP flux, comparable long-term fluxes and highest DOC rejection (approximately 80%). Thus, LSMM was proved to have a positive impact on membrane modification for surface water treatment.

5. Comparing the membrane's MWCO (measured using PEG and PEO as solutes), molecular weight distribution of NOM and NOM rejection, it is evident that MWCO was proved not a precise indicator for the prediction of NOM rejection. The experiments showed that the membrane with the highest NOM rejection (PES-LSMM) was not the one having the lowest MWCO.

6. Cleaning of membranes fouled with ORW was evaluated using four types of bench-scale UF cell system including a stirred UF cell, a SEPA cell, a single CF cell and a six-CF cell- in parallel system. The performance of three single cells in term of flux was similar for the first testing cycle and then deviated in subsequent cycles due to different degree of NOM deposition and the ease of cleaning corresponding with different cell geometries. The six-cell-in-parallel system behaved quite differently from the single cell CF system. The discrepancies require further investigation and as such are not currently recommended for membrane cleaning studies.

7. Cleaning efficiency at bench-scale would have no significant difference regardless of cell type used as long as a short cleaning frequency (i.e., every 30 min) is employed. The cleaning interval did not statistically affect the flux recovery when the stirred UF cell and the SEPA cell were used. However, SEPA cell is recommended for long-term cleaning tests (several hours) since its design simulates better a real spiral wound membrane module with permeate carriers and feed spacers below and on top of membrane sheets. Based on the limited numbers of tests conducted within the SEPA cell, it appears that LSMM addition has a positive impact on flux recovery after cleaning.

8. For all the membranes there was some irreversible fouling could not be restored completely by clean-in-place method even with rigorous chemicals. Only out-of-place cleaning with sponge could remove almost completely the fouling layer.

9. Given the LSMM additive was proven to have a positive impact with PES base membranes, it was then tried with other base polymers such CA, PEI, PS and PVDF. Based on DSC analysis, LSMM did not mix well with CA and PVDF, particularly at the higher LSMM concentration. For the other polymers, which were amorphous polymers like LSMM, the casting solutions were homogenous and easy to cast.

10. LSMM had a visible effect on MWCO, morphology and permeability but did not cause a statistically significant change in contact angle. Among the modified membranes, PES and PVDF membranes apparently had benefits from this hydrophilic additive in terms of higher flux changes and water production.

11. Overall, the results from this research imply that the incorporation of LSMM (not the hydrophobic nSMM) is possible for membrane modification for surface water treatment, in particular when PVDF base polymer is applied.

9.2 Recommendations

1. Test the LSMM membranes with different sources of water including ground water and coagulated surface-waters on the performance of these new membranes to evaluate the impacts of different water characteristics on membrane fouling.

2. Conduct a more extensive evaluation (at different manufacture conditions) of the benefits of LSMM addition for membranes made of the most promising base polymers i.e., PVDF, PES and PEI.

3. Make hydrophilic *hollow fibre* membranes and compare with commercial HF membranes in terms of performance, characteristics and cleaning efficiency.

4. Conduct post treatment for LSMM membranes with different chemicals such as ethanol, hexane, sodium hydroxide, sodium hypochlorite, acid solution and ultrasonic at 30°C in 5 hours.

5. The testing of new double-pass method has been solely conducted for PES-based membranes. Future study would involve in the evaluation of this new technique for different casting solutions. SEM images should be produced to investigate the membranes' physical structure.

6. Study the tensile strength of all new membranes, especially for the membranes made by double-pass casting method.
7. Check the concentration polarization of membranes (using different concentrations of PEG 6000). Even though concentration polarization is more severe for NF and RO, it has been claimed to contribute to fouling in UF to some extent.
8. Fabricate experimental membranes on backing materials to simulate the real commercial membranes. Then test the tailor-made membranes with backing materials using SEPA cell to simulate the real spiral wound membranes.
9. Analyse the hydrophobicity of membranes (contact angles) before and after filtration with MQ water (using commercial membranes to minimize the coupon differences) to further understand the impact of water itself (not foulants) on membrane surfaces.
10. Conduct a wider array of cleaning tests with a single cross-flow cell and compare those for the SEPA cell.
11. Determine the NOM deposition and TOC in the permeate after each cleaning test to evaluate the cleaning efficiency in term of NOM removal.
12. Employ a more advanced charge analyzer which can measure also the charge density of membranes for membrane surface charge determination.
13. Employ LC-OCD equipment to assess exactly the NOM fractions on membrane surfaces i.e., low MW acids, neutral amphiphilics (<350 Daltons), building blocks (300-500 Daltons), humics (~1000 Daltons), polysacharides (>20000 Daltons), hydrophobic fraction, etc.
14. Test in more details the impact of pre-compaction i.e., at different pressure (60, 70, 80 psi) and different duration (0.5 h; 1h, 2 h and 5 h). Generate the pre-compaction index:

$$DPC = \frac{\Delta J}{\Delta P} = \frac{(J_0 - J_1)}{\eta \Delta P} \qquad \text{(lmh/kPa)}$$

15. In comparing the performance of different filtration cell systems, considerate the hydraulic conditions in term of Reynold number i.e., compare the testing system running with the same Re, not the same cross-flow velocity Uc.

16. For MWCO calculation, all experimental membranes should be conducted SEM to determine exactly the thickness of top layer (based on magnification scale).

REFERENCE

Adam N. K., "The chemical structure of solid surface as deduced contact angles", in "Contact angle: wettability and adhesion", edited by R. F. Gould, Adv. Chem. Ser. 43, 52-56, (1964)

Aiken G.R., McKnight D.M. and Thurman E.M., "Isolation of hydrophilic organic acids from water using nonionic macroporous resins", Org.Geochem., 18, 567-573 (1992)

Alsari AM, Khulbe KC, Matsuura T,, "The effect of sodium dodecyl sulfate solutions as gelation media on the formation of PES membranes", J. Membr. Sci. 188, 279-293, (2001)

Amy G., Cho J., Yoon Y., Wright S., Clark M. M., Molis E., Combe C., Wang Y., Lucas P., Lee Y., Kumar M., Howe K., Kim K. S., Pellegrino J., and Irvine S., "NOM rejection by, and fouling of NF and UF membranes", AWWA Research Foundation, Denver, CO, (2001)

Amy G., Laabs C., Lee N., Merle T., Jekel M., Croue J. P., Jacangelo J., Lozier J., "Understanding low-pressure membrane fouling through analytical footprints of wastewater effluent organic matter (EfOM)", Proceeding in AWWA Membrane Technology Conference, Tampa, FL, (2007)

Anselme C. and Jacobs E. P., "Ultrafiltration", chapter 10 in "Water treatment membrane processes", J. Mallevialle, P. E. Odendaal and M. R. Wiesner, Eds., McGraw Hill; New York, NY, (1996)

Aptel P., and Buckley C. A., "Categories of membrane operations", Chapter 2 in "Water treatment membrane processes", J. Mallevialle, P. E. Odendaal and M. R. Wiesner, Eds., McGraw Hill, NY, (1996)

Arkhangelsky E., Kuzmenko D. and Gitis V., "Impact of chemical cleaning on properties and functioning of polyethersulfone membranes", J. Mem. Sci. 305, 176–184, (2007)

Arnal J.M., Garcia-Fayos B., Lora J., Verdú G. and Sancho M., "AQUAPOT: study of several cleaning solutions to recover permeate flow in a humanitarian drinking water treatment facility based on spiral wound UF membrane. Preliminary test (I)", Desalination 221, 331–337, (2008)

Baker R.W, "Membrane Technology and Applications", John Wiley&Son, Ltd, England, (2004)

Bessieres A., Meireles M., Coratger R., Beauvillain J., and Sanchez V., "Investigations of surface properties of polymer membranes by near field microscopy", J. Membr. Sci., 109, 271-284, (1996)

Bodzek M. and Konieczny K., "Comparison of various membrane types and module configurations in the treatment of natural water by means of low-pressure membrane methods", Sep. Purif. Technol. 14, 69-78, (1998)

Borisov S., Khotimsky V.S., Rebrov A.I., Rykov S.V., Slovetsky D.I. and Pashunin Yu.M., "Plasma fluorination of organosilicon polymeric films for gas separation applications", J. Membr. Sci., 125 (2), 319-329, (1997)

Bowen W. R., Calvo J. I., and Hernández A., "Steps of membrane blocking in flux decline during protein microfiltration", J. Membr. Sci., 101, 153-165, (1995)

Bowen W.R., Doneva T.A. and Yin H.B., Separation of humic acid from a model surface water with PSU/SPEEK blend UF/NF membranes, J. Membr. Sci. 206 (2002) 417.

Brink L.E.S. and Romijn D.J., "Reducing the protein fouling of polysulfone surfaces and polysulfone ultrafiltration membranes: optimization of the type of presorbed layer", Desalination, 78, 209-233, (1990)

Chan C.M., "Polymer Surface Modification and Characterzation", Hanser/Gardner Publications, New York, NY, (1994)

Chellam S., Jacangelo J.G. and Bonacquisti T.P., " Modeling and experimental verification of pilot-scale hollow fiber, direct flow microfiltration with periodic backwashing", Environ. Sci. Technol., 32 (1): 75-81, (1998)

Chen C-L. and Tsai D-S., "Permeation properties of microporous membranes prepared via coating of evaporated polydimethylsilane", J. Membr. Sci., 237(1-2), 163-165, (2004)

Cheryan M., Ultrafiltration Handbook, Technomic Publishing Com., Lancaster, PA, (1986)

Childress A.E. and Elimelech M., "Effect of solution chemistry on the surface charge of polymeric reverse osmosis and nanofiltration membranes", J. Membr. Sci., 119 253-268, (1996)

Cho J., Amy G. and Pellegrino J., "Membrane filtration of natural organic matter: comparison of flux decline, NOM rejection, and foulants during filtration with three UF membranes", Desalination, 127, 283-298, (2000)

Cho J., Amy G., Pellegrino J. and Yoon Y., "Characterization of clean and natural organic matter (NOM) fouled NF and UF membranes and foulants characterization", Water Supply, 17 (1), 183-190 (1999)

Dang T. H., Narbaitz M. R., Matsuura T. and Khulbe C. K., "A comparison of commercial and experimental ultrafiltration membranes via surface property analysis and fouling tests", Water Quality Res. J. of Canada, 41, 1, (2006)

Dang T.H., Narbaitz M.R. and Matsuura T., "Double-pass casting: A novel technique for developing high performance ultrafiltration membranes", J. Membr. Sci., 323, 45-52 (2008)

Deqian R., "Cleaning and regeneration of membranes", Desalination, 62, 363-371 (1987)

Dickson J.M., Childs R.F., McCarry B.E. and Gagnon D.R., "Development of a coating technique for the internal structure of polypropylene microfiltration membranes", J. Membr. Sci., 148 (1), 25-36, (1998)

Fang Y., "Separation of liquid mixtures by membrane", Ph. D. thesis, Department of Chemical Engineering, University of Ottawa, Ottawa, ON (1997)

Fievet P., Sbai M., Szymczyk A. and Vidonne A., "Determining the zeta-potential of plane membranes from tangential streaming potential measurements: effect of the membrane body conductance", J. Membr. Sci., 226 (1-2): 227-236, (2003)

Fievet P., Szymczyk A., Aoubiza B. and Pagetti J., "Evaluation of three methods for the characterisation of the membrane–solution interface: streaming potential, membrane potential and electrolyte conductivity inside pores", J. Membr. Sci., 168, 87–100, (2000)

Fritzsche K., Arevalo A. R., Connolly A. F., Moore M. D., Elings V. and Wu C. M., "The structure and morphology of the skin of polyethersulfone ultrafiltration membranes: A comparative atomic force microscope and scanning electron microscope study", J. Appl. Polym. Sci., 45, 1945-1956 (1992)

Garand-Sheridan A.-M., M.A.Sc. thesis, Department of Civil Engineering, University of Ottawa, Ottawa, ON (2008).

Gekas V. and Hallstrom B., "Microfiltration membranes, cross-flow transport mechanisms and fouling studies", Desalination, 77, 195-218, (1990)

Golander C.A. and Kiss E., "Protein adsorption on functionalized and ESCA-characterized polymer films studied by ellipsometry", J. Coll. Interface Sci., 121 (1): 240-253 (1988)

Green J.H. and Tylla M., "A comparison of ultrafiltration on various river waters", Desalination, 119 (1-3): 79-83, (1998)

Hamza A., Pham V.A., Matsuura T., and Santerre J.P., "Development of membranes with low surface energy to reduce the fouling in ultrafiltration applications", J. Membr. Sci., 131, 217-227 (1997)

Hermia J., "Constant pressure blocking filtration laws: Applications to Power-law non-Newtonian fluids", J. Trans. Inst. Chem. Eng., 60, 183-187 (1982)

Hester J. F., and Mayes A. M., "Design and performance of foul-resistant poly(vinylidene fluoride) membranes prepared in a single-step by surface segregation", J. Membr. Sci., 202, 119-135, (2002).

Hirose M, Itoh H, Minamizaki Y, Kamiyama Y., Proceedings of International Congress on Membranes and Membrane Processes, Yokohama, 178-179 (1996)

Ho J. Y. C., Matsuura T., and Santerre J. P., "The effect of fluorinated surface modifying macromolecules on polyethersulfone membranes", J. Biomater. Sci. Polymer Edn., 11(10), 1085-1104 (2000)

Ho W.S.W. and Sirkar K.K, "Overview", Chapter 1 in "Membrane handbook", Van Nostrand Reinhold, New York, NY, (1992).

Hong S. and Elimelech M., "Chemical and physical aspects of natural organic matter fouling of NF membranes", J. Membr. Sci., 132 (2): 159-181, (1997)

Huang J.Y., Takizawa S. and Fujita K., "Pilot-plant study of a high recovery membrane filtration process for drinking water treatment", Water Sci. Technol., 41 (10-11): 77-84, (2000)

Huisman I.H., Prádanos P. and Hernández A., "Electrokinetic characterisation of ultrafiltration membranes by streaming potential, electroviscous effect, and salt retention", J. Membr. Sci., 178, 55–64, (2000)

Huisman I.H., Tragardh G., Tragardh C. and Pihlajamaki A., "Determining the zeta-potential of ceramic microfiltration membranes using the electroviscous effect", J. Membr. Sci., 147, 187-194, (1998)

Johnson R. E. and Dettre R. H. "Contact angle: wettability and adhesion", edited by R. F. Gould, 43, 112-135, (1964)

Karimi A.A., Vickers J.C. and Harasick R.F., "Microfiltration goes Hollywood: the Los Angeles experience", Jour. AWWA, 91 (6): 90-103, (1999)

Kasemura T., Oshibe Y., Uozumi H., Kawai S., Yamada Y., Ohmura H., and Yamamoto T., "Surface modification of epoxy resin with fluorine-containing methacrylic ester copolymers", J. Appl. Polym. Sci., 47, 2207-2216 (1993)

Keesom W.H., Zelenka R.L. and Radke C.J., "A zeta potential model for ionic surfactant adsorption on a ionogenic hydrophobic surface, J. Colloid Interface Sci., 125 575-585. (1988)

Kennedy M., Kim S.M., Mutenyo I., Broens L. and Schippers J., "Intermittent crossflushing of hollow fiber ultrafiltration systems", Desalination, 118,175-188 (1998)

Kennedy M.D., Chun H.K., Yangali V.A.Q., Heijman B.G.J. and Schippers J.C., "Natural organic matter (NOM) fouling of ultrafiltration membranes: fractionation of NOM in surface water and characterisation by LC-OCD", Desalination, 178 (1-3): 73-83 (2005a)

Kennedy M.D., Kamanyi J., Amy G. and Schippers J.C., "Indicators for NOM fouling of UF membranes", Proceedings in Water Quality Technology Conference, AWWA, November 6-10, Quebec city, QB, (2005b)

Kesting R.E., Synthetic polymeric membranes: A structural perspective, John Wiley & Sons, New York, NY, (1985)

Khayet M, Khulbe KC, Matsuura T. "Characterization of membranes for membrane distillation by atomic force microscopy and estimation of their water vapor transfer coefficients in vacuum membrane distillation process". J. Membr. Sci. 238: 199–211 (2004)

Khayet M. and Matsuura T., "Preparation and characterization of polyvinylidene fluoride membranes for membrane distillation", Ind. Eng. Chem. Res., 40, 5710-5718 (2001)

Khayet M. and Matsuura T., "Surface modification of membranes for the separation of volatile organic compounds from water by pervaporation", Desalination, 148, 31-37 (2002)

Kilduff J. E., Mattaraj S., Sensibaugh J., Pieracci J. P., Yuan Y. and Belfort G. "Modeling Flux Decline During Nanofiltration of NOM with Poly(arylsulfone) Membranes Modified Using UV-Assisted Graft Polymerization", Env. Eng. Sci., 19, 477-495, (2002)

Kim K.J., Fane A.G., Ben Aim R., Liub M.G., Jonsson G., TessaroI.C., Broek A.P., Bargeman D., "A comparative study of techniques used for porousmembrane characterization: pore characterization", J. Membr. Sci., 87 (1-2): 35-46, (1994)

Kimura K., Hane Y., Watanabe Y., Amy G. and Ohkuma N. "Irreversible membrane fouling during ultrafiltration of surface water", Water Research, 38, 3431-3441, (2004)

Kimura K., Hane Y., Watanabe Y., Amy G. and Ohkuma N., "Irreversible membrane fouling during ultrafiltration of surface water", Water Res., 38 (14-15): 3431-3441, (2004)

Kuzmenko D., Arkhangelsky E., Belfer S., Freger V. and Gitis V. "Chemical cleaning of UF membranes fouled by BSA", Desalination 179, 323–333, (2005)

Laîné J. M., Hagstrom J. P., Clark M. M. and Malleviale J., "Effects of ultrafiltration membrane composition", Jour. AWWA, 81, 61-67 (1989)

Lee H.J., Amy G., Cho J.W., Yoon Y.M., Moon S.H. and Kim I.S., "Cleaning strategies for flux recovery of an ultrafiltration membrane fouled by natural organic matter", Water. Res., 35(14): 3301–3308, (2001)

Leenheer J.S., Croue J.P. and Krasner S.W., "Disinfection by-product formation reactivities of NOM fractions of a low-humic water", ACS Symposium, 76, 173-187, (2000)

Letterman R. D., Amirtharajah A. and O'Melia C. R., "Coagulation and Floculation", Chapter in "Water Quality and Treatment: A handbook of Community Water Supplies", Fifth edition, McGraw-Hill, New York, NY, (1999).

Liang H., Gong W., Chen J. and Li G., "Cleaning of fouled ultrafiltration (UF) membrane by algae during reservoir water treatment", Desalination 220, 267–272, (2008)

Loeb S. and Sourirajan S., Sea water demineralization by means of an osmotic membrane, Adv. Chem. Ser. 38, 117-132. (1962)

Maartens A., Swart P. and Jacobs E.P., "Humic membrane foulants in natural brown water: characterization and removal", Desalination, 115 (3): 215-227, (1998)

Madaeni S.S, Mohamadi T. and Moghadam M.K. "Chemical cleaning of reverse osmosis membranes", Desalination 134, 77-82, (2001)

Mallevialle J., Anselme C. and Marsigny O., "Effects of humic substances on membrane processes", Advances in Chemistry, 219, 749-767, (1989)

Mandeep, "Characterization and plasma protein binding studies of surface modified polyethersulfone", M.A.Sc. thesis, Department of Chemical Engineering and Applied Chemistry, University of Toronto, Toronto, ON (2001).

Martinez F., Martin A., Malfeito J., Palacio L., Prádanos P., Tejerina F. and Hernández A., "Streaming potential through and on ultrafiltration membranes: Influence of salt retention", J. Membr. Sci., 206, 431–441, (2002)

Meireles M., Aimar P. and Sanchez V., "Effects of protein fouling on the apparent pore size distribution of sieving membranes", J. Membr. Sci., 56, 13- 28, (1991)

Mosqueda-Jimenez D. B., "Impact of manufacturing conditions of Polyethersulfone membranes on final characteristics and fouling reduction", PhD thesis, Department of Civil Engineering, University of Ottawa (2003).

Mosqueda-Jimenez D. B., Narbaitz R. M. and Matsuura T., "Effects of preparation conditions on the surface modification and performance of polyethersulfone ultrafiltration membranes", J. Appl. Polym. Sci., 99 (6), 2978-2988, 2006

Mosqueda-Jimenez D. B., Narbaitz R. M. and Matsuura T., "Manufacturing conditions of surface-modified membranes: effects on ultrafiltration performance", Sep.Puri.Technol., 37(1), 51-67, (2004d).

Mosqueda-Jimenez D. B., Narbaitz R. M. and Matsuura T., Chowdhury G., Pleizier G., and Santerre J. P., "Influence of processing conditions on the properties of ultrafiltration membranes", J. Membr. Sci., 231(1-2), 209-224 (2004c).

Mosqueda-Jimenez D. B., Narbaitz R. M., and Matsuura T., "Impact of the membrane surface modification on the treatment of surface water", J. Env. Eng., 130, 1450-1459 (2004b).

Mosqueda-Jimenez, D. B., Narbaitz, R. M. and Matsuura, T. "Membrane fouling test: apparatus evaluation", J. Env. Eng., 130, 90-99. (2004a)

Mozia S. and Tomaszewska M., "Treatment of surface water using hybrid processes adsorption on PAC and ultrafiltration", Desalination, 162 (1-3): 23-31 (2004)

Mulder M., "Basic principles of membrane technology", Kluwer Academic Publishers, Dordrecht, Nethelands, (1996)

Muñoz-Aguado M.J., Wiley D.E. and Fane A.G., "Enzymatic and detergent cleaning of a polysulfone ultrafiltration membrane fouled with BSA and whey", J. Membr. Sci., 117, 175-187, (1996)

Nabe A., Staude E. and Belfort G., "Surface modification of polysulfone ultrafiltration membranes and fouling by BSA solutions", J. Membr. Sci., 133, 57-72 (2001).

Nguyen H.A., "Membrane fouling reduction by the incorporation of hydrophilic surface modifying macromolecules in ultrafiltration membrane manufacturing", M.A.S.c thesis, Department of Civil Engineering, University of Ottawa, Ottawa, ON (2005)

Nguyen, A. H., Narbaitz, R. M. and Matsuura, T. "Impacts of Hydrophilic Membrane Additives on the Ultrafiltration of River Water", J Environ Eng, 133, 515-524, (2007)

Norde W. and Rouwendal E., "Streaming potential measurements as a tool to study protein adsorption kinetics, J. Colloid Interface Sci., 139, 169-176 (1990).

Nunes S.P. and Peinemann K.-V., "Membrane Technology in the chemical industry", (2001).

Nystrom M., Lindstrom M. and Matthiasson E., "Streaming potential as a tool in the characterization of ultrafiltration membranes", Colloids Surfaces, 36, 297-312 (1989)

Pellegrino J., "Filtration and ultrafiltration equipment and techniques", Separation and Purification Methods, 29, 91-118, (2000)

Peng H., "The treatment of bilge water using a MF/UF hybrid membrane system: Membrane fouling, cleaning and the effect of constituents on flux decline", M.A.S.c. thesis, Department of Chemical Engineering, University of Ottawa (2002)

Pereira C.C., Nobrega R., and Borges C.P., "Membranes obtained by simultaneous casting of two polymer solutions", J. Membr. Sci., 192, 11-26 (2001)

Pham V. A., Santerre J. P., Matsuura T., and Narbaitz R. M., "Application of surface modifying macromolecules in polyethersulfone membranes: influence on PES surface chemistry and physical properties", J. Appl. Polym. Sci., 73, 1363-1378, (1999)

Pham V.A., "Surface modifying macromolecules for enhancement of polyethersulfone pervaporation membrane performance", M.A.S.c. thesis, Department of Chemical Engineering, University of Ottawa (1995)

Prakash R.A., Joshi S.V., Trivedi J.J., Devmurari C.V. and Shah V.J., "Structure–performance correlation of polyamide thin film composite membranes: effect of coating conditions on film formation", J. Membr. Sci., 211(1), 13-24, (2003)

Qin J. J., Oo M. H. and Li Y. "Development of high flux polyethersulfone hollow fiber ultrafiltration membranes from a low critical solution temperature dope via hypochlorite treatment", J. Membr. Sci., 247, 137-142 (2005)

Rana D., Matsuura T., Narbaitz R. M., and Feng C., "Development and characterization of novel hydrophilic surface modifying macromolecule for polymeric membranes", J. Membr. Sci., 249, 103-112 (2005).

Richter U., Kohler W. and Cabassud C., "Feed cycling in dead end filtration", Chem. Eng. Technol., 22(12): 1029-1033, (1999)

Sbai M., Fievet P., Szymczyk A., Aoubiza B., Vidonne A. and Foissy A., " Streaming potential, electroviscous effect, pore conductivity and membrane potential for the determination of the surface potential of a ceramic ultrafiltration membrane", J. Membr. Sci., 215, 1–9, (2003)

Schnitzer M. and Khan A.U., "Humic substances in the environment", Marcel Dekker,Inc., New York, NY, (1972)

Shen L.Q., Xu Z.K., Liu Z.M. and Xu Y.Y., Ultrafiltration hollow fiber membranes of sulfonated polyetherimide/polyetherimide blends: preparation, morphologies and anti-fouling properties, J. Membr. Sci. 218, 279, (2003)

Shim Y., Lee H.J., Lee S., Moon S.H. and Cho J., "Effects of natural organic matter and ionic species on membrane surface charge", Environ. Sci. Technol., 36 (17): 3864-3871, (2002)

Shon H.K., Smith P.J., Vigneswaran S. and Ngo H.H. "Effect of a hydrodynamic cleaning of a cross-flow membrane system with a novel automated approach", Desalination 202, 351-360, (2007)

Singh S., Khulbe K. C., Matsuura T. and Ramamurthy P., "Membrane characterization by solute transport and atomic force microscopy", J. Membr. Sci., 142, 111-127, (1998)

Sivakumar M., Susithra L., Mohan D.R. and Rangarajan R., "Preparation and performance of polysulfone-cellulose acetate blend ultrafiltration membrane", J. Macromolecular Sci., Part A-Pure Appl. Chem. 43, 1541-1550, (2006)

Sourirajan S. and Matsuura T. "Reverse Osmosis/Ultrafiltration Process Principles", National Research Council of Canada: Ottawa, ON (1985)

Suk D. E., Chowdhury G, Matsuura T., Narbaitz R. M., Santerre P., Pleizier G., and Deslandes Y., "Study on the kinetics of surface migration of surface modifying macromolecules in membrane preparation", Macromolecules, 35 (8), 3017-3021 (2002a)

Suk D. E., Pleizier G., Deslandes Y., and Matsuura T., "Effects of surface modifying macromolecule (SMM) on the properties of polyethersulfone membranes", Desalination, 149, 303-307 (2002b).

Suk D.E., Matsuura T., Park H.B. and Lee Y.M., "Synthesis of a new type of surface modifying macromolecules (nSMM) and characterization and testing of nSMM blended membranes for membrane distillation", J. Membr. Sci. 277, 177-185, (2006)

Szymczyk A., Fievet P., Mullet M., Reggiani J.C. and Pagetti J., "Comparison of two electrokinetic methods - electroosmosis and streaming potential - to determine the zeta-potential of plane ceramic membranes", J. Membrane Sci., 143, 189-195, (1998)

Takizawa S., Babel S., Pradhan N., Prathomrungsiyunkul T., Suwannarit K. and Yamazaki S., "Cross-flow ultrafiltration for surface water treatment in North Thailand", Water Sci.Technol., 41 (10-11): 69-76, (2000)

Tang Y. W., Santerre J. P., Labow R. S., and Taylor D. G., "Synthesis of surface-modifying macromolecules for use in segmented polyurethanes", J. Appl. Polym. Sci., 62, 1133-1145 (1996)

Thominette F., Farnault O., Gaudichet-Maurin E., Machinal C. and Schrotter J.-C. "Ageing of polyethersulfone ultrafiltration membranes in hypochlorite treatment", Desalination 200, 7–8 (2006)

Tragardh. G, "Membrane cleaning", Desalination, 71 (3): 325-335, (1989)

Tran-Ha M.H. and Wiley D.E. "The relationship between membrane cleaning efficiency and water quality", J. Membr. Sci. 145, 99-110, (1998)

Ulbricht M. and Belfort G., "Surface modification of ultrafiltration membranes by low temperature plasma II. Graft polymerization onto polyacrylonitrile and polysulfone", J. Membr. Sci., 111(2):193-215, (1996)

Wang J. W., Yue Z. R., Ince J. S. and Economy J. "Preparation of nanofiltration membranes from polyacrylonitrile ultrafiltration membranes", J. Membr. Sci., 286, 333-341 (2006)

Wang Y., Kim J.H., Choo K.H., Lee Y.S. and Lee C.H., "Hydrophilic modification of polypropylene microfiltration membranes by ozone-induced graft polymerization", J. Membr. Sci., 169 (2), 269-276, (2000)

Weber P. and Knauf R., "Ultrafiltration of surface water with MOLPURE FW50 hollow fibre module", Desalination, 119, 335-339, (1998)

Wiesner M.R. and Aptel P., "Mass transport and permeate flux and fouling in pressure-driven processes", Chapter 4 in "Water treatment: Membrane processes", McGraw Hill, New York, NY (1996)

Willem K., "Process of forming multilayered structures", U.S. Pat. No. 7208200 (2006)

Zeman J. L., and Zydney L. A., "Microfiltration and ultrafiltration: principles and applications", Marcel Dekker, New York, NY (1996)

Zhao Y.H., Zhu B.K., Kong L. and Xu Y.Y., "Improving hydrophilicity and protein resistance of poly(vinylidene fluoride) membranes by blending with amphiphilic hyperbranched-star polymer", Langmuir, 23, 5779-5787, (2007)

Zhao Z.P., Li J., Chen J. and Chen C.X., "Nanofiltration membrane prepared from polyacrylonitrile ultrafiltration membrane by low-temperature plasma: 2. Grafting of styrene in vapor phase", J. Membr. Sci., 251, 239-245, (2005)

Zheng Q. Z., Wang P, Yang Y. N., "Rheological and thermodynamic variation in polysulfone solution by PEG introduction and its effect on kinetics of membrane formation via phase-inversion process", J. Membr. Sci., 279, 230-237 (2006)

Zhu L. P., Zhang X. X., Xu L, Du C.-H., Zhu B.-K. and Xu Y.-Y., "Improved protein-adsorption resistance of polyethersulfone membranes via surface segregation of ultrahigh molecular weight poly(styrene-alt-maleic anhydride)", Colloids and Surfaces B-Biointerfaces 57,189-197 (2007)

ZularisamaA.W., IsmailaA.F., Salim M.R., Sakinaha M., and Ozaki H., "The effects of natural organic matter (NOM) fractions on fouling characteristics and flux recovery of ultrafiltration membranes", Desalination, 212, 191-208 (2007)

APPENDIX A

Effect of NOM storage and NOM characteristics on fouling test

A.1. Introduction

Settlement of natural organic matter (NOM) in water is a natural mechanism particularly in reservoirs. The settlement capacity of raw water can vary between 12 hours to several months depending on water sources (Stevenson, 1997). Normally, in water treatment, reservoirs or bank-side storages are employed for short term storage to primarily settle the troublesome solid particles, to provide a buffer in the event of pollution of the source or to stabilize the rapid fluctuations of the river with seasons. The disadvantages, however, are claimed for the thermal stratification which results in the increase of iron, manganese, ammonia, sulphide, silica, etc in the anaerobic condition; and an increase in algal mass. The stratification can be solved by re-mixing the water prior to sampling. In laboratory scale, the concern would be related to the change of the properties of surface water in terms of dissolved organic carbon (DOC), SUVA and particle size. For instance, Figure A.1 shows the NOM settlement after one day storage in the lab of a sample of ORW. NOM is present as brown flocs at the bottom of the bucket.

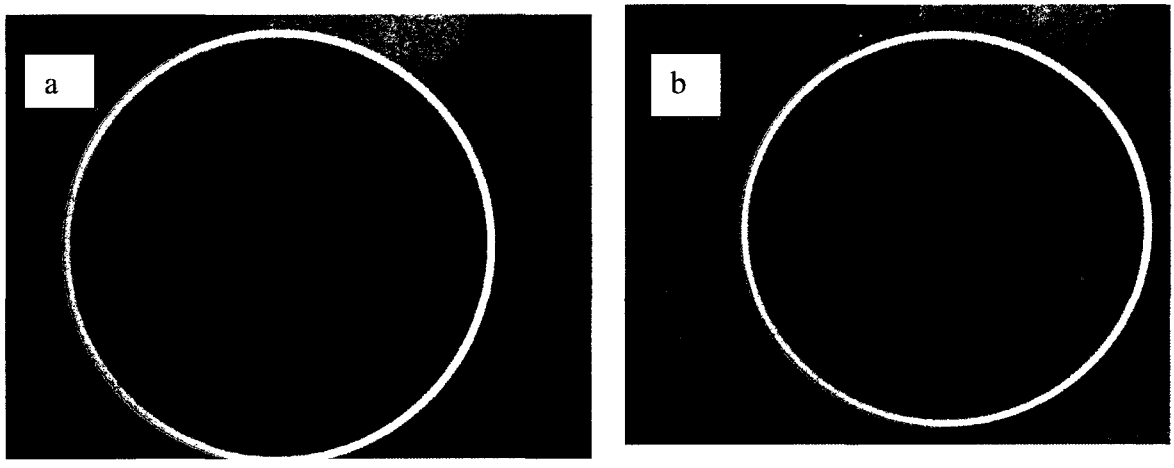

Figure A.1: NOM settlement (a) before and (b) after settling (after one day)

This appendix looked into the effect of storage on NOM characteristics over seven months. The Ottawa River water (ORW) was collected from the intake of the Britannia Water Treatment Plant (Ottawa, Ontario) in May 2007. It was stored in a closed barrel

without mixing or aeration condition and at 4°C. The barrel was constructed of high density polyethelyne and did not permit light to reach the water sample. Monthly analysis of this water was conducted for the following parameters: TOC, UV254, pH, conductivity, color, turbidity and NOM size distribution. Alkalinity, hardness and NOM fraction were randomly checked. The methods of analysis were described in detail in Chapter 3 (section 3.3). Four types of sample corresponding to four types of storage are described in Table A.1. The S1 follows regular procedure of storage applied for all experiments. S2, S3 and S4 were considered to evaluate the impact of temperature, acidification and mixing during the storage, respectively.

Table A.1: Type of samples

Sample	Type of storage	Description
S1	Regular storage	In fridge (4°C), no chemical addition, no mixing
S2	Store outside	Storage at normal temperature, no chemical addition, no mix
S3	Acidified NOM	In fridge, with acidification (pH=2), no mixing
S4	Regular store with mixing	In fridge (4°C), no chemical addition, with mixing right before sampling

A.2. Results and discussion

A.2.1 Original ORW

Table A.2: Characteristics of ORW in May, 2007 (original water)

Parameter	Unit	Value
TOC	mg/l	6.78
UVA254	m-1	0.31
Suva	l/mg.cm	4.54
pH		7.65
Conductivity	mS/cm	0.118
Colour		50
Turbidity	NTU	7.57
Alkalinity	mg CaCO3/L	44
Acidity	mg/l	80
Total Hardness	mg CaCO3/L	45.65
Calcium Hardness	mg CaCO3/L	43.48

It is clear from Table A.2 that Ottawa River water (ORW) has relatively high natural organic matter (NOM) content, low turbidity and hardness. It is considered to be a typical northern river with a yellowish color. Molecular weight of NOM is mostly in the range of 3k-30kDal (Figure A.2a) and NOM size varies between 200nm and 300nm (Figure A.2b). The main fraction of OWR-NOM is hydrophobic (80%), resulting to high MW (Figure A.3).

(a)

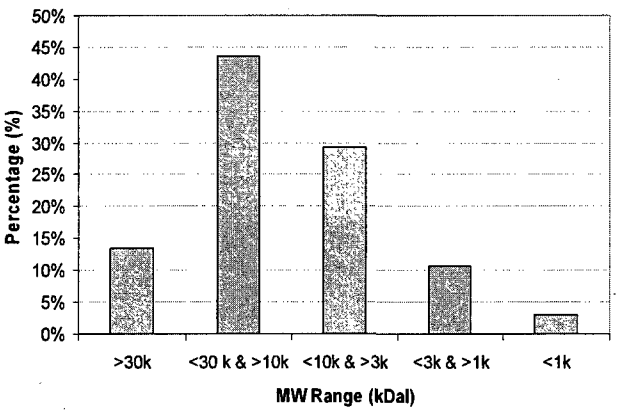

(b)

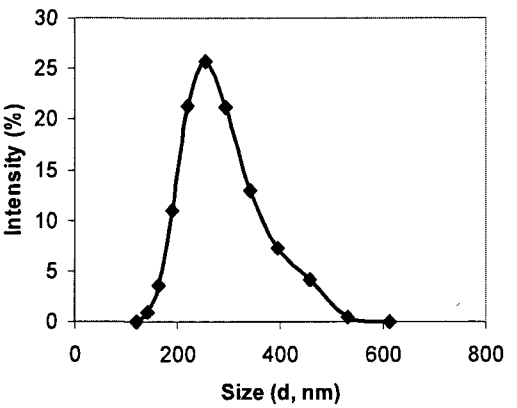

Figure A.2: NOM molecular weight distribution (a) and size distribution (b)

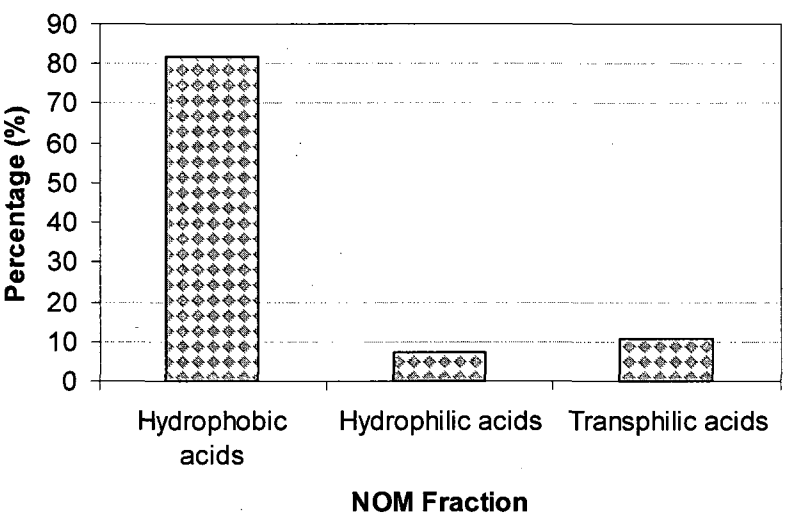

Figure A.3: NOM fractions

A.2.2 Impact of storage period (7 months)

The samples from the same water source S1 (in the fridge at 4°C, no chemical addition, no mix) were taken at the same day of every month and conducted with the same analysis. The results are presented in Table A.3.

Table A.3: Monthly record of S1

Parameter	Unit	May	June	July	August
TOC	mg/l	6.78	6.35	6.09	5.69
UVA254	m-1	0.31	0.29	0.26	0.26
Suva	l/mg/cm	4.54	4.55	3.82	4.55
pH		7.65	7.60	7.57	7.42
Conductivity	mS/cm	0.1180	0.1170	0.1160	0.1176
Colour		50	48	45	43
Turbidity	NTU	7.57	5.79	3.27	3.09

Upon storage, the values of TOC, color and turbidity decreased. This observation is logical since the three parameters are related to each other i.e., related to the presence of the NOM particles. The decrease is likely due to either the settlement of particles under gravity or the break-down of NOM by some anaerobic bacteria. Given the fact that lots of particles coagulated at the bottom of the container (Figure A.1) and the NOM size at the top of barrel, where samples were taken, was getting smaller over the storage period (Figure A.4). The NOM size distribution was obtained by using Zetasizer Nano series (See chapter E for details). The average NOM size decreased from 274.3 nm to 178.3 nm within the period from May to December. The statistical analysis showed that the NOM size reduction is dependent of the storage time. The storage also caused the hydrophobic fraction (which is composed of large MW particles) decreased while the fractions of hydrophilic (with lower MW particles) and transphilic of NOM (Figure A.5) increased.

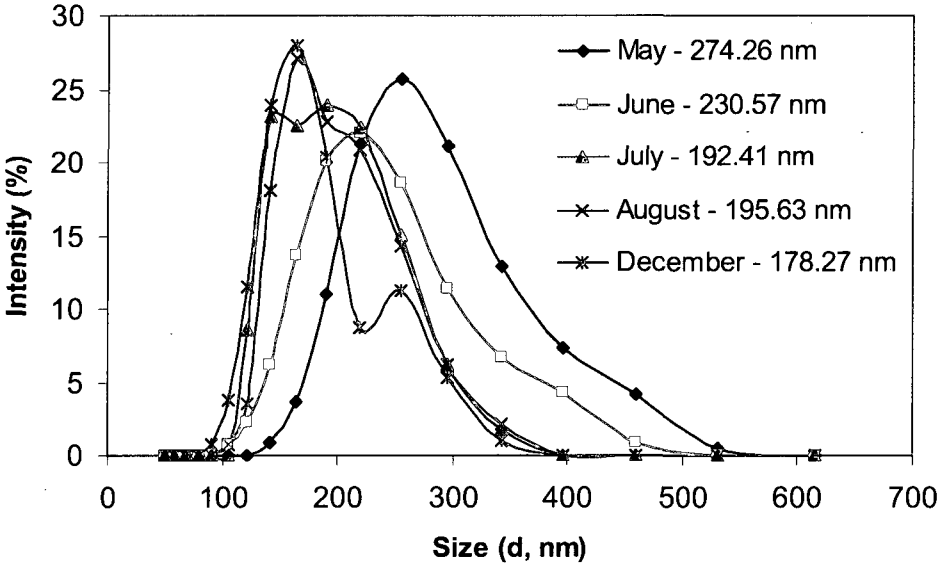

Figure A.4: NOM size distribution w.r.t to storage time (The values beside each month are average NOM size)

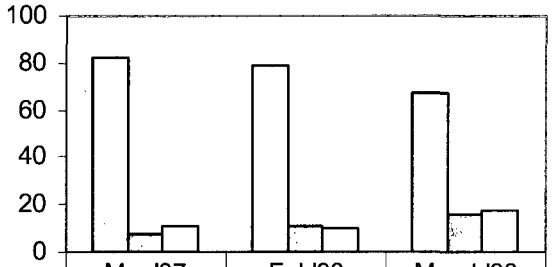

	May'07	Feb'08	March'08
Hydrophobic acids	81.992	78.642	67.022
Hydrophilic acids	7.386	11.133	15.610
Transphilic	10.622	10.224	17.367

Figure A.5: Isolation of NOM fractions

Normally, NOM is of concern for the membrane filtration tests since NOM removal is a crucial index in the evaluation of newly-made membranes. The reduction of NOM after 3 months (until July) and four months (until August) was 10% and 16%, respectively. Although fresh water is the best, the water could be safely stored for up to 3 months for the filtration test.

A.2.3 Impact of storage types

The storage duration had significant impacts on NOM characteristics (as seen in the previous section) and so did the type of storage. Four types of storage were tested including regular storage at 4°C (S1), room temperature storage (S2), cool temperature storage at 4°C with acidification (S3) and regular storage at 4°C with mixing right before sampling (S4). Those samples from 4 different types of storage were analyzed after two months (from May to July) at the same time (Table A.4). Surprisingly, the acidified samples yielded high TOC. Even though, the purpose of acidification is to control the growth and activity of bacteria, there might be a reaction between acid and NOM. The products from the reactions caused a higher conductivity, color and turbidity other than TOC. When the water was stored at room temperature, the TOC decreased much faster. The particle settlement again was confirmed in the result of S4. With the mixing, the settled particles from the bottom were remixed with the ones from the top, leading to the same TOC and a higher turbidity (S4 versus Original).

Table A.4: Comparison of different type of storage – in July (after two months)

Parameter	Unit	Original	S1	S2	S3	S4
TOC	mg/l	6.78	6.98	5.44	8.35	6.42
UVA_{254}	m-1	0.31	0.27	0.24	0.28	0.28
SUVA	l/mg.cm	4.54	3.82	4.42	3.34	4.47
pH		7.65	7.57	7.76	2.85	7.55
Conductivity	mS/cm	0.1180	0.116	0.136	0.463	0.114
Colour		50	80	44	120	67
Turbidity	NTU	7.57	3.27	7.83	7.94	13.18

The samples from different sources were characterized again in August (after 3 months of storage) in terms of NOM size distribution (Figure B.5). It was noticed that with the regular storage (S1), the NOM size followed a log-normal distribution (red diamond).

The samples stored at room temperature had a more complicated size distribution with several peaks. The samples with acidification had a wider range of particle sizes. The following conclusions can be made according to the analysis of Table A.4:

(i) Acidification modified the water characteristics (i.e., higher TOC, lower pH, higher color and conductivity). It would not be recommended to acidify NOM-containing water in the future.

(ii) Storing water samples at room temperature would also decrease the TOC due to higher NOM break-down and particle settlement (At high temperature, the water is less viscous and leads to an easier settling).

(iii) For regular refrigerated storage, samples without mixing have smaller particles than the fresh water samples while the samples with mixing have bigger particles. Maintaining slight mixing during storage maybe a better option but it needs to test to verify this is the case. If storage with mixing is not possible, it is recommended to keep the water at 4°C with no acidification and mix the water before sampling to at least guarantee the same TOC value as that of the raw water.

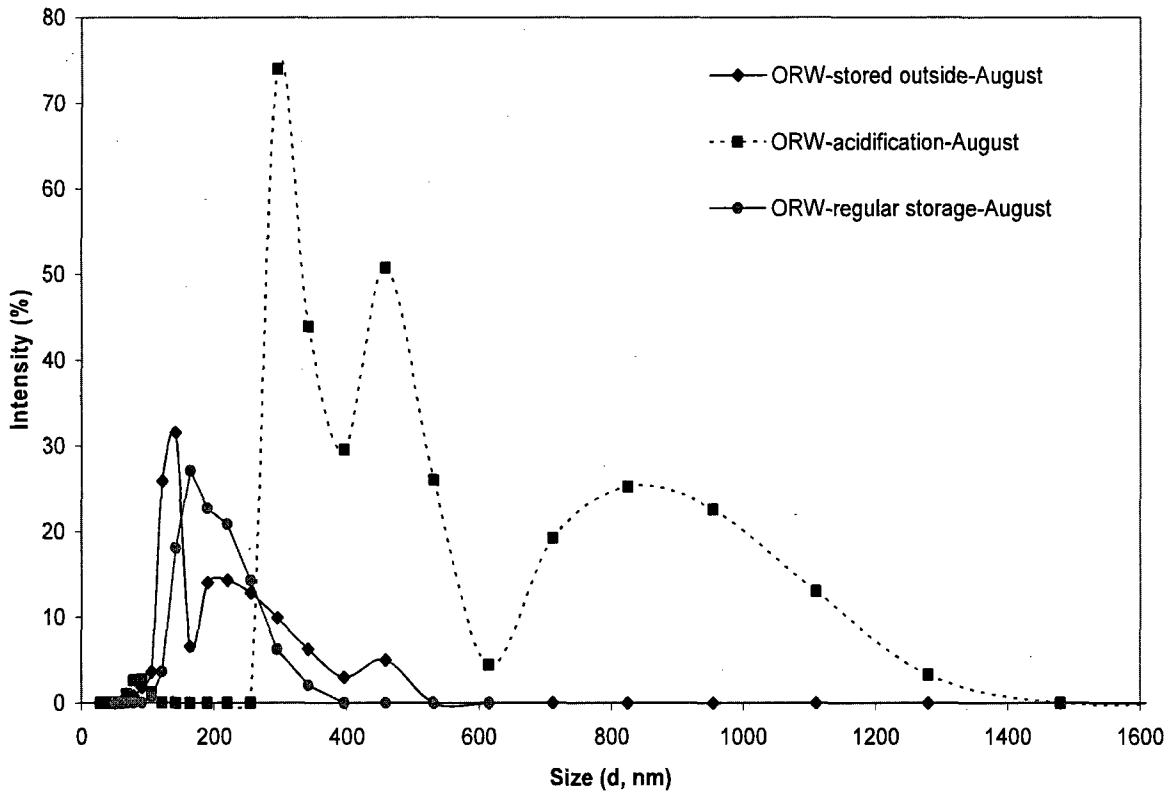

Figure A.6: NOM size distribution w.r.t to different storage types

A.2.3 Impact of NOM characterization on fouling tests

Due to time limitations, only NOM hydrophobic/hydrophilic fractionation and NOM size distribution were considered in this part of the study.

Which specific NOM fraction is mainly responsible for flux decline is not well understood. Some researchers claimed that the reason was the hydrophobic fraction (Cho et al., 2002) while the other found the hydrophilic fraction was the main cause (Zularisam et al., 2007). Factors such as types of tested membranes, testing protocol and water source might contribute to this controversy. In our test, the Ottawa river water (ORW) was isolated into three types of NOM fractions (i.e., three kinds of feed waters for filtration tests): hydrophobic, hydrophilic and transphilic fractions. Three different membranes (commercial PES PU, control PES and the modified PES LSMM) were tested with the hydrophobic water (HPO-ORW), hydrophilic water (HPI-ORW) the original ORW (mixed fractions). It was concluded that the fraction that mainly caused high flux reduction was hydrophobic for PES PU membranes, the mix of three fractions for control PES membranes and the hydrophilic fraction for PES LSMM membranes. Zularisam et al (2007) found that each fraction was susceptible to different fouling mechanism, leading to flux reduction at different rates. For instance, concentration polarization, adsorptive fouling and cake layer deposition were the dominant fouling mechanisms for hydrophobic (HPO), hydrophilic (HPI) and transphilic fractions, respectively. This shows clearly in Figure A.7 in which the flux reduction rates are different for different types of NOM fractions and membranes. In addition, the fouling mechanism modeling (see chapter K for details) revealed that for ORW (with NOM mixed fractions), the intermediate (n=1.5) blocking was the dominant mechanism for the tested membranes (Appendix L).

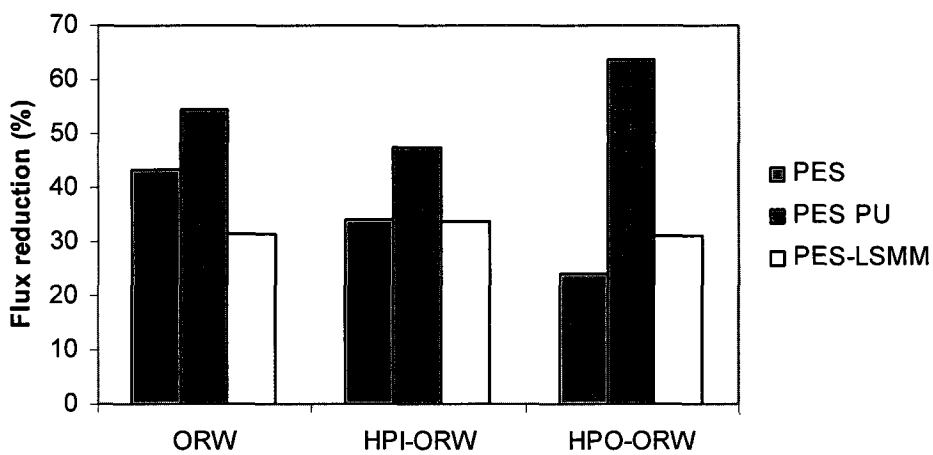

Figure A.7: Flux reduction with different water sources

APPENDIX B

Preliminary study of membrane charges with and without the incorporation of charged additive CSMM and hydrophilic additive LSMM

Zeta potential (the index of membrane charge) is the electrical potential at the actual shear plane between the charged surface and the bulk solution. For UF membranes, the streaming potential reflects the potentials of membrane pores rather than membrane surface (Childress and Elimelech, 1996). The streaming potential is related to zeta potential via a Helmholtz-Smoluchowski equation (Nystrom et al.1989; Keesom et al.1988; Norde and Rouwendal, 1990). Normally, the values of zeta potential, calculated from streaming potential, depend on various operational parameters such as pH, solute concentration, pressure, temperature, ionic strength and pore sizes. Nevertheless, in this study, the same conditions (pH = 7±0.5; temperature=22±0.5; same pressure range and electrolyte concentration or same ionic strength) were applied to focus on the comparison of PES membranes with and without LSMM additive.

In this study, the Zeta potential analysis of commercial, hydrophilic and charged membranes was measured by the system described in Appendix F. The hydrophilic membranes were prepared by blending PES membranes with LSMM additive. Details of LSMM are provided in Chapters 3, 5 and 8. For the charged membranes, the PES membranes were blended with charged additive CSMM. The synthesis of CSMM additive was similar to the procedure applied for LSMM or nSMM additives. After the pre-polymer was formed from the first step, it was end-capped with charged tail MDI-PPG-HBS to produce charged molecules. The average molecular weight of charged additive was 8.4×10^3 Dalton based on NMR spectroscopy. The Tg value recorded at the midpoint of the corresponding heat capacity transition was 114.2°C. The approach centers on developing the membrane surface charge by incorporating charged surface modifying macromolecules was to increase the negative charge, leading to more charge repulsion when filtering ORW since NOM contains mostly negatively charged particles. Several related aspects have been also considered including the effect of electrodes, membrane

batches and manufacturing conditions (i.e., additive concentration, evaporation time, migration manner and coagulation bath temperature).

B.1. Charges of LSMM-PES membranes and commercial membranes

Table B.1 presents the charge measurement of five commercial membranes and two experimental PES membranes. Description of the five commercial membranes is provided in Chapter 6. Since the electrodes (Ag/AgCl) used in the charge system were created manually in the lab (see details in Appendix F), it was of interest to compare the results obtained from different batches of electrode generation.

Table B.1 also shows that there is electrode effect on the charge performance, which was confirmed by ANOVA statistical analysis. The reason of this effect might lie in the control of Cl^- deposition on the electrodes, which affected the conductivity of electrodes to some extent. Analyzing membrane charge in replicate using two different electrodes is recommended. In addition, the incorporation of LSMM made PES membranes more neutral (from -6.3 mV for Control membranes to -3.14 mV for PES-LSMM membranes). The modified PES-LSMM membranes were the least negatively charged compared to the commercial ones.

Table B.1: Zeta potential measurement, ζ (mV)

	CA CQ	PES PX	PAN	PES PU	PES EWH	Control PES	PES-LSMM
Old electrode							
Mean	**-10.03**	**-3.84**	**-2.82**	**-4.65**	**-6.43**	**-5.97**	**-2.81**
Std	0.608	0.218	0.316	1.266	0.611	0.530	0.848
95% Confidence	0.842	0.246	0.358	1.432	0.692	0.600	0.960
New electrode							
Mean	**-7.87**	**-5.89**	**-3.49**	**-4.74**	**-3.89**	**-7.04**	**-3.63**
Std	0.495	0.148	0.098	0.172	1.231	0.349	1.397
95% Confidence	0.560	0.168	0.110	0.195	0.985	0.395	1.369
Overall							
Mean	**-8.84**	**-4.85**	**-3.20**	**-4.68**	**-5.14**	**-6.33**	**-3.14**
Std	1.393	1.118	0.470	0.962	1.406	0.700	1.109
95% Confidence	1.115	0.894	0.376	0.667	0.919	0.458	0.687

B.2. Effect of manufacturing conditions on surface charges

The main objective of this section is to quantify the migration of the charged additives to the membrane surface. Different concentrations of the additive (3.0 and 4.5 wt%), evaporation time (by putting in the 105°C oven for 0, 1.5 and 3.0 min before merging into the coagulation bath), the coagulation bath temperature (4°C vs 25°C) and migration manner (evaporation in oven vs migration in air) (Table B.2 and C.3) have been tried. The data in Table B.2 and B.3 was reported based on an average of four to six measurements for each sample.

Table B.2. Charge measurements of 4.5 wt% charged membranes

ζ (mV)	4.5-0e-4	4.5-1.5e-4	4.5-3e-4	4.5-1.5e-25	4.5-3.0e-25	4.5-3air-4	4.5-3air-25
Mean	-4.77	-5.02	-2.61	-7.26	0.71	-7.32	-3.20
Std	0.802	1.489	0.104	1.678	2.122	1.987	0.180
95% Confidence	0.907	1.685	0.118	1.471	2.401	2.248	0.203

Table B.3. Charge measurements of 3.0 wt% charged membranes

ζ (mV)	3-0e-4	3-1.5e-4	3-3.0e-4	3-1.5e-25	3-3.0air-25	3-3.0air-4*
Mean	-7.14	-5.75	-4.71	-5.83	-4.53	-6.40
Std	0.943	1.317	1.450	1.129	0.566	1.057
95% Confidence	0.924	1.290	1.421	1.277	0.641	0.846

***Nomenclature:** *XX – YY q - ZZ*

XX - Additive concentration: 3.0 wt% or 4.5 wt%;

YY - Duration of migration/evaporation: 0, 1.5 and 3.0 minutes

q - Manner of treatment: e-evaporation at 105°C in the oven; air-migration in air;

ZZ -Temperature of coagulation bath: 4°C and 25°C

Based on the above tables, it is surprisingly that the lower additive concentration (3.0 wt%) made the membranes more negatively charged than the higher additive concentration (4.5 wt%). It seems to indicate that 3.0% is sufficiently high to produce the full impact of the charged additive.

As illustrated in Figure B.1, the manufacturing conditions, such as evaporation time and migration manner did affect the migration of the charged additive to the membrane surfaces, however the changes were not always statistically significant. In addition, compared with the control PES (without additives, -5.9mV), most of the membranes became more neutral unfortunately. The increase of negative charge for some membranes was marginal.

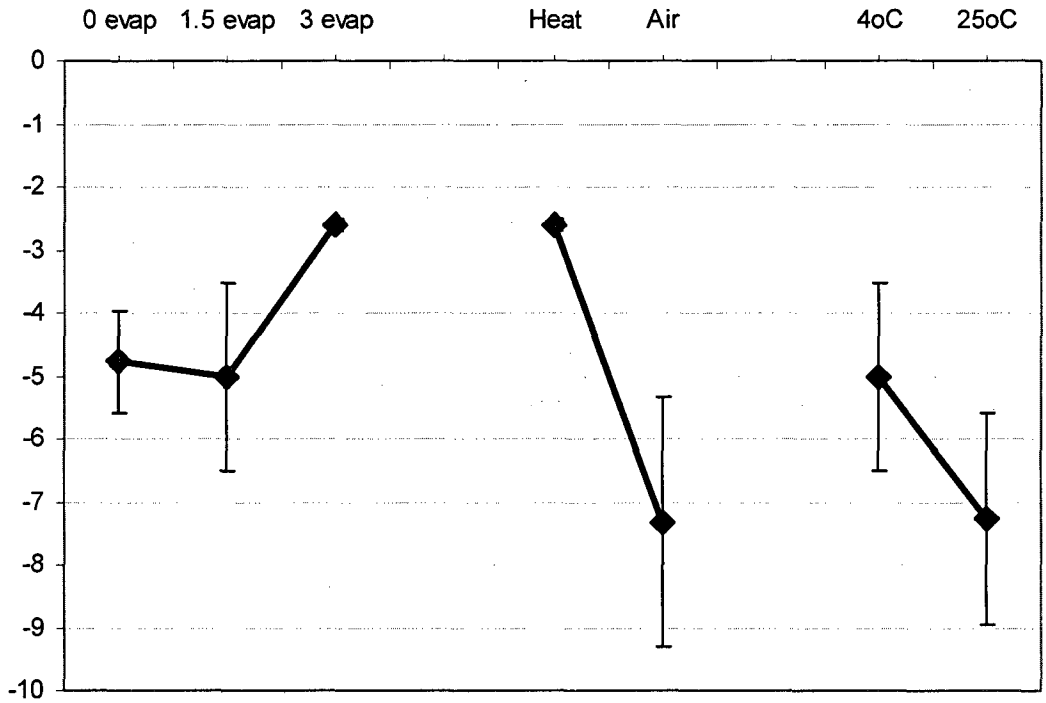

Figure B.1. Impacts of manufacturing conditions on surface charges

B.3. Effect of membrane batches

A second batch of membranes was cast using the same casting conditions. The charge measurements for the new membranes were performed immediately after they were manufactured. As shown in Table B.4, they were much more strongly charged. For the old batch, the membranes had been stored in DI water in the fridge for several days before being analyzed. Hence, the charges could have been possibly changed with batches due to the storage condition. Apparently, during the storage period, some of free ions were leached from the surface to some extent.

Table B.4. Charges of membranes of different batches

Membranes	New batch	Old batch
3-0e-4	-13.64	-7.14
3-1.5e-25	-12.54	-5.83
4.5-1.5e-25	-14.64	-7.26
4.5-1.5e-4	-16.97	-5.02

APPENDIX C

Post treatment

Several studies that post treatment with NaOH, NaOCl or some other chemicals could increase the fluxes or solute rejection (Qin et al., 2005; Wang et al., 2006). Given the fact that hydrophobic PES-nSMM membranes often had low PWP, an optional study of the impact of post treatment using chemicals (instead of physical post treatments like annealing or cooling) was tried. Some results have been reported in Chapter 4.

C.1. Description of tested membranes

Three membranes (PES PU, PES-nSMM1 and PES-nSMM2) have been employed to discover the effect of post treatment with 0.1M sodium hydroxide (NaOH) (Table C.1). A fouling test with river water was conducted to evaluate the improvement in membrane performance.

Table C.1: Tested membranes

Membrane	PES conc. (wt %)	SMM conc. (wt %)	Thickness (mm)	Casting technique
PES PU		Commercial membrane		
PES-nSMM1	18	0.5	0.2	Single pass
PES-nSMM2	18	3.0	0.2	Double pass

C.2. Procedure of Post treatment

Membranes were soaked in 0.1 M NaOH in 24 hours before being tested.

C.3. Results and discussions

The membranes were first characterized using the solute transport method (see Chapter 3 for details of this method). Pore characteristics are shown in Table C.2.

Table C.2: Responsive characteristics

Membrane	Condition	MWCO (kDal)	Mean pore (nm)	Pore density (# of pore/m2)	Water content (%)
PES-nSMM1	Without Post	**49.06** (3.83)	**2.50** (0.08)	**3.68** (0.48)	**77.64** (3.20)
PES-nSMM1	With Post	**37.60** (5.30)	**1.66** (0.16)	**23.25** (4.43)	**77.94** (0.27)
PES PU	Without Post	**60.33** (3.21)	**4.96** (0.23)	**17.83** (2.91)	N/A N/A
PES PU	With Post	**18.65** (0.93)	**1.36** (0.16)	**60.62** (3.50)	N/A N/A

Note:

- *Since the commercial PES PU membranes had a backing material, the determination of water content was not accurate and therefore not recorded.*
- *Pore characteristics of PES-SMM2 were not recorded.*
- *Data in the bracket represents standard deviation*
- *"With post" means with post treatment*

It is clear that post treatment with NaOH narrows the pore size, reducing the MWCO of membranes. The chemical might adsorb partly into the pores. This was consistent with observations of Qin et al., (2005). Their membranes were post-treated by means of a hypochlorite solution of 4000 ppm over 48 h. Their experimental results showed that the membrane flux was increased by five times and the pore size distribution became narrow after the hypochlorite treatment. Water content was almost the same with and without post-treatment.

As a result of pore constriction, DOC removal increased for the three membranes (Table C.3). Except for PES-nSMM1 membranes, the fluxes decreased with post treatment. This seems to follow the trade-off law of flux and solute removal. The low concentration of SMM or the casting method (single pass) likely caused the exception for PES-SMM1 membranes.

The performance effect of post-treatment using a NaOH solution was depended on membrane types. However, the test results were consistent with the previous studies that post treatment with chemicals narrows membrane pores.

Table C.3: Responsive performance of membranes with/without post treatment

Membranes	Condition	PWP (lmh)	Final flux (lmh)	DOC (%)	Norm. flux reduction (%)	Volume treated (l/m^2)*
PES-nSMM1	Without Post	**8.05** (7.27)	**10.87** (4.82)	**69.73** (4.06)	**24.74** (1.54)	**391.32** (10.32)
PES-nSMM1	With Post	**14.97** (13.60)	**20.16** (5.71)	**79.50** (0.35)	**35.75** (2.74)	**1100.58** (274.87)
PES-nSMM2	Without Post	**7.10** (5.10)	**12.79** (9.81)	**13.42** (9.49)	**50.41** (2.43)	**732.61** (555.05)
PES-nSMM2	With Post	**3.83** (1.62)	**2.05** (0.42)	**52.27** (8.57)	**51.00** (51.06)	**106.83** (13.26)
PES PU	Without Post	**120.66** (24.94)	**58.00** (19.23)	**72.46** (3.24)	**68.54** (10.66)	**3832.93** (914.18)
PES PU	With Post	**118.71** (49.43)	**44.36** (0.95)	**78.68** (0.21)	**67.64** (0.15)	**2820.87** (24.97)

- *Volume of water treated was accumulated after 50-h fouling test*
- *Data in the bracket represents standard deviation*

APPENDIX D

Impact of trans-membrane pressures (TMP)

The trans-membrane pressure used consistently in this thesis was 80 psig for precompaction and 50 psig for filtration. From the literature, the TMP for UF polymeric membranes however often ranges from 10-200 psig. High pressure usually results in higher fluxes but requires more energy and leads to an increasingly operational expenses. Thus, for practical and economic objectives, the selected TMP range for testing was from 10-80 psig. This optional study evaluated different operation pressures (50 psig or 30 psig) and pre-compaction pressures (80 psig or 70 psig) to further understand the impact of TMP. It is recommended by the manufacturer that pre-compaction pressure should be 1.2-1.5 times the operating pressure. In addition, intermittent release of pressure has been claimed to help recover the flux performance to some extent. It therefore was investigated and presented in this appendix as well.

D.1. Testing protocol

The test was conducted with two different cells: Amicon stirred UF cell 8400 (Dead-end) and crossflow cell (CF). Details about the two cells are described in Chapter 3.

D.1.1. UF cell:

The filtration was driven by nitrogen gas. By increasing the gas pressure, the fluxes were increased accordingly. At different pressures (0, 10, 20, 30, 40, 50 psig), the filtration flux was recorded when it reached a constant value. No pre-compaction was implemented. A variety of experimental membranes using different base polymers CA, PES, PS, PEI and PVDF) with or with out LSMM additive (0.5 wt% or 3.0 wt%) were used in these tests.

D.1.2. CF cell:

The impact of TMP on membrane performance using CF cells was evaluated using several protocols:

- With short compaction: Membranes were pre-compressed at 80 psig for one hour to make the membranes stable, then run with pure water (MQ water) at each pressure for

another hour. The pressure range was from 10 psig to 80 psig.

- With long compaction: UF membranes were pre-compacted at 50 psig for 24 hours then run at each pressure for hour as above.
- Without compaction + intermittent flushing: The system was run without pre-compaction at two different pressures 30 psig and 50 psig for 6 hours. There was an intermittent release of pressure chosen arbitrarily as two minutes every hour.
- With different pre-compaction pressures: Impact of pre-compaction pressure (80 psig versus 70 psig) in 60 min was evaluated in terms of membrane performance thereafter at 50 psig (flux and solute rejection).

D.2. Results

D.2.1 Using Amicon stirred UF cell 8400 (Dead-end filtration mode)

D.2.1.1 Comparison of LSMM-PES membranes with commercial membranes

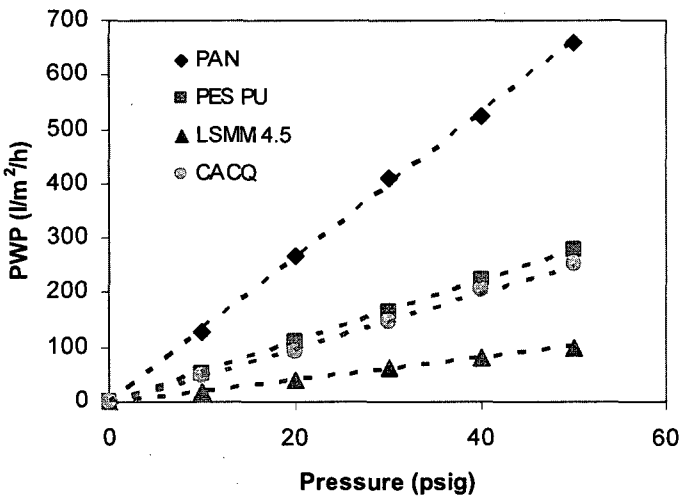

Figure D.1: Flux-pressure responses for commercial and experimental membranes (Using stirred UF cell)

The experimental membranes PES-LSMM (4.5 wt% of LSMM) was compared with other commercial membranes (PAN, PES PU and CACQ). Details of commercial membranes can be referred to in Chapter 6. According to Figure D.1, the PWP increased with increasing pressure. It agrees with the operation principle of almost pressure-driven membranes. Depending on the type of membranes, the effect of pressure on PWP varied. The PWP increase with increasing pressure was remarkable for PAN, similar for PES PU and CA CQ, and marginal for the experimental PES-LSMM membranes. It should be

noted that the experimental membranes were not as hydrophilic as the commercial ones; therefore the water penetration under pressure was not as significant. In addition, for the flux-TMP relationship is linear, these fluxes are below the critical fluxes.

D.2.1.2 Different LSMM-blended base polymers

Among the experimental membranes, the flux-pressure relation was also observed (Figure D.2) with different concentrations of LSMM additive.

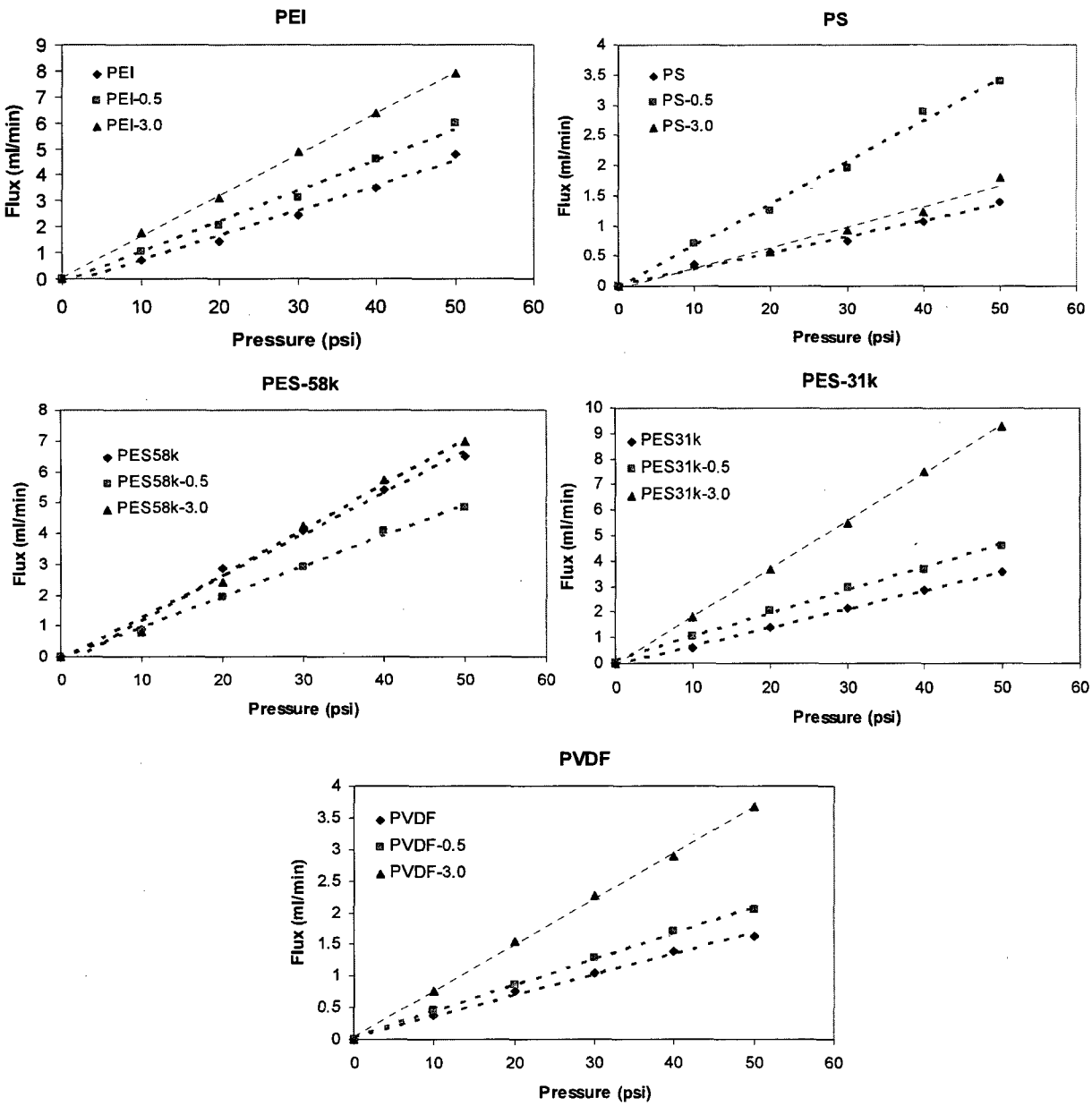

Figure D.2: Flux-pressure responses for experimental membranes with different concentration of LSMM additive (using stirred UF cell)

These membranes of different base polymers covered a wide range of hydrophilicity/ hydrophobicity spectrum: CA, PEI, PES, PS and PVDF. A description of their membrane characteristics is contained in Chapter 8. It is interesting that incorporation of LSMM absolutely enhanced the water flux and its relation with trans-membrane pressure. Except for the PS membranes, membranes with higher LSMM concentration increased the flux positively. Apparently, OH- group of PEG tail of the additive likely migrated to some extent to the membrane surface.

D.2.2 Using crossflow cell (Cross-flow filtration mode)

D.2.2.1 Impact of 24-hour compaction

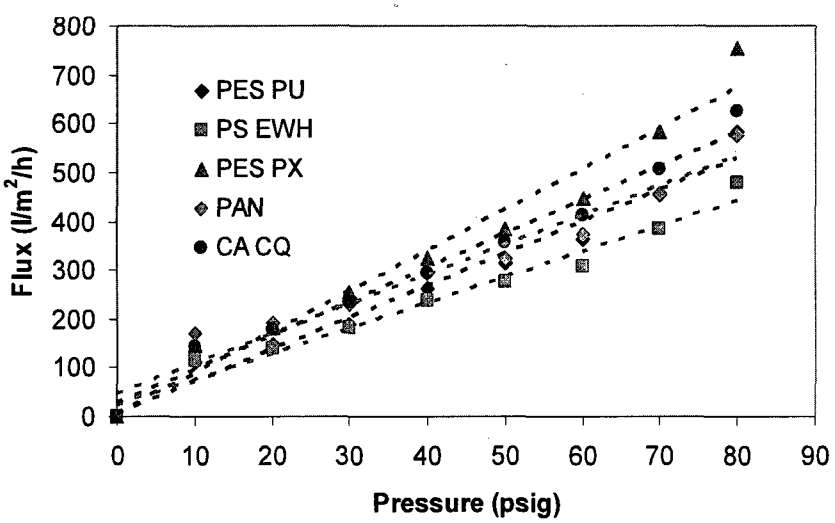

Figure D.3: Flux-pressure responses for commercial membranes without compaction (using crossflow UF cell)

First, it was noticed that the flux-pressure responses were in different way when different test cells were used (i.e., dead-end cell-Figure D.1 versus cross-flow cell-Figure D.3) although the same membranes were tested. Except for PAN membranes, all other membranes using cross-flow cells yielded higher flux with increasing pressure. This discrepancy could be attributed to the cell design. Nevertheless the linear regression was better in cases using the UF stirred cell (i.e., R^2 relation was absolutely high). Consequently, UF stirred cell was used more often for R_m, hydraulic membrane resistance, determination.

Second, Figure D.3 and Figure D.4 show the relationship of flux and pressure of the membranes with and without compaction (for 24 hours). It was obvious the fluxes were higher without compaction than those with compaction; the relationship between flux and TMP was relatively linear in both cases, however, their slopes were not the same. In the case of compaction, the flux almost doubled with a doubling of pressure at low pressure from 10-40psig, while the increase of flux was less at high pressure (35% increases at more than 40 psig). It means the impact was more significant at low pressure with compaction. However, the opposite impact occurred when the system was running without compression. The difference in fluxes at low pressure (from 10-40psig) was only about 20-25%, whereas it increased up to 60% at the highest pressure (80psig). Therefore, long term compaction is not recommended. Optimal pressure is from 50-60 psig, which gives effective fluxes and does not require as much energy as running at 80psig.

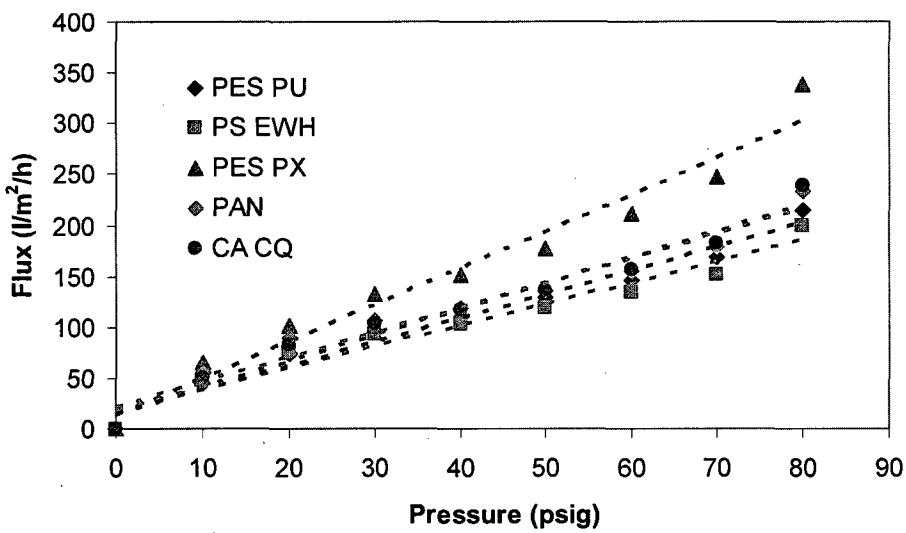

Figure D.4: Flux-pressure responses for commercial membranes with a 24-hour compaction (using crossflow UF cell)

In the collective plots which compare the behaviors of each membrane with and without compaction at 50 psig for 24 hours using MQ water and ORW (Figure D.5), it is clear that they show similar trends. The impact of compaction is evident when pressure was greater than 50 psig, with a deviation between two curves. The fluxes for NOM-containing feed water, as expected, were always lower than those using pure water as feed water.

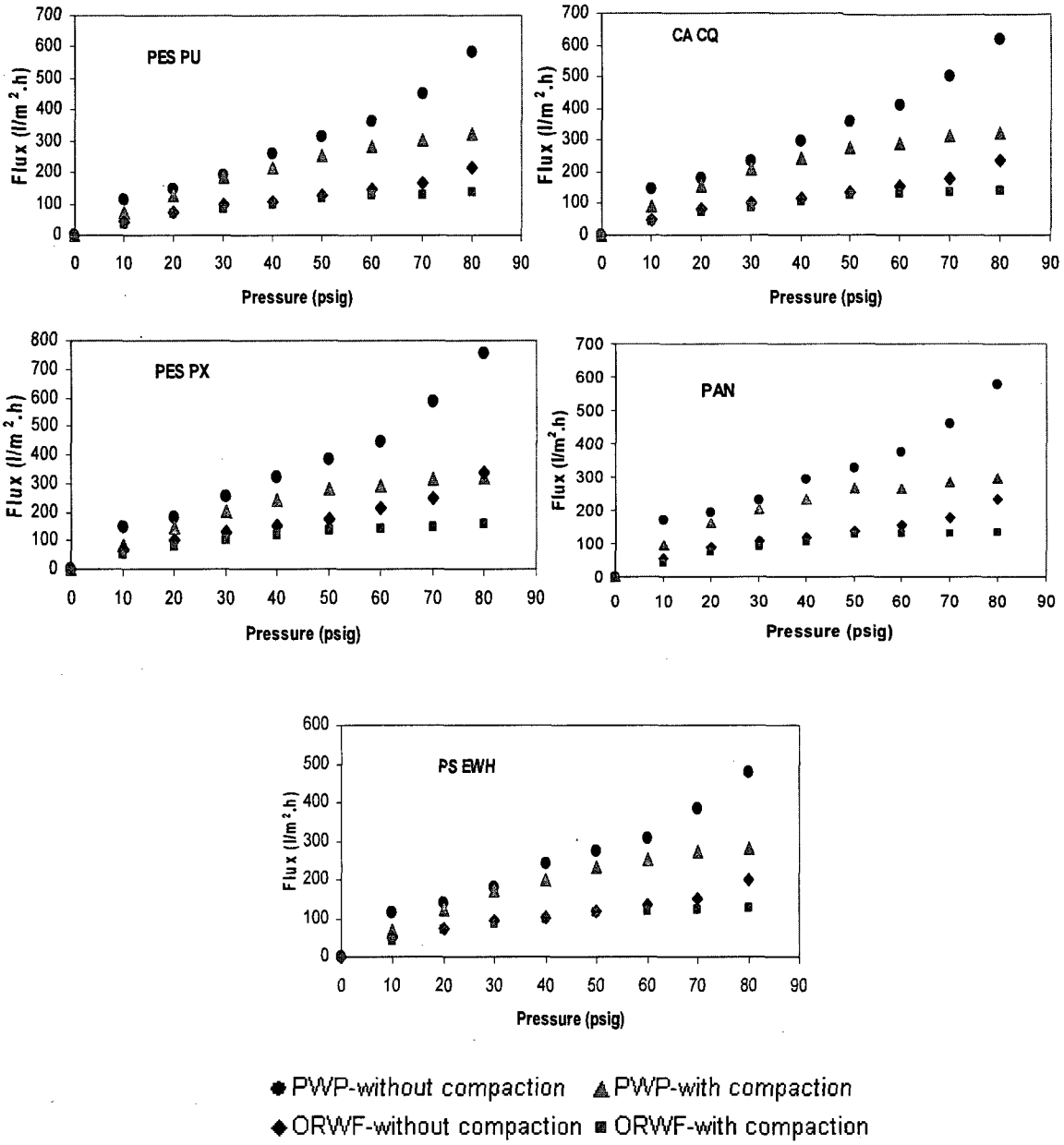

Figure D.5: Flux-pressure responses for different feed sources (pure water and NOM-containing water)

D.2.2.2 Impact of operating pressure and intermittent release of pressure

Logically higher operation pressure leads to higher fluxes if the pressure-driven system is used and pressure is applied continuously. Optimization of the operation pressure is

important since it affects the energy cost. In the result shown in Figure D.6, there were intermittent pressure releases of two minutes every hour.

(a) PES PU

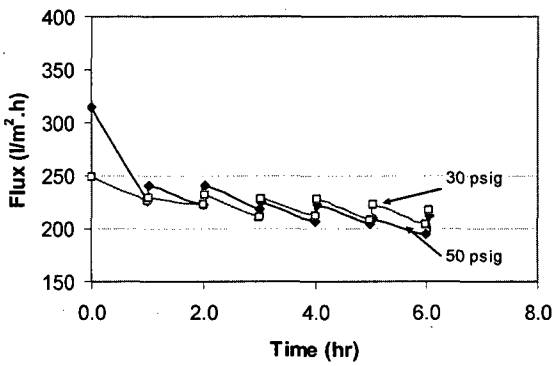

(b) CA CQ40

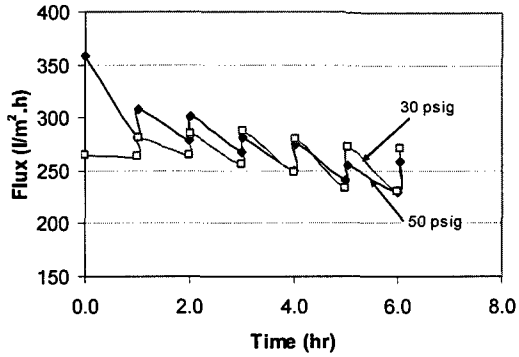

Figure D.6: Impact of operating pressure

As seen in Figure D.6, a higher operating pressure results in higher initial fluxes. The fluxes at lower operating pressure (30 pisg) however decreased more gradually and eventually became higher or similar to the 50 psig fluxes. Long term test (several days) should be conducted to confirm this observation. If it is true, lower operation than 50 psig can be applied for later UF membrane tests.

D.2.2.3 Impact of pre-compaction pressure

Three types of commercial membranes and one type of experimental PES-LSMM membranes were compacted for 60 min at 70 psig or 80 psig, and then at 50 psig for 100 hour long (50 hours with MW water and 50 hours with ORW). In all cases, higher compaction pressure led to higher initial permeation flux. The fluxes however reached almost the same state after long term run (100 hrs) (Figure D.7). In a long run, it may not be necessary to apply a high compaction pressure. Besides, the TOC removal was lower for all tested membranes at higher compaction pressure (Figure D.8). The possible explanation was that under the higher pressure, the turbulent condition increased, and leading to higher initial permeation flux. The high pressure likely deformed the support layer of membranes (which often has large finger-like structure), not the top selective layer, therefore their solute removal was not necessarily higher and the final fluxes were almost the same. Actually, higher water permeation under higher mass transfer rate would enhance the solute penetration to permeate side, resulting in lower TOC removal.

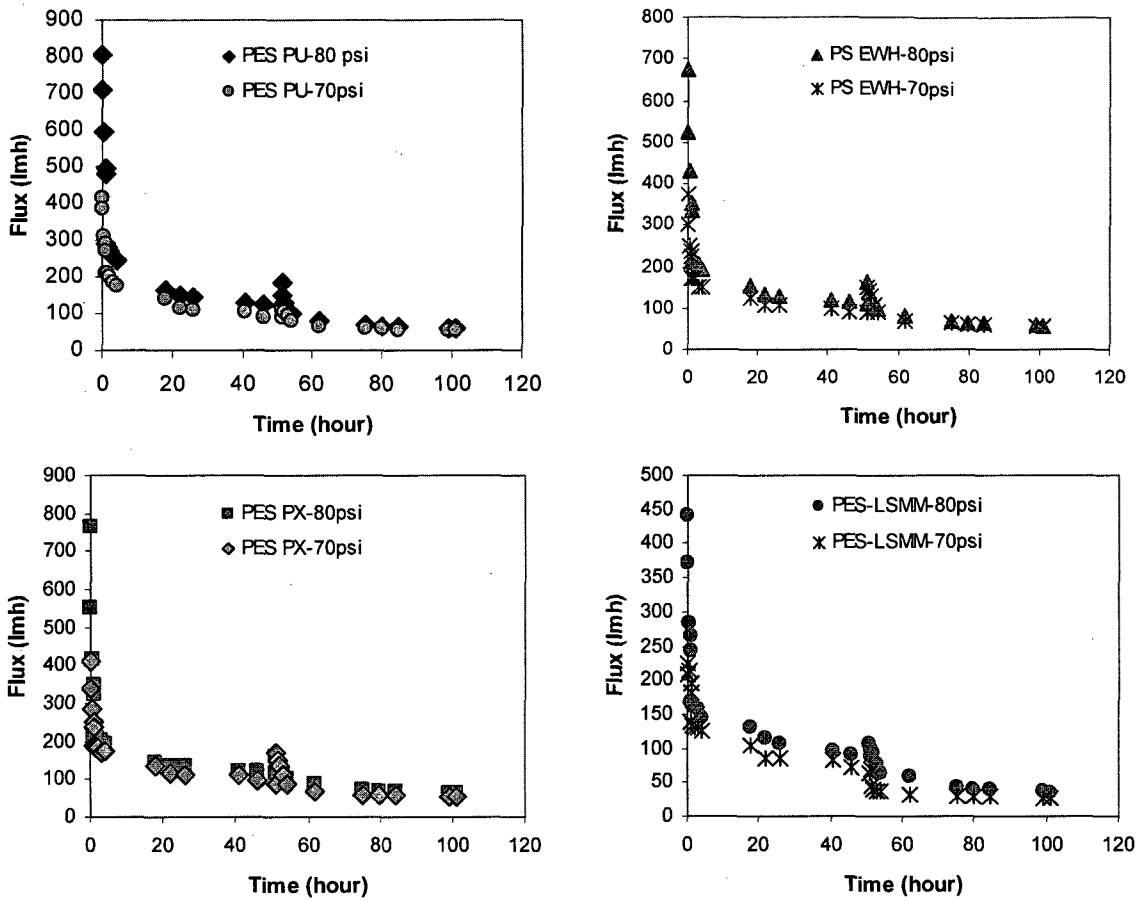

Figure D.7: Filtration fluxes at two different pre-compaction pressures

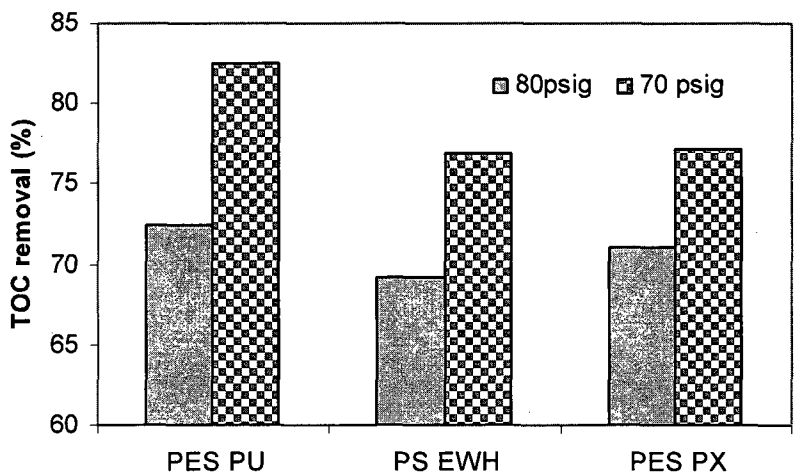

Figure D.8: TOC removal at two different pre-compaction pressures

APPENDIX E

Detailed Materials and Methods

Chapter 3 has briefly discussed the materials and methods for membrane and feed water characterization. This appendix aims at describing in more details the principles, preparation and analysis procedures for each method.

E.1. Characterization of natural organic matters

E.1.1 Total organic carbon (TOC)

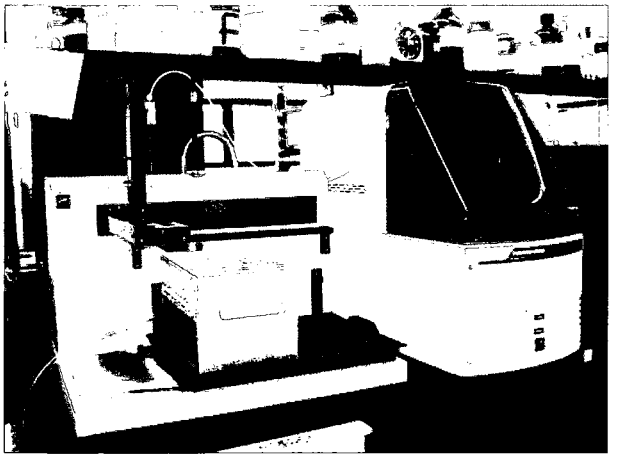

Figure E.1. Phoenix 8000 TOC analyzer

1.1.1. Method:

TOC is determined using a UV-Persulfate TOC analyzer (Phoenix 8000, Tekmar Dohrmann, Cincinnati, OH). This equipment uses the Standard Method 5310C, persulfate-ultraviolet oxidation method (APHA, 1999) in which organic carbons are oxidized to CO_2 and measured.

1.1.2. Preparing reagents and standards

- Glassware: All the glassware, containers and closures are thoroughly rinsed (3-5 times), then soaked in dilute (0.5%) nitric acid-containing beakers for over night, then rinsed profusely again before being dried in the oven for few hours. 40-ml vials (Kimble Glass Inc, Vineland, NJ) are used for storing samples.
- Standard solution: Potassium Hydrogen Phtalate (KHP).

- Reagents: Ultra pure water generated by Milli-Q water system (Millipore Cor., Billerica, MA); Phosphoric acid (H_3PO_4) 85% (Sigma-Aldrich, Milwaukee, WI) and Sodium Persulfate ($Na_2S_2O_8$) 98+% (Sigma-Aldrich, Milwaukee, WI).

1.1.3. Analysis procedure:

- Calibration: Standard solutions of 1ppm, 2ppm, 4ppm, 10ppm and 20 ppm are analyzed and a calibration curve is developed before testing.
- Each sample analysis is started by one cleaning, one blank, one standard solution and followed by samples.
- For each sample, four determinations are made and the first reading is discarded to minimize the impact of sample carryover from one sample to the next.

E.1.2 UV spectroscopy

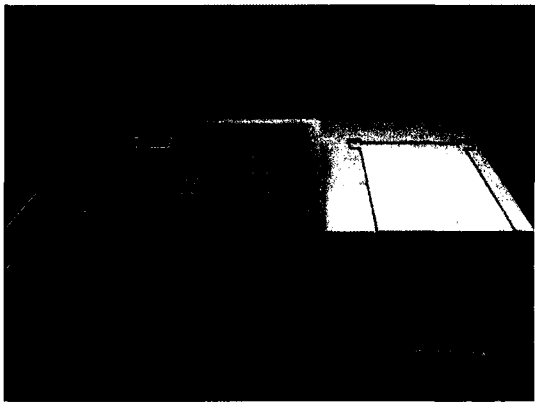

Figure E.2. Beckman Spectrophotometer

1.2.1. Method

UV absorbance at 254nm is conducted using a Beckman Spectrophotometer (DU-40, Beckman Coulter Inc., Fullerton, CA). Aromatic NOM is more supposed to be adsorbed by UV light so UV spectroscopy is helpful in measuring humic substances.

1.2.2. Preparing reagents and standards:

- A 1cm square quartz cell is employed. It should be cleaned thoroughly by MQ water.
- Ultra pure water for calibration

1.2.3. Analysis procedure:

- The spectrophotometer is calibrated to zero with MQ samples.
- Readings are taken in triplicate for each sample. After five to six samples, a blank with ultra pure water is checked.

E.1.3 Molecular weight/size by Ultrafiltration

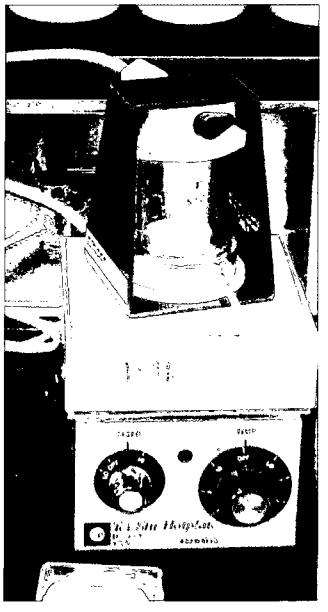

Figure E.3. Amicon UF Stirred Cell

1.3.1. Method:

Ultrafiltration-based molecular weight distribution is conducted using a 50-ml Amicon UF Stirred Cell (Micron 8050, Amicon Inc., Beverly, MA). A "Cascade" or "In Series" method is applied which is similar to a sieve shaker for particle size analysis. Figure E.4 shows the cascade method used in this study.

1.3.2. Preparing materials, reagents and standards:

- Membranes: Regenerated Cellulose membranes of MWCO of 500, 1000, 3000, 5000, 10000 and 30000 Daltons (Millipore, Billerica, MA) are used. They are soaked in ultra pure water to rinse the glycerine preservation coating then immerged in sample water.

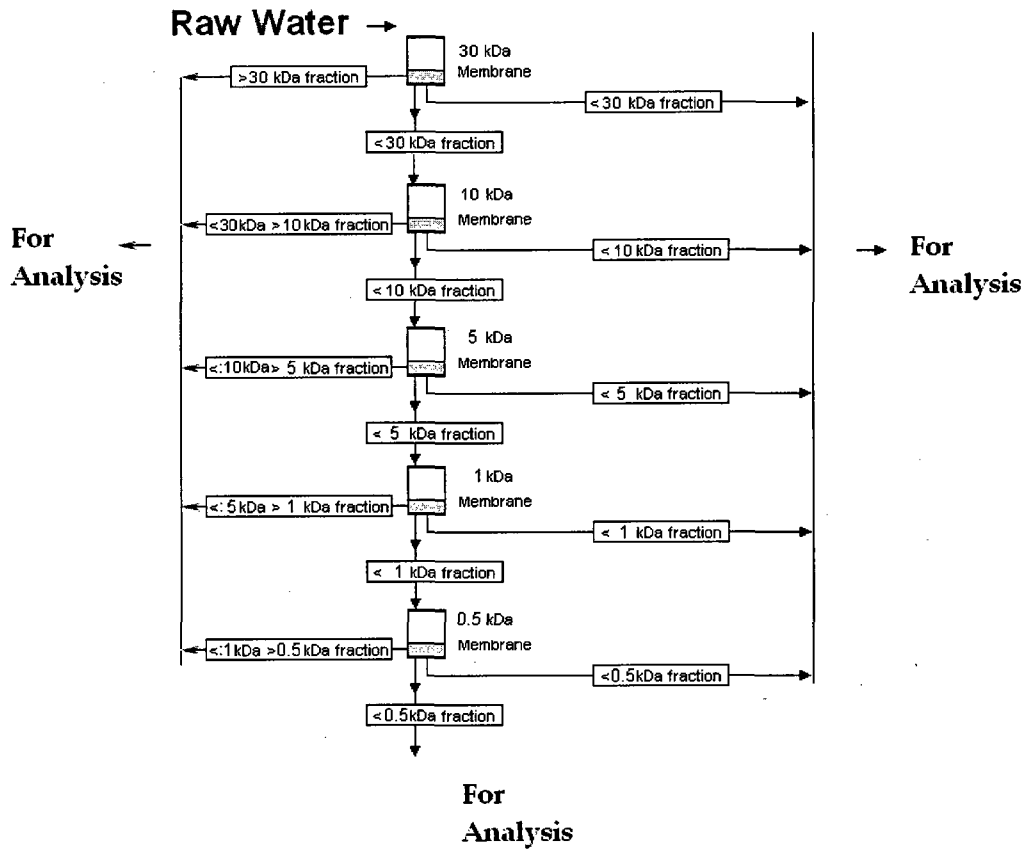

Figure E.4. "Cascade" method

1.3.3. Analysis procedure:

- Procedure:

  + The membranes are soaked with the shiny side down in MQ water and ORW to remove glycerin protection coating.

  + The cell is also cleaned with MQ water. The cell is filled with 50ml of MQ water and pressurized and the magnetic stirrer turned on. 75% of the water is allowed to run through the membrane and clean the system.

  + The cell is then filled (overfilled slightly) with 55ml of the water being fractionated.

  + The cell is pressurized to 35psi using air and stirred with a magnetic stirrer. The first 5ml of sample is discarded. 40ml of the permeate is collected and the pressure turned off. This step repeats four times for the first membrane.

  + Samples of the retentate and the permeate are set aside for later analysis.

+ The permeate is then required for use in the membranes of smaller pore sizes to complete the cascade analysis. For the later, the repeats reduce to three times or twice as long as it creates at least 30 ml for TOC analysis.

+ The fractions of NOM retained on each membrane are calculated by weight percent through a mass balance.

E.1.4 Molecular weight/size by Zetasizer Nano series

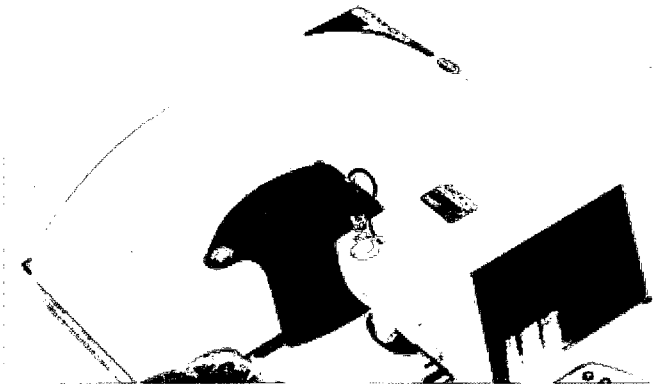

Figure E.5. Zetasizer Nano series

1.4.1 Method:

The Zetasizer Nano series performs Molecular weight measurements using a process called Static Light Scattering (SLS) and combining with the Debye plot. Static Light Scattering (SLS) is a non-invasive technique used to characterize the molecules in solution. The particles in a sample are illuminated by a light source such as a laser, with the particles scattering the light in all directions, then measure the time-averaged intensity of scattered light.

The molecular weight is determined by measuring the sample at different concentrations and applying the **Rayleigh equation.**

$$\frac{KC}{R_\theta} = \left(\frac{1}{M} + 2A_2C\right)P(\theta) \qquad [E.1]$$

Whereas: R_θ: The Rayleigh ratio - the ratio of scattered light to incident light of the sample.

M : Sample molecular weight.

A_2 : 2nd Virial Coefficient.

C : Sample concentration.

P_θ: Angular dependence of the sample scattering intensity, =1

K : Optical constant

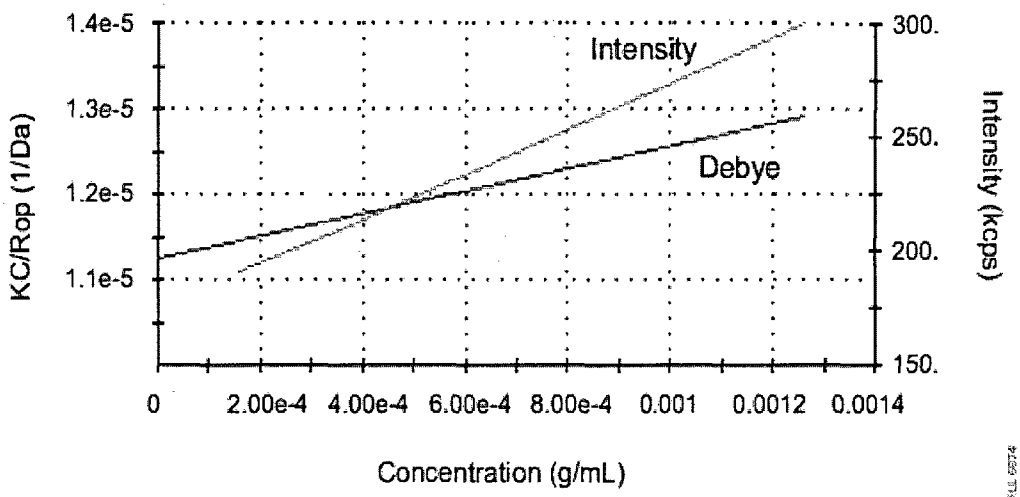

Figure E.6. Debye Plot

From this we can determine the Molecular weight (MW) from the Intercept and the 2nd Virial Coefficient (A_2) from the slope.

The 2nd Virial Coefficient (A_2) is a property describing the interaction strength between the particles and the solvent or appropriate dispersant medium.

- For samples where $A_2>0$, the particles 'like' the solvent more than itself, and will tend to stay as a stable solution.
- When $A_2<0$, the particle 'likes' itself more than the solvent, and therefore may aggregate.
- When $A_2=0$, the particle-solvent interaction strength is equivalent to the molecule-molecule interaction strength – the solvent can then be described as being a theta solvent.

1.4.2 Preparing materials, reagents and standards:

- Reagent: Ultra pure water
- Standard: Toluene solvent
- Cells: Disposable cuvettes (VWR International Co., Mississauga, ON)

1.4.3 Analysis procedure:

- Calibration: Build a curve with standard solution Toluene. The solvent must be filtered through 0.45μm filter.

- Preparing the samples. Five concentrations 2, 5, 10, 20 and 28mg/l of Toluene are prepared in 100-ml flasks.
- The samples are filled in the Disposable cuvettes (max. 15 mm), covered with caps and analyzed by Zetasizer Nano.

E.1.5 Isolation using XAD8/XAD4 resins

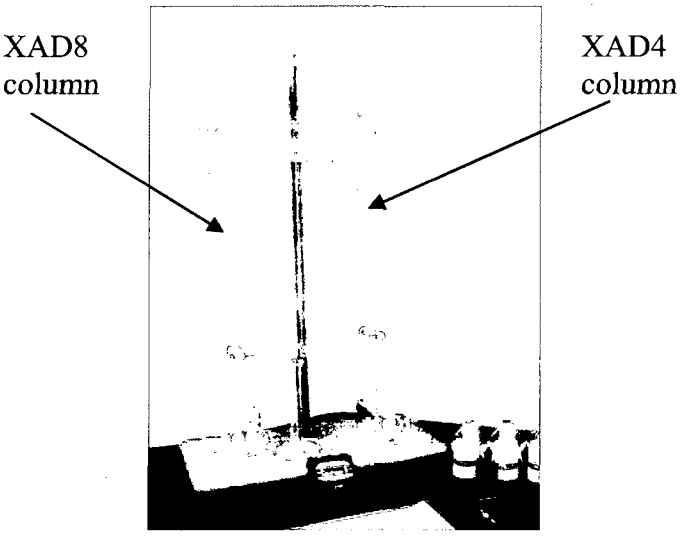

Figure E.7. XAD8 and XAD 4 columns

1.5.1 Method:

Hydrophobic, hydrophilic and transphilic fractions of NOM are isolated by using methyl methacrylate resins called XAD8 and XAD4. Those resins are packed in columns in series. The hydrophobic fraction which consists of large MW will be retained in XAD8 column. The transphilic fraction then is trapped in XAD4 column. The hydrophilic fraction is eluted from the effluent of the second column. TOC or UV of the feed, effluents after XAD8 and XAD4 column are recorded.

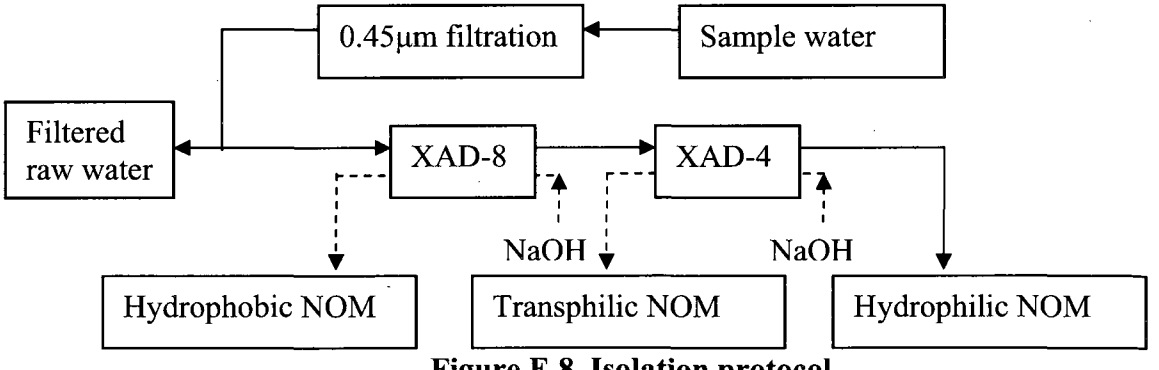

Figure E.8. Isolation protocol

1.5.2 Preparing materials, reagents and standards:

- Column: two 75cm length x 2.0 cm diameter glass columns
- Materials: Supelite XAD8 (Supelco, Bellefonte, PA), Amberlite XAD4 (Sigma-Aldrich, Milwaukee, WI)
- Reagents: Ultra pure water; 0.1N NaOH (Fisher Scientific, Hampton, NH); 0.1M HCl (Fisher Scientific, Hampton, NH)

1.5.3 Analysis procedure:

- Preparing column:

  + Clean the resin with methanol according to the manufacturers recommendations.

  + Rinse column with 0.1 N NaOH for ~1-3 hours.

  + Rinse column with five column volumes of hot MQ water between each sample.

  + Remove the column from the stand, secure a stopper at both ends and shake the column vigorously.

  + Rinse column once with MQ water and HCl acid

  + Run a sample of the MQ water and the effluent from the column through the TOC analyzer. The DOC of both should be the same. If the effluent has a higher DOC than the influent MQ water, repeat steps 3 and 4. Do this until the influent and effluent have the same DOC

- Procedure:

  + Obtain 350 ml of sample and vacuum filter with 0.45 μm to remove any precipitates, these would be humins. Store 50 ml for analysis (Named *Feed*)

  + Adjust the pH of a 300 ml sample to 2.0 with HCl. (01 drop of concentrated HCl)

  + Pass the sample of water through the column of XAD-8 resin (column 01)

  + Allow the first 100ml to go to waste. This portion is used only for eluting any remaining MQ water in the column.

  + Pass the remaining 200 ml of sample through the column 01 three times. Store 40 ml of them for analysis (Named *After XAD8*).

+ Pass the remaining 160 ml of sample through the column 02. Let the first 100 ml go to waste. Pass 60 ml of sample through the column 02 three times and then store for analysis. (Named *After XAD4*)

+ Elute the column 01 with 50 ml of 0.1M NaOH three times and collect (Named *Through XAD8*)

+ Elute the column 02 with 50 ml of 0.1M NaOH three times and collect (Named *Through XAD4*)

+ Conduct DOC and UV analysis of 5 samples *Feed, After XAD8, After XAD4, Through XAD8, Through XAD4* to determine the hydrophobic, hydrophilic and transphilic fractions.

E.2. Characterization of membranes:

E.2.1 Hydrophilicy

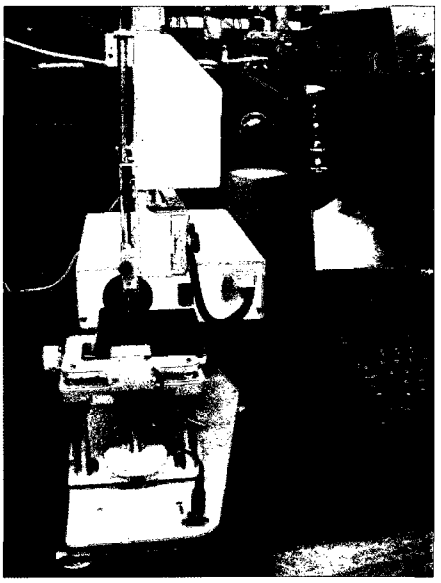

Figure E.9. VCA Optima goniometer

Method:

The hydrophilicity (contact angles) will be determined via a goniometer (VCA Optima, AST Products, Inc., Billerica, MA), which incorporates a digital camera and a computer controlled syringe pump. The contact angle is measured immediately after the sudden movement of the water drop by analyzing the

images taken by the camera and an automatic measurement program. The water drop volume ranges from 1.6 to 2.4 µl.

Preparing materials, reagents and standards:

- Reagent: ultra pure water
- Micro slides 25 x 75 x 1mm (VWR., Mississauga, ON)
- Syringe

Analysis procedure:

- The dry membranes are cut into 5 x 25mm pieces and fixed onto superfrost micro slides using electrical tape.
- Contact angles are measured using a goniometer. Repeat 5-6 times for each sample.

E.2.2 Pore property (Pore size, porosity)

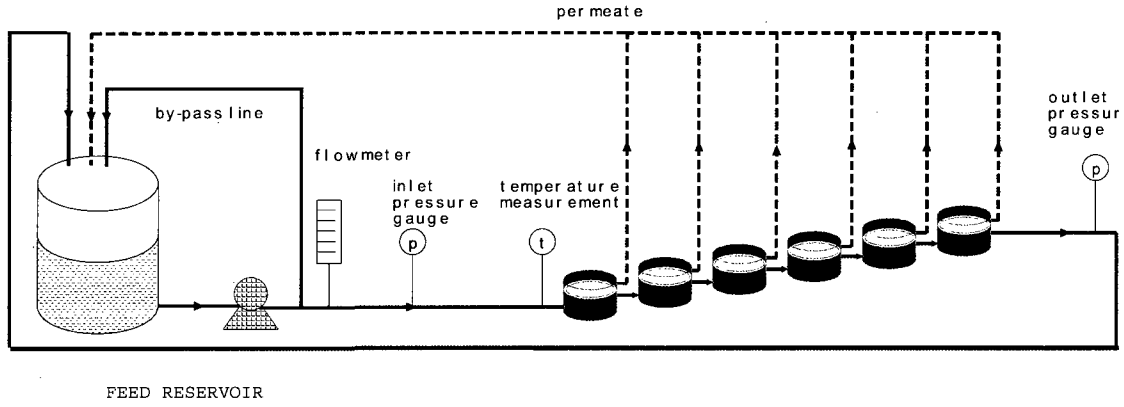

Figure E.10. System for Solute transport

2.2.1 Method:

Pore properties will be evaluated by solute transport method using different known molecular weights of polyethylene glycols (PEG) or polyethylene oxide (PEO) solutions. Those solutes are considered non-reactive, uniformly sized compounds that are theoretically not affected by adsorption, charge repulsion or other mechanisms since the removal mechanism is assumed to be solely size exclusion.

By plotting removal versus the size of solution, a sieving curve can be used to estimate the size of compound removed at 90%.

2.2.2 Preparing materials, reagents and standards:

- Standards: PEG and PEO (Sigma Aldrich, Milwaukee, WI)

2.2.3 Analysis procedure:

- The feed solutions are solutions of PEG with molecular weights of 10, 20, 35 kDal and PEO with molecular weight of 100 kDal. Their concentrations are approximately 100 mg TOC/L.
- The tests are run at 345 kPa (50 psig) pressure and room temperature (23±0.2°C). The feed and permeate samples are collected for TOC analysis.
- The membrane system is flushed with ultra-pure water for one hour after each PEG/PEO solution circulation.
- At the end of the hour the PWP rate is re-measured to corroborate that the solute transport tests had not altered the flux (i.e., fouled the membrane). The feed and permeate samples are collected and analyzed for total organic carbon (TOC).

E.2.3 Morphology (Roughness)

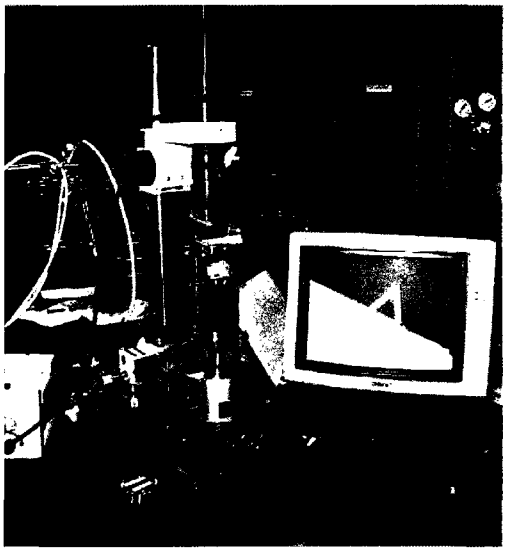

Figure E.11. AFM equipment

2.3.1 Method:

The roughness is determined based on Atomic Force Microscopy method AFM using a Nanoscope III equipped with a 1533D scanner (Digital Instruments, Gainesville, FL).

2.3.2 Preparing materials, reagents and standards:

- The tested membranes are cut into 0.5 x 0.5 cm pieces.

2.3.3 Analysis procedure:

Pieces of flat-sheet membranes are fixed over magnetic disks with two-sided adhesive tape. The laser beam of the AFM is focused on a pre-selected spot of the surface prior to the engagement of the cantilever. A tapping mode, AFM, in air is used to generate the AFM images.

E.2.4 Surface charge

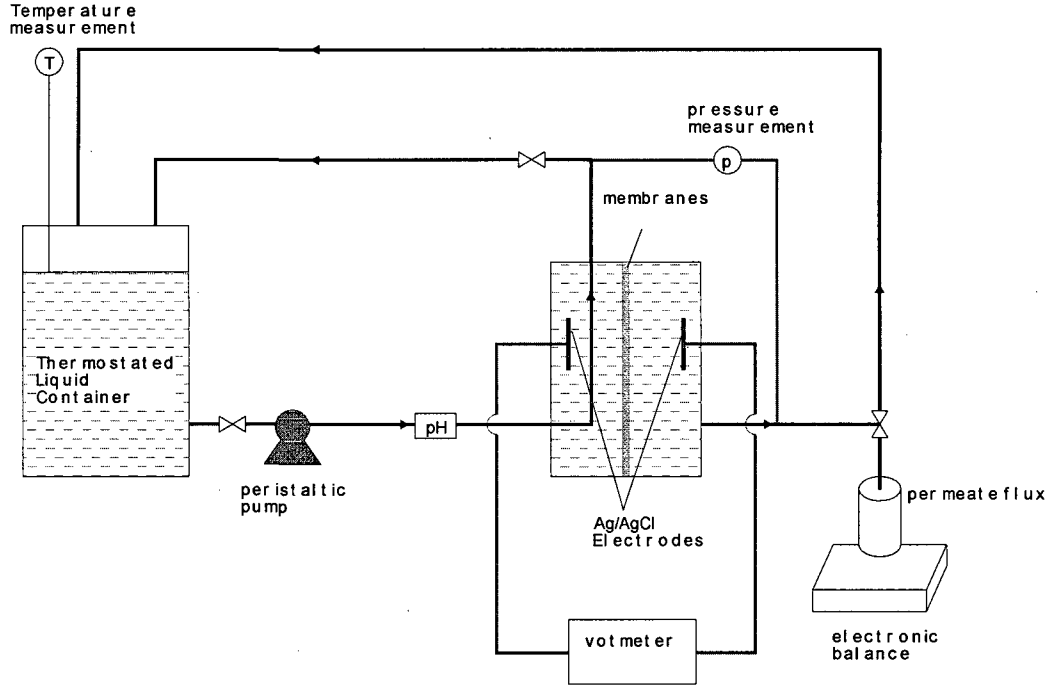

Figure E.12. System for Charge measurement

Method:

Zeta potentials are calculated from the relation of streaming potential versus differential pressure (Helmholtz-Smoluchowski equation):

$$\zeta = \frac{\Delta E}{\Delta p} \times \frac{\eta \kappa}{\varepsilon_o \varepsilon_r} \qquad [E.2]$$

Where ζ: Zeta potential

ΔE: streaming potential

ΔP: Pressure difference

η: viscosity of the permeate

κ: conductivity of the solution

ε_0:permittivity of the vacuum

ε_r: dielectric constant of the meadia

Its accuracy is ± 1.5mV (Nystrom, 1994)

Preparing materials, reagents and standards:

- Labview software (National Instruments, Austin, TX); Pressure transducer, thermocouple (Omega Technologies, Laval-STE Rose, QC); Peristaltic pump (Cole-Palmer Instrument Co., Mississauga, ON); UF Cell (GE Water & Process Technologies, Minnetonka, MN)
- Electrodes: Ag/AgCl electrodes are prepared via anodic deposition of chloride on silver from a 0.0001M HCl solution with a current density of 0.2 mA/cm2 (Ag/Pt electrodes). The electrodes are stored in 0.001M KCl solution overnight to prevent build-up of charge.
- Background Electrolyte: 0.001M KCl (Sigma Aldrich, Milwaukee, WI). Standard deviation of electrolyte concentration is smaller at low conductivity. Electrolyte is thermostated at 25°C.
- Thermostat, pressure sensor, pH probe, pump, electronic scale.
- Natural pH or pH = 3-6
- Pressure: 0.2, 0.4, 0.6, 0.8 and 1 bar (2.9; 5.8; 8.7; 11.6 and 14.5 psi)
- Temperature: room temperature
- Membranes

Analysis procedure:

- Preparation: A 0.001M KCl solution is circulated overnight at 0.2 bar to equilibrate the system. Membranes are put in a beaker containing KCl solution for 30 min before testing.
- Procedure: A minimum of 5 different pressures, ΔP, are applied and the streaming potentials, ΔE, are measured. The equivalent zeta potential can be deduced from the slope of ΔE vs ΔP plot.

For fouling membranes, membranes are fouled either by soaking in river water for two hours or running through ultrafiltration cell at 50 psi. Compare the differences.

- Effecting factors: pH (pH is adjusted with 0.1M NaOH and 0.1M HCl solutions), ionic strength (divalent ions), storage (dry or wet storage), different NOM concentrations (2, 5, 10mg/l, 20 mg/l and 28 mg/l are prepared in 200-ml flasks), different-base membranes

APPENDIX F

Manual of surface charge system

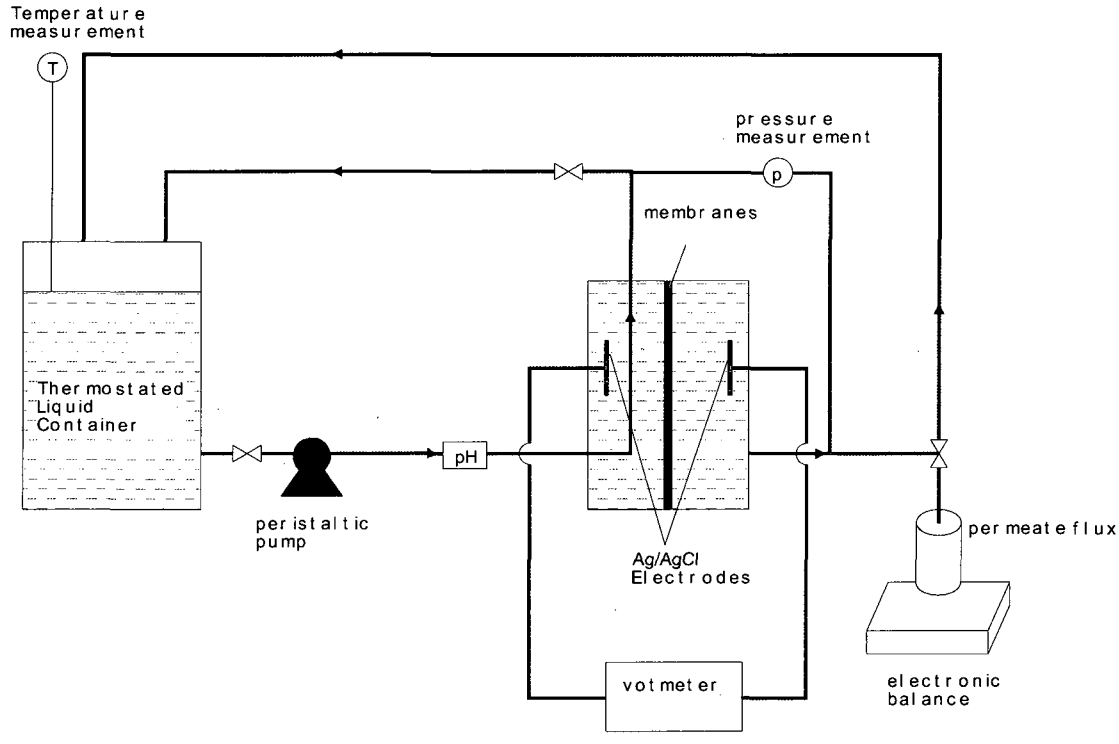

Figure F.1. Diagram of Zeta potential measurement system

F.1. Preparation:

F.1.1 Ag/AgCl Electrodes:

- Battery 1.5V
- Solution: 0.0001 M HCl
- Three silver wires
- Generation of electrodes: Silver/silver chloride (Ag/AgCl) electrodes are prepared using the battery 1.5V and HCl solution. Aligator clips were soldered onto the 1.5 V battery. The silver electrode (Φ=1.5mm, Aldrich, St. Louis MO) was attached to the positive side of the battery (working electrode) and another silver wire (reference electrode) is attached to the negative side. Both electrodes are immersed in the 0.0001 M HCl solution for 24 h. Under the current environment, Cl- moves toward and deposits onto working electrode. When the first working electrode is generated completely, it is taken off and the second working electrode is attached to the positive side. It is noted that the slower the Cl- deposition on Ag wires, the longer it stays.
- The electrodes are stored in a 0.5M KCl solutions until runs or between runs.
- After several runs (measurements) when the Cl-deposition is peeled off, the electrodes are cleaned by sand paper and MQ water and new electrodes are prepared following the above procedure.

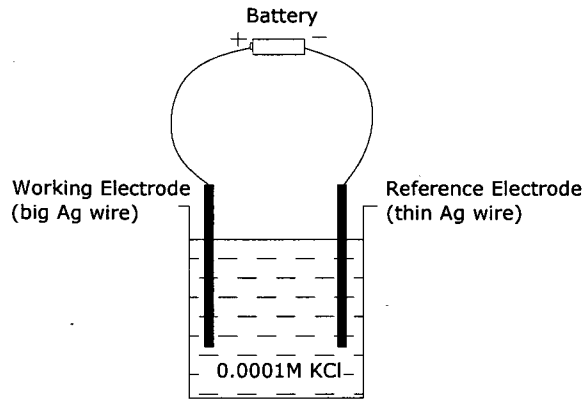

Figure F.1. Set-up for electrode generation

F.2.2 Electrolyte:

- 0.001M KCl solution: Mix 0.14912 g of KCl in 02 litres of MQ water

- *Note: The electrolyte reagent should be replaced every two samples because of increasing conductivity.*

F.3.3 pH Adjustment:

- Prepare 0.1M KOH and 0.1M HCl to adjust the pH ~7±0.5
- pH value of the electrolyte is shown on the Labview screen
- *Note: After experiment, make sure the pH electrode is filled with pH buffer of 7 to keep it out of drying.*

F.4.4 Temperature Adjustment:

- Prepare ice water or hot water (boiler) manually to adjust temperature of electrolyte to ~23±0.5
- Temperature value is shown on the Labview screen

F.5.5 Membrane preparation:

- Membranes are cut into coupons of 5cm diameter.
- Rinse membranes with MQ water, and then soak in 0.001 KCl for few hours.

F.6.6 Storage upon finishing:

- The Ag/AgCl electrodes should be stored in 0.001M KCl solution overnight to prevent build-up of charge.
- pH electrode should be stored in pH buffer of 7 to keep it out of drying.
- Put all chemicals (0.1M NaOH and 0.1M HCl) into the fridge.

F.2. Procedure:

- Check the electrodes if they are placed in the right order i.e., one before and one after the membrane sheet.
- Check if the computer recognizes the pH, temperature, pressure and streaming potential. If the values are abnormal (i.e., very high or negative), there must be a problem with the wire signals.

- Turn on the pump. Change the pressure by adjusting the dial on the pump to #0.5, 1, 1.5, 2.

Note: While increasing the pressure, make sure the pressure DOES NOT EXCEED 1 BAR (Max. 1 bar). Normally, the ideal operation pressure should be in the range of 0.1 – 0.6 bar.

- The thermostated electrolyte KCl is pumped from the container through the membrane. The difference in voltage (ΔE) between the silver chloride electrodes, placed on the feed and permeate sides of the membranes, is measured.
- A minimum of 5 different pressures, ΔP, are applied and the streaming potentials, ΔE, are measured.
- At each pressure level, record the charge when the pressure levels off (reaches constant condition). Time for pressure leveling depends on the types of membranes. It can be from several minutes to half an hour. Then, these measurements generate a set of data as shown in Table F.1.

Table F.1 Recorded streaming potentials

Pressure (bar)	Streaming potential (mV)
0	0
0.1	A
0.2	B
0.3	C
0.4	D
0.5	E

A-E: Values of streaming potentials

- Set up a spread sheet based on data from the table. Plot Pressure ΔP versus Streaming Potential ΔE. The equivalent zeta potential can be deduced from the slope of ΔE vs ΔP plot.

  Example: Slope = -40.722

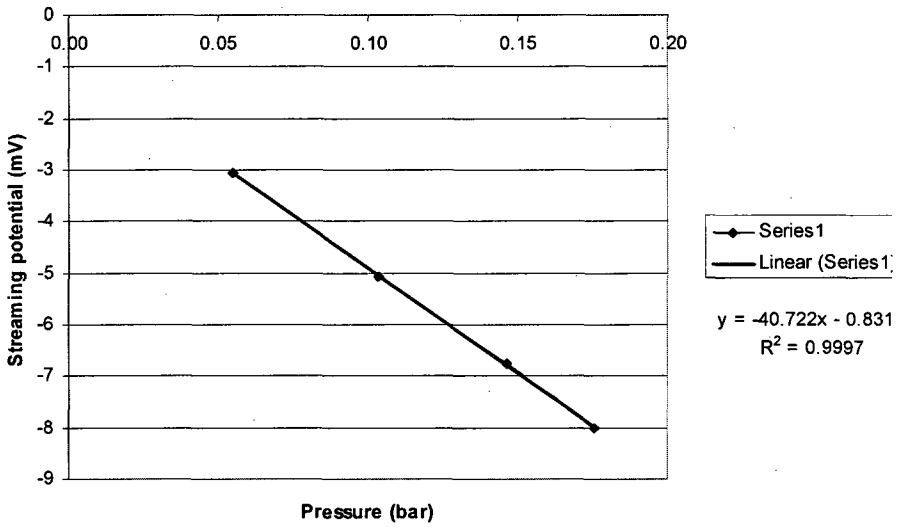

- Zeta potentials (ζ - mV) are calculated from the relation of streaming potential versus differential pressure (Helmholtz-Smoluchowski equation):

$$\zeta = \frac{\Delta E}{\Delta p} \times \frac{\eta \kappa}{\varepsilon_o \varepsilon_r}$$

Where η: viscosity of the permeate

κ: conductivity of the solution

ε_o:permittivity of the vacuum

ε_r: dielectric constant of the meadia

$\Delta E/\Delta P$: slope of the ΔE vs ΔP graph

Its accuracy is ± 1.5mV (Nystrom, 1994)

F.3. Calibration:

- Measure some charge-known membranes to calibrate the system before use.
- Reference membranes from the literature:

Membranes	Values of Zeta (mV)	Conditions
Zirfon membranes	0.8	pH6, 25°C, 0.001M KCl
Sulphonated PS 100kD	-19.8	pH6, 25°C, 0.001M KCl
Cellulose	-12	pH6, 23°C, 0.01M NaCl
Polyamide	-5	pH6, 23°C, 0.01M NaCl

PS 100kD Memtec	-3	pH6, 25°C, 0.001M KCl
PVDF, hydrophobic, 0.2mmm, Millipore	-4	pH6, 25°C, 0.001M KCl
PVDF, hydrophilic, 0.2mmm, Millipore	-22	pH6, 25°C, 0.001M KCl
PS 30kD Amicon	-16	pH6, 25°C, 0.001M KCl
PS 30kD Millipore	-12	pH6, 25°C, 0.001M KCl
PS 100kD Millipore	-17	pH6, 25°C, 0.001M KCl
Regenerate cellulose, 30kD, Amicon YM30	-2	pH6, 25°C, 0.001M KCl
Regenerate cellulose,100kD, Amicon YM100	-10	pH6, 25°C, 0.001M KCl
Polycarbonate, nuclepore, 0.2mmm	-18	pH6, 25°C, 0.001M KCl
PS 30kD, Millipore	-6.2	pH6, 30°C, 0.001M KCl
PS 100kD, Millipore	-7.8	pH6, 30°C, 0.001M KCl
PS 300kD, Millipore	-4	pH6, 30°C, 0.001M KCl
PS, 10kD	-22	pH6, 25°C, 0.001M KCl

Note: You can test some membranes that you have, but check their charges from the literature

F.4. Trouble shooting

F.4.1. If the membranes are porous and easy to break, use a low pressure range. It has been reported that the charges behave differently at low or high range of pressures. At low pressures, flow is through the larger pores, which give a more real estimate of the charge since the pores act as a channel where flow can not be disturbed. At high pressures, flow passes through the smaller pores, which may disturb the flow and alter the actual charge, negating some of the assumptions used to quantify charge.

F.4.2. If there is no response from the zeta potential (no data shown on the screen or it remains 213 mV), it is recommended to:

- run the system for at least a day at a constant pressure with membrane
- soak membrane in the electrolyte 0.001KCl solution

F.4.3. Failure to change the electrolyte and regenerate electrodes may lead to inaccurate readings.

APPENDIX G

Comparison of two contact angle analyzers (CAAs)

Two goniometers were compared in a study conducted by Camille Amelot, a French exchange student, under the instruction of the author. The first goniometer (C860 701) is an old style from Sherr Tumico, Germany. The water drop images reflected on the round glass plate are observed intuitively and contact angles are measured manually. The second goniometer is a VCA Optima (AST Products, Inc., Billerica, MA) which applies more recent technology. Water drop images are snapped by the inside digital camera and contact angles are automatically calculated by the Pendant drop software. Either of the two goniometers can be used for measurement of membrane hydrophobicity. This study aimed at comparing their precisions to have a better application.

G.1. Principles of measurement

G.1.1. Goniometer model C860 70 (Sherr Tumico, Germany) - Old CAA

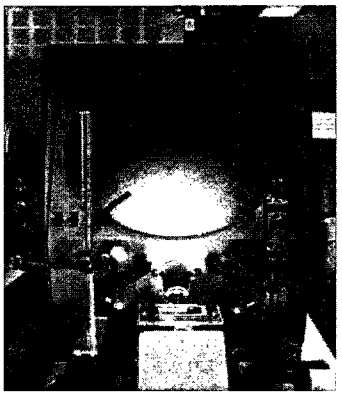

Figure G.1. *C860 70* goniometer

Step 1: Select membrane pieces and stick them on micro-slides.

Step 2: Place micro-slide on the supporting plate

Step 3: A syringe with full water is clamped above the micro-slide to place a water drop onto the membrane. Manually add water by pressing the syringe until the water drop starts expanding.

Step5: View the droplet clearly and turn the round glass plate so that the centre of round glass plate is on the left edge of water drop image (Figure G.2).

Step 6: Measure the contact angle θ

Step 7: For each micro-slide, repeat the measurement 3-4 times. Calculate the average angle θ.

Step 8: Repeat 3 times for each membrane.

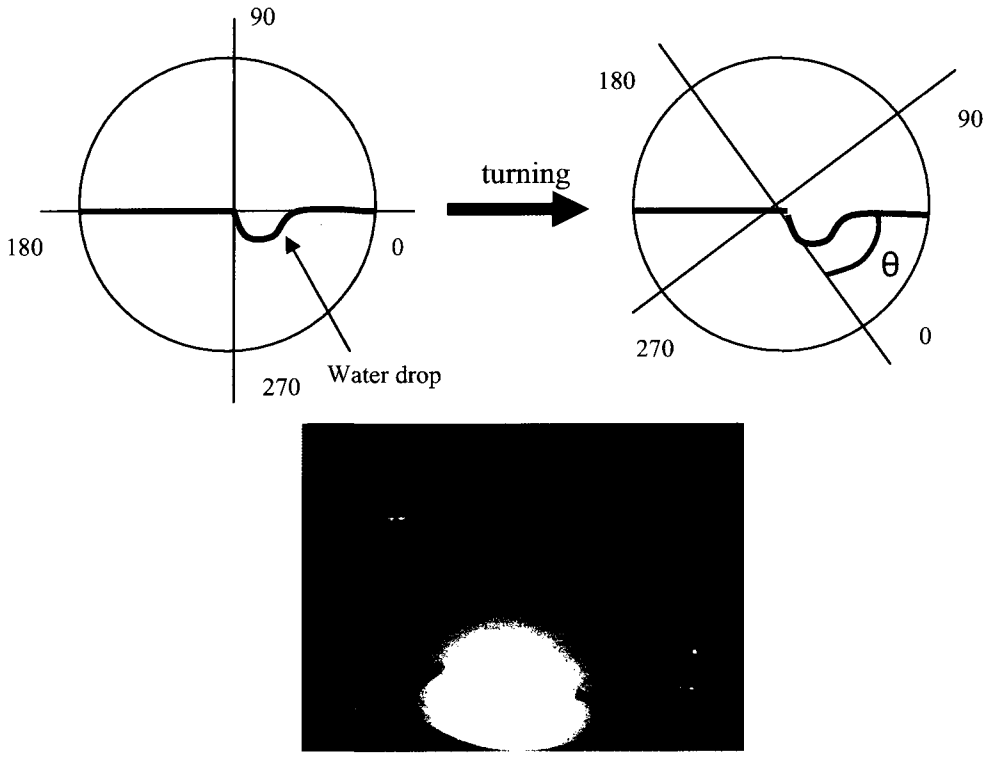

Figure G.2: Measure of contact angle

G.1.2. VCA-Optima (AST Products, Inc., Billerica, MA) – New CAA

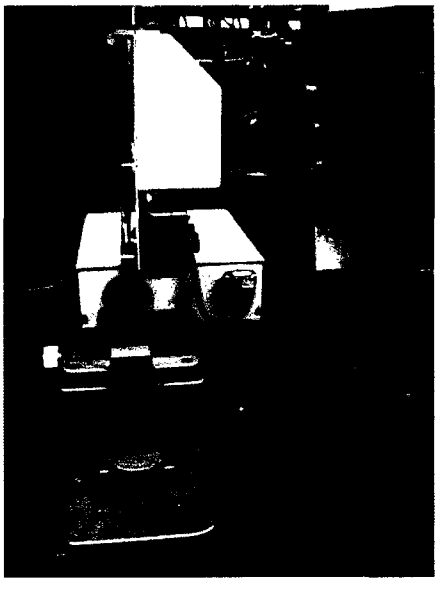

Figure G.3: VCA-Optima

Step 1: Select membrane pieces and stick them on micro-slides.

Step 2: Place micro-slides on the support plate

Step 3: A syringe with full water is clamped above the micro-slide to place a water drop onto the membrane. The volume of water drop ranges from 0.25 to 2.25μL. When the drop starts expanding, water addition is stopped.

Step 4: The average angle θ is automatically measured using the software (Figure G.4)

Step 5: For each micro-slide/membrane coupons,

repeat the measurement 3-4 times.

For each membrane sheet, randomly select at least 3 coupons at different places to be measured. The mean contact angle is the average of 9-10 measurements.

Note: High θ means that the membrane is more hydrophobic.

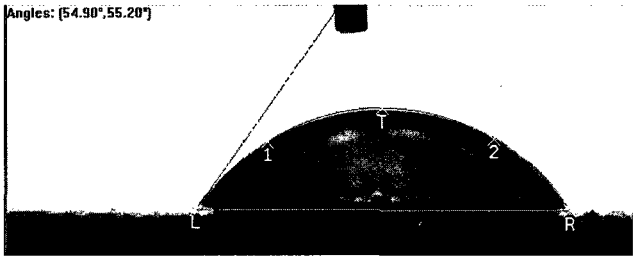

L: Left marker

R: Right marker

T: Top marker

1: Marker 1

2: Marker 2

Figure G.4: Measurement of water drop by a software

G.2. Results

Indeed, with the old CAA, it is difficult to produce a good drop and hard to control the drop volume. The VCA-Optima, on the other hand, produces a more precise volume of water drop. Moreover, more measurements can be done on one sample i.e., around fifteen measures per sample using VCA-Optima, while with the old goniometer only three or four measurements can be done per membrane sample.

Table G.1 presents the advancing contact angles analyzed by the two CAAs for 19 membranes. Interestingly, higher contact angle values were obtained via the new CAA for all cases except for sample No.5. The average deviation of each CAA is almost the same (4.5° for the new CAA and 4.4° for the old CAA). However the data difference between two CAAs is from 0 to 15.6°. The possible reason lies in the equipment itself. The new CAA seems to be more reliable and has been used widely in membrane research field. In case where the new CAA is not available, the old CAA can be used with at least five degree adjustment.

Table G.1: Comparison of advancing contact angles measured by two CAAs

No	Membranes	New CAA		Old CAA		Difference
		Average	Std	Mean	Std	Mean
1	0.5SMM-200-very fast	**91.6**	4.5	**83.2**	2.3	8.5
2	0.5SMM-250-very fast	**89.8**	2.5	**82.5**	1.6	7.3
3	1.5SMM-200-fast	**87.2**	4.6	**73.2**	5.5	14.0
4	1.5SMM-200-slow	**90.9**	3.7	**75.3**	6.7	15.6
5	1.5SMM-250-fast	**80.6**	7.5	**80.9**	1.6	-0.3
6	1.5SMM-250-slow	**89.6**	3.4	**84.7**	2.9	4.9
7	3SMM-200-fast	**85.5**	7.6	**73.0**	6.8	12.6
8	3SMM-200-slow	**86.0**	7.4	**74.1**	3.8	11.9
9	4.5SMM-200-slow	**91.6**	3.9	**82.0**	4.9	9.5
10	4.5SMM-250-slow	**84.9**	5.4	**83.5**	7.6	1.3
11	4.5SMM-200-fast	**85.0**	4.3	**75.3**	4.4	9.7
12	4.5SMM-250-fast	**96.1**	4.9	**81.5**	5.2	14.6
13	Double 3SMM	**86.4**	4.4	**80.6**	2.9	5.8
14	0.5LSMM-200-very fast	**67.4**	3.3	**60.2**	4.4	7.2
15	0.5LSMM-250-very fast	**72.9**	3.0	**65.0**	3.1	8.0
16	4.5LSMM-200-very fast	**72.0**	4.1	**63.9**	1.9	8.2
17	4.5LSMM-250-very fast	**69.3**	2.7	**59.4**	6.5	10.0
18	Double LSMM	**61.6**	4.9	**59.7**	5.2	1.9
19	Control PES	**69.5**	4.2	**58.8**	6.3	10.7
	Average		4.5		4.4	

Note: All membranes used PES as a base polymer. The abbreviation of membrane sample expresses: Concentration of additive-type of additive-film thickness-casting speed.

In the membrane modification field, the alternation of contact angles due to the incorporation of additives is of great concern. Tables G.2 and G.3 report the contact angle changes because of the addition of hydrophobic SMM and hydrophilic LSMM. Apparently, the new CAA shows a greater change in contact angle compared to the old

CAA as a result of blending the hydrophobic SMM into the membranes (Table G.2). Nevertheless, the opposite was observed for the hydrophilic LSMM membranes (Table G.3). The old CAA reported larger changes in contact angles associated with the addition of LSMM membranes (i.e., membranes are more hydrophilic).

Table G.2: Changes of PES-SMM membranes with control PES membranes

SMM membranes	SMM increase (^{0}) – new CAA	SMM increase (^{0}) – old CAA
0.5SMM-200-very fast	22.1	13.7
0.5SMM-250-very fast	20.3	13.0
1.5SMM-200-fast	17.7	3.7
1.5SMM-200-slow	21.4	5.8
1.5SMM-250-fast	11.1	11.4
1.5SMM-250-slow	20.1	15.2
3SMM-200-fast	16.0	3.5
3SMM-200-slow	16.5	4.6
4.5SMM-200-slow	22.1	12.6
4.5SMM-250-slow	15.4	14.0
4.5SMM-200-fast	15.5	5.8
4.5SMM-250-fast	26.6	12.0
Double 3SMM	16.9	11.1
	Prove more hydrophobic	Prove less hydrophobic

Table G.3: Changes of PES-LSMM membranes with control PES membranes

LSMM membranes	LSMM decrease(^{0})- new CAA	LSMM decrease(^{0})- old CAA
0.5LSMM-200-very fast	2.1	9.3
0.5LSMM-250-very fast	-3.4	4.5
4.5LSMM-200-very fast	-2.5	5.6
4.5LSMM-250-very fast	0.2	10.1
Double LSMM	7.9	9.8
	Prove less hydrophilic	Prove more hydrophilic

Given that the VCA manufacture claims the instrument has a precision of $\pm 0.1^{\circ}$, the much larger deviation obtained in those experiments may be a result of membrane variability and/or exaggerated claims by the manufacture.

In fact, only one CAA should be used to record the contact angle changes regardless of whether hydrophobic or hydrophilic additives are blended though. In our study, the VCA goniometer has been used consistently.

APPENDIX H

Contact angles as a function of drop age (time)

Chapter 5, section 5.4.2.2 has presented the change of contact angles as a function of time or drop age for all the tested membranes. This index indicates the absorbance or the wettability of membrane surface and will be discussed in details in this appendix.

H.1. Introduction and Procedure

If surface tension acting on solid, liquid, solid-liquid interfaces is balanced, it is said that thermodynamic equilibrium exists between the liquid and solid surfaces (Adam, 1964). However, if the surface is previously wetted (Adam, 1964) or the surface roughness is increased (Johnson and Dettre, 1964), there is a contact angle hysteresis. Also it was reported that the wettability is time dependent with a tendency to progress from the hydrophobic to the hydrophilic state. When the membranes are completely wet, the contact angles reach zero eventually.

To evaluate the absorbance or the wettability of membrane surface, it is necessary to capture a sequence of images during the interaction between a water drop and membrane surface. In this study, 12 frames of drop images were recorded automatically within a minute by the camera installed in the VCA Optima goniometer and controlled by Pendant drop software.

Table H.1. Typical report from the program for each measurement:

Capture time (sec)	Left angle (°)	Right angle (°)	Width (mm)	Height (mm)	Area (mm^2)	Volume (µl)
0	67	65.6	1.706	0.569	2.285	0.745
10	67.5	65.9	1.706	0.562	2.286	0.729
20	66.4	64.9	1.706	0.559	2.285	0.729
30	66	64.7	1.706	0.554	2.285	0.719
40	66.5	64.5	1.706	0.55	2.285	0.711
50	64.1	62.9	1.713	0.547	2.306	0.704
60	65.5	63.9	1.706	0.542	2.286	0.697
70	63.9	63	1.706	0.539	2.286	0.689
80	64.7	63.3	1.698	0.535	2.265	0.683
90	64	61.8	1.706	0.534	2.285	0.685
100	64.2	62.5	1.698	0.53	2.265	0.675
110	63.7	61.7	1.706	0.53	2.286	0.677
Mean	65.292	63.725	1.705	0.546	2.284	0.704
Stdev	1.353	1.411	0.004	0.013	0.011	0.023

Based on Table H.1, the volume of water drop is seen to decrease with capture time, so the water seems to be absorbed into the membranes.

H.2. Results:

The change of contact angles as a function of time/drop age was determined for membranes with and without LSMM addition (Figure H.1 and Figure H.2)

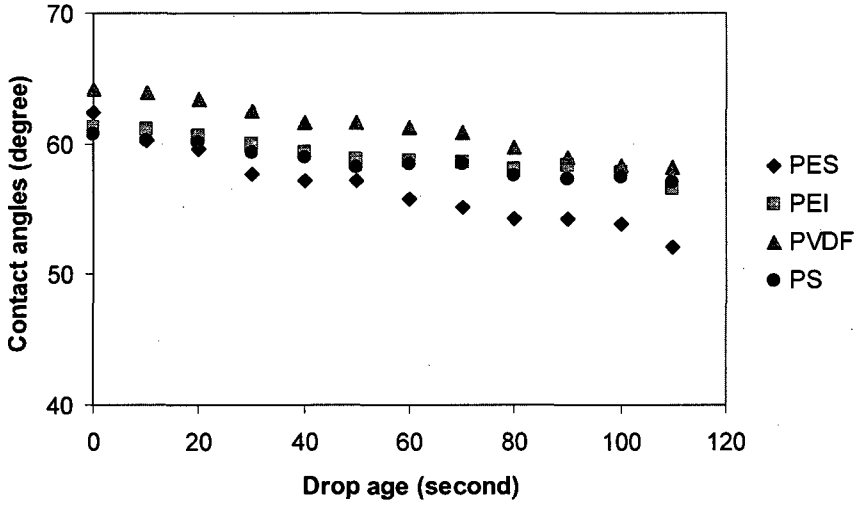

Figure H.1. Control membranes (without additives) of different base polymers

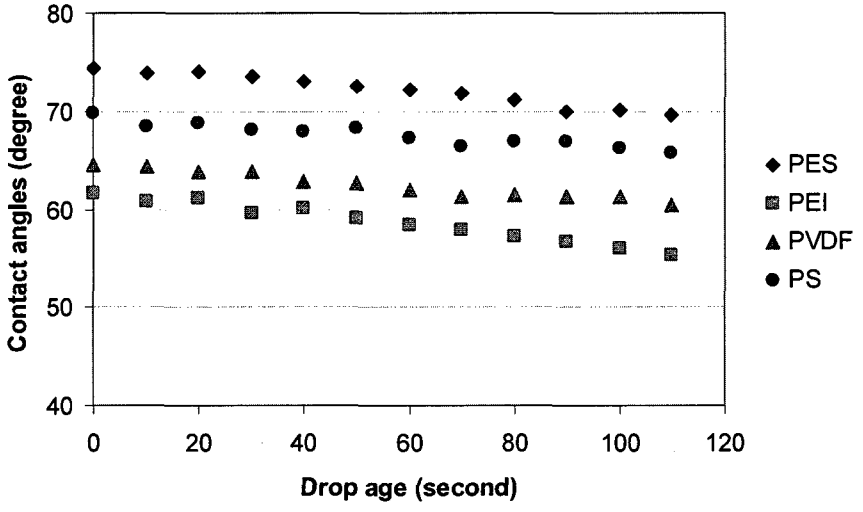

Figure H.2. LSMM membranes (with 3.0% wt of LSMM additive) of different base polymers

Interestingly the evolution of water drops for PEI and PS control membranes is the same but differs a bit from PVDF and especially PES membranes. It means that the PES

membranes might be wetter than the others. Data of advancing contact angles however shows that the four membranes statistically have the same hydrophobicity (same advancing contact angles – Chapter 8). The control PES membranes may possibly be a more absorbent material as they have the largest drop in contact angle (Figure H.1).

Incorporation of the hydrophilic LSMM seems to significant alter the water absorbance with time even thought only PEI and PVDF membranes became more hydrophilic. Obviously, the PVDF-LSMM and PES-LSMM membranes become less susceptible to absorbance. Unfortunately, roughness data is not available to elucidate better this response.

More observations about the evolution of the water drop as a function of drop age are discussed in Chapter 5.

APPENDIX I

Effect of drying methods on hydrophobicity measurement

I.1. Drying methods

To measure the contact angles or membrane hydrophobicity, the membranes need to be dried. There are several techniques can be used for drying membranes. In this study, three methods of drying have been employed: a chemical drying with ethanol solvent, a physical drying in an oven at 75°C, and a natural drying. The objective of this study is to explore the impact of drying methods on contact angle measurements.

- Chemical drying method: Pieces of membranes were sequentially submerged in four ethanol/water solutions (25, 50, 75 and 100% w/w ethanol) to exchange with the water from the membranes. The soaking in each of these solutions lasted at least 6h. Afterwards, each membrane sheet was placed between filter papers at room temperature so that ethanol can be evaporated, resulting in dry membranes.
- Physical drying method: Membrane samples were basically put in an oven at 75°C for at least two days until the weight of dry membranes were unchanged.
- Natural drying method: This is the simplest way in which each membrane sheet was placed between filter papers to dry at room temperature for 7 days.

These three different drying methods have advantages and disadvantages which are given in the Table I.1.

Table I.1: Advantages and Disadvantages of the different drying methods (studied by a French exchange student)

Methods of drying	Physical	Chemical	Natural
Advantages	- water in membranes is evaporated significantly - higher contact angles - short time (2 days)	Water in membranes is exchanged with ethanol	- Neither power nor chemicals are used - Inexpensive and easy
Disadvantages	- use energy - membranes become wrinkled or stuck to the tray due to the heat	- use chemicals - long time (~8 days)	- long time (7days)

Figure I.2 represents the advancing contact angles of the membranes with and without LSMM for the three methods of drying. It is clear that LSMM has not a real effect on the surface of the membrane statistically. Indeed, the contact angles are approximately the same with and without the additive. There is a lot of incoherence of these values. For example, there was a decrease of the contact angles between the control PVDF membrane and the PVDF membranes with LSMM 0.5% when the natural drying method was used but no change was observed between them when physical drying method was applied.

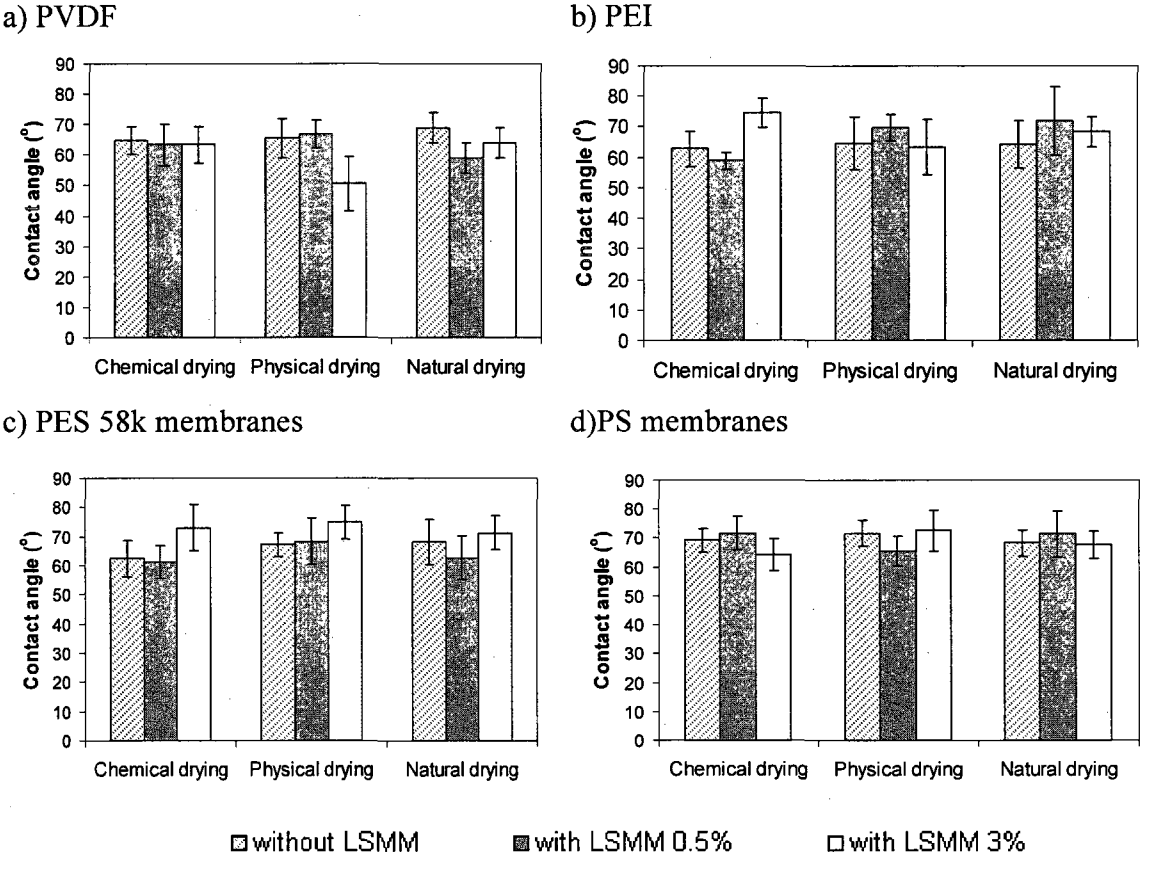

Figure I.1: Advancing contact angle for each polymer as a function of the different drying methods

I.2. ANOVA statistical analysis

To confirm the observation from previous section, a statistical analysis was conducted. First, membranes dried by the same method (e.g., chemical drying method) were analyzed to assess the impacts of base polymers (PES, PEI, PS and PVDF) and concentration of LSMM additive (0 wt%, 0.5 wt% and 3.0 wt%). Table I.2 shows the

statistical analysis for responsive contact angle with two variables (base polymers and %LSMM) using ANOVA-two way model.

Table I.2: ANOVA-two way model for contact angles

Source	DF	SS	MS	F	P*
Main effects					
Base Polymers (A)	4	686.6	171.7	6.73	***0.003***
%LSMM (B)	2	136.7	68.4	2.68	0.101
Interaction					
A x B	8	502.7	62.8	2.46	0.063
Error	15	382.8	25.5		
Total	29	1708.8			

**If P≤0.05, the effect is significant*

It is found that for the same drying method (i.e., chemical drying), only base polymers have impacts on contact angle (P=0.003, ≤0.05). The addition of LSMM concentrations is statistically not important.

The impact of drying methods is illustrated in Table I.3 using the Balanced ANOVA-Mixed model. The condition of this model is that: three factors (base polymer, drying method and LSMM concentration) are crossed; one factor base polymer is random; and the other two (%LSMM and drying method) are fixed. The base polymer is chosen random since the number of levels of base polymer is the highest (4 types of polymers) whilst there are only three levels for drying method (chemical, physical and natural methods) and only three levels for LSMM concentration (0 wt%, 0.5 wt% and 3.0 wt%). Results would be a bit different if other factor is chosen. According to Table I.3, base polymer is the only main effect on the contact angles. Nevertheless, the Balanced ANOVA-Mixed model provides a more complex analysis regarding the interaction of three variables (not two variables as in ANOVA-two way model). As seen in the results, P values are less than 0.05 for the (Base Polymers x Drying methods) and (Base Polymers x Drying methods x LSMM concentration) interactions. Analytical interpretation (from the model) renders that if the 3-factor interaction is significant, any lower order interactions and main effects involving terms of the significant interaction are not considered meaningful. This means contact angle is actually affected by all three

factors. Figure I.2 depicts a comprehensive understanding via interaction of three main effects.

Table I.3: Balanced ANOVA-Mixed model for contact angles

Source	DF	SS	MS	F	P
Main effect					
Base Polymers (A)	3	414.28	138.09	7.56	***0.000***
Drying methods (B)	2	64.11	32.05	2.06	0.209
LSMM conc. (C)	2	27.26	13.63	0.19	0.833
Interaction					
A x B	6	93.46	15.58	0.85	0.539
B x C	4	153.13	38.28	0.68	0.622
A x C	6	435.10	72.52	3.97	***0.004***
A x B x C	12	679.79	56.65	3.10	***0.004***
Error	36	657.81	18.27		
Total	71	2524.95			

**If P≤0.05, the effect is significant*

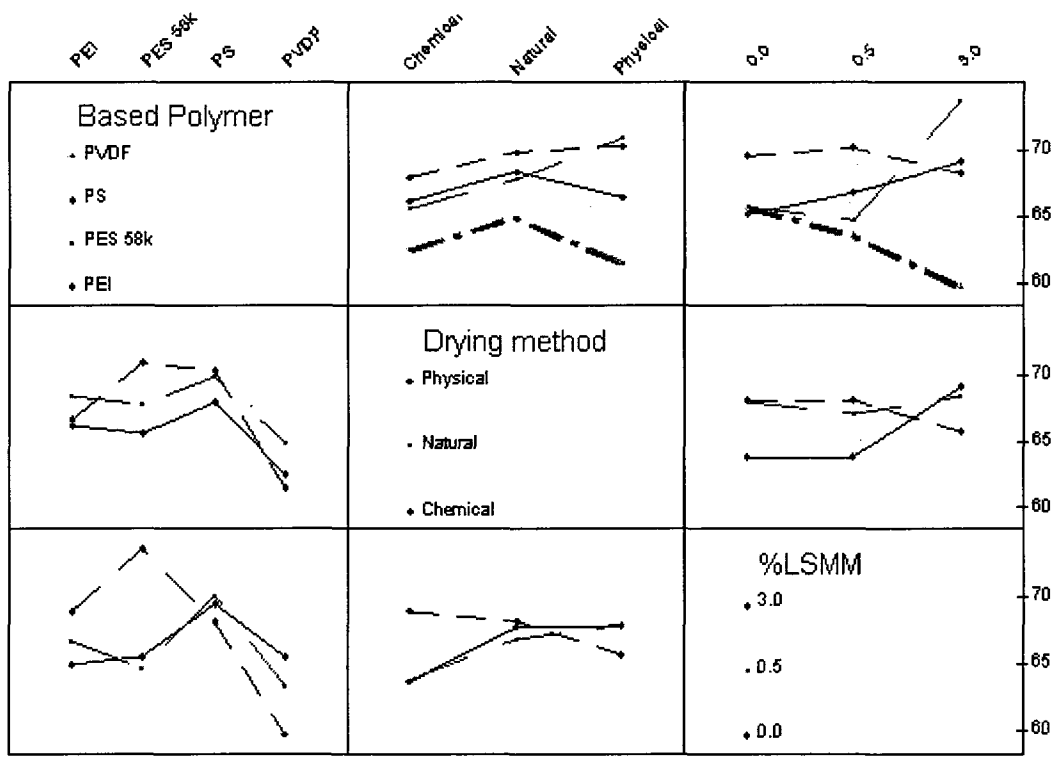

Figure I.2: Interaction Plot

Even though there is some evidence of the effect of drying method on contact angle (as shown in Table I.3), the analytical analysis does not show which one has the best impact. It should be noted that if drying method or LSMM concentration is chosen as random factor for the Balanced ANOVA-Mixed model, there is no significant effect shown for these two factors on contact angles. The natural drying method, which is the easiest and cheapest technique, thus can be safely applied to dry membranes for contact angle analysis.

APPENDIX J

Impacts of chemicals and protocols on cleaning tight UF membranes

The chemicals, protocols, test cells, cleaning frequency and tested membranes for the cleaning of tight UF membranes are described in details in Chapter 3, section 3.8. Chapter 7 has presented the impacts of test cells, cleaning frequency and membrane types. This appendix, therefore, solely shows the effects of the remaining factors such as cleaning chemicals, cleaning protocols and the impact of additive incorporation.

J.1. Effect of chemicals

Impact of chemical cleaning on functional properties of PES membranes has been investigated extensively by Arkhangelsky et al. (2007). They reported that higher dosages of cleaning agents in the first step resulted in complete restoration of the initial flux but led to more severe fouling, thus requiring higher cleaning frequency. In addition, the bonding character between the foulant and membrane surface changes between suspended and adsorbed stages. The reason was that hypochlorite treatment dislodged the PVP component from the membrane matrix, causing decreases in contact angle and flux values and an increase in pore size. Accordingly, each successive cleaning of the PES surface led to increasingly severe fouling and more significant flux drops. The chlorine treatment of PES membranes led to enlarged pore sizes as depicted by AFM, and more charged membrane as depicted by streaming potential measurement. This was explained by the partial scission of the C-S bond which decreased the polymer integrity. The microscopic changes in polymer structure were well pronounced at macroscopic levels. The mechanical strength of chlorine-cleaned membranes became lower as the total chlorine concentration increased. Similarly, Qin et al. (2005) reported a five-fold increase in membrane flux and a narrowed pore size distribution after the hypochlorite treatment. Thominette et al. (2006) also reported a decrease in elastic elongation of PES membranes exposed to hypochlorite solution.

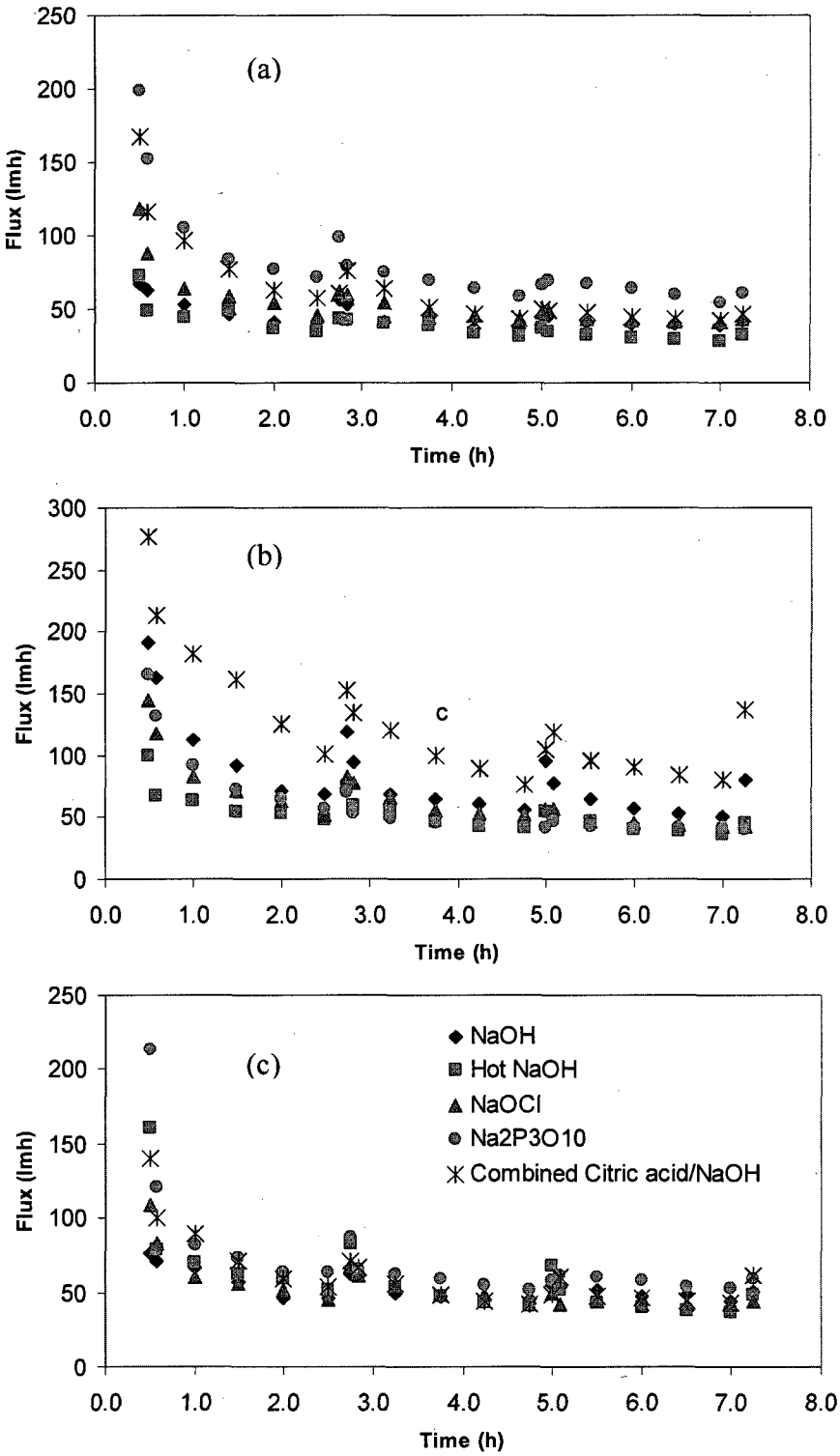

Figure J.1: Three-cycle flux performance with different cleaning chemicals for (a) PES, (b) PES PU and (c) PES-LSMM

The experiments in this appendix evaluated the impact of three cleaning cycles using a number of cleaning agents for three types of PES membranes: the commercial PES PU membranes, the experimental control PES membranes and the experimental PES-LSMM membranes. ORW was used a feed water for the filtration tests.

Figure J.1 illustrates that the optimal chemical for cleaning clearly depends on the type of membranes. Sodium tripolyphosphate appears best for the control PES membranes. A combination of citric acid and NaOH solutions apparently is most effective for commercial PES PU membrane. All chemicals perform similarly on the modified PES-LSMM; the most promising chemical for these modified membranes is probably sodium tripolyphosphate.

This study reconfirms that the commercial membrane is most effectively cleaned by the combined method. For the experimental membranes, the sodium tripolyphosphate is most effective. Chlorine group or high pH did not benefit the tailored/experimental membranes.

J.2. Effect of protocols

Table J.1 summarizes the flux recovery of the three membranes after different cleaning protocols.

Table J.1: Flux recoveries of experimental and commercial membranes after cleaning

Cleaning method	Control PES		PESPU		PES-LSMM	
	Mean	*Std*	*Mean*	*Std*	*Mean*	*Std*
BW only	**83.09**	28.53	**82.10**	21.05	**80.61**	11.09
BW and NaOH	**129.38**	19.30	**108.41**	14.90	**106.15**	15.09
BW with hot water	**88.44**	28.08	**69.58**	12.54	**98.54**	11.85
Cross-flushing	**68.10**	23.51	**69.41**	21.70	**70.35**	22.98
Chemical only (NaOH)	**85.72**	8.04	**75.45**	11.29	**87.21**	7.27

It is worth noting that the fouled membranes were not completely recovered during any of the cleaning tests. In other words, NOM deposited on the membrane surface could not

be entirely removed without scrubbing (physical removal). This was concluded by visually examining the membranes after each cleaning protocol.

In all cases, flux does not recovery fully following backwashing; however backwashing in combination with chemical cleaning can achieve up to 130% flux recovery. It is possible that the backwashing or cross-flushing (physical actions) only removes the reversible fractions of NOM from membrane surface while the chemicals would clean the adsorbed fractions. Combining the two methods would mostly "refresh" the membranes. Without physical cleaning, which partly dislodges the bulky NOM solutes on the membrane surface, the chemical itself can not completely clean the foulants. If cleaning only consisted of backwashing, the post-cleaning flux was greater for the control PES membrane, presumably because of its larger pores.

J.3. Effect of the modifying additive LSMM

The impact of additive was evaluated by comparing the net water production (P_{water}), an indicator of good membranes:

$$P_{water} = \int_{t_0}^{t_f} J(t)dt - J_{wf} \times \Delta t_c \qquad [J.1]$$

Where: P_{water}: net water product (L/m^2)

$J(t)$: flux as a function of time ($L/m^2/h$)

t_o: initial time of the fouling experiment (h)

t_f: time at the end of fouling test (h)

Δt_c: time period for cleaning (h)

($J_{wf} \times \Delta t_c$): flux loss due to cleaning

In most cases, Δt_c was 25 minutes (the sum of 10 min for BW and 15 min for chemical circulation). In case of short fouling duration (30 min), Δt_c was shorter, 15 minutes, with only 5 min for chemical cleaning.

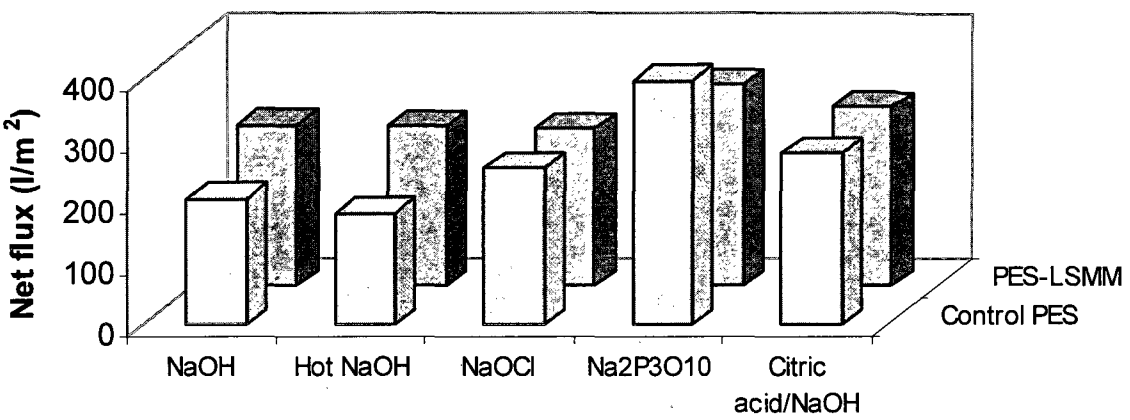

Figure J.2. Impact of modifying additive on net water production (L/m^2) with different cleaning chemicals

Figure J.2 presents the net water product for the PES membranes with and without LSMM. In most cases using different chemicals, the addition of LSMM increased the water production. Interestingly, the sodium tripolyphosphate reagent achieved the highest average net flux for both types of membranes, followed by the combined acid citric and NaOH. The cost of using sodium tripolyphosphate was reasonable, thus it could be considered as PES membranes are used.

APPENDIX K

Empirical modeling

In analysis, a descriptive model of the system can often be built as a hypothesis of how the system could work or try to predict how an unforeseeable factor could affect the system. A mathematical model uses mathematical language to describe a system by a set of variables and a set of equations that establish relationships between the variables. Two types of empirical modeling were used in this research to describe the fouling phenomenon occurring on membrane surface: Fouling Resistance Modeling and Fouling Mechanism Modeling.

K.1. Fouling Resistance Modeling

According to the first modeling approach, fouling can be quantified by the resistance appearing due to formation of cake or gel layer on membrane surface during the filtration and the resistance removal can be determined via cleaning (Madaeni et al., 2001, Munoz-Aguado et al., 1996). The flux (J) through the cake and membrane can be described by Darcy's law:

$$J = \frac{\Delta P}{\mu R_t} \qquad [K.1]$$

Where J: solute-containing water flux ($l/m^2/h$)

ΔP: transmembrane pressure (N/m^2)

μ: viscosity of water at temperature T (Ns/m^2)

R_t: total resistance (m^{-1}), may include the effects of membrane itself, solute adsorption, gel formation, cake formation, etc.

$$R_t = R_m + R_f \qquad [K.2]$$

Whereas R_m membrane resistance. This index refers to the resistance of membranes with pure water only.

$$R_m = \frac{\Delta P}{\mu J_{wo}} \qquad [K.3]$$

J_{wo}: Initial flux with pure MQ water ($l/m^2/h$)

R_f: resistance appears after fouling with solute-containing water

$$R_f = \frac{\Delta P}{\mu J_{wf}} \quad [K.4]$$

J_{wf}: flux at the end of fouling test period (L/m^2/h)

Residual solute resistance of the fouled membranes $R_{sw} = \frac{\Delta P}{\mu J_{wf}} - R_m$ [K.5]

Residual solute resistance of the cleaned membranes $R_{sc} = \frac{\Delta P}{\mu J_{wc}} - R_m$ [K.6]

Where J_{wc}: Pure water flux after cleaning test (l/m^2/h)

Flux recovery is a method for quantification of cleaning efficiency:

$$FR = \frac{J_{wc}}{J_{wo}} x100\% \quad [K.7]$$

Solute resistance removal is another method for this evaluation and can be estimated from:

$$RR = \frac{R_{sw} - R_{sc}}{R_{sw}} x100\% \quad [K.8]$$

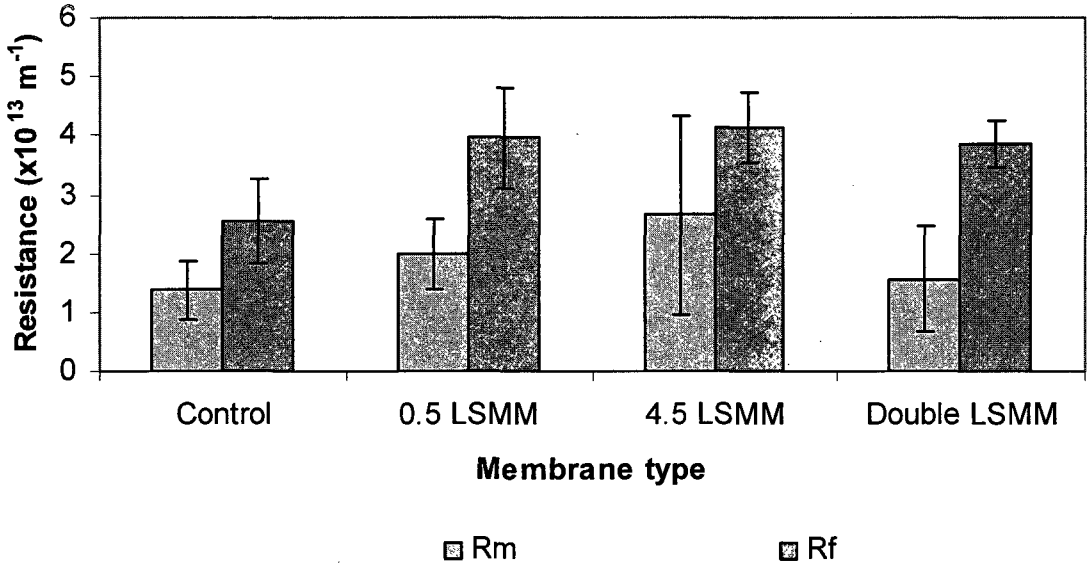

Figure K.1. R_m and R_f of PES-LSMM membranes

Figure K.1 depicts the resistances of PES-LSMM membranes and the control (without blending the additive LSMM). Statistically, the membrane resistances are the same for membranes with or without LSMM. The solute resistance seems however stronger for the

modified LSMM membranes mostly because the incorporation of LSMM made the pore size smaller.

The effect of different testing apparatus was one of this thesis objectives and its results have been presented in Chapter 7. This appendix only summarizes and compares the cleaning efficiency (4-hour cleaning interval) using equations derived from the above model.

Table K.1. Effect of different testing apparatus on flux recovery and solute resistance removal

	Stirred UF cell	SEPA cell	Single CF cell	CF cells in parallel
Rm	4.26±0.07	3.53±0.82	3.03±0.71	3.57±0.16
Rsw	11.32±2.51	8.13±1.92	12.09±4.30	27.90±11.96
Rsc	0.50±0.47	1.04±0.02	1.14±0.11	3.49±0.41
RR	95.55±3.17	87.21±2.78	90.58±2.27	87.50±3.54
FR	89.43±8.93	77.26±4.33	72.66±2.65	50.58±1.84

With the same membrane (commercial PES PU), the residual solute resistances were slightly dissimilar for different kinds of test cells due to the cell designs. Considerable evidence for cell effect was observed in resistance removal and flux recovery. However, from a statistical point of view, the SEPA cell and single CF cell performed similarly.

K.2. Fouling Mechanism Modeling

General fouling equation

To study the mechanisms leading to membrane fouling, the common practice consists of assuming that one of the four fouling mechanisms (e.g., cake formation, intermediate blocking, pore constriction (standard blocking) and complete blocking) takes place. The differential rate laws corresponding to all possible fouling mechanisms were proposed by Hermia (1982) for dead-end filtration under constant applied pressure:

$$\frac{dJ}{dt} = kJ(J)^{2-n} \qquad [K.9]$$

Where k is a fouling coefficient and n is a dimensionless filtration constant, which depends on the type of filtration. n has values of 0, 1, 1.5 and 2 for cake filtration, intermediate blocking, standard blocking and complete blocking, respectively.

Single mechanism

The filtration experiments in this study however used cross-flow mode filtration. Cross-flow mode has been claimed to enhance mass transfer processes that induce back transport from the membrane surface, leading to lower net flux of foulant to the membrane surface (Kilduff et al., 2002). The unifying equation for cross-flow filtration applied in this study was:

$$\frac{dJ}{dt} = -k(J - J^*)(J)^{2-n} \qquad [K.10]$$

Where J* is a critical flux and n can take the same values as in equation [K.1]

Determination of k, J* with corresponding n was performed using MATLAB 7.0 (Math Works, Natick, MA).

Table K.2 presents the regressed model coefficients as well as the mean square residual (MSR). It appears that the best fitted (i.e., has the lowest MSR) mechanism varies for every single case. Mosqueda-Jimenez et al., (2006) on their study using the same feed water found that cake formation was the best fitted model which was definitely not true for this case. The difference likely arose from the difference in membranes tested and testing protocols.

Table K.2: Fitting parameters for single fouling mechanism model

	n	k	J*	MSR
PES - 0.5LSMM				
	0.0	0.0001	45.3169	4.0400
	1.0	-0.0004	10.0524	1.8932
	1.5	-0.0184	50.4742	0.2712
	2.0	-0.1083	45.9350	0.8980
PES - 0.25nSMM				
	0.0	0.0009	6.9391	0.4376
	1.0	-0.0017	2.4673	0.4177
	1.5	-0.0362	6.5900	0.3281
	2.0	-0.0379	6.4376	0.4286
PES - 0.5nSMM				
	0.0	0.0003	6.3364	1.0663
	1.0	-0.0211	10.5017	0.5231

	1.5	-0.0185	10.6172	0.9807
	2.0	-0.2672	10.5195	0.5843
PES - 1.5nSMM				
	0.0	0.2957	1.6436	0.4681
	1.0	0.0045	3.4272	0.6870
	1.5	-0.0612	1.5849	0.3584
	2.0	-0.5279	1.7952	0.0515
PES - 3.0nSMM				
	0.0	0.0052	2.8620	2.0494
	1.0	-0.0067	2.1613	1.9776
	1.5	-0.0566	2.4426	2.8842
	2.0	-0.0157	0.0952	1.3758
PES - 4.5nSMM				
	0.0	0.1062	1.2006	0.0114
	1.0	-0.0838	1.2260	0.0067
	1.5	-0.1141	1.3028	0.0089
	2.0	-0.1632	1.2480	0.0089

Two examples of data fitting are shown in Figure K.2, where the blank circles represent the experimental data while the lines represent the fit curves for different fouling mechanisms.

It is observed that good fit came along with smooth curve of data. The flux performance of 0.5% LSMM, 3.0% SMM and 0.25% SMM modified membranes was not decreased evenly, resulting rather high MSR. For the case of 4.5% SMM, the data responded smoothly, so the best fit was obtained easily and perfectly. It is worth noting that the values of J* which is the critical flux were close to the final fluxes after 50-hour testing period. In addition, when the degree of fouling became more serious (from n=0 to n=2), the fluxes often decreased more slowly and k were observed decreasingly. In other words, the smaller values of k represent less dramatic flux decline. It was confirmed in several studies (Kilduff et al., 2002; Mosqueda-Jimenez et al., 2006).

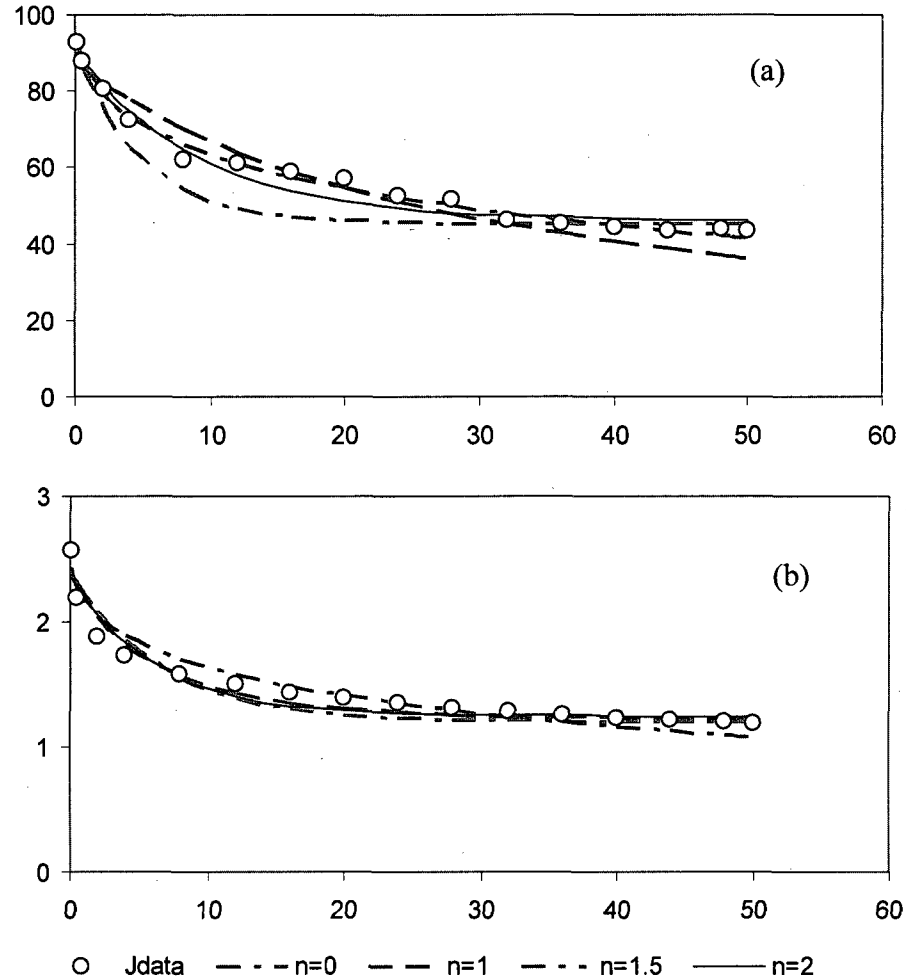

Figure K.2. Flux reduction with time for different single mechanism model. (a) Modified membranes with 0.5 wt% LSMM, (b) Modified membranes with 4.5 wt% SMM

Increasing concentration of SMM affected the fouling mechanism since the best fit model changed without a clear pattern. Although the data was not fully analyzed for all the cases, however between 0.5 SMM and 1.5 SMM (as shown in Figure K.3), increasing concentration of SMM led to smaller mean pore sizes, thus the chances of pore constriction or completely blocking were higher. In addition, the MWCOs of PES-3.0 nSMM and PES-4.5nSMM membranes were from 3.5-5 kDal with mean pore sizes are less than 0.5nm. The loose NF membranes often have MWCOs ranging from less than 1 kDal to several kDal for the treatment of drinking water (Wang et al., 2009). So they can be considered as loose nanofiltration (NF) membranes, for which the major fouling mechanism was found to be intermediate or complete blocking (Bodzek et al., 2002).

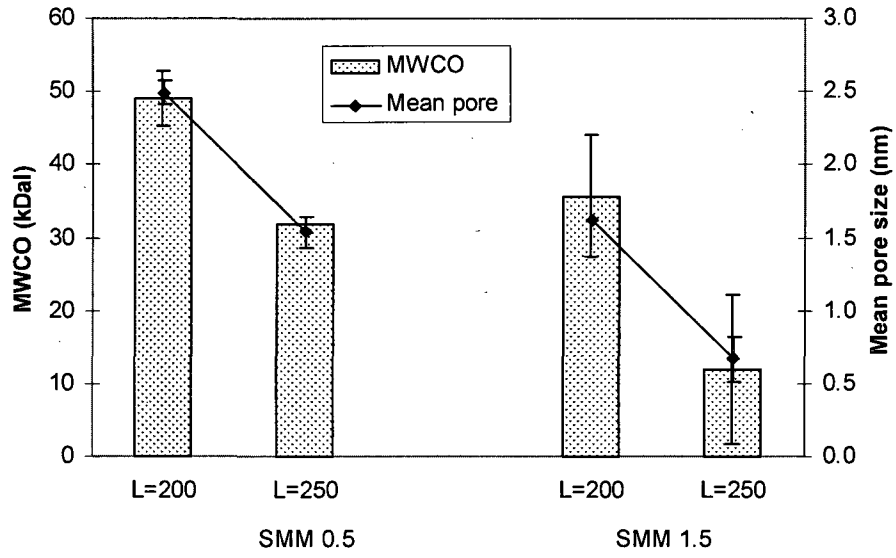

Figure K.3. Pore characteristics

Combined mechanisms

The single mechanism modeling in some cases does not fit well the experimental data due to the possible fact that more than one mechanism affecting membrane fouling. Ho and Zydney (2000) developed a model that combines cake formation and pore constriction for dead-end filtration. Kilduff et al., (2002) modified it for cross-flow filtration mode by incorporating a back transport term.

The area of open pores was expressed as:

$$A_{open} = A_T \exp\left[-\alpha C_b t\left(\frac{\Delta P}{\mu R_m} - J^*\right)\right] \qquad [K.11]$$

Where A_T ($=A_{open} + A_{blocked}$) is the nominal membrane area (m^2)

A_{open}: area of unblocked or open pores (m^2)

$A_{blocked}$: area of membrane blocked by foulant (m^2)

α: pore blockage parameter (m^2/kg)

C_b: bulk concentration of the solute (kg/m^3)

ΔP: applied pressure (Pa)

μ: solution viscosity (kg/m/s)

R_m: membrane resistance (m^{-1})

The rate of cake resistance, which is assumed to be equal to the mass of solute transported to the surface, was obtained by integration analytically of the following equation from $R_{c,0}$ to R_c:

$$\frac{dR_c}{dt} = \alpha_c (A_T - A_{open}) C_b \left(\frac{\Delta P}{\mu (R_m + R_c)} - J^* \right) \qquad [K.12]$$

Where α_c: specific resistance of the cake ($m^{-1}kg^{-1}$)

$R_{c,0}$: resistance of the initial deposit (m^{-1})

Finally the modeled flux was calculated with the equation:

$$J_T = \frac{A_{open} \Delta P}{\mu R_m} + \frac{(A_T - A_{open}) \Delta P}{\mu (R_m + R_c)} \qquad [K.14]$$

Parameters such as α, α_c, R_c and J* were optimized using Microsoft Excel Solver and MATLAB 7.0 (Math Works, Natick, MA).

Mosqueda-Jimenez et al., (2006) found that the combined mechanism fitted the experimental data better than the single one with a smaller mean square error (MSR). It is confirmed again by this study (Figure K.4).

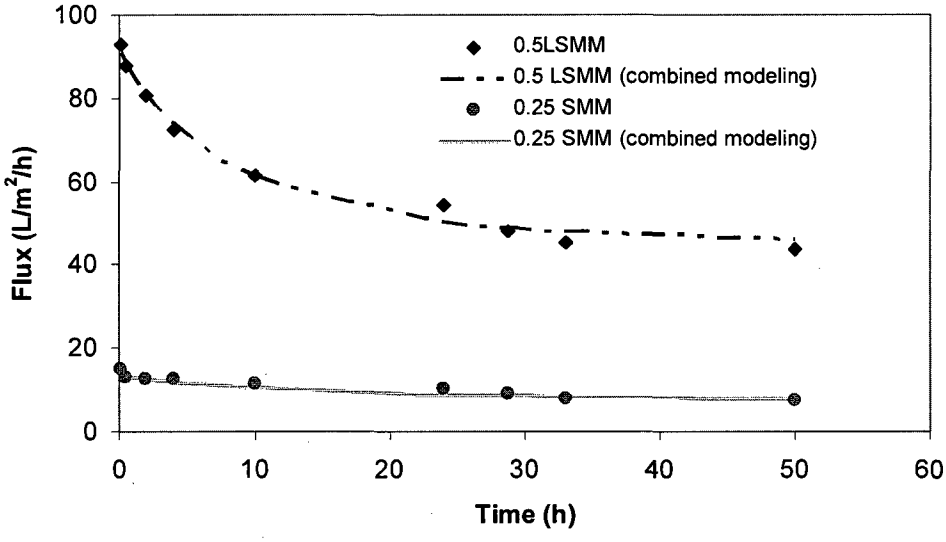

Figure K.4A. Flux reduction with time for combined-mechanism model for PES-LSMM membranes

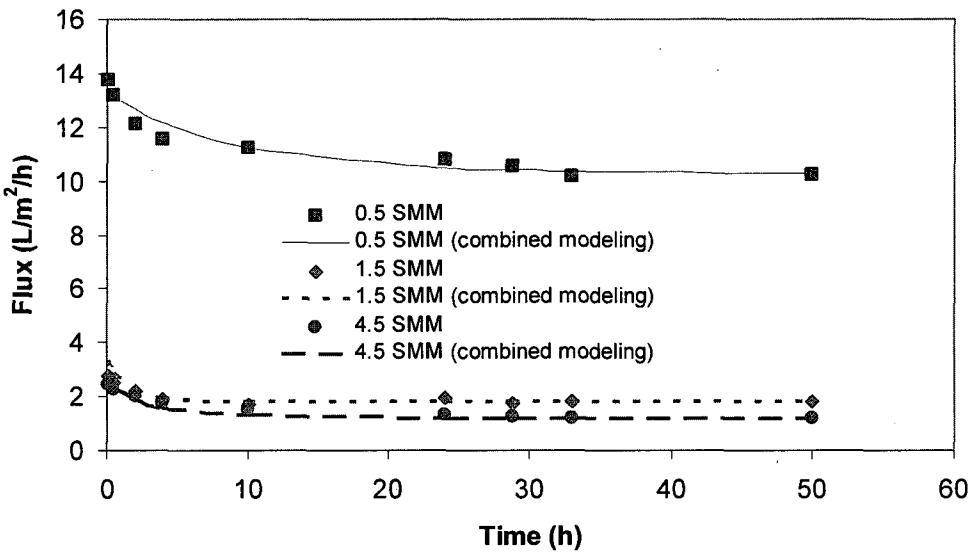

Figure K.4B. Flux reduction with time for combined-mechanism model for PES-nSMM membranes

The MSR of combined-mechanism model are all smaller than those of single mechanism model (Table K.3), proving the combined simulates better the fouling mechanism. Choi et al., (2005) claimed that their autopsy of fouled membranes suggested that the irreversible fouling layer was initially formed by pore blocking of small particles followed by strong interaction of fouling layer with mainly dissolved materials and by fouling layer compaction due to permeation drag.

Table K.3: Fitting parameters for combined fouling mechanism model

Membranes	α	α_c	$R_{c,0}$	J*	MSR	MSR (Single)$^+$
PES-0.5 LSMM	0.2849	3.59E+18	1.45E+16	45.212	0.039	0.271
PES-0.25 nSMM	0.2786	8.50E+19	1.00E+17	7.412	0.086	0.328
PES-0.5 nSMM	0.3020	1.05E+20	1.01E+17	10.255	0.011	0.523
PES-1.5 nSMM	0.3885	1.50E+22	3.89E+17	1.795	0.006	0.052
PES-3.0 nSMM	0.1885	1.50E+19	3.69E+17	2.690	0.202	1.376
PES-4.5 nSMM	0.5619	1.50E+22	5.05E+17	1.182	0.001	0.007

$^+$: *the smallest MSR obtained from single model.*

Again, for the case of 3.0 SMM, since the data was not smooth, the fitting flux was awkward. Its MSR was small because the values of fluxes were small, so the difference was not significant. Regardless to the case of 3.0 SMM, the specific cake resistance parameter α_c, pore block parameter α and the resistance of the initial fouling layer $R_{c,0}$ seem to be slightly affected with the increasing concentration of SMM. Moreover, the higher the flux permeation, the lower the resistance. This agrees with the fact that higher SMM concentration membranes had very little NOM deposition on the surface at the end of the experiment (membranes were almost white) or the DOC removals were lower for the higher SMM concentration (Figure K.5). The possible explanation for that phenomenon lies on the chemical interactions of the additive on membrane surfaces. It was observed during the film hardening period that the solvent exchange took a long time and it happened strongly. The coagulation bath (originally 100% iced pure water) changes its color due to the leakage of solvent. The membrane surfaces were therefore very rough (see SEM images in Appendix O) and porous on the top layer.

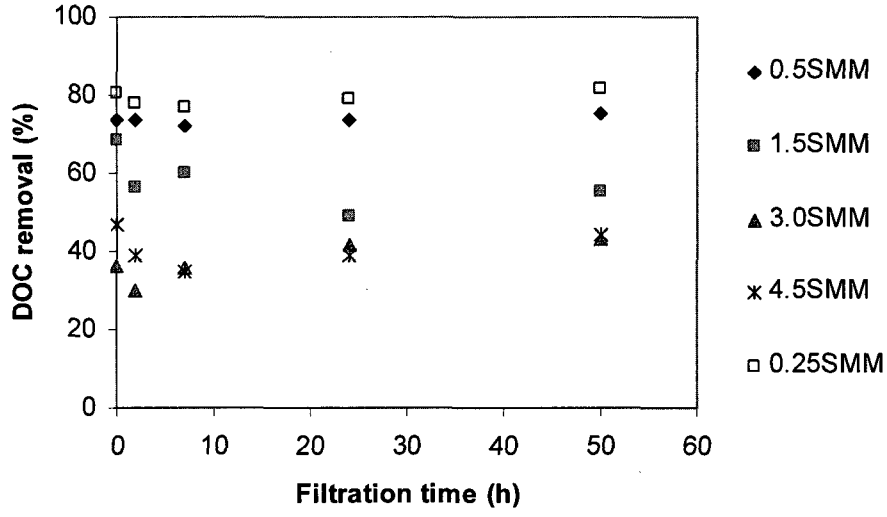

Figure K.5. DOC removal as a function of filtration time

APPENDIX L

ANOVA test results

Analysis of variance (ANOVA) is a general technique that can be used to test the hypothesis that the means among two or more groups are equal, under the assumption that the sampled populations are normally distributed. ANOVA is similar to regression in that it is used to investigate and model the relationship between a response variable and one or more independent variables. Analysis of variance, however, differs from regression in two ways: the independent variables are qualitative, and no assumption is made about the nature of the relationship (that is, the model does not include coefficients for variables). In fact, analysis of variance extends the two-sample t-test for testing the equality of two population means to a more general null hypothesis of comparing the equality of more than two means, versus them not all being equal. The ANOVA test is conducted in this study using Minitab 15 statistical software (Minitab Inc., State College, PA).

L.1. ANOVA methods

L.1.1 One- way ANOVA

To test the equality of means and to assess the differences in means, you use the one-way ANOVA procedure. This performs a comparison of the means of a number of replicate experiments performed where *a single input factor* is varied at different settings or levels. The object of this comparison is to determine the proportion of the variability of the data that is due to the different treatment levels or factors as opposed to variability due to random error. The model deals with specific treatment levels and is involved with testing the null hypothesis H0: $\mu 1 = \mu 2 = \ldots = \mu\alpha$ where μi represents the level mean. Basically, rejection of the null hypothesis indicates that variation in the output is due to variation between the treatment levels and not due to random error. If the null hypothesis is rejected, there is a difference in the output of the different levels at significance α and it remains to be determined between which treatment levels the actual differences lie.

L.1.2 Two-way ANOVA

A two-way analysis of variance tests the equality of means by *two variables or factors.* For this procedure, the data must be balanced (i.e., same number of observations) and factors must be fixed.

If the experimenter only considers two levels of interest for an experiment, factors A and B, such as predetermined levels for temperature settings or the length of time for process step, the factors A and B are said to be *fixed factors* and the model is a *fixed-effects model.* The various hypotheses that can be tested using this ANOVA concern whether the different levels of Factor A, or Factor B, really make a difference in the response, and whether the AB interaction is significant. For the two-way ANOVA, the possible null hypotheses are:

1. There is no difference in the means of factor A
2. There is no difference in means of factor B
3. There is no interaction between factors A and B

The alternative hypothesis for cases 1 and 2 is: the means are not equal.

The alternative hypothesis for case 3 is: there is an interaction between A and B.

The null hypothesis (H_0), in which the effect of any particular independent variable on each of the response variables does not exist, was rejected if P-value ≤ 0.05 ($\alpha = 0.05$ or 5%). Therefore, for the P-values to be statistically significant they should be ≤ 0.05.

L.1.3 General Linear Model/Balanced ANOVA

General Linear Models (GLM) are used to perform unvaried analysis of variance with balanced and unbalanced designs, analysis of covariance, and regression for each response variable.

Calculations are done using a regression approach. A "full rank" design matrix is formed from the factors and covariates and each response variable is regressed on the columns of the design matrix. Factors may be crossed or nested, fixed or random. Covariates may be crossed with each other or with factors, or nested within factors.

Minitab displays a factor level table, an ANOVA table, multiple comparison confidence intervals for pair-wise differences between main factors, and the corresponding multiple comparison hypothesis tests.

L.1.4 Balanced ANOVA-Mixed model ANOVA-Fit the restricted form of the model

A mixed model is one with both fixed and random factors. There are two forms of this model: one requires the crossed, mixed terms to sum to zero over subscripts corresponding to fixed effects (this is called the restricted model), and the other does not. Minitab fits the unrestricted model by default, but you can choose to fit the restricted form. The reasons to choose one form over the other have not been clearly defined in the statistical literature.

The choice of model form does not affect the sums of squares, degrees of freedom, mean squares, or marginal means. It does affect the expected mean squares, error terms for F-tests, and the estimated variance components.

In the unrestricted model, all these random variables are independent. The remaining terms in this model are fixed. In the restricted model, any term which contains one or more subscripts corresponding to fixed factors is required to sum to zero over each fixed subscript.

The organization of the output is the same for restricted and unrestricted models: a table of factor levels, the analysis of variance table, and as requested, the expected mean squares. The differences in the output are in the expected means squares and the F-tests for some model terms.

If an interaction is significant, any lower order interactions and main effects involving terms of the significant interaction are not considered meaningful.

L.2. Results

L.2.1 One-way ANOVA

To demonstrate the application of one-way ANOVA, a data set from the evaluation of manufacturing conditions for PES-nSMM membranes (Chapter 4) was analyzed. Table L.1 presents the P-values of five independent variables (PES concentration, nSMM concentration, casting speed, film thickness and post treatment). Each variable varied at two or three different levels. Based on this analysis, one can see if the different levels affect the membrane performance (i.e., solute rejection, flux reduction or final flux).

Apparently, only additive concentration had significant impacts on the DOC removal, flux reduction and final flux. Post treatment has impact solely on the flux reduction.

Table L.1: P-values of the independent variables obtained from the analysis of variance (one-way ANOVA) for the performance variables

	P-values		
Source of variation	**Solute rejection**	**Flux reduction**	**Final Flux**
PES concentration (wt%)	0.07 – NO	0.744- NO	0.207 - NO
nSMM concentration (wt%)	0.014 - YES	0.004 – YES	0.041 - YES
Casting speed (m/s)	0.167 - NO	0.385 – NO	0.097 - NO
Thickness of membrane film (mm)	0.684 - NO	0.400 – NO	0.091 - NO
Post treatment	0.429 - NO	0.039 – YES	0.220 - NO

L.2.2 Two-way ANOVA

This type of statistical analysis was applied to evaluate the significance of base polymers (PES, PEI, PS and PVDF) and LSMM concentration (0 wt%, 0.5 wt% and 3.0 wt%) on membrane hydrophobicity using the same drying method (e.g., chemical drying method). Table L.2 shows the statistical analysis for responsive contact angle with two variables (base polymers and %LSMM) using two-way ANOVA model.

Table L.2: Two-way ANOVA model for contact angles

Source	**DF**	**SS**	**MS**	**F**	**P***
Main effects					
Base Polymer (A)	4	686.6	171.7	6.73	***0.003***
%LSMM (B)	2	136.7	68.4	2.68	0.101
Interaction					
A x B	8	502.7	62.8	2.46	0.063
Error	15	382.8	25.5		
Total	29	1708.8			

**If P≤0.05, the effect is significant*

It is found that for the same drying method (chemical drying), only base polymers impact contact angle and surface energy (P=0.003, ≤0.05). The percent of LSMM is statistically not important.

To test if the effect of the variables involved in the membrane casting is statistically significant, the ANOVA test was employed and the results presented in Table L.3. The SMM type (hydrophobic versus hydrophilic) and the casting method (single-pass versus double-pass) were chosen as the independent variables, while the response variables were selected as characteristics (MWCO, Mean pore size, Pore density, Contact angles) and performance.

Table L.3: P-values of the independent variables obtained from two-way ANOVA model for the characteristic variables (α = 0.05)

Source of variation	MWCO[a]	Mean pore size	Pore density	Contact angles
Main effects				
A: SMM type	***0.000***[b]	***0.000***	***0.001***	***0.000***
B: Casting method	0.216	***0.036***	0.160	***0.050***
Interactions				
AB	***0.002***	***0.016***	0.117	***0.024***

[a] *MWCO = Molecular weight cut-off*

[b] *If P-value ≤ 0.05 the effect is statistically significant*

Results of Table L.3 indicate that at a significance level of α = 0.05, there is significant evidence for all main effects and for a two-factor interaction: membrane type × casting method. According to ANOVA interpretation, if the interaction is significant, any main effects involving terms of the significant interaction are not considered meaningful. Based on Table L.3, the MWCO, mean pore size and contact angles all depend on both the type of polymeric additives and the casting method.

L.2.3 General Linear Model (GLM) /Balanced ANOVA

Table L.4 presents results analyzed using GLM to assess the impact of base polymer and LSMM concentration. Since the interaction effect was significant for all membrane characteristic parameters, the type of base polymers and LSMM concentration both had impacts on these responsive parameters.

Table L.4: P-values of the independent variables obtained from GL model for the characteristic variables ($\alpha = 0.05$)

	MWCO	Mean pore size	Pore density	Geometry Std. Dev.	Porosity	Contact angles	Water content
Main effects							
Base polymer	***0.001***	***0.000***	0.177	0.073	0.078	***0.004***	***0.000***
%LSMM	0.142	***0.043***	0.571	0.425	0.796	0.876	***0.047***
Interaction							
Polymer x LSMM	***0.000***	***0.000***	***0.008***	***0.000***	***0.000***	***0.029***	***0.000***

Comparison of the two methods (two-way ANOVA and GLM) for contact angle analysis showed different results. LSMM concentration had no impact in two-way ANOVA (Table L.2), but it did in GLM. The reasons causing this discrepancy have not been clearly defined in the statistical literature.

L.2.4 Balanced ANOVA-Mixed model ANOVA

The impact of drying methods (natural drying, chemical drying and physical drying methods), which was presented in Appendix I, was analyzed using Balanced ANOVA-Mixed model- restricted form (Table L.5). The condition of this model is that: three factors (base polymer, drying method and LSMM concentration) are crossed; one factor base polymer is random; and the other two (%LSMM and drying method) are fixed. The base polymer is chosen randomly since the number of levels of base polymer is the highest (4- 4 types of polymers) whilst there are only three levels for drying method (chemical, physical and natural methods) and only three levels for LSMM concentration

(0 wt%, 0.5 wt% and 3.0 wt%). Results would be completely different if other factors were chosen randomly. According to Table L.5, base polymer is the only main effect on the contact angles. It is consistent with the results from two-way ANOVA model (Table L.2).

Nevertheless, the Balanced ANOVA-Mixed model is a more complex one regarding the interaction of three variables (not two variables as in two-way ANOVA model). As seen in the results, P values are less than 0.05 for AC and ABC interaction. Analytical interpretation (from the model) renders that if the 3-factor interaction is significant, any lower order interactions and main effects involving terms of the significant interaction are not considered meaningful. This means contact angle is actually affected by all three factors.

Table L.5: Analysis using Balanced ANOVA-Mixed model for contact angles

Source	DF	SS	MS	F	P
Main effect					
Base Polymers (A)	3	414.28	138.09	7.56	***0.000***
Drying methods (B)	2	64.11	32.05	2.06	0.209
%LSMM (C)	2	27.26	13.63	0.19	0.833
Interaction					
A x B	6	93.46	15.58	0.85	0.539
B x C	4	153.13	38.28	0.68	0.622
A x C	6	435.10	72.52	3.97	***0.004***
A x B x C	12	679.79	56.65	3.10	***0.004***
Error	36	657.81	18.27		
Total	71	2524.95			

**If P≤0.05, the effect is significant*

Even though there is little evidence of the effect of drying method on contact angle, the statistical analysis does not show which one has the highest impact. It should be noted that if drying method or LSMM concentration is chosen as random factor for the Balanced ANOVA-Mixed model, there is no significant effect shown for these two factors on contact angles. The natural drying method, which is the easiest and cheapest technique, hence can be applied to dry membranes for contact angle analysis.

APPENDIX M

Mathematical equations for MWCO and pore characterization

Porosity, pore density and mean pore size were obtained through the solute transport method (Singh et al., 1998). It is essentially a continuation of the ultrafiltration test in which the feed is changed to solutions of different known molecular weight solutes for one-hour periods. The feed (solute) concentrations were 100 mg/L solutions of PEG with molecular weights of 1.5, 6, 10, 14, 20, 35 kDal and PEO with molecular weight of 100 kDal. Solute diameters were calculated from the following expressions for the Stokes radius (a) of PEG and PEO as a function of their molecular weights (M):

$$a_{PEG} = 16.73 \times 10^{-10} M^{0.557} \qquad [M.1]$$

$$a_{PEO} = 10.44 \times 10^{-10} M^{0.587} \qquad [M.2]$$

These equations were derived by Singh et al. (1998) from empirical expressions of PEG and PEO's intrinsic viscosities and the Stokes-Einstein equation for diffusivity, assuming that the particles with Stokes radius would diffuse at the same rate as the particle under study.

Based on the solute (PEG, PEO) separation data, the pore size distribution of the membranes was computed using the log-normal probability function. It is predicted to be an accurate way to describe UF membranes sieving curves, i.e., the solute separation, $f(\%)$, versus the solute diameter (d_s) follow the log-normal relationship:

$$\frac{df(d_p)}{dd_p} = \frac{1}{d_p \ln\sigma_p \sqrt{2\pi}} \exp\left[-\frac{1}{2}\left(\frac{\ln(d_p/\mu_p)}{\ln\sigma_p}\right)^2\right] \qquad [M.3]$$

where d_p is the pore diameter, μ_p is the geometric mean of the pore diameter and, σ_p is the geometric standard deviation (GSD) of the pore diameter. These parameters are denominated geometric, because they correspond to a log-normal distribution $\mu_p = d_s @ f = 50\%$ (solute diameter that corresponds to 50% separation of PEG obtained from the PEG separation data), and σ_p, is calculated by:

$$\sigma_p = \frac{d_s @ f = 84.13\%}{d_s @ f = 50\%} \qquad [M.4]$$

where d_s is the solute diameter ($d_p = d_s$). Their geometric means ($\mu_p = \mu_s$) and their geometric standard deviations (GSD) ($\sigma_p = \sigma_s$) were considered to be the same. μ_s is the geometric mean, and σ_s is the GSD of the solute diameter. Library functions from Microsoft Excel for the standard normal distribution and base-10 logarithm (i.e., NORMSINV and LOG10, respectively) were used to compute solute separation f(%) at a predetermined pore size base on PEG separation data. These f values were then used together with the value of μ_p and σ_p obtained from equation [M.4] to compute the pore size distribution of the membrane based on equation [M.3]. This model is based on an assumption that dependence of solute separation on the steric and hydrodynamic interaction between solute and pores is ignored, thus the pore size equals the solute size. (Singh et al., 1998).

Calculations of pore density (number of pores per unit area, N) and surface porosity (ratio of the area of pores to the total membrane surface area, S_p) were based on the Hagen-Poiseuille equation modified for a porous membrane, assuming laminar flow (Porter, 1990):

$$J_i = \frac{N_i \pi d_i^4 \Delta P}{128 \eta \delta} \qquad [M.5]$$

where

J_i = solvent flux for pores with diameter d_i (m^3/m^2-s)

N_i = density of pores with diameter d_i (dimensionless)

ΔP = pressure difference across the pores (Pa) (345 kPa in this study)

η = solvent viscosity (N-s/m^2) ($\eta = 9.34 \times 10^{-4}$ at water temperature of 23°C)

δ = length of the pores, considered equivalent to the thickness of the skin layer (no tortuosity) (m) (approximately $\delta = 2 \times 10^{-7}$ m)

Thus, total flux (J, i.e., the final PWP) through the membrane was the summation of all fluxes through the pores with different sizes:

$$J = \Sigma J_i = \frac{\pi \Delta P}{128 \eta \delta} \Sigma N_i d_i^4 = \frac{\pi \Delta P N}{128 \eta \delta} \sum_{d_{min}}^{d_{max}} f_i d_i^4 \qquad [M.6]$$

where

f_i = fraction of pores with diameter d_i

Therefore,

$$N = \frac{128\eta\delta J}{\pi\Delta P\sum_{d_{\min}}^{d_{\max}} f_i d_i^4} \qquad [M.7]$$

The surface porosity was the same as the void volume of the membrane skin (Porter, 1990):

$$S_p(\%) = \left(\frac{\pi}{4}\sum_{d_{\min}}^{d_{\max}} N d_i^2\right)\times 100 = \left(\frac{N\pi}{4}\sum_{d_{\min}}^{d_{\max}} f_i d_i^2\right)\times 100 \qquad [M.8]$$

As an example, the sieving curves of 18 wt%PES-LSMM membranes manufactured under different conditions (different thickness, LSMM concentrations and different casting techniques) and simulated by the above model are presented in Figure M.1.

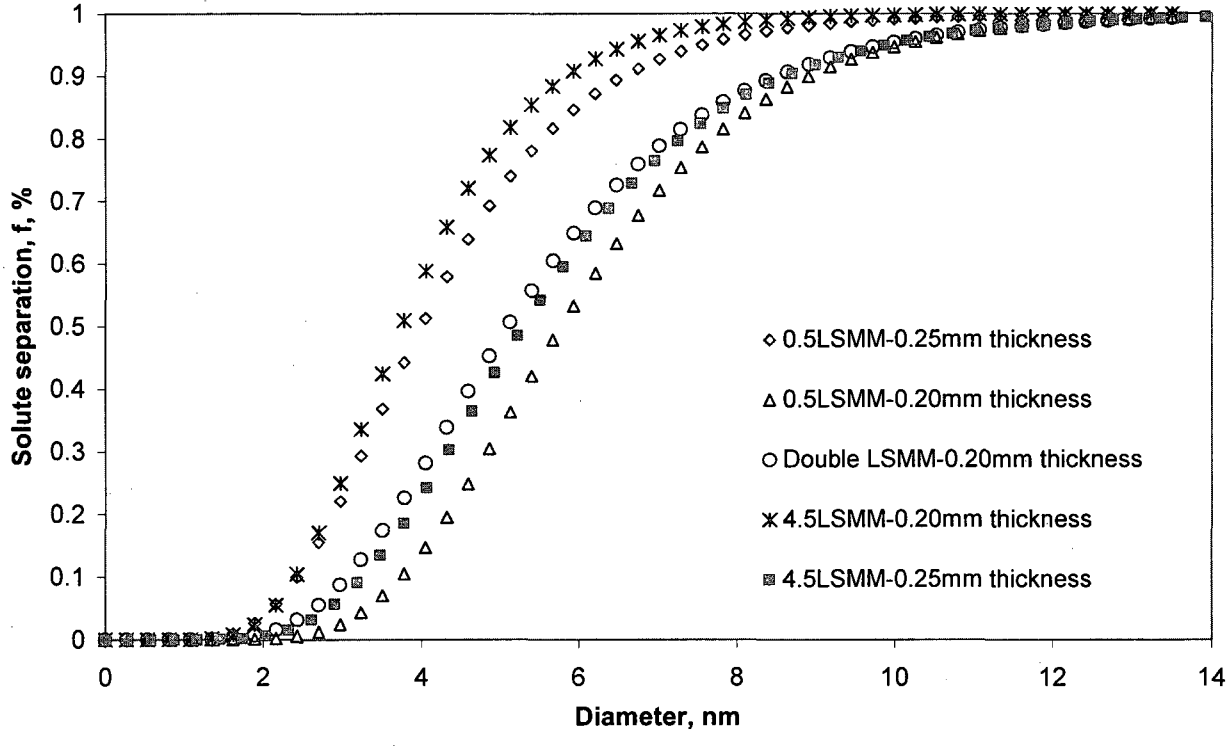

Figure M.1 Simulated sieving curve of LSMM modified membranes (The double LSMM has LSMM concentration of 0.5 wt%)

It is obvious that for low LSMM concentration, the thinner membranes (0.2 mm thick) have a larger mean pore size, accordingly increasing the MWCO. For the higher additive concentration (4.5 wt%), the opposite is observed. Membranes of 0.25mm thickness are having higher mean pore sizes. The explanation of those phenomena may lie in the impact of shear stress. Since the shear stress is directly proportional to casting velocity, solution viscosity and inversely proportional to film thickness (Shear stress = (viscosity)*(velocity/thickness)), the shear stress increases by either increasing the casting velocity, increasing viscosity or by decreasing the thickness. High shear rate often leads to greater molecular orientation and leaves bigger gaps (pores) between two aligned macromolecular nodules. The pore sizes are therefore larger.

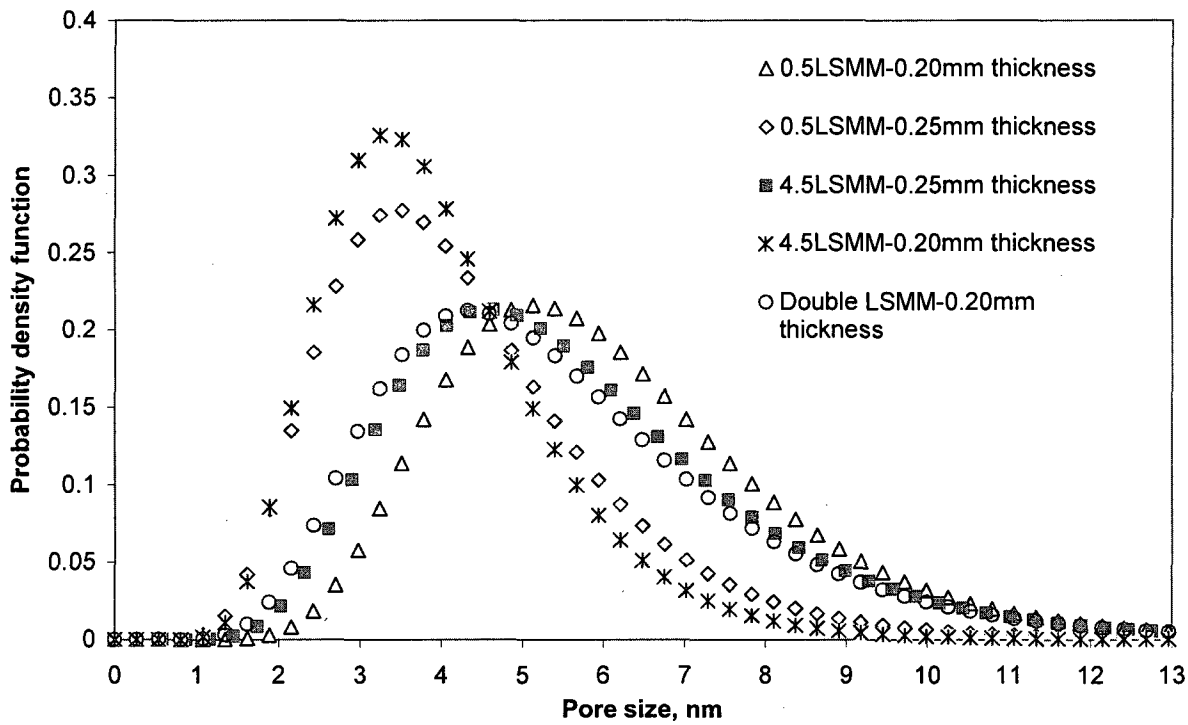

Figure M.2 Simulated pore size distribution of LSMM modified membranes

The probability density function plot in Figure M.2 gives an indication of the pore size distribution for the different membranes. It is observed that those membranes that had larger mean pore sires had a smaller most probable size of the pores (mode, maximum in the probability density function curves). It is worth noting that because of the assumptions (chapter 5- section 5.4.2.1) made to generate the model, the pore size distributions in Figure M.2 represents just an approximation of the actual data. Table M.1

shows the detailed values of the mean pore size, pore density and MWCO of the hydrophobic nSMM membranes.

Table M.1. Pore density and Surface porosity of SMM membranes (18%PES)

Membranes	Mean pore size (nm)	Pore density (# of pores/m^2)	MWCO (kDal)
0.5 nSMM-0.2mm thickness	2.50	3.68	49.06
0.5 nSMM-0.25mm thickness	1.54	6.58	31.86
1.5 nSMM-0.2mm thickness	1.62	21.29	35.71
1.5 nSMM-0.25mm thickness	0.67	10.76	11.94
3.0 nSMM-0.2mm thickness	0.56	55.17	4.65
Double 3.0 nSMM -0.2mm	2.48	39.17	21.35

According to Table M.1 and the two figures (M.1 and M.2), some conclusions and interpretations about the impact of manufacturing conditions on pore characteristics can be made as following:

- LSMM concentration: No clear trend is evident (from Figures M.1 and M.2).
- nSMM concentration: An obvious trend can be seen from nSMM membranes that higher nSMM concentration leads to smaller mean pore sizes and MWCO. The possible explanation is that nSMM additive is less viscous than LSMM (nSMM casting solution is less viscous then LSMM casting solution), thus the shear stress is less, leading to denser membranes (see SEM images in Appendix O).
- Thickness (0.25mm vs 0.20 mm): Thicker membranes lead to lower shear stress, accordingly smaller pore sizes and MWCO.
- Casting technique (double vs single pass): Double pass method increases the pore sizes of membrane with the same amount of SMM additive again due to the effect of shear stress as explained above.

APPENDIX N

Topography of membranes

The study of the skin layer morphology of synthetic polymeric membranes can help to elucidate the separation mechanism, since the pore structure and especially surface images determine the intrinsic permeation properties. Membrane topography may be characterized by several roughness parameters and measured by AFM. One of the parameters most commonly employed is the mean roughness or R_a (or arithmetic roughness average), which, according to Singh et al. (1998), is the mean value of the surface height relative to the centre plane. The centre plane is defined as that plane that encloses equal volumes above and below it. In other words, R_a is the arithmetic average of the absolute value of the surface variation from the mean. For a better interpretation of the relationship between membrane surface morphology and fouling phenomenon, AFM was employed in this study. Some results have been reported in Chapters 6 and 8. Table N.1 reports the absolute values of roughness R_a for the commercial membranes, control membranes (different base polymers but without blending additives) and the modified membranes (with the incorporation of 3.0 wt% hydrophilic LSMM additive).

Table N.1 Roughness (R_a) of membranes

Commercial membranes	R_a (nm)	*Control membranes*	R_a (nm)	*Modified membranes*	R_a (nm)
PES-PX	1.669	CA	0.67	CA-LSMM	1.34
C-XM	0.935	PEI	2.40	PEI-LSMM	2.26
PS-EWH	1.906	PS	1.05	PS-LSMM	2.39
PES-PU	0.666	PES58k	0.89	PES58k-LSMM	1.10
CA-CQ	0.689	PES31k	1.27	PES31k-LSMM	2.73
PES-MIL	1.789	PVDF	4.32	PVDF-LSMM	1.64
PAN	1.320				
PS-FO100	1.525				
PS-FO50	1.738				

There is no clear trend for the change of roughness when adding the additives according Table N.1. The CA membranes are often the smoothest ones while the PS membranes are almost the roughest membranes.

Figure N.1 shows three-dimensional images of the membrane surfaces for unmodified, surface-modified and commercial membranes. All AFM images in Figure N.1 are presented at the same scale to facilitate the comparison among them, i.e., 0.5 μm × 0.5 μm scanning area with 40 nm in the Z direction. Light areas correspond to elevated regions (peaks that represent the nodules), while dark areas correspond to low regions (valleys that represent the pores) (Khayet et al., 2004).

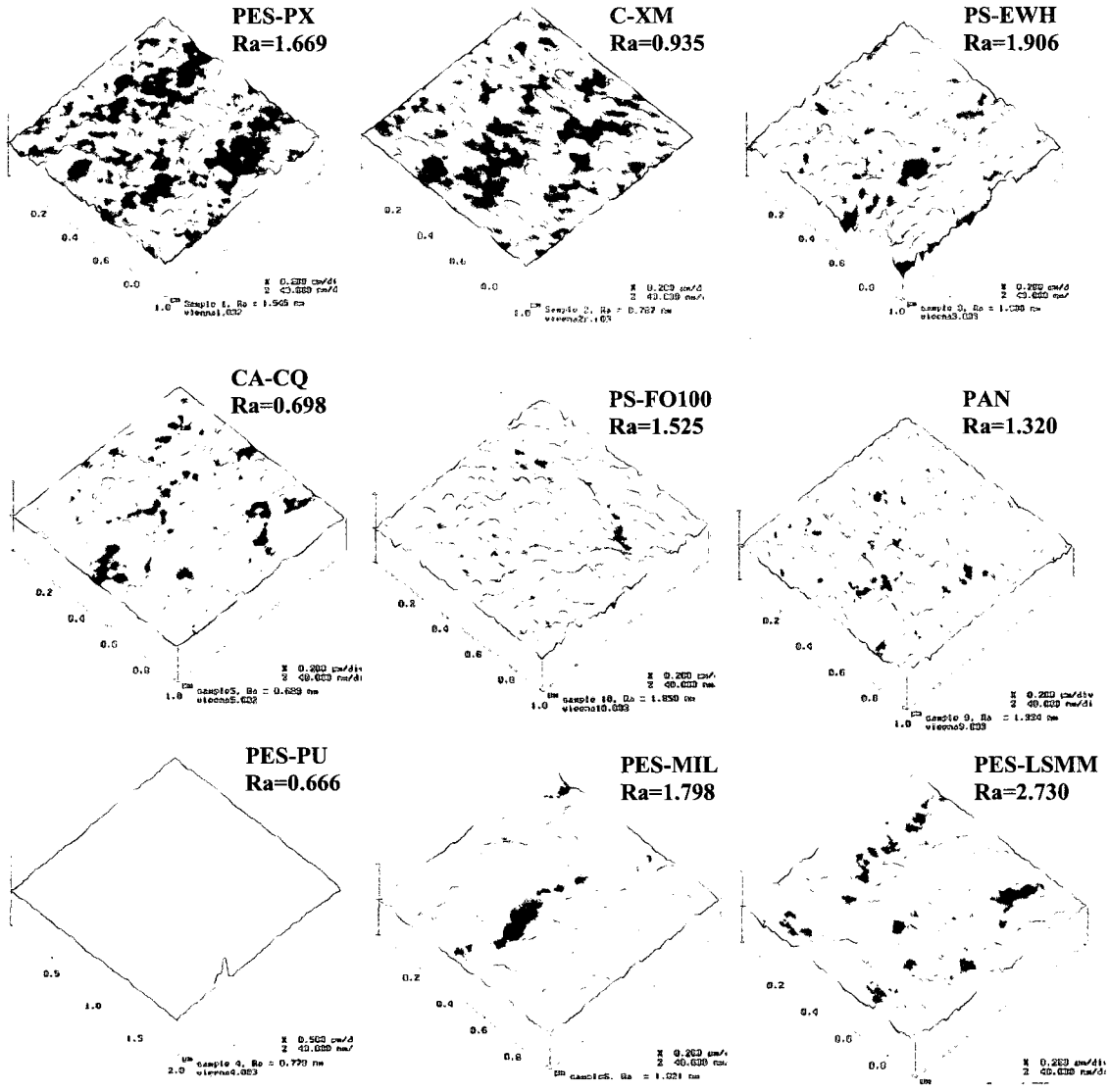

Figure N.1. AFM images of membrane surfaces

Surface roughness is usually related to many other parameters. Singh et al. (1998) found that roughness became higher when MWCO increased since high MWCO had less tightly

packed nodules aggregates in the skin layer. The same trend was observed by many other researchers (Fritzsche et al., 1992; Bessieres et al., 1996). It was confirmed again in this study that PU40 and XM40 membranes, which had lowest values of MWCO (data is presented in Chapter 6), showed the smoothest surfaces. Hirose et al. (1996) found that an increase in surface roughness resulted in a higher water permeation flux. For PVDF membranes, Khayet et al. (2001) observed that the measured pure water flux increased with the increase of roughness and the roughness parameter was higher for membranes having larger pore sizes and nodule sizes as well as higher surface porosity.

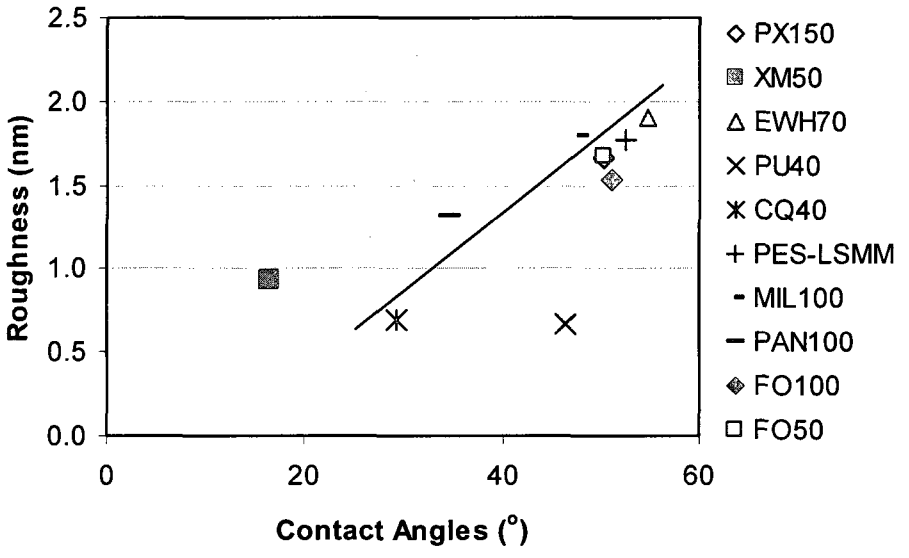

Figure N.2. Relationship of roughness and hydrophilicity for commercial and PES-LSMM membranes

Figure N.2 shows that roughness increased with an increase in the contact angles except for XM50. The water permeation rate increases with a decrease in the contact angle, (i.e., increase in hydrophilicity). In fact, both cellulose (XM50) and cellulose acetate (CQ40) membranes that correspond to the lowest contact angles showed the highest PWP values (Chapter 6). Then, from the trend shown in Figure N.2, it is concluded that the smoother membranes have higher values of PWP. This seems contradictory to the results reported by Khayet et al. (2004) and Hirose et al., (1996). It should, however, be noted that these results involves membranes made of many different materials. On the other hand the data shown by Khayet et al. (2002) and Hirose et al. (1996) were obtained from membranes prepared from the same base polymeric material. It should also be emphasized that

cellulose and cellulose acetate membranes were the smoothest and the most hydrophilic among the tested membranes.

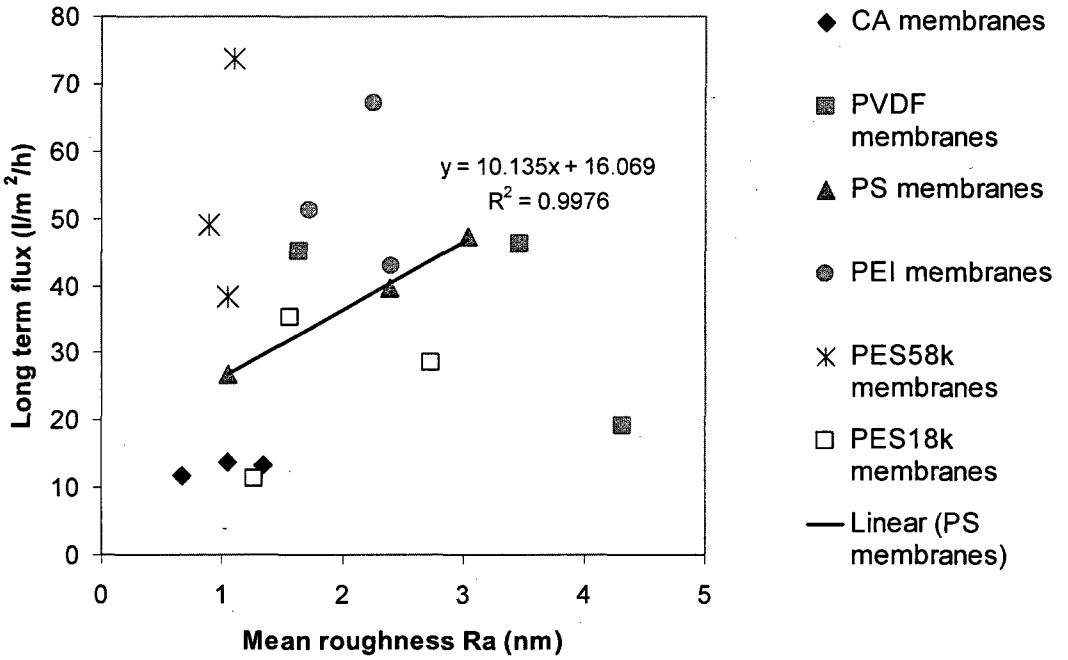

Figure N.3. Scatter plot of final permeate flux as a function of mean roughness for membranes prepared using LSMM with different concentrations (0; 0.5 and 3.0 wt%)

Figure N.3 depicts the relationship of mean roughness and long term flux (i.e., after 50 hours of pure water permeation test). Only for PS membranes, there are correlation between roughness and water permeation rate. Nevertheless this trend might be observed for PS membranes under this particular testing system solely.

APPENDIX O

Scanning electron microscopy (SEM) images

SEM is known a powerful tool for the interpretation of the relationship between membrane surface morphology and fouling phenomenon. A key limit of SEM is that high-resolution SEM, which requires high-energy electrons, can cause structural and chemical changes at polymer surfaces. To minimize beam damages, membrane samples must be coated with a heavy metal, such as gold, platinum or palladium. Despite this limitation, SEM has still been used in a number of studies in the membrane field because of its simple and clear three-dimensional images of surfaces.

Some SEM images were previously presented in Chapters 4 and 5. In this appendix, some cross-section images are depicted in Figure O.2 and the surface images are presented in Figure O.1. Table O.1 shows the membrane code and the corresponding variables.

Table O.1 Description of membranes

Membrane code	PES (wt%)	nSMM (wt%)	Thickness (mm)	Casting speed (cm/s)
M1	18	4.5	0.20	0.25
M2	18	4.5	0.20	1.5
M3	18	4.5	0.25	0.25
M4	18	4.5	0.25	1.50
M5	16	4.5	0.20	1.50
M6	14	4.5	0.20	1.50
M7	18	3.0	0.20	0.25
M8	18	3.0	0.20	1.50
M9	18	1.5	0.20	0.25
M10	18	1.5	0.20	1.50
M11	18	1.5	0.25	0.25
M12	18	1.5	0.25	1.50
M13	18	0.5	0.20	1.50
M14	18	0.5	0.25	1.50
M15	18	0.0	0.20	1.50

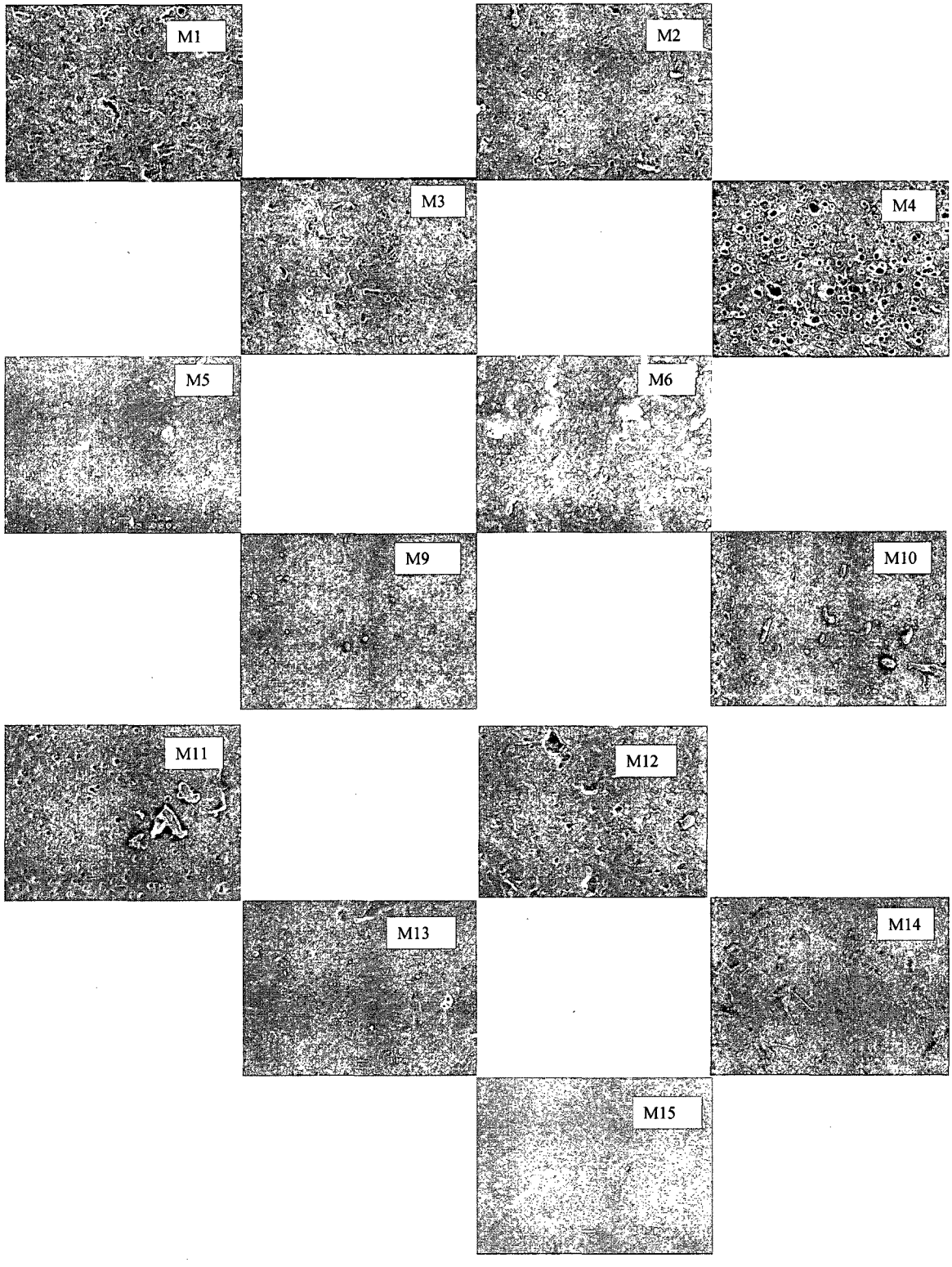

Figure O.1 SEM surface images of 15 membranes

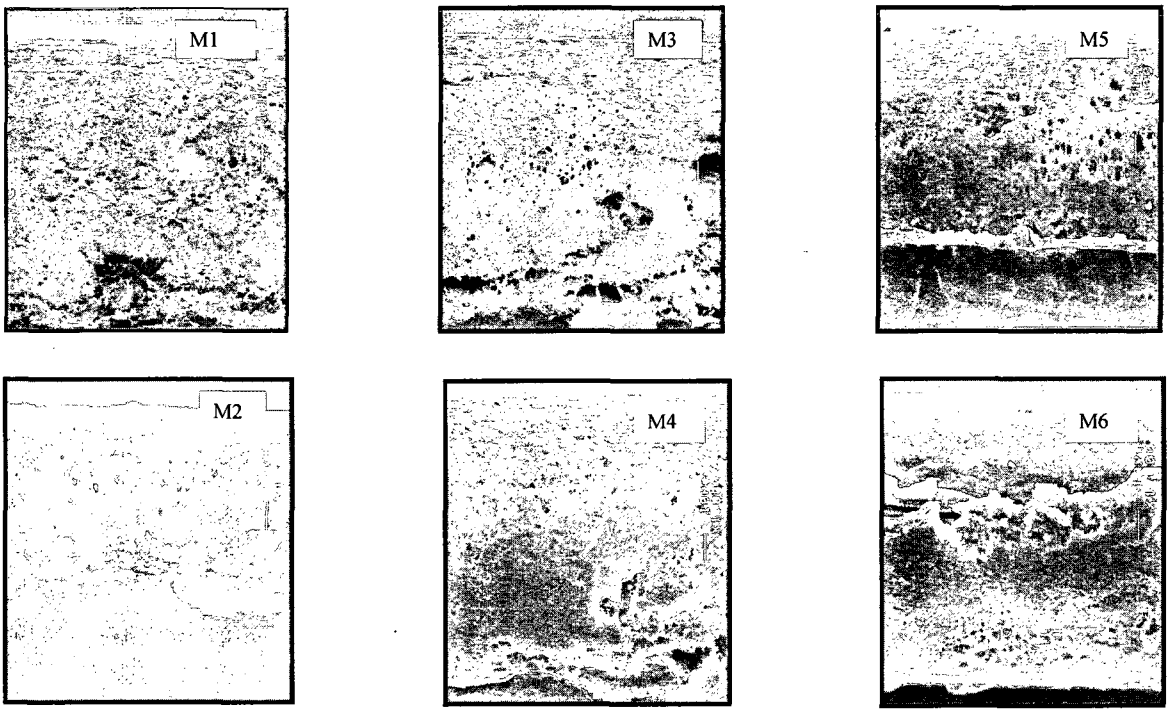

Figure O.2 SEM cross-sections of 6 membranes

Even though the surface and cross-section in some cases do not show the clear images, it is possible to distinguish the smooth or rough surface, finger-like, layer or spongy structures. In general, the hydrophobic nSMM membranes can be distinguished with rough surfaces and spongy cross-section structures (See Figures O.1 and O.2). It is worth noting that nSMM casting solutions are quite not viscous. When we added more nSMM additive, the solutions became even less viscous (i.e., viscosity of 3 wt% nSMM+18 wt% PES is 622 cP while for the 4.5 wt% nSMM+18 wt% PES, viscosity is 573cP). Their membrane surfaces are not shiny and smooth but rough and dry with colonies of chemical aggregation. Especially when the amount of nSMM added are very low (0.5 or 1.0 wt%), no trace of shallow holes can be seen on the surfaces (M13 and M14). The PES-nSMM membranes are however very hydrophobic. Their contact angles are up to 91°. Increasing evaporation times can result in contact angles of more than 120°. It is interesting that higher percentage of nSMM does not guarantee more hydrophobic, even the opposite happens.

Table O.2: Advancing contact angles of some nSMM membranes (blending with 18 wt% PES base polymer)

	0 wt% nSMM	0.5 wt% nSMM	1.5 wt% nSMM	3.0 wt% nSMM	4.5 wt% nSMM
Contact angles (degree)	71.6	89.7	89.6	86.0	84.8

The discrepancy due to casting speed (fast or slow) affects quite obviously the surface and the cross-sections (see M1 vs M2, M3 vs M4). Slower speed, slower shear stress, thus denser (cross-section) membranes obtained since low shear rate often leads to poor molecular orientation and leaves small gaps (pores) between two aligned macromolecular nodules. Membranes therefore became less porous. Higher PES content seems to make the membranes more rough and spongy (viscosities of 18 wt%, 16 wt% and 14 wt% of PES are 573 cP, 550.1 cP and 366.7 cP respectively). Effect of thickness only shows clearly in M9, M10 (smoother) versus M11, M12 (rougher) when the percent of additive is 1.5 wt%. Again the explanation for this effect possibly lies in the effect of shear stress in which the thickness is adversely proportional to the shear rate. Refer to chapter 4 for a full interpretation of the impact of nSMM additive on modified membranes.

APPENDIX P

Analysis of solution viscosity

Viscosity is a measure of the resistance of a fluid which is being deformed by either shear stress or extensional stress. In general terms it is the resistance of a liquid to flow, or its "thickness".

The viscosity of a casting solution indicates how easy it will be to cast and form a film. The more viscous the solution, the easier the solution to cast. For some solutions that are less viscous such as celulose acetate solution, it is often required to reduce the temperature of the solution by refrigerating. Viscosity increases as temperature decreases. When considering the casting mode (casting speed or casting technique), knowledge of solution viscosity is more important since it shows the shear stress effect against spreading movement of the casting bar. Some analysis of solution viscosities have been reported in Chapter 5. This appendix however will describe the detailed procedure of solution viscosity measurement.

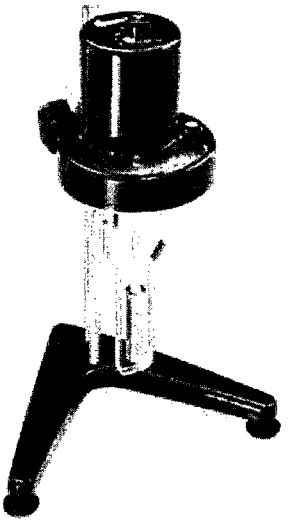

Figure P.1. Rotational viscometer

The solution viscosity in this study was measured by a rotational viscometer LVT C2443 (Brookfield Co., Middleboro, MA) (Figure P.1). The data was obtained by multiplying the dial reading number (corresponding to the torque required to rotate a spindle at constant speed) with the spindle factor. Depending on the solution characteristic, a specific spindle is chosen.

P.1. Preparation and calibration:

P.1.1 Type of viscosmeter

Two viscometers were tried including a RVT100463 model and a LVF-C2443 model from Brookfield Company. A standard solution with a known viscosity of 12980cP was tested. The results using RVT100463 and LVF-C2443 viscometers were 16065 cP and 13600 cP, respectively. The final decision of choosing viscosity was for the second one LVF-C2443.

P.1.2 Solution container

A 20-ml adaptor which is equipped with the viscosmeter was used as a solution container. In cases where the adaptor is not available, a 125-ml bottle (that is often used for making casting solution) can be utilized.

P.1.3 Type of spindle, rpm and position of spindle

After several tests, spindle #3, rpm60 and centered position were selected since they gave the value closest to standard solution. Data was obtained was multiplied by the dial reading number (corresponding to the torque required to rotate a spindle at constant speed) and spindle factor (based on the catalogue, with spindle #3, rpm60, the spindle factor is 20)

P.1.4 Calibration

Several solutions with known viscosities can be used for calibration. In our study, Glucose solution, which had viscosity of 12980 cP, was used. In cases where there is not enough solution for viscosity analysis, a relative calibration could be set up for standard solution (see Table P.1 and Figure P.2) with an appropriate ratio.

Table P.1:Calibration for Standard solution (Glucose) 12980 cP:

Position	Value (cP)
1	12640.00
2	12340.00
3	11080.00
4	9160.00
5	1140.00

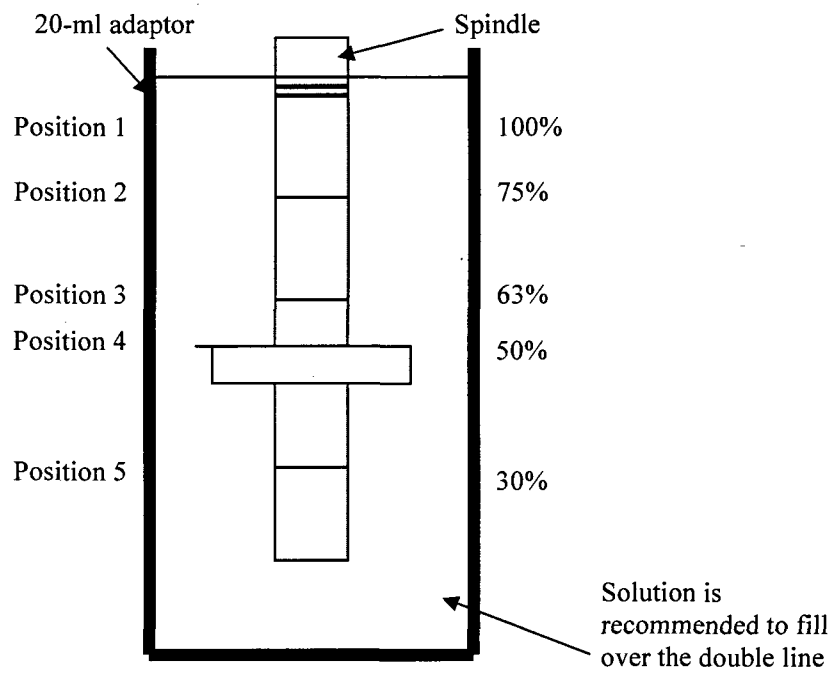

Figure P.2. Calibration positions in solution container

P.2. Viscosities of several casting solutions:

Table P.2 presents the viscosities of several solutions using the Rotational viscometer. Obviously from Table P.2 that higher base polymer concentration leads to higher viscosity. This could be due to a greater agglomeration at higher concentrations. With the same PES concentration and additives (either SMM or LSMM), similar viscosities are obtained.

Table P.2: Viscosities of solutions with and without additives

Membranes	Viscosity (cP)
4.5 wt% SMM-18 wt%PES	573.0
4.5 wt%SMM-16 wt%PES	550.1
4.5 wt%SMM-14 wt%PES	366.7
3 wt% SMM-18 wt%PES	622.0
3 wt% LSMM-18 wt%PES	671.4
Control PES (18 wt%PES)	410.0
Control PES (20 wt%PES)	656.0

APPENDIX Q

Behavior of different membrane coupons on a membrane sheet

In membrane manufacturing, the ideal membrane sheets should perform equally regardless of the location within the sheet. However, to achieve that ideal performance is something beyond the control. Even commercial membranes face the same problems. This was proved by our preliminary test with six NF270 membrane coupons (cut from the same membrane sheet). Their performance was different to some extent. The difference was not avoidable but the desired membranes should have as small discrepancy as possible. The discrepancy of membrane coupons on a membrane sheet has been known among membrane researchers in our group but it has not been written down. This however will be discussed in this appendix so that students who are new to membrane field in general or membrane manufacture in particular would have some ideas.

The difference among membrane coupons of a membrane sheet comes from the casting step. This relates to the nucleation of polymer-lean phase (de-mixing).

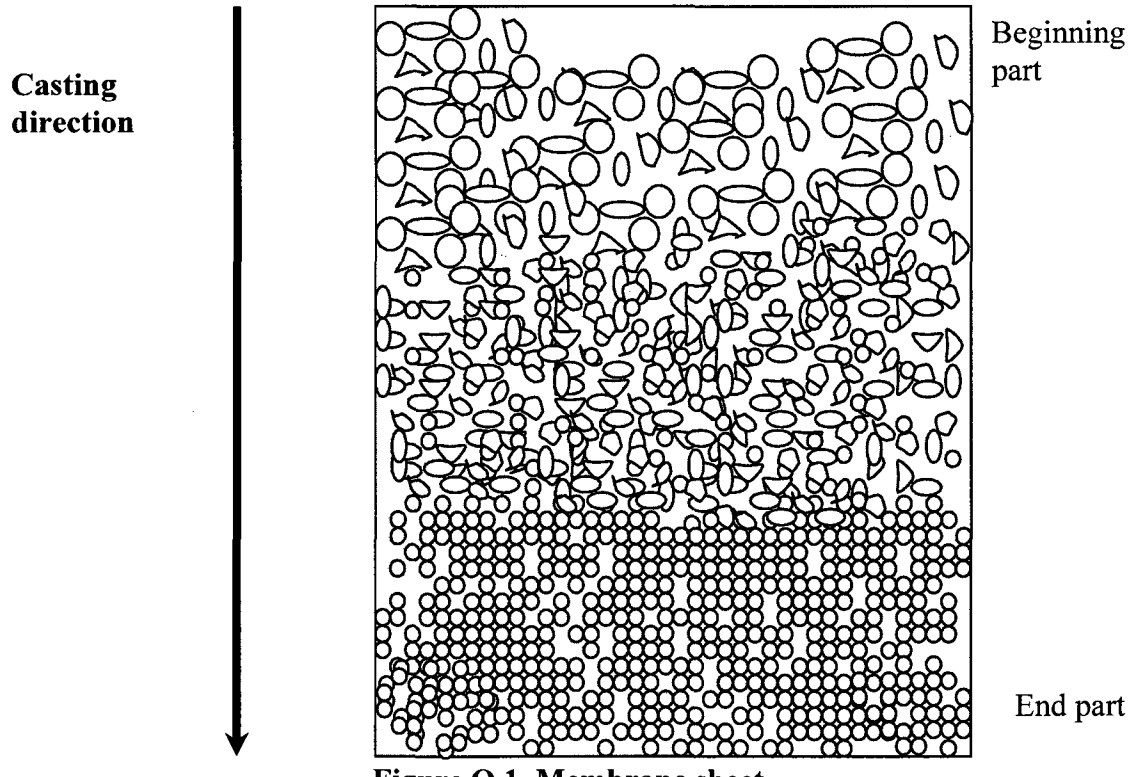

Figure Q.1. Membrane sheet

Following the casting direction (same as gelation direction) in Figure Q.1, there is instantaneous demixing in the "beginning part" resulting in more porous part while there is a delayed demixing at the "end part" of the film. That causes the "end part" more dense. Observations were conducted by putting membrane sheets on a light box. As a trade-off, the "beginning part" obtains higher flux but lower solution rejection. To optimize the two benefits, the chosen coupons were often cut close to the "end part" and "intermediate part" (Figure Q.2).

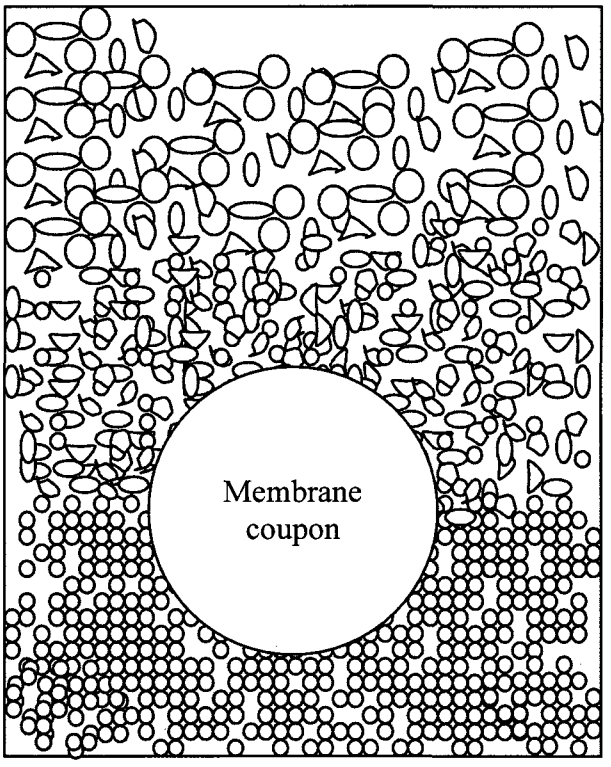

Figure Q.2. Chosen location for membrane coupons

A filtration test was conducted to further confirm the idea of chosen location for the best membrane coupons. Three membrane coupons from the same PES-LSMM membrane sheet were cut from three different zones, namely UF1, UF2 and UF3 membranes. Two others were cut from two zones of the control PES membrane sheet (UF4 and UF5). Characteristics of these membranes are presented in Table Q.1.

Table Q.1: Characteristics of tested membrane coupons

Membrane code	Characteristics	Part in membrane sheet
UF1	Not very porous, PES-LSMM membranes	End
UF2	Half porous, PES-LSMM membranes	Intermediate
UF3	Very porous, PES-LSMM membranes	Beginning
UF4	Half porous, Control PES membranes	Intermediate
UF5	Not very porous, Control PES membranes	End

Those tested membranes were cut into a 5cm-diameter coupons and placed randomly into crossflow cell-in-series system. Details of this system can be found in Chapter 3.

The differentiation in performance can be seen clearly from Figure Q.3. From the same PES-LSMM membrane sheet, the three UF1, UF2 and UF3 membrane coupons behave differently in terms of flux. The same dissimilarity is observed for the two coupons of control PES membranes (UF2 and UF5) as well. In addition, as expected the dense membranes (i.e., not very porous membranes) had the lowest fluxes while the very porous membranes had much higher fluxes. Control PES membranes had higher fluxes than the modified PES-LSMM ones.

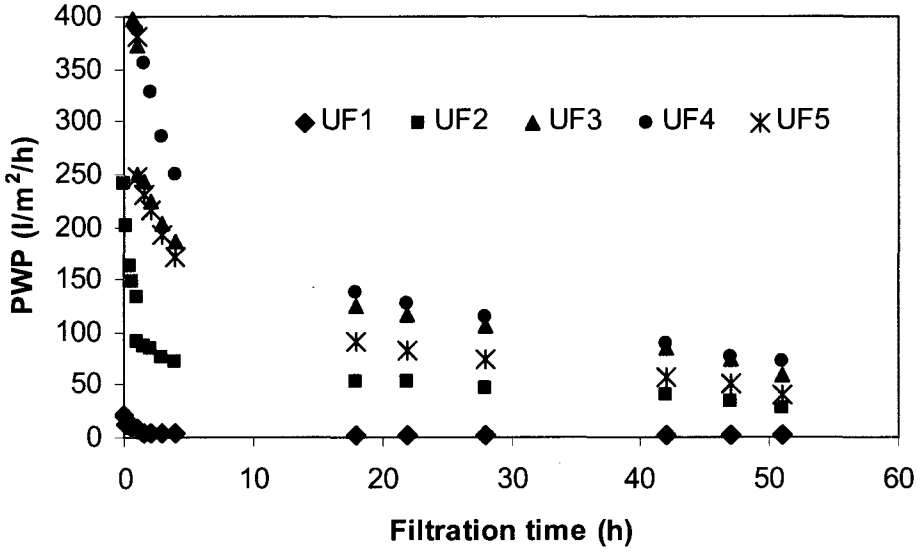

Figure Q.3. PWP as a function of filtration time

APPENDIX R

Impact of compaction

PES, used as a base polymer in most part of this thesis, is a typical amorphous polymer with good chemical compatibility and superior thermal stability but is susceptible to compaction under high pressure. The operating pressure used in this research was 50 psi. Moreover, the membranes were pre-compacted at 70 (sometimes 80 psi) for 30 min with MQ water prior to the filtration test. Although the degree of compaction (regressed slope of water flux-time plot within the first 5 mins of filtration test, after the pre-compaction period) was not significant; it was possible to observe a change in flux during the subsequent 50 psi operation (Figure R.1).

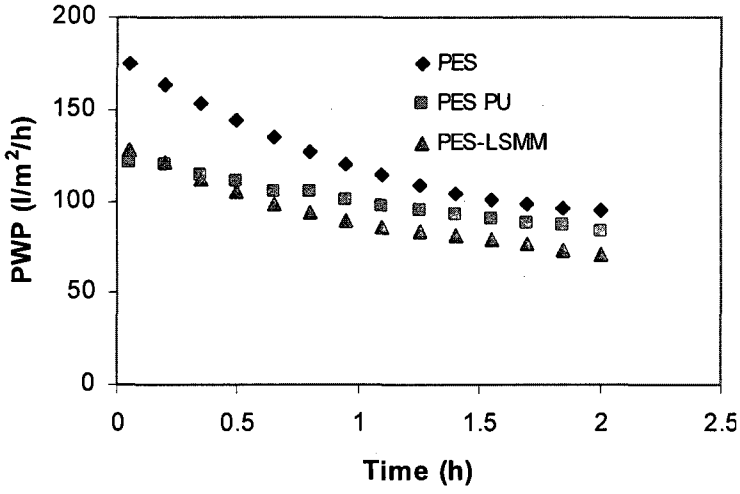

Figure R1. Pure Water Permeation as a function of time (using 6-CF cell system)

From Figure R.1, the control PES was the most compacted. The reason to monitor the degree of compaction via the permeation test with MQ water is that the overall flux drop during the fouling test may be due to both compaction and fouling. It is expected that the impact of compaction is less than that of the gel layer created by NOM adsorption (fouling). To confirm this, a series of similar permeation tests were conducted in which the feed water was switched from MQ water to ORW, the hydrophobic fraction (HPO-ORW) and the hydrophilic fraction of river water (HPI-ORW). The two last waters were obtained by isolation using XAD8/XAD4 resins. It is interesting that with contaminant-free water, the degree of compaction (determined by the initial slope of the flux-time plot) of the experimental membranes was significantly greater than for the commercial

PES PU. The explanation may be due to the fact that PES PU has backing material while the tailor-made membranes have none. The degree of compaction for three membranes presents the same trend for the hydrophilic (HPI-ORW) and hydrophobic fractions (HPO-ORW) of ORW i.e., all decrease when switching from HPI-ORW to HPO-ORW water source. The difference between the two water sources is that HPI-ORW contains mostly low MW particles while HPO-ORW is composed of high MW compounds. It seems that the impact of pressure is more for water with low MW solutes since the membrane resistance is less. Compression force acts stronger without hindrance or diffusion forces. It seems that the incorporation of the LSMM additive enhances the mechanical strength, leading to a higher capacity for resisting pressure compaction.

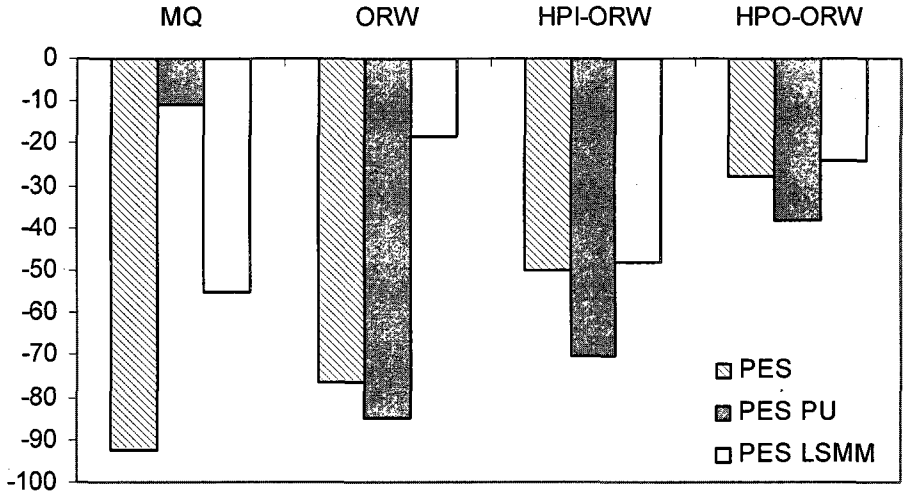

Figure R.2: Degree of compaction during filtration test with different water sources

It is concluded that the degree of compaction due to foulant-free water (MQ water) in some cases was comparable with foulant-containing water (ORW) and should not be ignored. In other words, even though PES is an amorphous polymer and has high compaction resistance such that it is recommended for high pressure applications, compaction occurs regardless of the water filtered. Secondly, incorporation of an additive enhances the membrane resistance to pressure compaction.

APPENDIX S

Summary of the LSMM project

Incorporation of hydrophilic additives – a promising approach for membrane surface modification in water treatment?

S.1. ABSTRACT

Blending surface modifying macromolecules (SMMs) in casting solutions has achieved certain impacts in the modification of membrane surface. The first type of SMM membranes incorporated with hydrophobic SMMs and was successful in certain membrane separation processes that require surfaces of hydrophobic nature, such as VOC removal by pervaporation and seawater desalination by membrane distillation. Then, hydrophilic SMMs (or LSMMs) were developed based on assumption that more hydrophilic PES ultrafiltration (UF) membranes would produce better performance for surface water treatment applications. This paper summarizes our recent work in the development of LSMM-containing UF membranes including the use of an alternative casting method to improve the quality of UF membranes and the evaluation of UF membranes prepared with a LSMM and different base polymers. Indeed, the hydrophilic surface modifying macromolecules (LSMMs), upon being congregated at the membrane surface during processing, have enhanced the flux performance, increased the regeneration capacity of membranes via cleaning, and proved to be well compatible with several typical UF base polymers including PES and PVDF. This paper will summarize the key results and discuss about LSMMs, which have most likely the properties of additives, based on a series of our previous and on-going studies.

Key words

Flux enhancement; hydrophilic additive; ultrafiltration.

Abbreviation

CA	Cellulose acetate
DMAc	N,N-dimethylacetamide
HDI	Hexane 1,6- diisocyanate
LSMM	Hydrophilic surface modifying macromolecules
MDI	Methylene bis-p-phenyl diisocyanate
NMP	1-methyl-2-pyrrolidinone
NOM	Natural organic matters
PCL	Polycaprolactone polyol
PE	Polyesters
PEG	Polyethylene glycol
PEI	Polyetherimide
PES	Polyethersulfone
PPG	Polypropylene glycol
PPO	Polypropylene polyol
PS	Polysulfone
PVDF	Polyvinylidene fluoride
PVP	Polyvinylpyrrolidone
SMM	Surface modifying macromolecules
TDI	Toluene 2,4- diisocyanate
UF	Ultrafiltration

S.2. INTRODUCTION

The hydrophilic surface modifying macromolecules (LSMM) project, originally called H-PHIL SMM, was the invention of articles creating a hydrophilic membrane surface. A step towards blending hydrophilic macromolecules is to try to increase the surface energy (or decrease the contact angles) since high surface energy is usually equivalent with better wettability. The water permeability of the membranes, as a result, will increase.

The development of these additives is not a trivial matter. Many different formulations are developed; however, many did not mix well with the base polymers. Even if the

additive and the base polymer(s) mix well, the casting does not necessarily produce reasonably good quality membranes, often due to solution viscosity or bubble problems. This raises an interest of using a new casting technique to recover this problem. The mixing capability of LSMM with different base polymers and the regeneration ability of these modified membranes are also other aspects of interest.

S.3. MATERIALS AND METHODS

S.3.1 LSMM synthesis and characteristics

Generally, LSMM has a following formula:

$$C\text{-}\{P\text{-}A\text{-}P\text{-}[B]_r\}_q\text{-}P\text{-}A\text{-}P\text{-}C$$

Basically, the synthesis of LSMM involves in two steps: synthesizing a segmented block oligomeric copolymer$\{P\text{-}A\text{-}P\text{-}[B]_r\}_q$ by reacting a diisocyanate A with an oligomeric polyol $[B]_r$, and then end-capping the copolymer with a hydrophilic oligomer C to produce the macromolecule. The desired structure of LSMM is such that its polymeric backbone remains buried in the membrane while the hydrophilic tail (OH^-) aligns itself with the interface thereby imparting hydrophilic properties to the membrane surface (Dang et al., 2008a).

Specifically, Rana et al., (2005) disclosed an LSMM synthesis via employing MDI and PPG dissolved in DMAc solvent, then end-capped with PEG. Figure S.1 showed the schematic synthesis of LSMM.

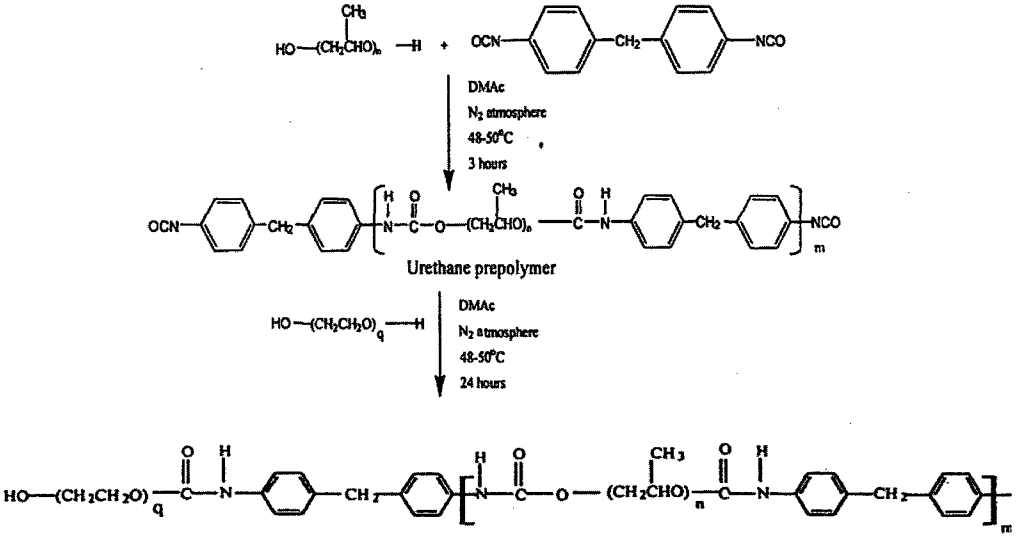

Figure S.1. LSMM synthesis scheme (after Rana et al., 2005)

Nitrogen content in LSMM-PEG was 5.92%. The characteristics of LSMM may change from batch to batch. In current study, it has Mn (number average molar mass) = 1.28x104, Mw (weight average molar mass) = 3.63x104 and its polydispersity index in NMP solvent is 2.83. Mn and Mw also change as percents of the diisocyanate or oligomeric polyol as well as hydrophilic oligomer components differ. LSMM is compatible well with most common solvents such as NMP and DMAc. Since these solvents are often used for dissolving mostly polymers such as PVDF, CA, PEI, PS, etc. This additive could probably be mixable with them. The first test of compatibility has been with PES, a relatively hydrophobic polymer with Tg ~ 230 degree, good thermal and mechanical properties. The modification of PES via incorporating LSMM will be discussed in the following section.

S.3.2 PES-LSMM fabrication

The membranes are modified by incorporating LSMM during mixing the casting solutions. Practically, the solution cast should contain: 0-6 wt% of LSMM; 10-25 wt% of the relatively hydrophobic base polymer (any one or a combination of PES, PS, PEI, PE and PVDF); 0-20 wt% of the hydrophilic pore forming polymer miscible with the base polymer (any one or a combination of PVP and PEG) and the rest of solvent(s). The reason that higher content of LSMM is not recommended is this would lead to difficult-to-process and brittle membranes. Optimization of each component's contents requires dozens of membrane processing and testing. Like while, this optimum ratio may work for a specific solute, not the others.

S.3.3 Membrane analysis

All the membranes were subjected to several morphological and physical/chemical analyses including scanning electron microscopy (SEM), atomic force microscopy (AFM), contact angle analysis, solute transport test, cross-flow ultrafiltration with surface water and cleaning tests. Details of these characterizations were described thoroughly by Dang et al., (2008a, b, c).

S.4. DISCUSSIONS

S.4.1 Characteristics of PES based membranes

During the past four years, several studies on PES base-LSMM membranes have conducted for the treatment of surface water. Rana et al., (2005) rendered that with the addition of LSMM, contact angles became slightly decrease, smaller mean pore sizes and higher solute (PEG) rejection were observed. In their study, the percent of LSMM was challenging in the range of 1.5 to 6 wt%. To illustrate the low ability of combining high LSMM content, they tried with 12 and 20 wt% LSMM. Those membranes were very brittle and even difficult to separate from the support material during casting. The percent of PES base polymer was kept constant at 20 wt%. What they found was that the more LSMM added, the more hydrophilic membranes were as well as was the water permeation rate. It seems that LSMM functions well as a hydrophilic additive. Although it does not make a very significant change (i.e., ten degree lower), for membrane modification it is recognizable.

Following this approach, Nguyen (2005) tested different concentrations of base polymer (15, 18 and 21 wt% of PES), LSMM (1.5, 3 and 4.5 wt%) and PVP (PVP:PES = 1, 2 and 3) to obtain the optimum ratio for NOM removal. In addition, diverse types of LSMM (LSMM200, LSMM 400 and LSMM 600 which generated by end-capping with PES having MW of 200, 400 and 600 respectively) were mixed in casting solutions. The values for each parameter were selected based on the study of hydrophobic SMM additives (Mosqueda-Jimenez et al., 2004). According to Nguyen (2005), no significant change on contact angle screening was observed by varying the PES content. 18 wt% of PES was eventually chosen since it was considered the "safe" number. This percentage was also preferred mostly in recent researches especially with SMM-blended modification (Mosqueda-Jimenez et al., 2004, Zheng et al., 2006, Zhu et al., 2007). Basically the concentration should not be low to avoid making brittle membranes or high to produce very tight membranes. The ratio PVP:PES of 1 to 3 was recommended in the membrane literature due to especially easy-to-cast factor (Mosqueda-Jimenez, 2003). They however disclosed that beside increasing the casting solution viscosity and facilitating the membrane manufacturing, the addition of PVP did not have any favorable impacts to membrane characteristics and performance. More widespread pore size

distribution made them more susceptible to mechanical compaction. No improvement in fluxes and NOM removal. Fouling was severe for membranes with PVP (Nguyen et al., 2007). The same results were found for the case of using different LSMM types (or different PEG end-group molecular weights) except the impact of LSMM400 and LSMM600 on membrane hydrophilicity was somewhat greater than that of LSMM200. The effect of LSMM content so far is most controversy since they don't show clear impacts. Current study showed that the optimum values could be 0.5 LSMM – higher percent made no difference. In addition, low percent of additive polymer helps reduce the capital costs in real application. Other than that, there are several advantages including easy to mix and cast, clear solution compatible well base polymer(s) and solvent.

Table S.1: Characteristics and performance of PES-LSMM and control PES membranes

No	Characteristic parameters	Control	LSMM	No	Performance parameters	Control	LSMM
1	MWCO (kDal)	71.68	69.65	9	Pure water permeation (lmh)	128.66	70.52
2	Mean pore size (nm)	4.60	4.35	10	R_m (10^{-10} m^{-1})	0.1	0.19
3	Pore density (# pore/m^2)	23.64	13.44	11	R_{fouled} (10^{-10} m^{-1})	0.26	0.38
4	Contact angle (°)	71.57	70.15	12	Flux reduction (%)	62.8	60.49
5	Surface tension (dyne/cm)	40.72	41.54	13	NOM removal (%)	76.65	78.57
6	Surface charge (mV)	-6	-3	14	NOM deposition (mg/m^2)	3	4.15
7	Roughness (nm)	1.27	1.72	15	Water production (l/m^2)	3458.3	2190.2
8	Water content (g/m^2)	126.84	126.94				

Note:

- Analysis methods for parameters No 1- 7, 9, 12-14 were referred to Dang et al., 2006

- Analysis methods for parameters No 8 and No 15 were referred to Dang et al., 2008b

- Analysis methods for parameters No 10 and 11 were referred to Bartlett et al., 1995

It can be seen from the above summarized data that the incorporation of LSMM made the membranes tighter with smaller mean pore sizes and lower MWCO, slightly increase the surface tension. Even though it is not superior in terms of fluxes, the solute rejection is enhanced and flux reduction is less. Certain success on synthesis and modification of PES-LSMM has brought to the doubt whether this kind of tail made membrane could be able to compete with the commercial UF membranes. The overview could be more critical if these modified membranes are compared with the UF commercial membranes. It would indicate the capability of these membranes in the membrane market.

S.4.2 Comparison with commercial UF membranes

Study by Dang et al., (2006) pointed out interestingly that the newly modified membranes was in the range of tight UF membranes with relatively smooth surface, small pore size and MWCO of approximately 60 kDal. This MWCO was somewhat a bit different from the MWCO in Table S.1 because of different LSMM content in membranes. The LSMM concentrations were 0.5 and 4.5 wt% for the membranes reported in Table S.1 and S.2 respectively. 4.5 wt% LSMM is the most favorable concentration that was concluded by Nguyen (2005).

Table S. 2: Pore characteristics and MWCO of tested membranes

Membranes	Measured MWCO (kDal)	Pore density (# of pores/m^2)	Mean Pore size (nm)	Contact angle (^{o})	Rough-ness (nm)
PX150	120.87	4.52	6.83	50.17	1.669
XM50	64.13	15.14	5.43	**16.50**	0.935
EWH70	80.39	9.41	5.90	54.75	1.906
PU40	58.06	**19.90**	**4.80**	46.33	**0.666**
CQ40	**57.59**	19.55	5.14	29.36	0.689
PES-LSMM	*61.64*	*15.79*	*5.05*	52.47	*1.806*
MIL100	98.52	6.63	6.19	47.67	1.789
PAN100	98.21	7.52	5.40	34.53	1.320
FO100	98.91	6.51	6.33	51.00	1.525
FO50	66.01	13.42	5.12	50.28	1.738

Note: The bold numbers indicate the highest value for pore density and lowest values for pore size, roughness and MWCO.

According to the summary of membrane characteristics in Table S. 2, the cellulose acetate (CQ40) and polyethersulfone (PU40) membranes appeared to be the most promising in terms of fluxes and fouling potentials since efficient membranes should have small pore sizes, high pore density and high surface porosity (Alsari et al., 2001). Considering the MWCO of membranes, molecular weight distribution of NOM and NOM rejection, it is noted that MWCO was proved not a truly precise indicator for the prediction of NOM rejection. The experiments showed that the membrane with the highest NOM rejection (PES-LSMM) was not the one having the lowest MWCO.

In term of flux, the commercial membranes such as FO50, MIL100 or XM50 were elevated at the start-up, but drop quickly in the first six hours (Dang et al., 2006). However, if high frequent cleaning is applied, the PES-LSMM may not be able to compete with the above commercial membranes in term of water production. Nevertheless, it is worth noting that while PES-LSMM membranes had much lower initial flux than cellulose acetate or cellulose membranes, they had the highest (TOC) rejection (80%) and the lowest flux reduction (62%). For the commercial membranes, the range of TOC rejections and flux reductions were 62-80% and 68-80%, respectively. This TOC rejection was relatively high compared with the 20% to 40% reported in the literature.

S.4.3 Cleaning PES-LSMM membranes

Improved amenability to cleaning is another potential benefit of surface modified membranes. Replicate of cleaning tests has been carried out currently. Both fouled membranes were subjected to backwashing in 10 min or chemical cleaning (NaOH) with duration of 15min each (Figure S.2). If cleaning was just by backwashing, the post cleaning flux was greater for the control PES membrane, presumably because of its larger pores, however when chemical cleaning was used the post-cleaning flux was higher for PES-LSMM membranes (Dang et al., 2008c).

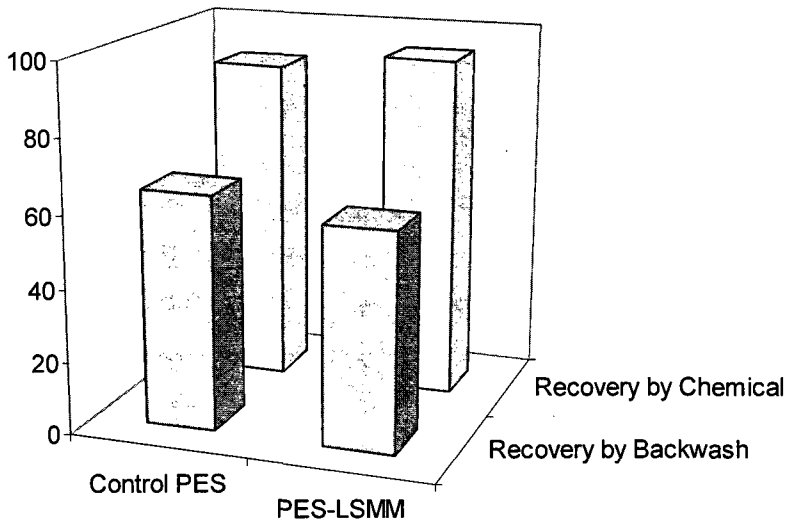

Figure S.2. Flux recovery

S.4.4 Improvement of LSMM membranes – double casting

In trying to improve the capability of LSMM containing dopes, we initially experimented with changing the LSMM and PES concentrations. Alternatively, our most recent approach has evaluated a new casting technique, hereafter called "Double casting". This approach consists of spreading the casting solution in one direction (Step 1 and 2 in Figure S.3) and re-spreading it in the opposite direction immediately afterwards (Step 3 Figure S.3) and proceeding to gelation, which different from the conventional thin film composite approach of producing a multilayered structure. The hypothesized impact on membrane morphology are depicted somewhere in Dang et al., (2008a).

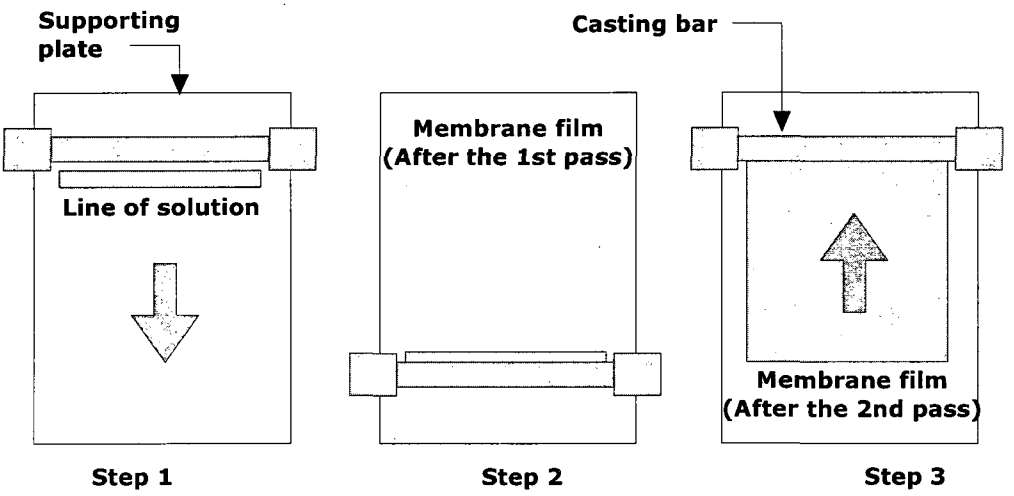

Figure S.3: Schematic representation of casting steps

Since the objective of this study was to observe the change of hydrophilicity of the membranes, advancing contact angles and contact angles as a function of drop age were recorded (Figure S.4). Obviously, the double casting method did have some effects on the membrane surface, especially the hydrophilicity. With the replicate of ten measurements, the advancing contact angles were decreased up to three degrees with respect to the standard deviation. In addition, the surface of the Double-PES-HI tended to draw more water into the membrane pores as the time passes. It was hypothesized by the authors that the since the membrane casting period was doubled, more hydrophilic SMMs would migrate to the membrane surface, lowering the hydrophilicity, and thereby enhancing the contact angles.

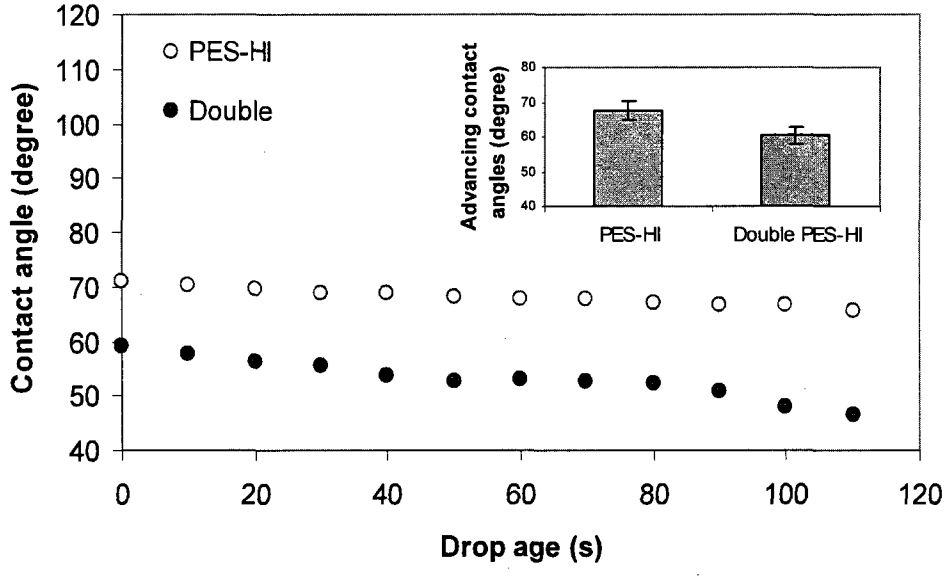

Figure S.4: Contact angles

Nevertheless, just a slight difference in NOM rejection and fluxes was achieved since this method was found to be more suitable for hard-to-cast solutions (Dang et al., 2008a).

S.4.5 Blending LSMM with other UF base polymers

The specific design of a membrane for use in a particular separation is governed by many factors such as hydrophobicity, porosity, mechanical strength and tendency to foul. Change of base polymer, one of membrane forming compounds, may impart membranes

with alternative properties and performance. The hydrophilic SMM has proved to have positive impacts on PES ultrafiltration membranes up to this point. It is of interest to investigate the effect of LSMMs blending with various host polymers on the performance of UF membranes. Five polymers selected as the base polymers to cover a wide range of hydrophilicity/phobicity spectrum were CA, PEI, PES, PS, and PVDF (Dang et al., 2008b). Apparently, LSMM was mixable well with all the base polymers. However, solutions with lower LSMM percent (0.5 wt %) were easier to cast. Whereas incorporation of a larger amount of LSMM (3.0 wt %) made the formation of membranes with good appearances more difficult especially for CA and PVDF. In addition, LSMM had a visible effect on those membranes in terms of MWCO and morphology (Dang et al., 2008b).

The change of flux due to the incorporation of LSMM in the casting solutions is presented in Figure S.5, where the % flux change is defined by the following equation.

$$\% \text{ Flux change} = \frac{J_{withLSMM} - J_{withoutLSMM}}{J_{withoutLSMM}} x100 \qquad [S.1]$$

Whereas $J_{withLSMM}$ ($l/m^2/h$) and $J_{withoutLSMM}$ ($l/m^2/h$) are the pure water fluxes corresponding to the membranes prepared from the same host polymer with and without LSMM blending. The figure shows the change of the above parameter as a function of operating period. Positive flux change illustrates the increase in the pure water flux by SMM blending. Furthermore, the line slopes indicate the effect of SMM blending on the membrane compaction, i.e., the upward trend indicates less compaction, horizontal line equal compaction and downward trend the stronger compaction of the membranes in which LSMM is blended.

Although the additive did not make the membranes more hydrophilic, it significantly improved the permeability of the membranes prepared with all the base polymers. For the PVDF-LSMM membrane the flux change was over 200 percent. It was found that beside PES, PVDF could be a promising candidate for membrane modification using LSMM based on pure water flux enhancement.

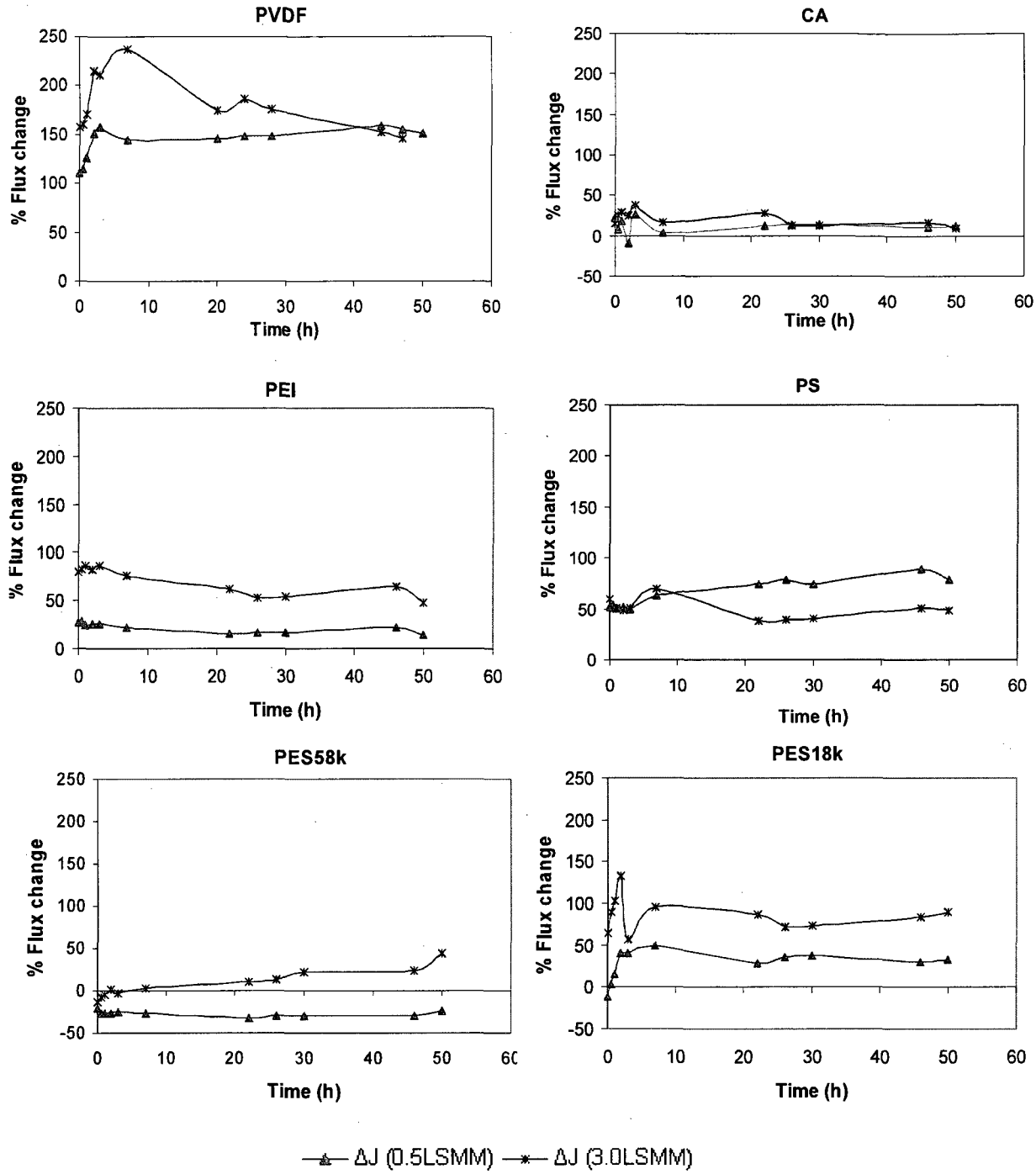

Figure S.5: Percent of flux change as a function of filtration time

S.5. CONCLUSIONS

The evaluation in terms of mixing capability, comparison with the commercial UF membranes, experience of new casting method, regeneration ability, and compatibility

with other base polymers has shown that the surface modification of membranes via the addition of a surface modifying additive to the cast solution has promise. LSMM was compatible with several base polymers such as PES and PVDF polymers. It absolutely enhances flux performance. The incorporation of this additive improves the cleaning, especially chemical cleaning as well. Future researches on fabrication of LSMM hollow fiber UF membranes would be of interest to obtain the full understanding of the effects of these surface active molecules.

S.6. REFERENCE

Alsari A.M., Khulbe K.C., Matsuura T. (2001). The effect of sodium dodecyl sulfate solutions as gelation media on the formation of PES membranes. *J. Membr. Sci.*, 188, 279-293.

Bartlett M., Bird M.R., Howell J.A. (1995). An experimental study for the development of a qualitative membrane cleaning model, *J. Membr. Sci.* 105, 147-157

Dang T.H., Narbaitz M.R., Matsuura T. (2008a). Double-pass casting: A novel technique for developing high performance ultrafiltration membranes. Submitted to *J. Membr. Sci.*

Dang T.H., Narbaitz M.R., Matsuura T. (2008c). Optimised cleaning methods for tight UF membranes in surface water treatment. *In preparation.*

Dang T.H., Narbaitz M.R., Matsuura T. and Khulbe C.K. (2006). A comparison of commercial and experimental ultrafiltration membranes via surface property analysis and fouling tests. *Water Qual.Res. J. of Canada*, 41 (1), 85-94

Dang T.H., Narbaitz M.R., Matsuura T. and Rana D. (2008b). Performance of a newly-developed hydrophilic additive blended with different UF base polymers. Submitted to *J. Appl. Polm. Sci.*

Mosqueda-Jimenez D.B. (2003). Impact of manufacturing conditions of Polyethersulfone membranes on final characteristics and fouling reduction", PhD thesis, Department of Civil Engineering, University of Ottawa.

Mosqueda-Jimenez D.B., Narbaitz R.M., and Matsuura T. (2004). Impact of the membrane surface modification on the treatment of surface water. *J. Environ. Eng.*, 130, 1450-1459.

Nguyen A.H., Narbaitz R.M., Matsuura T. (2007). Impacts of hydrophilic membrane additives on the ultrafiltration of river water, *J. Environ. Eng.*,133 (5): 515-522.

Nguyen H.A. (2005). Membrane fouling reduction by the incorporation of hydrophilic surface modifying macromolecules in ultrafiltration membrane manufacturing", M.A.S.c thesis, Department of Civil Engineering, University of Ottawa, Ottawa, ON.

Rana D., Matsuura T., Narbaitz R.M., Feng C. (2005). Development and characterization of novel hydrophilic surface modifying macromolecule for polymeric membranes. *J. Membr. Sci.* 249: 103-112.

Zheng Q.Z., Wang P., Yang Y.N. (2006). Rheological and thermodynamic variation in polysulfone solution by PEG introduction and its effect on kinetics of membrane formation via phase-inversion process. *J. Membr. Sci.* 279 (1-2): 230-237.

Zhu L.P., Zhang X.X., Xu L., Du C.H., Zhu B.K., Xu Y.Y. (2007). Improved protein-adsorption resistance of polyethersulfone membranes via surface segregation of ultrahigh molecular weight poly(styrene-alt-maleic anhydride), *Coll. Surf. B-Biointerfaces* 57 (2): 189-197.